NOVEL HYBRID MATERIALS: FUNCTIONALIZED POLYOXOMETALATES AS POTENTIAL METALLOLIGANDS

by

KRISTOPHER MIJARES

MChem , The Nottingham Trent University, 2002

AN ABSTRACT OF A DISSERTATION

submitted in partial fulfillment of the requirements for the degree

DOCTOR OF PHILOSOPHY

Department of Chemistry
College of Arts and Sciences

KANSAS STATE UNIVERSITY
Manhattan, Kansas

2008

Abstract

Polyoxometalates are self-assembled metal-oxygen anionic clusters formed primarily by Mo, W and the Group V transition metals. Their structural, chemical and physical diversity have attracted much attention from fields such as catalysis, imaging, magnetic materials, medicine and photochromism. While many of these inorganic systems are easy to prepare, their conversion to hybrid inorganic-organic materials through functionalization is an ongoing challenge.

Two approaches used for functionalization involve the insertion of metal-nitrido fragments into a lacunary polyoxometalate or the direct replacement of the terminal oxo ligands with the isoelectronic organoimido $[NR]^{2-}$, hydrazido $[NNR_2]^{2-}$, nitrosonium $[NO]^{+}$ and diazenido $[NNR]^{+}$ ligands. The later process has been proven successful with a variety of different nitrogenous ligands.

One of our group's goals has been to synthesize a functionalized hexamolybdate species capable of metal coordination, with the ultimate goal of forming self-assembled networks. However, previous results have been unsuccessful due to the electron withdrawing effect of the cluster which is transmitted to the metal binding site. In order to overcome this effect, several new organoimido delivery reagents (phosphineimines, isocyanates and arylamines) containing electron donating substituents have been synthesized and characterized. Attempts to attach these species to hexamolybdate are described. The synthesis and characterization of biarylimido ligands bearing remote σ-donor functionalities and their incorporation into the hexamolybdate cluster will be described.

A new and exciting avenue of polyoxometalate chemistry will be demonstrated through the successful metal coordination of the biarylimido functionalized hexamolybdate to a ruthenium(II) metalloporphyrin. This also brings the hexamolybdate polyoxometalate one step closer to being capable of forming the supramolecular architectures mentioned earlier.

A chromium(V) nitrido polyoxometalate has been synthesized and characterized from a lacunary Keggin precursor, in collaboration with our colleagues in Paris. The ability of this complex as a nitrogen transfer reagent will be explored.

An alternative synthetic route to the osmium-nitrido-Dawson species, $[(OsN)P_2W_{17}O_{61}]^{4-}$ will also be described. These nitrido species could be an entry point to other derivatives through reactions with various nucleophiles and electrophiles.

NOVEL HYBRID MATERIALS: FUNCTIONALIZED POLYOXOMETALATES AS POTENTIAL METALLOLIGANDS

by

KRISTOPHER MIJARES

MChem , The Nottingham Trent University, 2002

A DISSERTATION

submitted in partial fulfillment of the requirements for the degree

DOCTOR OF PHILOSOPHY

Department of Chemistry
College of Arts and Sciences

KANSAS STATE UNIVERSITY
Manhattan, Kansas

2008

Approved by:

Major Professor
Eric A. Maatta

Copyright

Abstract

Polyoxometalates are self-assembled metal-oxygen anionic clusters formed primarily by Mo, W and the Group V transition metals. Their structural, chemical and physical diversity has found use in fields such as catalysis, imaging, magnetic materials, medicine and photochromism. While many of these inorganic systems are easy to prepare, their conversion to hybrid inorganic-organic materials through functionalization is an ongoing challenge.

Two approaches used for functionalization involve the insertion of metal-ligand fragments into a lacunary polyoxometalate or the direct replacement of the terminal oxo ligands with the isoelectronic organoimido $[NR]^{2-}$, hydrazido $[NNR_2]^{2-}$, nitrosonium $[NO]^{+}$ and diazenido $[NNR]^{+}$ ligands. The latter process has been proven successful with a variety of different nitrogenous ligands.

One of our group's goals has been to synthesize a functionalized hexamolybdate species capable of metal coordination, with the ultimate goal of forming self-assembled networks. However, previous results have been unsuccessful due to the electron withdrawing effect of the cluster which is transmitted to the metal binding site. In order to overcome this effect, several new organoimido delivery reagents (phosphineimimines, isocyanates and arylamines) containing electron-donating substituents have been synthesized and characterized. Attempts to attach these species to the hexamolybdate are described. The synthesis and characterization of biarylimido ligands bearing remote σ-donor functionalities and their incorporation into the hexamolybdate cluster will be described.

A new and exciting avenue of polyoxometalate chemistry will be demonstrated through the successful coordination of the biarylimido functionalized hexamolybdate to a ruthenium(II) metalloporphyrin. This also brings the hexamolybdate polyoxometalate one step closer to being capable of forming the supramolecular architectures mentioned earlier.

A chromium(V) nitrido polyoxometalate has been synthesized and characterized from a lacunary Keggin precursor, in collaboration with our colleagues in Paris. The ability of this complex as a nitrogen transfer reagent will be explored.

An alternative synthetic route to the osmium-nitrido-Dawson species, $[(OsN)P_2W_{17}O_{61}]^{4-}$ will also be described. These nitrido species could be an entry point to other derivatives through reactions with various nucleophiles and electrophiles.

Table of Contents

List of Figures

List of Tables

Acknowledgements

I would first and foremost like to thank my major professor, Dr. Eric A. Maatta. His guidance, understanding and support throughout my time here at Kansas State University will never be forgotten. You have truly influenced my life in a positive way and helped me develop both as a person and as a scientist, for this I will always be grateful. Thank you for my time in Paris and at K-State. I would also like to thank our colleagues in Paris, Dr. Anna Proust, Dr. René Thouvenot, Dr Bernie Hasenknopf and Dr. Vanina Lahootun for their warmth and hospitality during my time in Paris.

I would like to thank my committee, Dr. Chris Levy, Dr. Paul Smith, Dr. Michael Kanost and Dr Robert Larson for their professionalism and understanding with scheduling the final defense. As well as Dr. Ohm Prakash for his help with NMR interpretation.

To all my friends in Manhattan who have my made my time here so memorable. I want to thank Dr. Leila Maurmann for her unlimited help and patience with the various NMR experiments, without her, the coordination work would not have been possible. Also my group mates, Dr. Lou Wojcinsksi and Dr. Jeff Karcher for their endless help and support in and out of the lab and the office conversations. I want to especially thank the "Brits" (Alex, Ben, Dipesh, Jamie and Michelle) for the laughter, the tears and indeed understanding the importance of a good decent pint and a good film!

Thanks to various people in the department that made my life considerably easier during my time here especially, Jim Hodgson (thanks for all my glassware, the conversations and advise) Earline Dikeman, Tobe Eggers, Richard Bachamp, Ron Jackson, Connie Cusimano, Kim Ross, Donna Wright, Mary Dooley, Arlon Meek. Thanks must also go to Dr. John Desper for the x-ray crystal structure analysis, as well as to Dr. Takeo Iwamoto and Dr. Hirosima Yasuaki for the MS data.

To my mum and dad, without your support, love and sacrifices I would not have been able to do any of this. I love you both very much.

Finally, to my wife. Krista, your love, support and encouragement throughout my time at KSU gave me the motivation to persevere and grow as a person. For this I am truly thankful for and will always be indebted to you. I love you.

Dedication

To my wife, my mum and my dad, thank you so much for everything.

I love you all.

CHAPTER 1 - Introduction

1.1 Polyoxometalates

Polyoxometalates (POMs) are self-assembled metal-oxygen anionic clusters formed primarily by Mo, W and the Group V transition metals.[1,2] Each nano-sized assembly is accompanied by counter ions such as alkali metal cations, ammonium cation or polyalkylammonium cations. Assembly of these metal-oxide structures can be achieved via stoichiometric control or pH control (Fig 1-1).

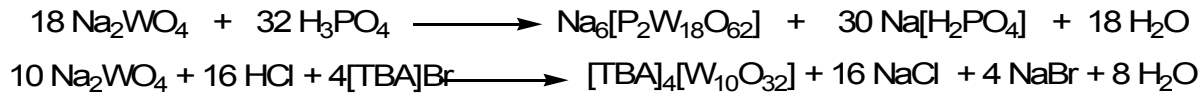

Figure 1-1: Syntheses of POMs in acidic conditions.[3] ([TBA] = (n-C4H9)4N)

POMs can be classified into two broad groups, isopoly and heteropoly anions (Figure 1-2). Typically the isopolyanionic framework is composed of one type of metal atom (termed 'addenda' atoms), which are often molybdenum or tungsten atoms. Heteropolyanions or 'mixed addenda' clusters, typically possess one (sometimes two) hetero atoms which are located in the center of the framework, e.g. phosphorus in $[P_2W_{18}O_{62}]^{6-}$. So far over 70 different heteroatoms have been incorporated into various POMs.

Figure 1-2: Molecular formula of Isopoly and Heteropoly anions[1]

(M = addenda metal, O = oxygen, X = heteroatom).

Historically, Berzelius is credited for reporting the first POM in 1826,[4] namely the ammonium salt of $[PMo_{12}O_{40}]^{3-}$. This heteropoly salt was later utilized by Svanberg and Struve[5] for the gravimetric and volumetric determination of phosphorus. However it would be almost another 100 years before its structure was determined by Keggin[6]. It is important to remember that there

are hundreds of structures pertaining to POMs both isopoly and heteropoly; three of the most common structures are shown in Figure 1-3.

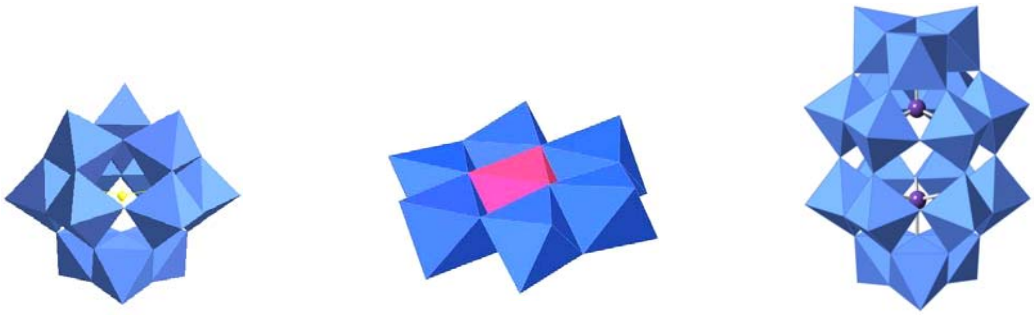

(a) (b) (c)

Figure 1-3: Polyhedral representation of a) Keggin, b) Evans-Anderson and c) Dawson POMs.[2]

The Keggin structure (Figure 1-3a) is perhaps the most commonly adopted structure and has a diameter of ~ 1.2 nm. It is composed of 12 vertex- and edge-sharing MO_6 octahedra surrounding a central XO_4 tetrahedron; X can be a wide range of elements typically from Group 4 or 5 metals (e.g. P^{5+}, As^{5+}, Si^{4+}, Ge^{4+}).[2] Any POMs with a general ratio of 1:12 are labeled as 'Keggin' and those with a ratio of 2:18 are labeled as 'Dawson' types.

POMs are structurally and compositionally diverse and they also typically exhibit rich electrochemistry.[7(a)] This can be attributed to their fully oxidized framework. It is common for POMs (those without *cis*-$[MO_2]$ units) to display multiple and reversible one- or two-electron reductions often leading to mixed valence species referred to as 'heteropoly blues' due to their characteristic intense blue coloring. Perhaps this was why initial efforts of POM research focused greatly on their behavior as 'heteropoly acids'

$$[PW_{12}O_{40}]^{3-} + 23\,OH^- \longrightarrow HPO_4^{2-} + 12\,[WO_4]^{2-} + 11\,H_2O$$

$$[CrMo_6O_{26}H_6]^{3-} + 9\,OH^- \longrightarrow Cr(OH)_3 + 6\,[MoO_4]^{2-} + 6\,H_2O$$

Figure 1-4: Cluster decomposition of POMs by hydroxide.[1]

and more recently as catalysts[8]. In their fully oxidized state POMs tend to be thermally, oxidatively and hydrolytically stable. However cluster decomposition can occur even at mildly

basic conditions[1] (Figure 1-4). Physically, POMs can range anywhere between 6-25 Å in diameter with ionic weights upwards of 10,000 amu.[1]

Table 1-1: Timeline of industrial processes catalyzed by heteropoly compounds.[2]

Reaction	Year	POM Catalyst
$CH_2{=}CHCH_3 + H_2O \rightarrow CH_3CH(OH)CH_3$	1972	$H_4[SiW_{12}O_{40}]^a$
$CH_2{=}C(CH_3)_2 + H_2O \rightarrow (CH_3)_3COH$	1984	$H_3[PMo_{12}O_{40}]^a$
$^nTHF + H_2O \rightarrow HO\text{-}[\text{-}(CH_2)_4\text{-}O\text{-}]^n\text{-}H$	1985	$H_3[PW_{12}O_{40}]^b$
$CH_2{=}CH_2 + O_2 \rightarrow CH_3COOH$	1997	Pd-HPA[c]
$CH_2{=}CH_2 + CH_3COOH \rightarrow CH_2CH_2O_2CCH_3$	2000	$H_4[SiW_{12}O_{40}]/SiO_2^c$

([a] Homogeneous, [b] Biphasic (liquid-liquid), [c]Heterogeneous; HPA = heteropolyanion)

Industrially, POMs have been utilized mainly as acid-, oxygenation- and photo-catalysts. In the early 1970's Japan developed and commercialized the heteropoly salt, $H_4[SiW_{12}O_{40}]$ for the homogeneous catalytic hydration of propene to 2-propanol (Table 1-1).[2]

1.2 Keggin Polyoxometalates

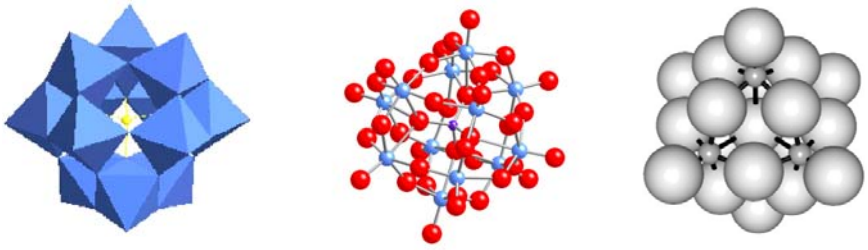

(a) (b) (c)

Figure 1-5 Various structural representations of a Keggin POM. a) Polyhedral; b) Ball and stick model (red = oxygen, blue = metals, purple = addenda metal atom); c) Space filling model.[7(b)]

As mentioned previously, Berzelius is credited for the discovery and documentation of the first fully recognized POM; $(NH_4)_3[PMo_{12}O_{40}]$.[7] However structure resolution is credited to Keggin, thus heterolopolyanions of the $[XMo_{12}O_{40}]^{n-}$ type are often described as a 'Keggin type' (Figure 1-5).[7]

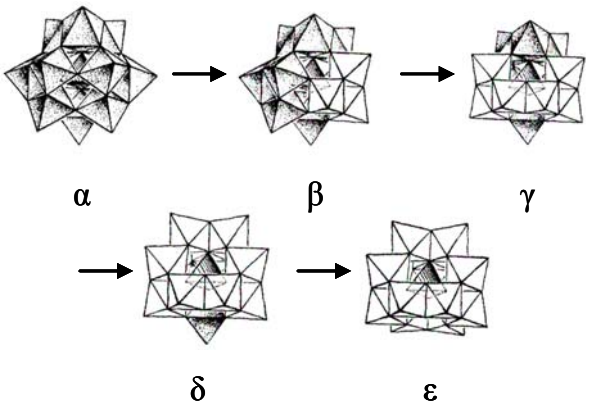

Figure 1-6: Baker-Figgis isomers of the Keggin Structure (α). Rotation of one, two, three or four Mo_3O_{13} units (unshaded) by π/3 produces the β, γ, δ and ε isomers, respectively.[1]

Keggin POMs overall exhibit virtual tetrahedral (T_d) symmetry, with a central XO_4 tetrahedral unit surrounded by 12 MoO_6 octahedral units which are arranged into four groups of three edge sharing Mo_3O_{13} units. Each of the four Mo_3O_{13} groups are linked to the central PO_4 unit and to each other by their corresponding edges. It was later found by Baker and Figgis that when groups of one, two, three or four of the Mo_3O_{13} units are rotated by π/3, different isomers of the Keggin POM can be related (Figure 1-6).[9]

In addition to the isomeric forms of the complete (or "plenary") Keggin structure, there are also "lacunary" derivatives in which one, two or three oxo-metal vertices have been removed by treating the complete Keggin ion with a suitable base such as bicarbonate. An example illustrating the formation of the lacunary $[XM_{11}O_{39}]^{n-}$ system is shown in Figure 1-7. It has also been shown that certain lacunary species can be synthesized via stoichiometric and pH control.[10]

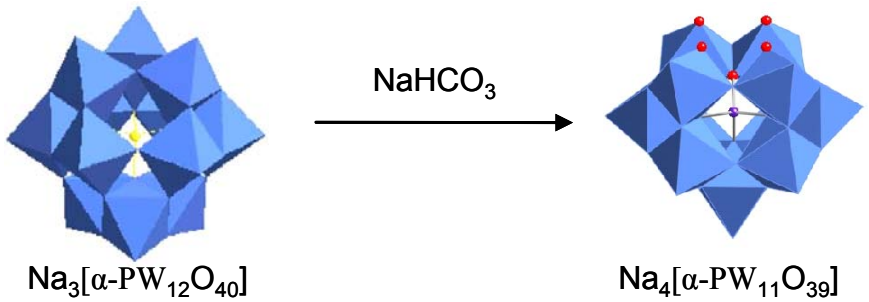

Figure 1-7: Synthesis of the mono-lacunary Keggin species, $[\alpha\text{-}PW_{11}O_{39}]^{7-}$ via the abstraction of one $[W^{VI}O]^{4-}$ unit.[3]

The removal of an M-O unit from the Keggin exposes a 'cavity' within the lacunary species (Figure 1-7). This cavity presents five oxygen donors in a roughly square pyramidal arrangement and therefore is ideally suited for incorporating an added $[ML]^{n+}$ unit in a pseudo-octahedral geometry. Exploitations of such vacant sites have afforded an enormous range of complexes (M = e.g., Co(II), Co(III), Zn(II), Ni(II), etc.; L = H_2O, halide, NH_3, pyridine, etc.).[11] However it should be noted that not all lacunary Keggins are hydrolytically or thermodynamically stable and can often revert back to their parent Keggin. Similar lacunary species are also known with the Dawson series of POMs.

1.3 FUNCTIONALIZED POMs

1.3.1 - Transition metal

As described in the preceding section, the range of POMs can be further extended through functionalization of the clusters with transition metal cations. The ability of both heteropoly and isopoly POMs to incorporate transition metals has truly extended their structural, chemical and physical diversity. All first row and most of the second row transition metals have been incorporated into various Keggin and/or Dawson clusters.[1] Derivatives containing multiple transition metal cations as well as organometallic species have been prepared. The resulting modified clusters can exhibit desirable properties such as magnetic behaviour[12] or catalytic activity[13]; examples are illustrated in Figure 1-8.

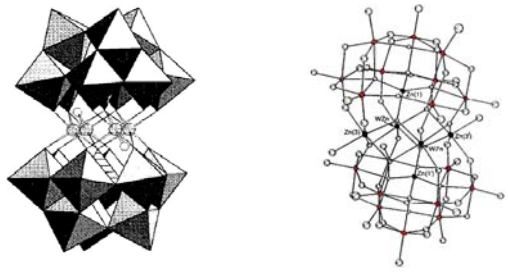

(a) (b)

Figure 1-8: Structural representations of a) the magnetic POM[12] $[(Fe^{II})_4(H_2O)_2\text{-}(PW_9O_{34})_2]^{10-}$ b) the oxidation catalyst[13] $[WZn_3(H_2O)_2(ZnW_9O_{34})_2]^{12-}$ (red = W; black = Zn).

1.3.2 - Main Group Elements

Although halide ions $[X]^-$ are formally isoelectronic with oxide ions $[O]^{2-}$, there are few examples of halide functionalized POMs. One such species is $[H_2NaW_{18}O_{56}F_6]^{7-}$(Figure 1-9).[14] However, the fluoride ion does not occupy a terminal position, being instead contained within the cluster leaving it unavailable for further chemical reactions.

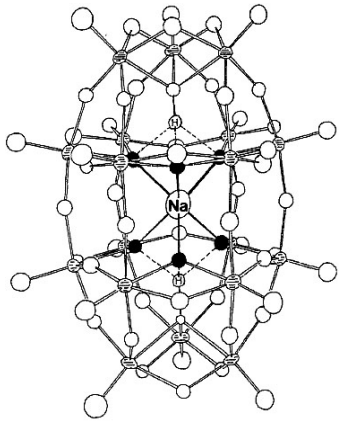

Figure 1-9: Ball and Stick representation of $[H_2NaW_{18}O_{56}F_6]^{7-}$
(Open circle = oxygen; blackened circles = fluoride; grey circles = tungsten).[14]

As with the halides, there are few known POMs clusters incorporating sulfur and selenium. Klemperer[15] reported the first thio-POMs, $[W_5O_{18}MS]^{3-}$ (M = N, Ta) from a reaction between $[MW_5O_{19}]^{3-}$ and hexamethyldisilathiane. Another example of a thio POM is γ-$[SiW_{10}Mo_2S_2O_{38}]^{6-}$, in which the POM acts as a tetradentate ligand to a $\{Mo_2S_2O_2\}^{2+}$ species (Figure 1-10).[16]

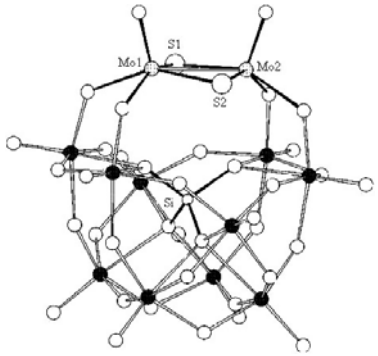

Figure 1-10: Molecular structure of γ-$[SiW_{10}(Mo_2S_2)O_{38}]$.[6-16]

1.3.3 - Alkoxo- and Group 14 derivatives

Alkoxo-ligands are one of the most common functionalities appended to POMs. Their syntheses encompass O-alkylations,[17] esterifications with alcohols,[18] controlled hydrolysis of metal alkoxides[19] and self-assembly from alcohols and POMs.[7] A majority of the alkoxo ligands are incorporated into POM clusters via μ^2 or μ^3 binding with one exception: the Lindqvist derivatives of $[(MeO)XW_5O_{18}]^{n-}$ (X = Ti, Zr, Nb, Ta, Mo, W)[19] display terminal alkoxo ligands.

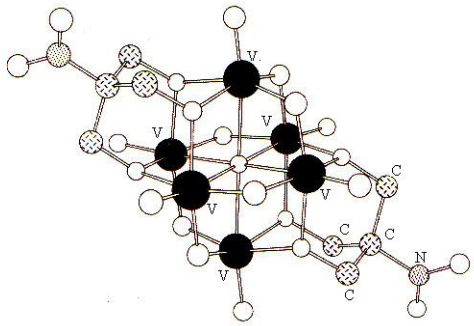

Figure 1-11: The tris-alkoxo Lindqvist POM, trans-$[V_6O_{13}\{O_2NC(CH_2O)_3\}_2]^{2-}$.[20]

Zubieta exploited tris-alkoxo ligands to stabilize epolyoxovanadate cores (Figure 1-11).[20] Similar tris-alkoxo-derivatives were prepared by Gouzerh in the form of the Anderson-Evans POM, $[XMo_8O_{18}\{H_3C(CH_2O)_3\}_2]^{n-}$ (X = Mn, Os).[21]

Although alkylidenes $[R\text{-}C]^{3-}$ are isoelectronic to the oxo ligands of POMs, so far there are no known examples of alkylidene-functionalized POMs. In the late 1970's examples of organosilyl[22] and organogermyl[23] POMs were reported by Knoth and Pope. Almost 20 years later, the first organostannyl ligands were incorporated into various Keggin[22], Dawson[23] and Lindqvist[24] POMs (Figure 1-12).

The organostannyl POMs are significant because they provide a versatile way to attach a broad range of organic substituents onto a POM via the tin sites leading to hybrid organic-inorganic materials.

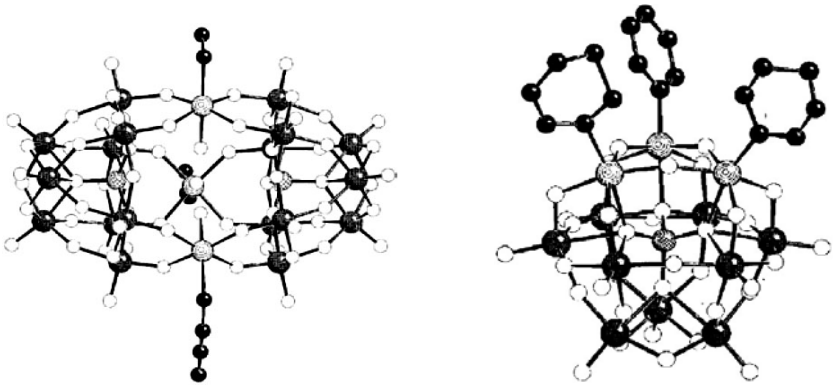

(a) (b)

Figure 1-12: Molecular models of (a)[17] α-$[(SiW_9O_{34})_2(^n\text{-}BuSnOH)_3]^{14-}$ and (b)[17] β-$[SiW_9O_{37}(SnPh)_3]^{7-}$.

1.3.4 - Lindqvist Polyoxomoletalates

The Lindqvist[25] family of POMs have the general formula, $[M_6O_{19}]^{n-}$, (M = Mo, W, Nb, Ta, V) (Figure 1-13).[26] Unlike the Keggin structures, homometallic unsubstituted Lindqvist POMs do not exhibit isomerism. Lindqvist POMs contain three distinct type of metal-oxygen bonds, as revealed through x-ray crystallography (Table 1-2). A central oxygen atom is bound to six metal atoms, with local octahedral symmetry.

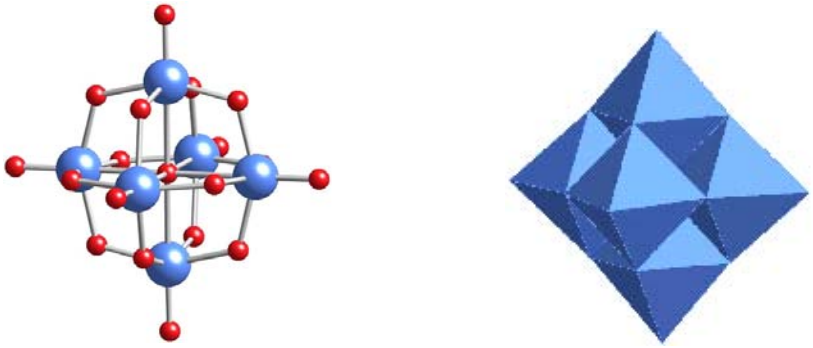

Figure 1-13: Structural representation of the Lindqvist POM, a) Ball and Stick Model (big/ blue = Metal; small/red = oxygen) b) Polyhedron.

Each metal atom is capped by a terminal oxo ligand via a formal triple bond (one σ-bond and two π-bonds), and shares four bridging (μ_2) oxo ligands with adjacent meal atoms. These hexa-metalates have an idealized octahedral symmetry.

Table 1-2: Selected bond lengths (Å) of some Lindqvist ($[M_6O_{19}]^{n-}$) isopolyanions.

Lindqvist POM	M-O(terminal)	M-O(bridging)	M-O(central)	Refs.
$[Mo_6O_{19}]^{2-}$	1.68	1.93	2.32	27
$[Ta_6O_{19}]^{8-}$	1.80	1.99	2.38	1
$[W_6O_{19}]^{2-}$	1.69	1.92	2.38	28

1.3.5 - Synthetic routes for the surface modification of hexamolybdate with organoimido ligands.

The terminal oxygens of hexamolybdate ($[Mo_6O_{19}]^{2-}$) can be substituted by various nitrogenous ligands such as organoimido $[NR]^{2-}$, hydrazido $[NNR_2]^{2-}$, nitrosonium $[NO]^{+}$ and diazenido $[NNR]^{+}$ species. Over the years, the ability to substitute a terminal oxo-ligand by an isoelectronic imido ligand has attracted considerable attention. This interest has been fuelled by the possible role of organoimido ligands in nitrogen transfer reactions,[27] as intermediates in the catalytic ammoxidation of propylene into acrylonitrile[28] and in olefin aziridination[29]. Given that

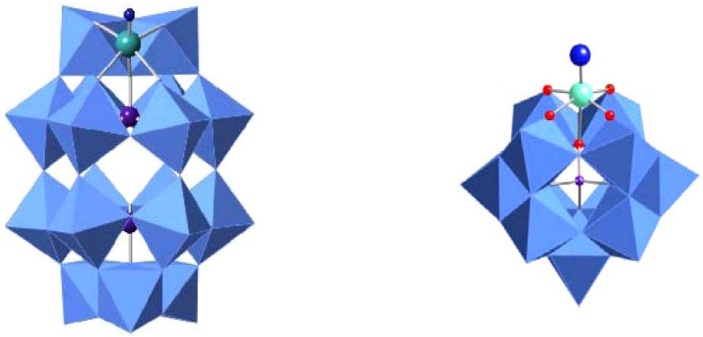

Figure 1-14: Polyhedral representations of (a) the nitrido-Dawson ion $[(MN)P_2W_{17}O_{61}]^{n-}$ and (b) the nitrido-Keggin ion $[(MN)PW_{11}O_{39}]^{x-}$ (M = Re, Os).[30]

the close-packed structures of the Lindqvist and Keggin systems resemble those observed in catalytically-relevant metal oxides such as MoO_3, it is not surprising that organoimido polyoxometalates have drawn widespread interest.

A variety of nitrogenous functionalities have been substituted into various POMs, and these will be discussed later in more detail. In the simplest form, metal nitride units $[MN]^{n+}$ were incorporated into both a Lindqvist[31] and a Keggin[32] POM by Zubieta. However the first series of fully characterized metal-nitride POMs were reported in 2002 and 2006 by Maatta and Proust.[30] They showed that both Re- and Os-nitrido species can be incorporated in both Dawson and Keggin type POMs, respectively. In particular, the $[M(N)\text{-}P_2W_{17}O_{61}]^{x-}$ and $[M(N)\text{-}PW_{11}O_{39}]^{x-}$ (M = Os, Re) (Figure 1-14).[30]

The most common method for incorporating nitrogenous ligands into a Lindvist POM is via direct substitution. In 1995, Maatta and Hill reported a *p*-pyridylimido vanadium(V) complex.[33] (Figure 1-15) They demonstrated that the pyridyl nitrogen (σ-donor / π-acceptor) remote functionality was capable of coordinating a second metal center producing new types of bimetallic complexes.

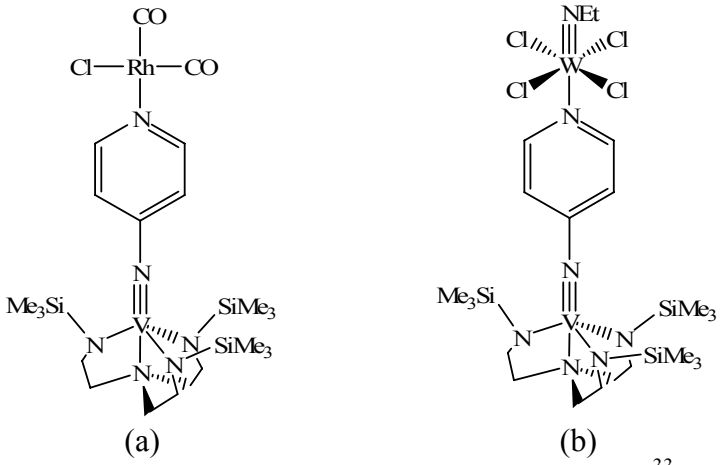

Figure 1-15: Bimetallic systems reported by Maatta and Hill,[33] Vanadium(V) organoimido complexed with (a) rhodium and (b) tungsten.

With this knowledge, Maatta and Forster successfully incorporated the *m*-pyridylimido remote functional group into the hexamolybdate dianion in an attempt to convert the dianion into a metalloligand.[34] Other remote functionalities have also been attached to the hexamolybdate with varying degrees of success such as carboxylic acid, p-pyridine, styrene, crown ether, phenol and hydro-quinoline groups.

Several routes to functionalizing hexamolybdates have been established over the past 2 decades. The method developed by the Maatta[35] group relies on the direct reaction of the

tetrabutylammonium hexamolybdate salt, $[TBA]_2[Mo_6O_{19}]$, with an organoimido delivery reagent. The organoimido deliver reagent can be a phosphineimine ($R\text{-}N{=}PPh_3$) or an isocyanate (R-NCO); the reactions are conducted under an inert atmosphere using mild heat. Though the detailed mechanism is not yet known, it was proposed that substitution (i.e. hexamolybdate

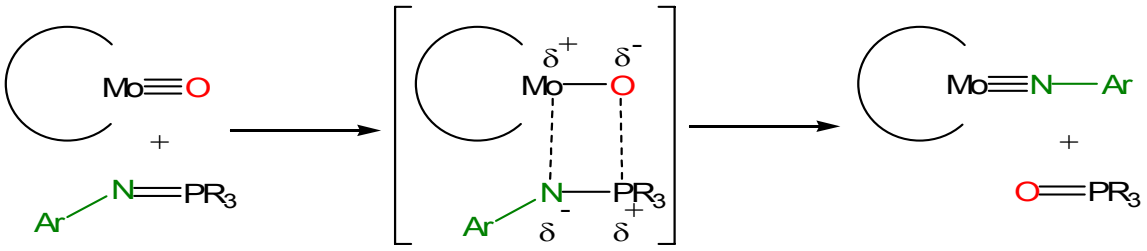

Figure 1-16: Proposed mechanism for the substitution of $TBA_2[Mo_6O_{19}]$ with a phosphineimine delivery reagent. (Maatta's phosphineimine protocol).[35]

functionalization) occurs via an interaction between the terminal molybdenum-oxygen multiple bond and the phosphorus-nitrogen double bond. The resulting transition state, resembling that of the Wittig (net) [2 + 2] intermediate,[35] rearranges to form the desired functionalized POM (Figure 1-16). As is the case of the Wittig reaction, a by-product of the reaction is triphenylphosphine oxide which can be removed.

Substitutions involving isocyanates are suggested to proceed via a similar four-membered transition state (Figure 1-17). However, the reaction by-product in this route (isocyanate protocol) is carbon dioxide which can be allowed to dissipate from the mixture (i.e. minimal workup required). The only disadvantage to this protocol is the generally longer reaction times (Figure 1-10). This has made the isocyanate protocol extremely attractive over that of the phosphineimine protocol; however it should be noted that not all isocyanates nor phosphineimines are able to functionalize the hexamolybdate dianion.

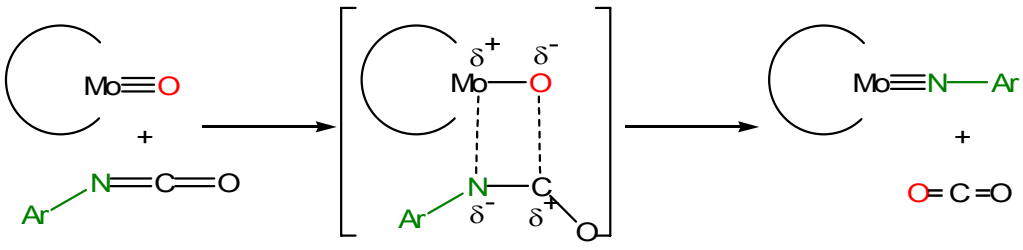

Figure 1-17: Proposed mechanism for the substitution of $[TBA]_2[Mo_6O_{19}]$ using an isocyanate delivery reagent (isocyanate protocol).[35]

Over the last few years, new methods for the functionalization of hexamolybdate have been introduced by Peng[36] and Wei[37]. Both of these approaches utilize an arylamine delivery reagent in the presence of N,N'-dicyclohexylcarbodiimide (DCC) under reflux and inert atmosphere. Peng's protocol utilizes $[TBA]_2[Mo_6O_{19}]$ and DCC as a dehydrating agent/activating reagent (Figure 18). Although the mechanism is not fully understood, it was proposed that DCC serves two purposes: (i) to form an activated intermediate species where a terminal molybdenum-oxygen of hexamolybdate interacts with the arylamine and (ii) as a sacrificial dehydrating reagent. Peng's protocol has reported high yields but as with Maatta's phosphineimine method, a by-product in (N,N'-dicyclohexylurea) requiring separation is formed.

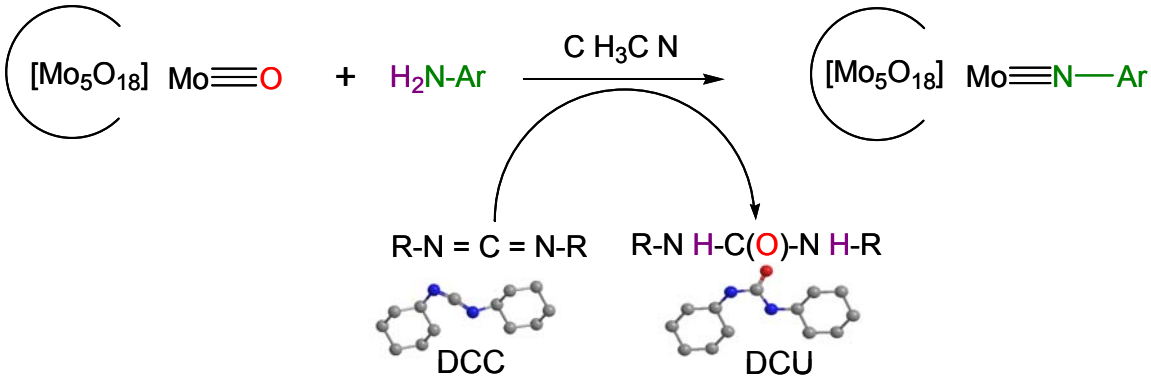

Figure 1-18: Reaction Scheme for the functionalization of $[TBA]_2[Mo_6O_{19}]$ with DCC and an arylamine (Peng's protocol).[36]

Recently Wei,[36,37] in collaboration with the Peng group, introduced a fourth method for hexamolybdate functionalization. As with Peng's method, Wei utilized the arylamine aided by DCC. However the Wei protocol uses the octamolybdate anion $[TBA]_4[Mo_8O_{26}]$) instead of hexamolybdate, and the reaction also requires the addition of the corresponding arylamine hydrochloride salt (Figure 1-19). The hydrochloride salt of the arylamine serves to assist the conversion of the octamolybdate to the hexamolybdate.[38] In this method, the urea by-product is

accompanied by an uncharacterized molybdenum fragment from the conversion of octamolybdate to the hexamolybdate.

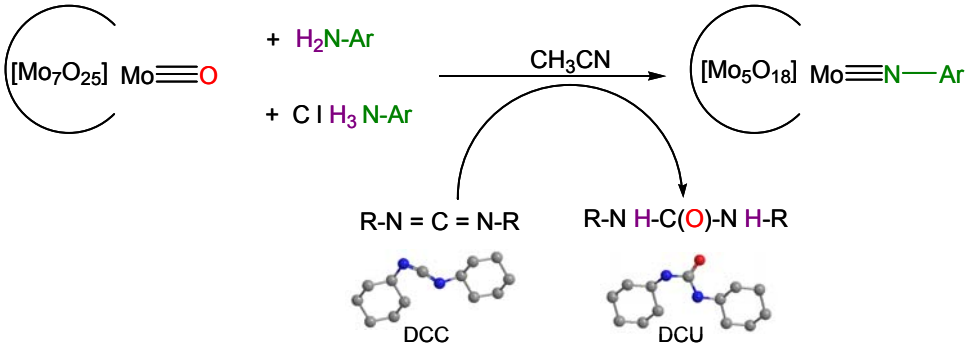

Figure 1-19: Reaction scheme for the production of imido-hexamolybdates from $[TBA]_4[Mo_8O_{26}]$, DCC, an arylamine and its hydrochloride salt (Wie's protocol).[37,38]

Clearly a variety of methods are available to functionalize hexamolybdate with an organoimido species. With these tools at hand, the only limitation should be our imagination. However in practice not all isocyanates nor phosphineimines are capable of forming functionalized hexamolybdates.[39]

Over the years the Maatta group has synthesized various organoimido- functionalized Lindqvist POMs, of the general formula $[(R)N\text{-}Mo_6O_{18}]^{2-}$, ranging from simple ^{n}-butyl-imido[40], diisopropylphenylimido,[40] and cyclohexylimido[40] species (Figure 1-20) to the more elaborate ferrocenylimido[41] hexamolybdate (Figure 1-21b).

This series led to a better understanding of the effects of imido substitution on the hexamolybdate polyanion. The addition of an organoimido functionality to a POM was found to increase the electron density of the cluster, particularly with the Lindqvist type hexamolybdate POM, $[Mo_6O_{19}]^{2-}$. This was supported by the observed upfield shift of the imido substituted molybdenum atom (^{95}Mo NMR)[40] and the upfield shift of the remaining terminal oxygen atoms (^{17}O NMR).[40] The observed lengthening of the bridging oxo-molybdenum bonds at the imido-substituted sites (from single crystal X-ray data) and the observation of more negative reduction potentials (from cyclic voltammetry studies) each support the idea of increased electron density of the cluster with increasing organoimido substitution.[40]

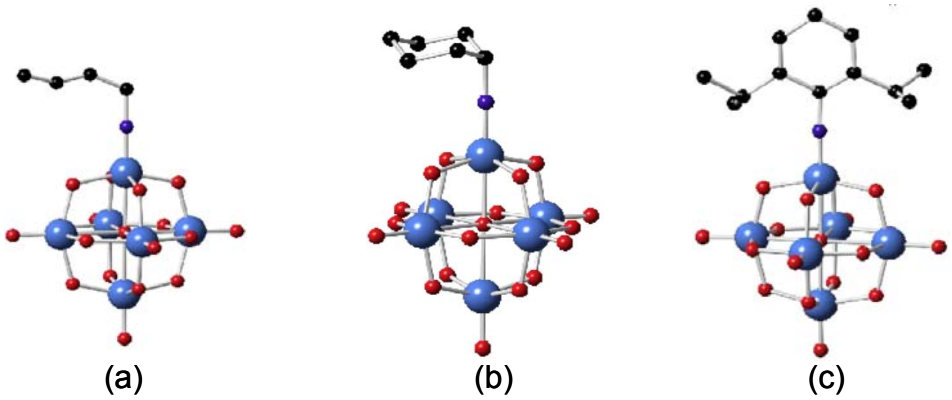

Figure 1-20: Representations of (a) ^{n}-butylimido- (b) cyclohexylimido- and (c) diisopropylphenylimido-hexamolybdate structures.[33]

The Maatta group also reported a polymerizable styrylimido–hexamolybdate (Figure 1-21a) capable of forming copolymers with divinylbenzene and 4-methylstyrene.[42] Recently, the Peng group produced hexamolybdate clusters immobilized onto a polymeric backbone, produced via carbon-carbon (Suzuki) coupling of the aceteylinicimido-hexamolybdates and various arylhalides.[43]

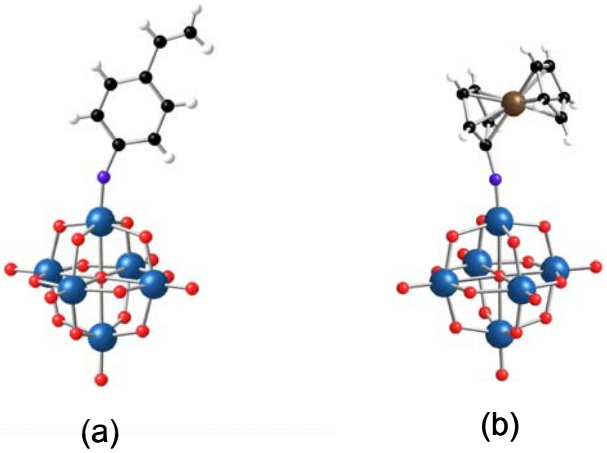

Figure 1-21: Molecular Representation of (a) styrylimido-[26b] and (b) ferrocenylimido-hexamolybdate[41].

1.4 - Scope

This thesis will outline the pursuit of transforming hexamolybdate, $[Mo_6O_{19}]^-$ into a metalloligand capable of metal coordination and electronic communication, with the ultimate goal of forming self-assembled networks. This goal was successfully achieved by the functionalization of hexamolybdate with biarylorganoimido ligands bearing remote σ-donor functionalities with a propensity for metal coordination. Herein will also be described the successful syntheses of several new organoimido delivery reagents (phosphineimimines, isocyanates and arylamines) and attempts to utilize in the formation of new imido-hexamolybdates.

The latter part of this thesis will describe the successful and reproducible synthesis of a new chromium (V) nitrido-Keggin POM, $[Cr(N)PW_{11}O_{39}]^{5-}$ and preliminary attempts to utilize it for N-transfer to an olefin. I will also describe the synthesis and characterization of an osmium-nitrido-Dawson species, $[(OsN)P_2W_{17}O_{61}]^{4-}$.

[1] Pope, M.T., *Heteropoly and Isopoly Oxometalates: Springer, Berlin*, **1983**.
[2] Borras-Almenar, J.J., Coronado, E., Muller, A., Pope, M., *Polyoxometalate Molecular Science: Kluwer, Dordrecht*, **2001**.
[3] Klemperer, W.G. *Inorganic Syntheses* **1990**, 27, 71-74.
[4] Berzelius, J.J. *Pogg. Ann.* **1826**, *61*, 380.
[5] Svanberg, K. Struve, H., *J. Prakt. Chem.* **1848**, *44*, 257-291.
[6] Keggin, J. *Nature*, **1933**, *131*, 908.
[7] (a) Baker, L., Glick, D., *Chem. Rev.* **1998**, *98*, 3.
(b) Bridgeman A.J., Cavigliasso, G., *Faraday Dicsuss.* **2003**, *124*, 239.
[8] Gates, B.C. KAtzer, JR., Schuit, G.C.A, *Chemistry of Catalytic Processes: McGraw-Hill* **1979**, 311.
[9] Muller, A., Peters, F., *Chem. Rev.* **1998**, *98*, 239.
[10] Radkor and Beer, *Polyhedron* **1995**, *14 (15-16),* 2139-2149.
[11] (a) Baker, L.C., Figgis, J.S., *J. Am. Chem. Soc.* **1970**, *92*, 3794.
(b) Baker, L.C., Pope, M.T., Shibata, M., Fang, J.H., Koh, L.L., *J. Am. Chem. Soc.* **1966**, *88*, 2329.
(c) Bushey, P.A., M.S. Thesis, Georgetown University, 1974.
[12] Coronado, E., Gomez-Garcia, C.J., *Chem. Rev.* **1998**, *98*, 273-296.
[13] (a) Tourne, C.M., Tourne, G.F., Zonnevijlle, F., *J. Chem. Soc. Dalton Trans.* **1991**, 143.
(b) Hill, C.L., Prosser-McCartha, C.M., *Coord. Chem. Rev.* **1995**, *143*, 407.
(c) Neumann, R., *Prog. Inorg. Chem.* **1998**, *47*, 317.
[14] Jorris, T.L, Kozik, M., Baker, L.C.W., *Inorg. Chem.* **1990**, *29*, 4584.
[15] Klemperer, W.G., Schwartz, C., *Inorg. Chem.* **1985**, *24*, 4459.
[16] Cadot, E., Bereau, V., Marg, B., Secheresse, F., *Inorg. Chim. Acta.* **1995** *239*, 39.
[17] Knoth, W.h., Harlow, R.L, *J. Am. Chem. Soc.* **1981**, *103*, 4265.
[18] Day, V.W., Klempere, W.G., Schwartz, C., *J. Am. Chem. Soc.* **1987**, *109*, 6030.
[19] Klegg, W., Elsegood, M.R.J., Errington, R.J., Havelock, J., *J. Chem. Soc., Dalton Trans.* **1996**, 681.
[20] (a) Khan, I., Zubieta, J., *Prog. Inorg. Chem.* **1995**, *43*, 1.
(b) Chen, Q., Zubieta J., *Inorg. Chem.* **1990**, *29*, 1456.
[21] Hasenknopf, B., Delmont, R., Herson, P., Gouzerh, P., *Eur. J. Inorg. Chem.* **2002**, 1081.
[22] Knoth, W.H., *J. Am. Chem. Soc.* **1979**, *101*, 2211.
[23] Zonnevijlle, F, Pope, M.T., *J. Am. Chem. Soc.* **1979**, *101*, 2731.
[24] Krebs, B, (in M.T. Pope, A. Muller) *Polyoxometalates: from Platonic Solids to Anti-Retroviral Activity, Kluwer Academic Publishers*, **1994**.
[25] Pope, M., Muller, A., *Angew. Chem. Int. Ed. Engl.* **1991**, *30*, 34.
[26] (a) Moore, A., *PhD Thesis, Kansas State University* **1998**.
(b) Kwen, H., *PhD Thesis, Kansas State University* **2000**.
[27] (a) Sharpless, K.B., Patrick, D.W., Truesdale, L.K., Biller, S.A., *J. Am. Chem. Soc.* **1975**, *97*, 2305.

(b) Chong, A.O., Oshima, K., Sharpless, K.B., *J. Am. Chem. Soc.* **1977**, *99*, 3420.

[28] (a) Graselli, R.K., Burrington, J.D., *Ind. Eng. Chem. Prod. Res. Develop.* **1984**, *23*, 393.
(b) Burrington, J.D., Kartisek. C.T., Graselli, R.K., *J. Catal.* **1983**, *81*, 489.

[29] Nugent, W.A., Mayer, J.M., *Metal-Ligand Multiple Bonds, Wiley: New York* **1988**,.

[30] (a) Dablemont, C., Hamaker, C., Thouvenot, R., Sojka, Z., Che, M., Maatta, E.A., Proust, A., *Chem. Eur. J.* **2006**, *12*, 9150.
(b) Kwen, H., Tomlinson, S., Maatta, E.A., Dablemont, C., Thouvenot, R., Proust, A., Gouzerh, P., *Chem. Comm.*, **2002**, 2970.

[31] Kang, H., Zubieta, J., *Chem. Comm.* **1988**, 1192.

[32] Abrams, M., Costello, C., Shaikh, S., Zubieta, J., *Inorg. Chim. Acta.* **1991**, *180*, 9.

[33] Hill, P.L., Yap, G.P.A., Rheingold, A.L., Maatta, E.A., *J. Chem. Soc. Chem. Comm.* **1995**, 732.

[34] Forster, G.D., Liable-Sands, L., Rheingold, A.L., Maatta E.A., unpublished results.

[35] Stark, J., Young, V., Maatta, E.A., *Angew. Chem. Int. Ed. Engl.* **1995**, *34*, 2547.

[36] Wei, Y., Xu, B., Barnes, C, Peng, Z., *J. Am. Chem. Soc.* **2001**, *123*, 4083.

[37] Wu, P., Qiang, Li, Ning, G., Wei, Y., Wang, Y., Wang, P., Guo, H., *Eur. J. Inorg. Chem.* **2004**, 2819.

[38] Hao, J., Ruhlmann, L., Zhu, Y., Li, Q., Wei, Y., *Inorg. Chem.* **2007**, *46*, 4960.

[39] Karcher, J., *PhD Thesis, Kansas State University*, **2007**.

[40] Strong, J., Yap, G., Ostrander, R., Liable-Sands, Rheingold, A., Thouvenot, R., Gouzerh, P., Maatta, E.A., *J. Am. Chem. Soc.* **2000**, *122*, 639.

[41] Stark, J., Young, V., Maatta, E.A., *Angew. Chem. Int. Ed. Engl.* **1995**, *34*, 2547.

[42] Moore, A., Kwen, H., Beatty, A., Maatta, E.A, *Chem. Comm.* **2000**, 1793.

[43] Xu, B, Lu, M., Kang, J., Wang, D., Brown, J, Peng, Z., *Chem. Mater.* **2005**, *17*, 2841.

CHAPTER 2 - Can organoimido functionalized hexamolybdates act as metalloligands?

2.1 - Introduction – Functionalized Hexamolybdates

Over the last three decades, an increasing number of hexametalate[1a] derivatives with the general formula $[M_6O_{19}(L)]^{2-}$ (M = Mo, W, V) have been reported, where the surface is appended with various organo ligands (L). These organic/inorganic hybrid materials have either been found to exhibit synergistic[1b,2] or an additive combination of properties (e.g. redox, photochemical, ferromagnetic).[3] The focus of our group centers around developing functionalized hexamolybdate dianions $[Mo_6O_{18}(L)]^{2-}$ capable of metal coordination with a long term goal of forming supramolecular[1a] architectures. A number of functionalized hexamolybdate dianions[3-7] have been successfully synthesized (Chapter 1), in which an isoelectronic exogenous ligand, L, (i.e. organoimido) has replaced one or more terminal oxo ligands on the surface of the cluster.[4] The following discussion will highlight the path that led to the successful coordination of an organoimido functionalized hexamolybdate to a transition metal complex via the remote functionality (σ-donor) of the exogenous ligand, effectively transforming the derivatized hexamolybdate dianion into a metalloligand.

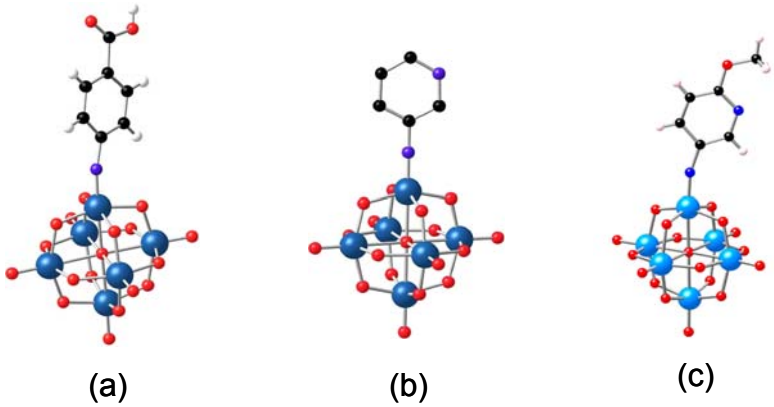

Figure 2-1: Molecular structures of (a) carboxyphenylimido-, (b) pyridylimido- and (c) methoxypyridylimido-hexamolybdates.[15]

With the synthetic routes (Chapter 1) developed and established by Maatta[5,6,7,8,9] Peng[10,16] and more recently Wei,[11,12,13,14] a number of hexamolybdate compounds modified with organoimido ligand have been reported[4] and now form a significant sub- class of POM hybrid materials. Preliminary attempts at metal coordination within the Maatta group produced the carboxyphenylimido-, 3-pyridylimido- and methoxypyridylimido-hexamolybdates as synthesized by Moore.[15] (Figure 2-1) Each remote functionality was chosen by Moore[15] for their propensity for metal coordination but none of were found capable of the desired metal coordination when attached to the hexamolybdate.

There are only a few examples of organoimido functionalized hexamolybdates reported to demonstrate metal coordination via a covalently bound remote functionality.[8,16] One such example is the (previously mentioned) ferrocenylimido-hexamolybdate (Fe^{2+} coordinated via cyclopentadienylimido ligand) by Maatta.[8] Another was the terpyridyl-phenylimido-hexamolybdate reported by Peng *et al.*[16] (Figure 2-2). This terpyimido hexamolybdate was demonstrated to coordinate Fe^{2+}.[16(b)]

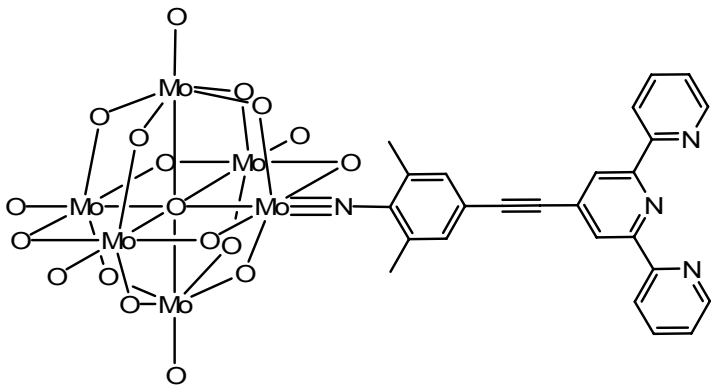

Figure 2-2: Structural representation of terpyimido-hexamolybdate.[16]

Hexamolybdates can undergo poly-substitution. As demonstrated by Strong,[6] all six terminal oxo ligands can be replaced by isoelectronic organoimido ligands (Figure 2-3). It was observed (by cyclic voltammetry studies) that the electron density of the cluster increases with increasing organoimido incorporation.[5] This effect was credited to the imido ligand's enhanced ability as an electron donor relative to terminal oxo ligands.

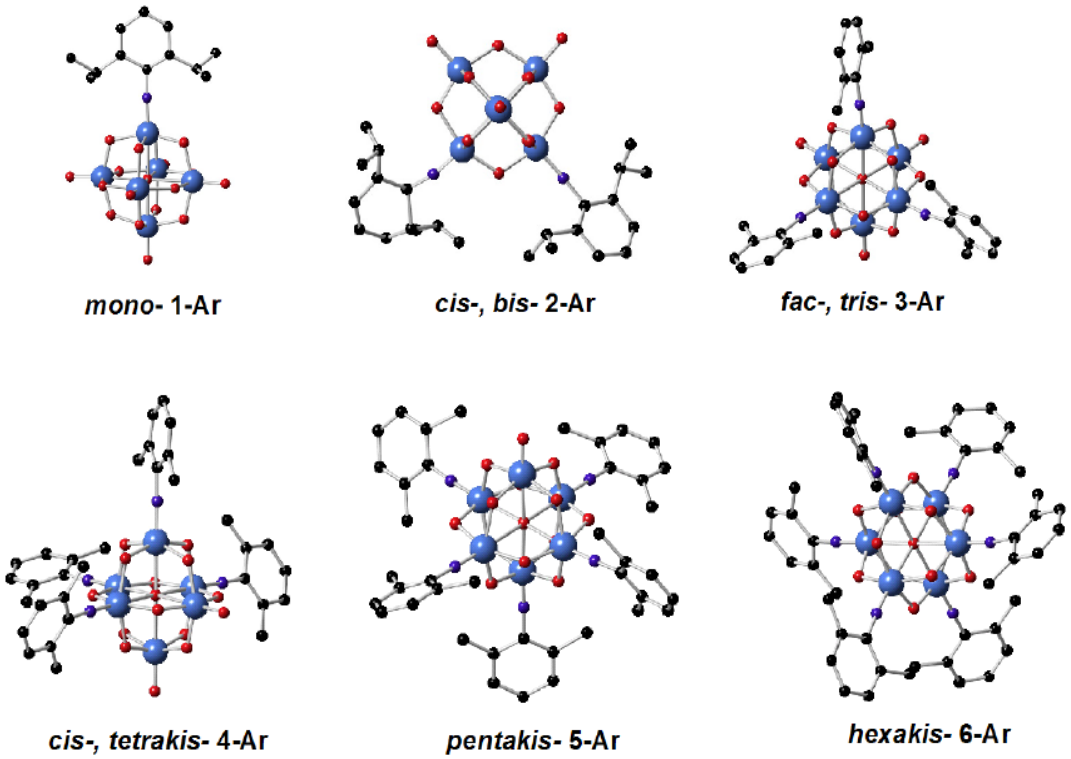

Figure 2-3: Molecular structures of mono-, bis-, tris-, tetrakis-, pentakis-, and hexakis-(2,6-diisopropylphenylimido)hexamolybdate.[5]

The overall octahedral nature of hexamolybdate wherein each terminal oxo ligand is related to another by either 90° or 180° makes it well suited for constructing discrete supramolecular structures such as those shown in Figure 2-4. In theory, metal coordination can be used as a supramolecular "glue" and the multiply substituted functionalized hexamolybdates used as "building blocks" for constructing highly ordered structures that may exhibit unique physical, chemical and electronic properties.

With this in mind, one can imagine supramolecular structures bearing one or more of these organoimido ligands bound to a single hexamolybdate cluster coordinated to a common metal center (Figure 2-4). Metal coordination of two mono-functionalized (Figure 2-3) hexamolybdates onto a transition metal such as silver should produce a linear or "dumb-bell" structure (Figure 2-4). If multiply-appended hexamolybdate complexes were accessible, the formation of more elaborate supramolecular structures would be possible (Figure 2-4). Development of the synthetic methods needed to provide this type of substitution onto hexamolybdate will be crucial in producing these architectures. Strong demonstrated astonishing

control of substitution at hexamolybdate, through variations in reactions conditions (e.g. reaction times, temperature, stoichiotmetry) (Figure 2-3).[40] Unfortunately this degree of structural organization by an organoimido appended hexamolybdate cluster is yet to be reported for imido ligands capable of binding metal centers and thus the ability to use hexamolybdates as "building blocks" is still in its infancy.

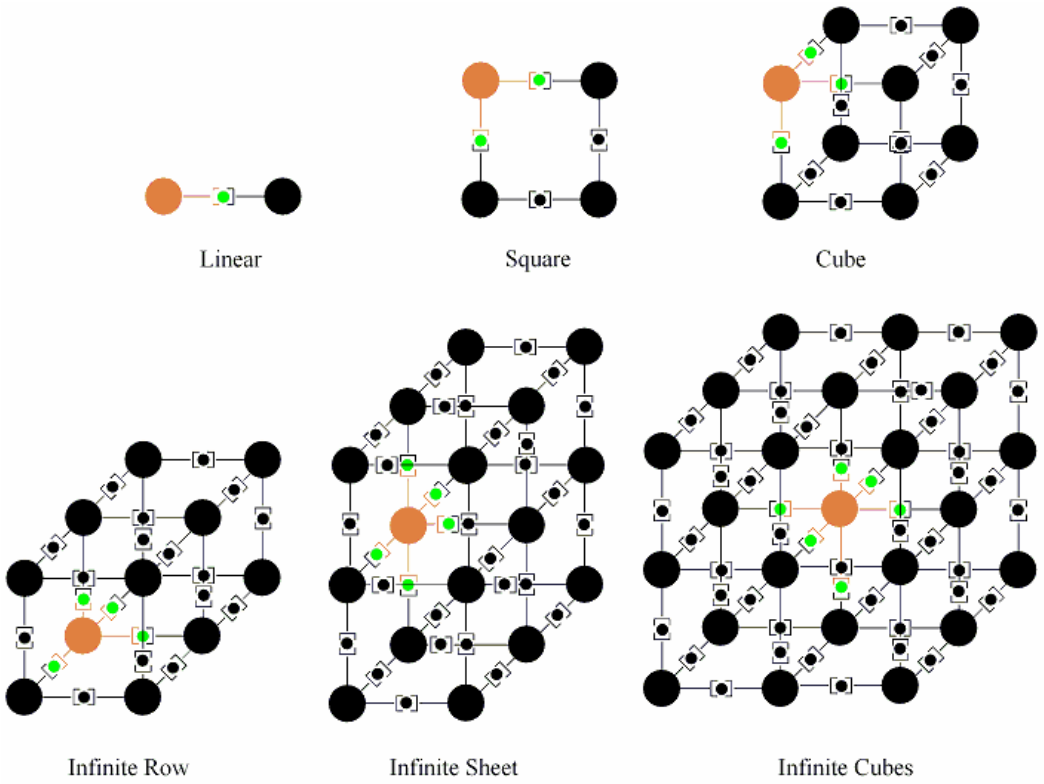

Figure 2-4: Supramolecular structures possible with increasing organoimido substitution. (Orange = organoimido substituted hexamolybdate; Green = coordinated metal atom)[17]

The initial step in synthesizing an organoimido hexamolybdate complex is the preparation of the hexamolybdate dianion, $[Mo_6O_{19}]^{2-}$. The hexamolybdate cluster is conveniently prepared from modified literature methods,[18,19,20] as its tetrabutylammonium ($[^{n}-(CH_3)(CH_2)_3)_4N^+]$; $[TBA]^+$) salt which is readily soluble in organic solvents such as acetone, acetonitrile, dichloromethane and pyridine. After reaction with the chosen imido delivery reagent (Chapter 1), successful functionalization can be detected via infra-red spectroscopy (FT-IR). It has been observed that mono-functionalized hexamolybdate complexes exhibit a "shoulder-/strong band" feature in the $[Mo\text{-}O_{terminal}]$ stretching region of the IR spectrum at ca. 960-980 cm^{-}

[1] (shoulder) and 950 cm^{-1} (strong), respectively. The observation of this shoulder (in conjunction with evidence from ^1H NMR spectra) is a reliable indicator of successful functionalization.[15,21]

2.1.1 - Hurdles to Hexamolybdate Coordination.

The inability of various functionalized hexamolybdates to bind transition metals (via a remote functionality) has been reported elsewhere[15,21] and is attributed to the electron withdrawing effects of the attached cluster fragment, $[Mo_6O_{18}]^{2-}$. The lack of coordination demonstrates that the cluster (Figure 2-5; Part A) exerts a deactivating effect on the remote functionality (Part C) through the organoimido ligand (Part B). In order to rationalize this effect, it is necessary to recall that each cluster contains six (d^0) molybdenum ions, each in their highest oxidation state (+6) rendering the cluster as an efficient electron sink (i.e. an electron 'sponge').

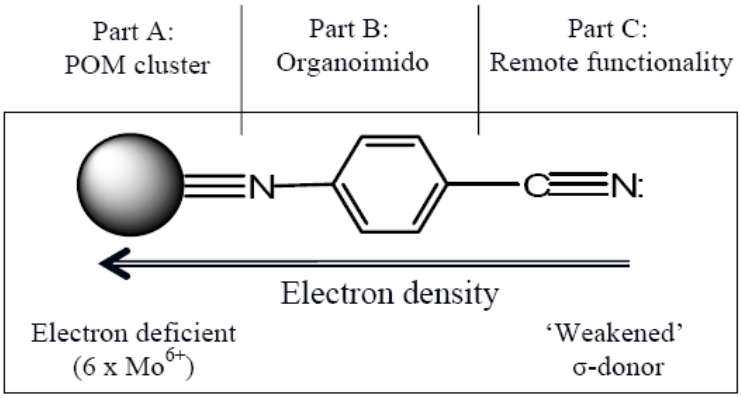

Figure 2-5: The segments of an organoimido functionalized hexamolybdate complex illustrating electron withdrawal from the remote functionality (σ-donor).[15] (Black sphere = $TBA_2[Mo_6O_{18}]$)

Several attempts were undertaken within our group to overcome the "electron- sponge" behavior of hexamolybdate.[15,21] The first step was to increase electron density at the organoimido substitutent. Moore[15] prepared *p*-methoxy-*m*-pyridylimido-hexamolybdate (Figure 2-6). The addition of the methoxy group (an electron donor) served two purposes: (i) to increase electron density at the imido ligand and, (ii) offering the potential of a bidentate coordination mode for a suitable transition metal (Figure 2-6).[15]

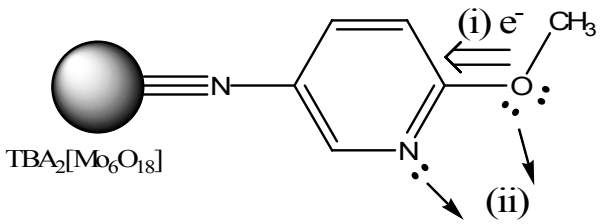

Figure 2-6: Representation of two possible ways to improve σ-donor ability by (i) electron donation from the –methoxy group and (ii) bidentate coordination.[15]

Unfortunately, the introduction of the methoxy group was insufficient to overcome the electron withdrawing influence of hexamolybdate and metal coordination was never observed. Also, it was observed in its single crystal X-ray (solid state) structure, that the non-bonding electrons of the methoxy oxygen were rotated away from those of the pyridyl nitrogen, although this does not preclude adoption of the bidendate motif in solution.

With this in mind, a series of benzonitrile and pyridyl-biaryl organoimido delivery reagents containing multiple electron donor groups (dimethyl and tetramethyl cyanophenyl species) were envisioned and synthesized. Each was designed with the intent that the methyl substituents would provide increased electron density and in turn greater σ-donor capabilities for the cyano function. In the following sections, I will describe several successful (and attempted) syntheses of new organoimido delivery reagents, including aryl amines ($Ar\text{-}NH_2$), phosphinimines ($R\text{-}N{=}PPh_3$) and isocyanates (R-NCO). I will also describe the synthesis of other biphenyl- and pyrimidylphenyl reagents and attempts to introduce these as organoimido ligands into the hexamolybdate.

2.2 - Results and Discussion

2.2.1 - Synthesis of Dimethyl and tetramethylphenylimido delivery reagents

Initially, attention was focused on molecules such as **1** and **2** (Figure 2-7) as well as the tetramethyl substituted analogue **3**, where Y can be $–NH_2$ or $–CO_2H$ (which could later be converted to their $–N=PPh_3$ and -NCO organoimido delivery reagents, respectively). The proximity of the methyl groups to the nitrile (-CN) function in **2** made it a more attractive initial target than **1**.

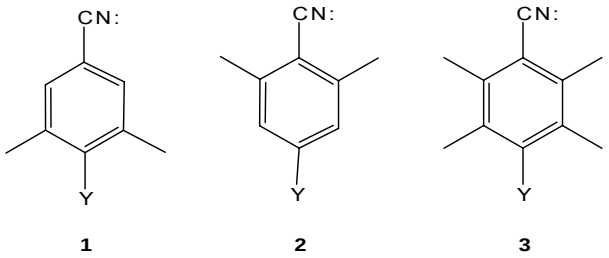

Figure 2-7: Series of methyl substituted cyanobenzene compounds as precursors for the syntheses of organoimido delivery reagents. (Y = $-CO_2H$, $-NH_2$)

The synthesis of target molecule **2** began from commercially available 3,5-dimethylaniline, **4** (Figure 2-8). The amino group of **4** was converted into a carboxamide in order to favor nucleophilic (halogenation) substitution at the *para* position. Formation of the carboxyamides and subsequent halogenations proceeded with ease. However the syntheses of **6a** proved unsuccessful, thus **5b** (^{t}butyl-carboxamide) was synthesized. The cyanation of the **7** was achieved by a procedure adapted from the literature using copper(I) cyanide under harsh (130^{o}C) reaction conditions (Figure 2-8).[24]

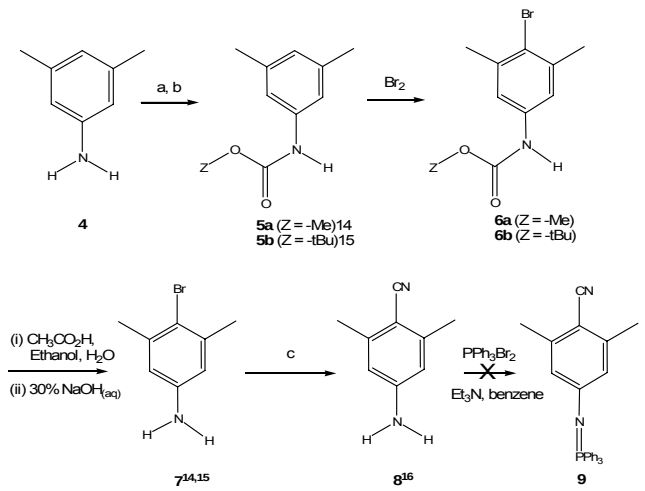

Figure 2-8: Schematic for attempted synthesis of **9**. (a^{22} = thionyl chloride, CH_2Cl_2, 0^oC; b^{23} = NaOH, di-tbutyldicarbonate, 1,4-dioxane, 0^oC; c^{24} = CuCN, 2-pyrrollidinone, 4 days, reflux)

After numerous attempts, the desired phosphinimine delivery reagent **9** proved inaccessible. Hindered by the inconsistent synthesis, purification problems and extremely low yields of **8,** focus was shifted to the tetramethyl analogues (Figure 2-9). Retrosynthetic analysis of the desired target molecule **10**, identified a cheap and readily available starting reagent in the form of 1,2,4,5-tetramethylbenzene, **15**.

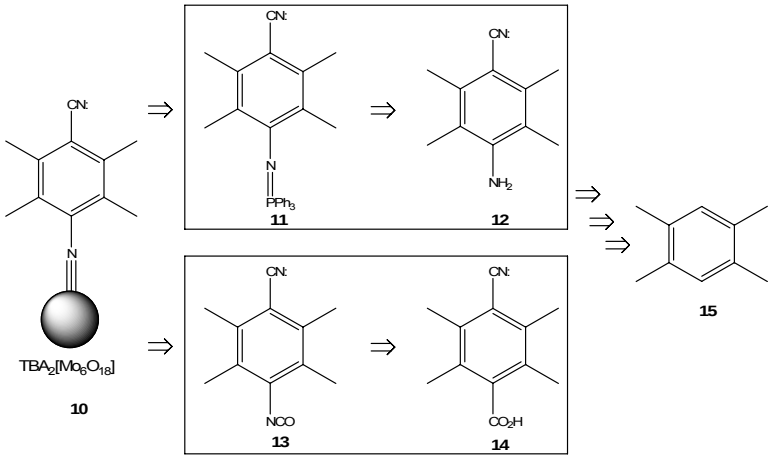

Figure 2-9: Retrosynthetic analysis of target molecule, **10** (4-cyano-2,3,5,6-tetramethyl-phenylimido hexamolybdate).

The new tetramethyl imido delivery reagents of interest became **11** and **13** which maybe accessed via the correspoinding amine **12** and carboxylic acid **14**. The tetramethylbenzene compounds **16** and **17** were synthesized from 15 through a series of substitutions according to modified literature methods[25] (Figure 2-10).

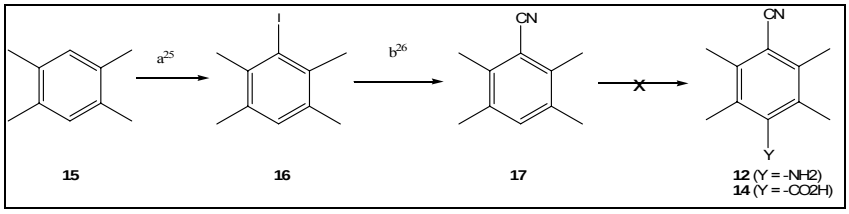

Figure 2-10: Schematic for the synthesis of **12** and **14** from 1,2,4,5-tetramethylbenzene. (a^{25} = I_2, H_5IO_6, H_2SO_4, H_2O, CH_3COOH; b^{26} = CuCN, $(Me_2N)_3PO$, 100°C)

Cyanation of **16** imparted an unfortunate deactivating effect on the *para*-position rendering it inert to substitution. This made the synthesis of **12** and **14** via this method impossible. An alternative route was undertaken using di-halogenated tetramethylbenzenes and various substitution reactions outlined in the literature (Figure 2-11).[25,27,28,29]

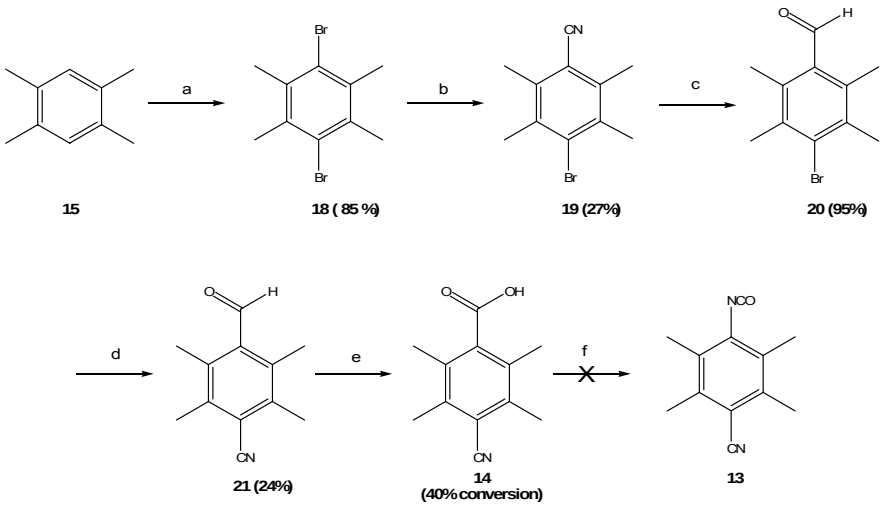

Figure 2-11: Schematic for the synthesis of **17** and isocyanate **13**. (a^{25} = I_2, Br_2, CH_2Cl_2; b^{28} = CuCN, DMF, 8 hours, reflux; c^{28} = DIBAL-H, toluene, CH_2Cl_2; d^{28} = CuCN, DMF, 8 hours, reflux; e^{29} = pyridinium chlorochromate (2 mol%), H_5IO_6, CH_3CN; f^{31} = diphenyl phosphoryl azide, 1,8-bis(dimethylamino)-naphthalene, THF, reflux, 14 hours)

The low yield of the desired mono-cyano product **19** was attributed to a competing side reaction that resulted in formation of di-cyano-tetramethylbenzene (di-CTB) as the major product.[27] This was evident from the '95%' conversion (based on **15**) quoted in literature,[28] with only 30% of this being the mono-substituted product, **19**. Despite various attempts at altering the reaction conditions to favor mono-substitution (e.g. increased dilution and lowered reaction temperatures) the major product was always di-CTB. Further attempts were made to selectively convert one of the cyano groups of di-CTB to the aldehyde[28] or the amine[30] with no success.

The oxidation of **21** yielded the carboxyphenyl, **14**. However **14** was never isolated as the pure compound upon acid-base workup and was prone to decomposition during column chromatography. Nevertheless, conversion to the isocyanate imido delivery reagent, **13** was attempted via a modified literature method[31] using diphenylphosphoryl azide (DPPA) and 1,8-bis(dimethylamino)-naphthalene (Proton Sponge). Unfortunately no evidence of **13** was observed by either FT-IR or MALDI-ToF mass spectra.

Functionalization of hexamolybdate with the dimethyl- and tetramethyl-cyanophenyl moieties should not be dismissed as impossible. Further studies are needed in order to facilitate the conversion of the carboxylic acid to the isocyanate, as well as improving the overall yield of the cyanation (i.e. average of 24%) (Figure 2-11). Other tetramethylphenyl systems should also be considered, especially those containing σ-donor groups other than cyano (e.g. pyridyl nitrogen), which may yield better results.

2.2.2 - Ligand extension via phenyl spacer groups: a series "extended" isocyanates and phosphinimines as novel imido delivery reagents.

As mentioned previously, the primary cause of 'σ-donor deactivation' is attributed to electron withdrawal by hexamolybdate. However, other factors such as proximity and conjugation between the hexamolybdate cluster and the σ-donor site were considered previously.[21] As a starting point, Kwen[21] proposed the use of ligands containing 'extended spacer groups' such as imines (e.g. **22** and **23**). The increased separation was intended to decrease the electron withdrawing effect of the cluster (Figure 2-12), which in turn should lead to a more basic donor favoring the ability for metal coordination. Unfortunately the imines were found to

be unstable during their conversion to the phosphinimine.[21] This made the Schiff bases **22** and **23** unsuitable imido delivery reagents.

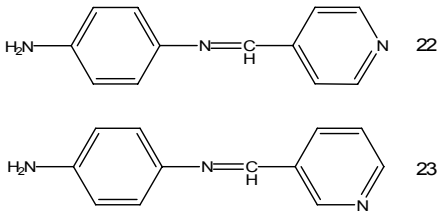

Figure 2-12: Kwen's Schiff Base ligands.[21]

In light of this, the Schiff base motif was discarded in favor of the bi-aryl substituents, **27** – **29** and **38** – **40** (Figure 2-13 and 2-14). Although the biaryl ligands are shorter than the imines they do not suffer from hydrolytic decomposition. The biaryl ligands offer a versatile way of forming the organoimido moiety (through a preformed aryl containing the amino or carboxy functionality) with desired remote functionality (preformed on another aryl (Figure 2-13)).

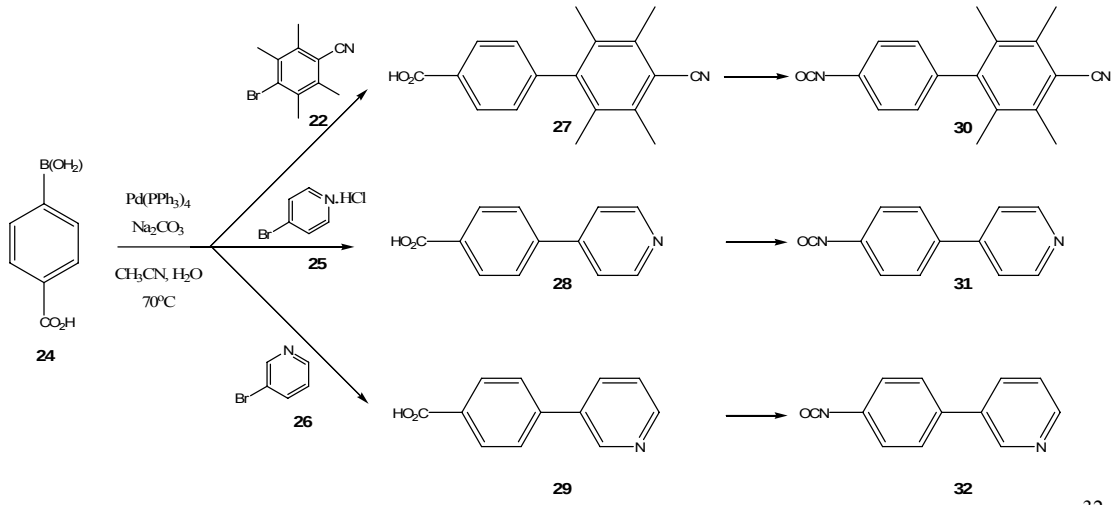

Figure 2-13: Syntheses of *p*-carboxybiaryl ligands (bearing the extended spacer group)[32] and their conversion to the isocyanate[31] organoimido delivery reagent.

Subsequent conversion of these amino or carboxy biaryl ligands to their corresponding phosphinemine or isocyanate, respectively gave access to the necessary organoimido delivery reagent. This was also a good opportunity to recycle the previously synthesized *p*-cyano-tetramethylbromobenzene **19**, as a preformed remote functionality. (Figure 2-13)

The carboxylic acids **27**, **28** and **29** were successfully synthesized using methods adapted from literature.[32] However their conversion to the isocyanates **30**, **31** and **32** (organoimido delivery reagents) were met with varying degrees of success using methods adapted from the literature.[31] However purification of the isocyanates resulted in decomposition during column chromatography, recrystallization was likewise unsuccessful. Despite the lack of pure isocyanate samples, functionalization of hexamolybdate was attempted. Unfortunately the formation of the characteristic shoulder feature in the IR spectrum (*ca.* 960 cm^{-1}) was not observed. Several attempts were made, with varying reaction conditions such as time, temperature, concentration and stoichiometry. The lack of success was not completely surprising since not all isocyanate compounds are capable of functionalizing hexamolybdate.[17]

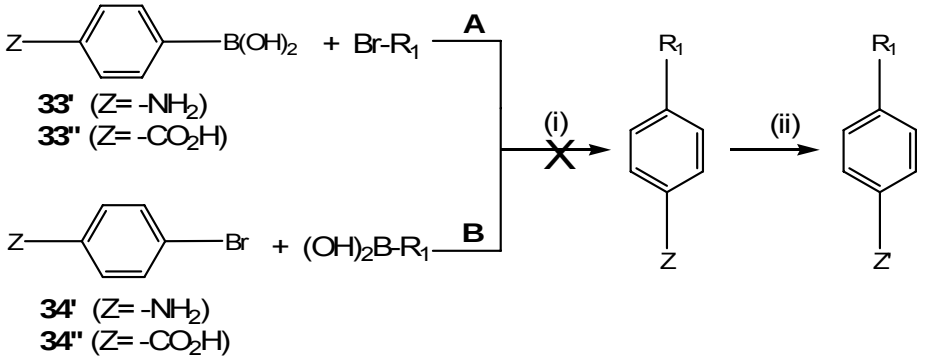

Figure 2-14: Attempted syntheses of p-aminobiaryl ligands (bearing extended spacer) via routes A and B. ((i) = $Pd(PPh_3)_4$, $NaCO_3$, CH_3CN, H_2O; (ii) = PPh_3Br_2, Et_3N, toluene).[21]

With this knowledge, focus quickly shifted to the amino equivalents in order to access the phosphinimines **41**, **42** and **43** (Figure 2-14). However, the high cost of **33'** (*p*-aminophenylboronic acid; $53 per gram; Sigma-Aldrich) and failed attempts at its synthesis prompted a search for an alternative. This was found in **34'** (i.e. Route B of Figure 2-14), obtained via a modified literature method (Figure 2-15).[33a] Conversions of the arylbromides containing the remote functionality to their corresponding boronic acids (**35**, **36** and **37**)[33a] also proved unfruitful. The carboxylic acid **33''** was explored as an optional route to access the

Table 2-1: Table of *p*-aminobiaryls not accessed via Suzuki coupling.

	R_1		Z	R_1		Z'	R_1
35	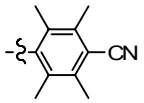	38	$-NH_2$	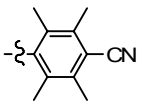	41	$-N=PPh_3$	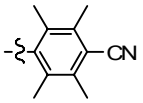
36	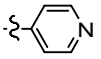	39	$-NH_2$	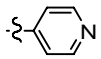	42	$-N=PPh_3$	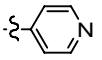
37	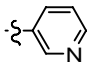	40	$-NH_2$	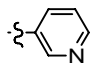	43	$-N=PPh_3$	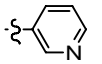

isocyanates. However the extreme cost of **33''** ($450/1g)[33b] made this an unviable starting material and synthesis of the alternative **34''** (via a literature method)[33a] was also found to be unsuccessful.

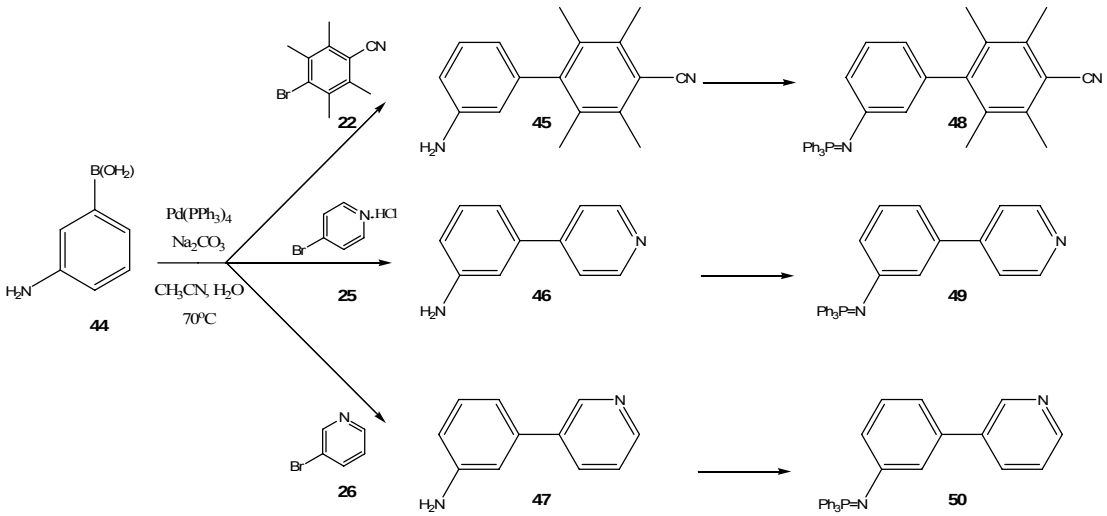

Figure 2-15: Syntheses of m-aminobiaryl ligands **45 - 47** (bearing the extended spacer group)[32] and the phosphinimine imido delivery reagents (**48 - 50**).[21]

An alternative route to the desired amino-biaryl ligands (**38** – **40**) was needed and (Table 2-1) came in the form of the relatively cheap and commercially available[34] *m*-aminophenylboronic acid, **44**. (Figure 2-15) Subsequent Suzuki coupling reactions of **44** with the desired σ-donor (as the corresponding arylbromide) yielded ligands **45**, **46** and **47**.[32] Compound **45** was found to precipitate *in situ* during the reaction.

Table 2-2: Series of *m*-aminobiaryls and their phosphinimine derivatives.

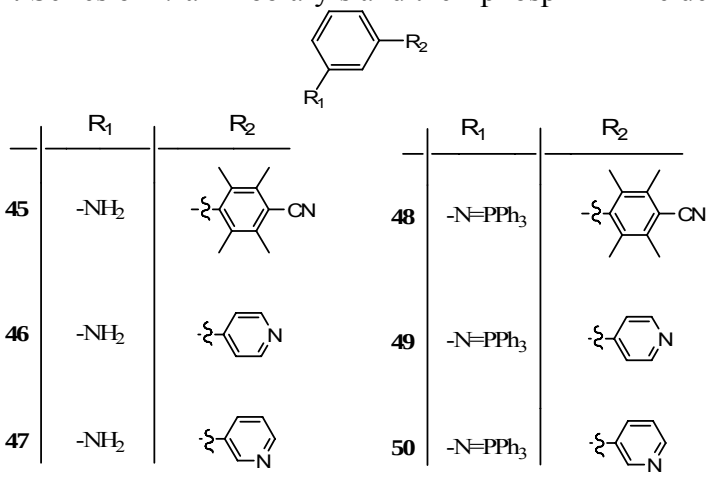

Unfortunately **45** proved insoluble in solvents typically used for conversion to the phosphinimine (i.e. benzene and toluene) or for hexamolybdate functionalization (i.e. acetonitrile or pyridine) (Table 2-2). The synthesis of **48** was attempted in benzene and held at reflux temperatures. After 48 hours, no significant amounts of the desired phosphinimine could be detected by ^{31}P NMR. However, a fragment corresponding to [**48** + **^{1}H**]$^{+}$ at 511.56 amu was observed by ESI-MS (ElectroSpray Ionization-Mass Spectrometry; M/Z calculated = 510.62 amu). Although this suggested formation of some **48**, the compound was not successfully isolated for further reaction with hexamolybdate.

Initially, syntheses of phosphinimines **49** and **50** were thought to have been successful. The ^{1}H NMR spectra showed the (AA'BB') pattern typical of triphenylphosphine along with the absence of the amino protons. It should be noted that the chemical shifts and multiplicities of the desired phosphinimines are virtually indistinguishable from the triphenylphosphine oxide (PPh_3=O) formed in the presence of water. This rendered characterization by ^{1}H NMR unreliable. The lack of new chemical shifts in the ^{31}P NMR spectrum of **49** was a good indication of the failed synthesis. In contrast, the ^{31}P NMR spectrum of **50** showed a new weak and broad signal at 4.56 ppm (relative to H_3PO_4). This is in the range of literature values for aryl phosphinimines.[35] Interestingly, masses corresponding to [M/Z + ^{1}H] for **49** and **50** were observed by ESI-MS at 431.403 and 431.439 amu, respectively (calculated M/Z = 430.49 amu). The ESI-MS spectra of **49** and **50** strongly suggested the presence of the phosphinimines albeit in low quantities.

Functionalization of hexamolybdate was nevertheless attempted with crude samples of both **49** and **50** in pyridine under argon. Unfortunately, after 8 days at reflux temperatures the IR spectrum shoulder at ~960 cm^{-1} (characteristic of functionalization) was not observed. As with the isocyanates, these results were not completely surprising, since it is known that not all phosphinimines are capable of hexamolybdate functionalization.[17]

2.2.3 - Successful functionalization of hexamolybdate with 3-(pyridin-3-yl)-phenylamine.

In light of the unfruitful grafting of the organoimido ligands onto hexamolybdate via the R-NCO and R-$NPPh_3$ reagents, a more recent method introduced by Wei *et al* was explored.[11-14] Wei utilized the amine along with its hydrochloride salt as the organoimido delivery reagents. Unlike the Maatta and Peng protocols, this method does not employ hexamolybdate but rather

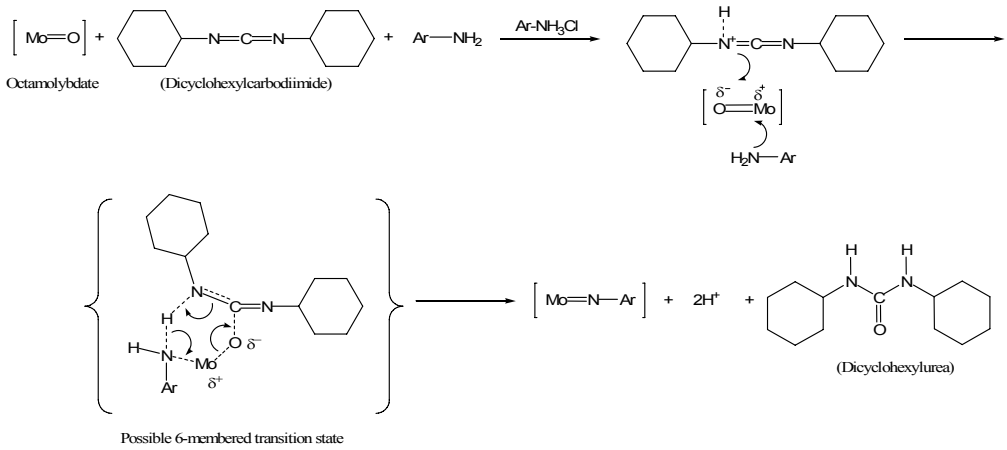

Figure 2-16: Postulated mechanism reported by Wie[36] for hexamolybdate functionalization via the amine, hydrochloride amine, DCC and octamolybdate.

a related POM, octamolybdate $[TBA]_4[Mo_8O_{26}]$. A structural rearrangement must occur in order to yield the final organoimido-appended hexamolybdate $TBA_2[Mo_6O_{18}(L)]$. The mechanism of this functionalization protocol has not been studied in detail but a proposed mechanism was discussed by Wei.[36] It suggested that the dicyclohexylcarbodiimide (DCC) serves as a dehydrating agent with an activating effect on a terminal Mo-O bond of the cluster. (Figure2-16)

The function of DCC bears some resemblance to its use in biochemistry as a coupling reagent for the formation of amide bonds.[37] Decreased reaction times, typically less than 24 hours, are an advantage of Wei's protocol over previous methods (Figure 2-17). Functionalization of hexamolybdate with **45** was not attempted, due to the lack solubility in acetonitrile but reactions were conducted using **46** and **47**.

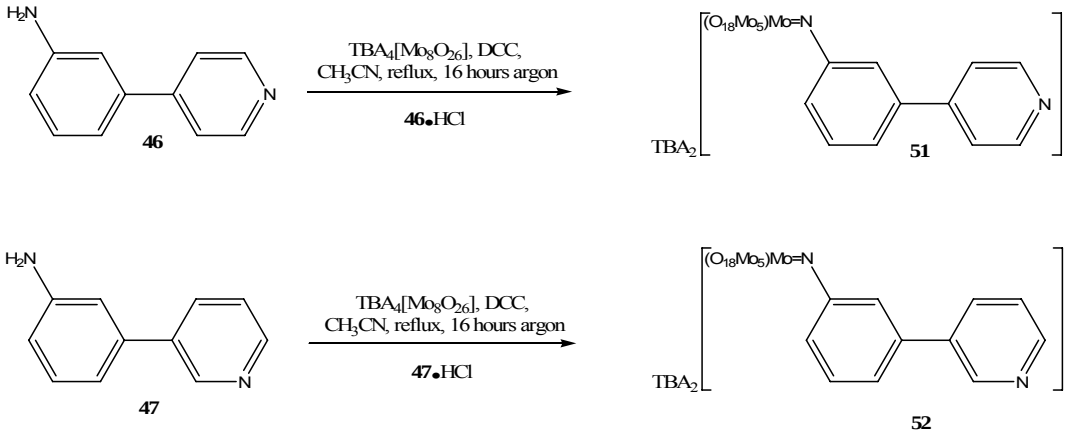

Figure 2-17: Functionalization of hexamolybdate adapted from Wei's method.[14] (DCC = dicyclohexylcarbodiimide)

As outlined in Wei's method,[14] an equivalent of tetrabutylammonium octamolybdate was dissolved in anhydrous acetonitrile, along with three equivalents of DCC, an equivalent of the arylamine and an equivalent of the corresponding amine hydrochloride salt. The resulting orange suspension was stirred at reflux temperature under argon (Figure 2-17). After 16 hours, an off-white precipitate was collected from the cooled reaction mixture (urea by-product) and the red filtrate was concentrated under reduced pressure. Both crude reaction mixtures from **51** and **52** were found to contain the characteristic shoulder at 960 cm^{-1} in the IR spectra. This indicated the successful functionalization of hexamolybdate with the biarylamine ligands. Red-orange crystals of **51** were obtained after triple recrystallization by slow vapor diffusion of diethyl-ether into a concentrated acetonitrile solution. The red-orange crystals were found to contain the dicyclohexylurea by-product as excess [TBA^+] as determined by ^1H NMR spectroscopy. Crystals of **51** suitable for single x-ray crystallography have yet to be obtained.

Red-orange crystals of the hybrid POM **52** were successfully grown from a concentrated acetonitrile solution by slow vapor diffusion of diethylether over 20 days in 31% yield. It was

characterized fully by ^{1}H NMR, electronic spectroscopy, cyclic voltammetry and elemental analysis. The molecular structure of **52** was determined by single crystal x-ray crystallography (Figure 2-18).

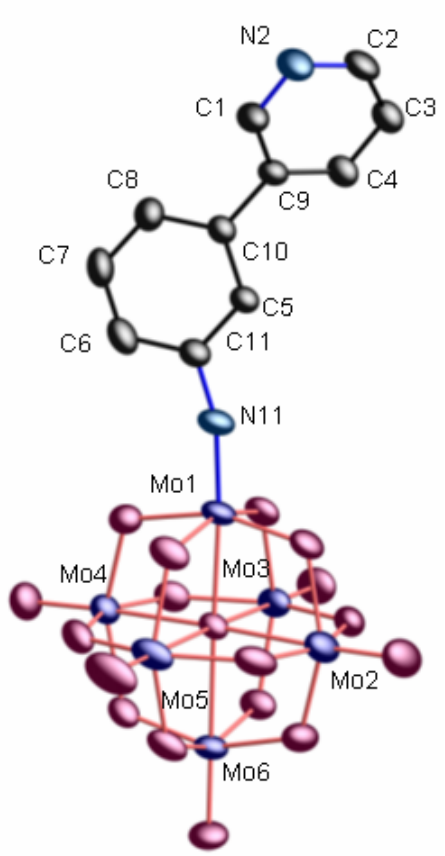

Figure 2-18: Thermal ellipsoid plot (50% probability) for **52**.
(Hydrogens and TBA^{+} omitted for clarity; oxygen = red ellipsoids)

Table 2-3: Molybdenum-nitrogen bond distance and angles for complexes $TBA_2[Mo_5O_{18}(Mo{\equiv}N\text{-}\mathbf{L})]$

L	Mo-N length (Å)	Mo-N-C angle (°)
^{n}-butyl-[42]	1.720(16)	175.4(17)
Cyclohexyl-[42]	1.719(10)	177.7(7)
2,6-(^{i}Pr)$_2$C$_6$H$_3$-[42]	1.739(15)	176.3(15)
4-cyanophenyl-[21]	1.727(7)	164.0(7)
4-iodophenyl-[17]	1.737(5)	156.4(4)
2,6-(CH$_3$)$_2$-4-Br-C$_6$H$_2$-[13]	1.731(4)	176.3(4)
3-(pyridin-3-yl)phenyl- (**52**)	1.746(3)	164.3(3)

As with other reported mono-organoimido hexamolybdates structures,[5-6,8-15] the organoimido moiety of **52** was observed to occupy a terminal position with an Mo1 - N11 distance of 1.746 Å and an (Mo1 - N11 - C11) angle of 164° (Table 2-3 and Figure 2-20). The Mo1 - N11 bond in **52** is slightly longer than other examples reported in literature(Table 2-3)[5-6,8-15] This may indicate weaker Mo≡N bond character as a possible consequence of decreased conjugation between the cluster and the biarylimido ligand.

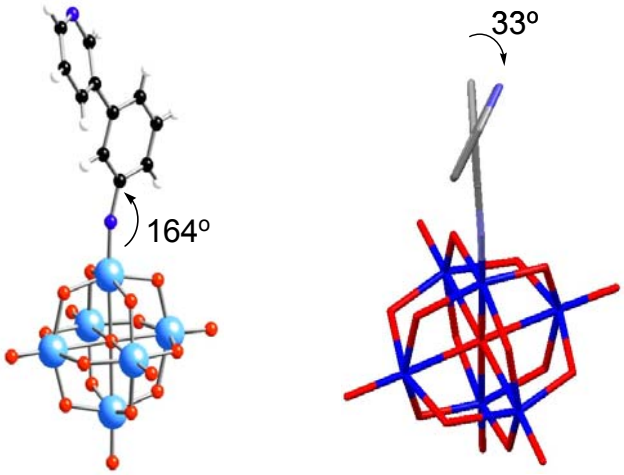

Figure 2-19: Molecular representations of **52**: (a) Ball and stick and (b) Wire model depicting the 33° torsion angle between the aryl rings. (Blue = Mo, Red = O; Black/Grey = C; White = H)

A noticeable feature of **52** was the deviation from linearity of the imido linkage (Mo1 - N11 - C11) by 16° (Figure 2-19). This is not unusual and is consistent with other structures of hexamolybdates appended with monoaryl organoimido ligands.[5-6,8-15] Also in the solid state, the pyridyl nitrogen (N2) is directed away from the cluster (Figure 2-19 and 2-20)

A weak interaction between the pyridyl nitrogen N2 and an H-C unit of a methylene carbon of a neighboring $[TBA]^+$ cation was noted with a distance of 3.325 Å (N21-C21-2). In the solid state, the planes of the biaryl rings were observed to be twisted by 33° relative to each other (Figure 2-19b). Furthermore, weak interactions between hydrogen atoms on C25 and C26 (of the biaryl) and bridging oxygens O12 and O23 of a neighboring cluster was inferred by C-O separations of 3.245 Å and 3.504 Å, respectively (Figure 2-20).

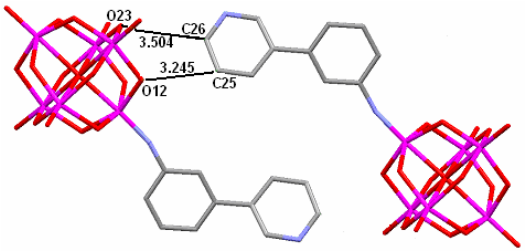

Figure 2-20: Wireframe model of **52** from crystal structure.
(Atomic distances in Å; Hydrogens and counter cations omitted for clarity)

The proton assignments of **47** and **52** were determined from the observed chemical shifts, multiplicities, and COSY (2D homonuclear correlation spectroscopy NMR spectra). The upfield region, between 0 and 3.2 ppm, of the ^{1}H NMR spectrum of **52** was assigned to the $[TBA]^{+}$ protons (Figure 2-21). As expected, the integration of these protons (72 x ^{1}H) are consistent with presence of two $[TBA]^{+}$ units per biaryl-imido hexamolybdate (8 x ^{1}H). This was later confirmed by elemental analysis and single x-ray crystallography.

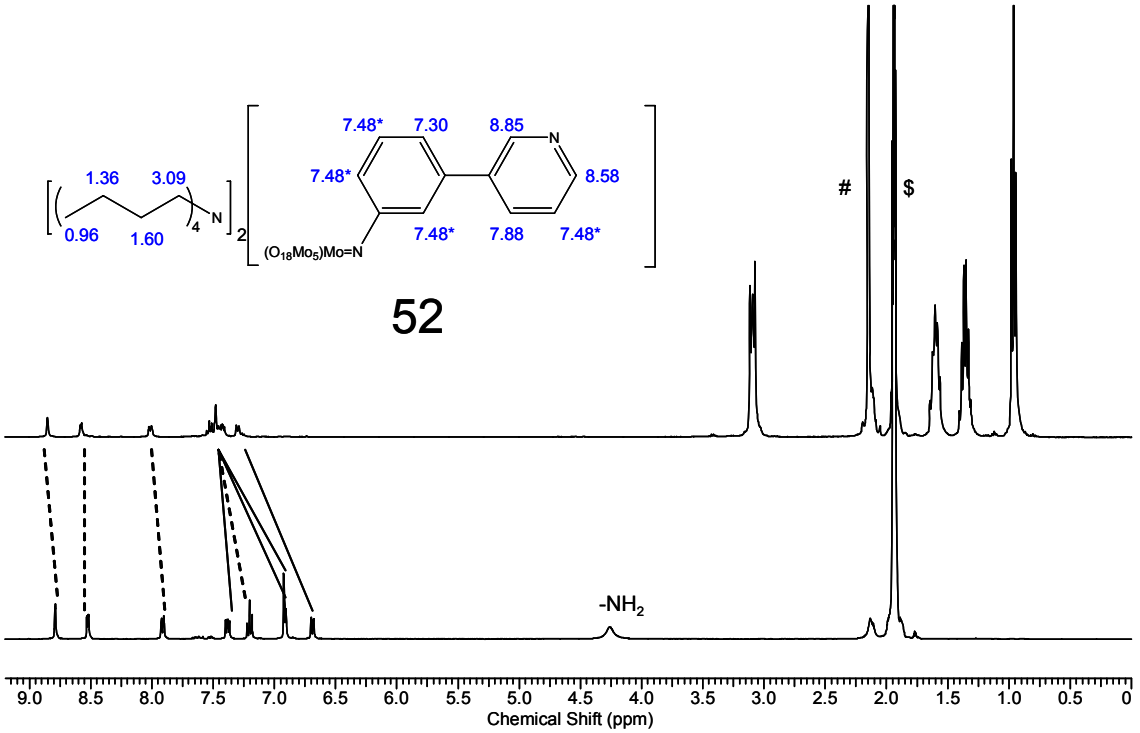

Figure 2-21: ^{1}H NMR spectra (400 MHz, CD_3CN) of **52** (top) and **47** (bottom).
($ = H_2O; # = CH_3CN; dashed lines = pyridyl protons; solid lines = phenylimido protons)

Deshielding of the ligand protons coupled with the disappearance of the amino protons were good indicators of successful functionalization. The appearance of the complex multiplet at 7.48 ppm in the ^{1}H NMR spectrum of **52** presented two setbacks: (i) proton assignments based on multiplicities were no longer possible and (ii) the small Δδ values (within the complex multiplet) rendered 2D correlation NMR techniques such as COSY and NOESY ineffective (Figure 2-23).

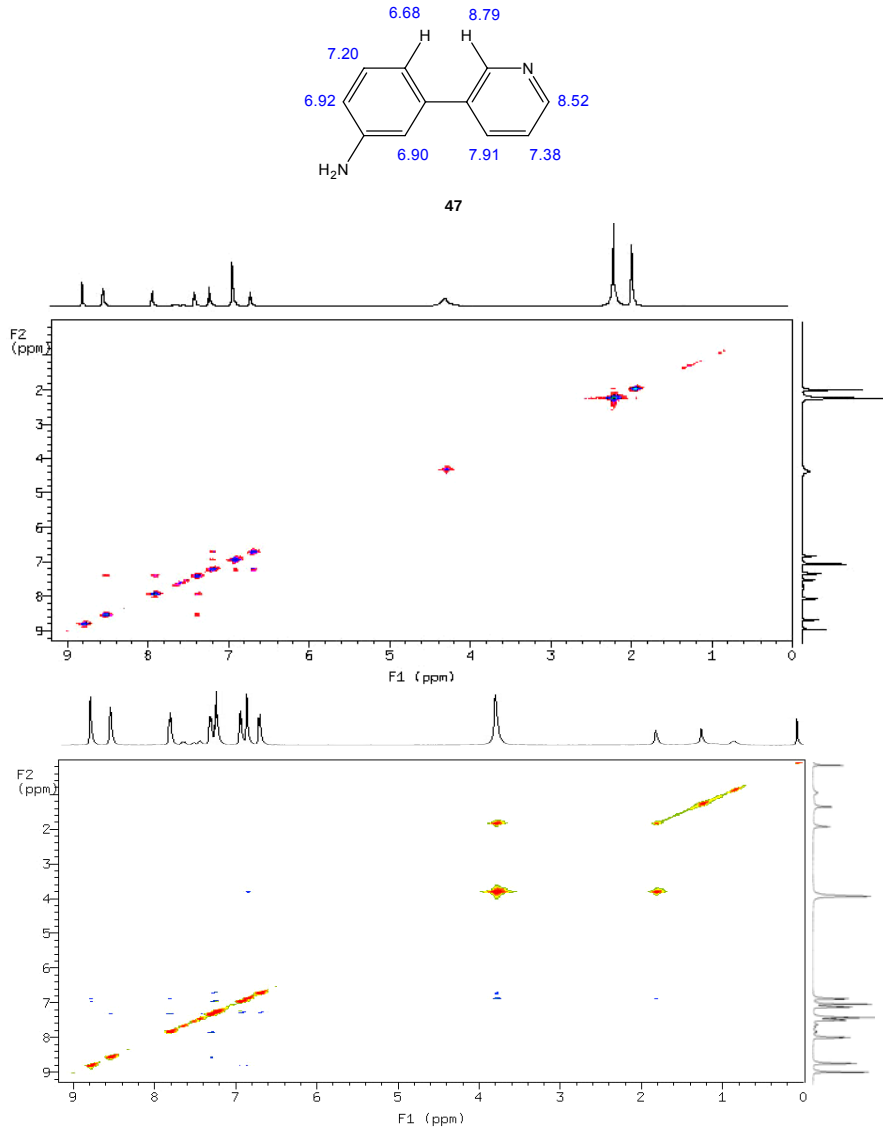

Figure 2-22: 400 MHz COSY (top) and NOESY (bottom) spectra of **47** (CD_3CN).

As a comparison to **52**, the COSY spectra of **47** showed four cross peaks from the scalar coupling between six aromatic protons of the biaryl appendage (Figure 2-22 and Table 2-4). In

contrast, only two cross peaks were observed in the COSY NMR spectrum of **52**, assigned to the protons of the pyridyl section of **52** (7.48, 7.88, 8.58 ppm) (Figure 2-23). The NOESY spectrum (Figure 2-23) showed some of the COSY signals as well as interaction between the N-H protons and that of a pyridyl.

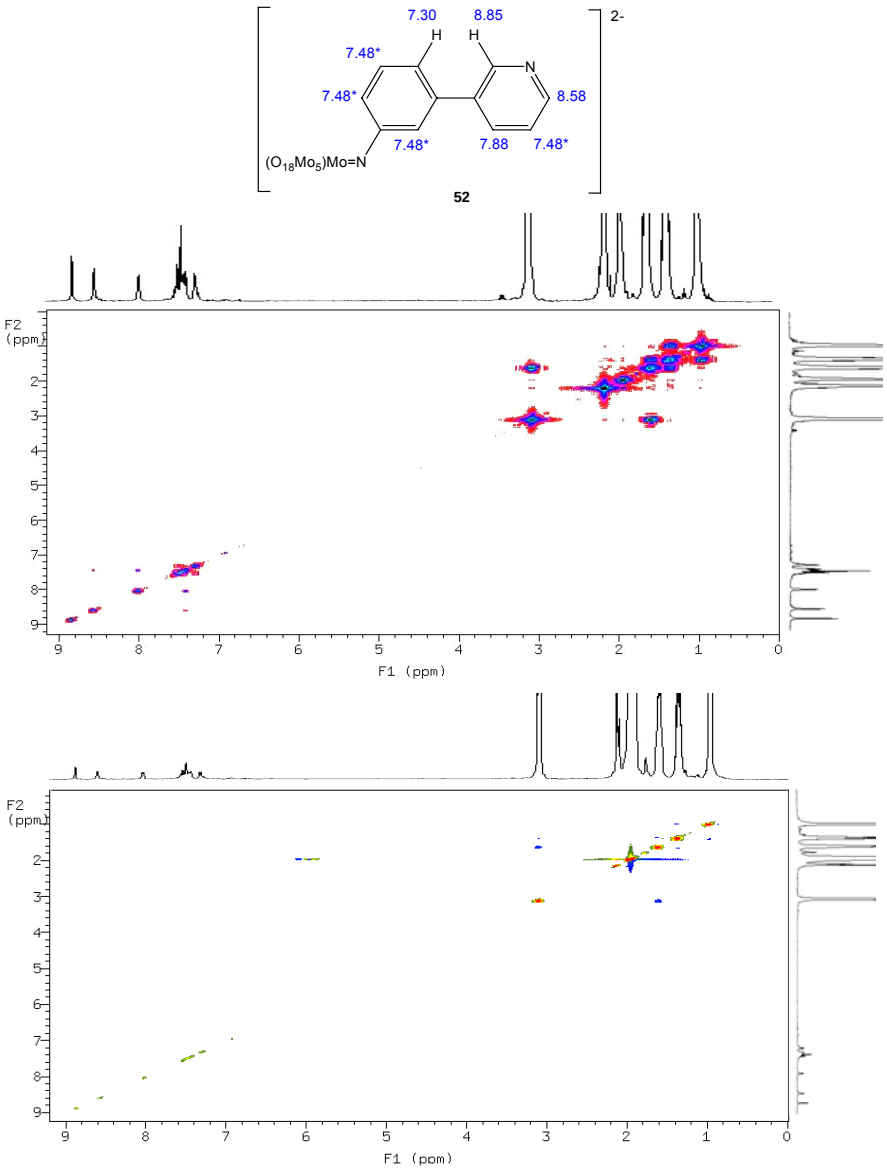

Figure 2-23: 400 MHz COSY (top) and NOESY (bottom) spectra of **52** (CD_3CN).

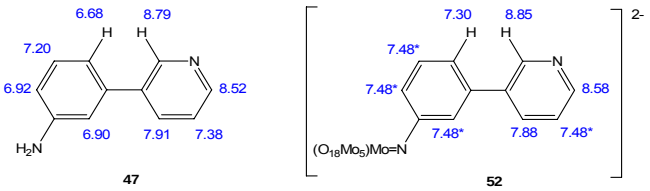

Figure 2-24: ^{1}H NMR (ppm) assignments for **47** and **52** (CD_3CN).

(7.48* = median value (7.41 – 7.55 ppm) of the complex multiplet of the phenylimido ring)

Table 2-4: Selected ^{1}H-^{1}H NMR (CD_3CN) COSY/NOESY data of **47** and **52**.

Complex	Protons (ppm)	COSY	NOESY
47	6.68 and 7.20	yes	-
	7.20 and 6.92	yes	-
	7.91 and 7.38	yes	-
	7.38 and 8.52	yes	-
	6.90 and 7.91	-	not observed
	6.68 and 8.79	-	yes
52	8.01 and 7.48*	yes	-
	7.48* and 8.58	yes	-
	7.48* and 8.01	-	not observed
	7.30 and 8.85	-	yes

The small Δδ of the complex multiplet at 7.48 ppm was assigned to the phenylimido imido-hexamolybdate section of the biaryl. Unfortunately this rendered NOESY NMR as an ineffective tool for further assignment of the protons. Thus the cross peaks expected from the phenylimido ring of **52** were interpreted as indistinguishable from the strong diagonal signal in the spectrum.

The NOESY spectra of **47** also suggested possible interaction between the protons at 6.68 and 8.79 ppm, *i.e.* those the adjacent to the biaryl C-C bond. This interaction strongly suggested that rotation about the C-C bond is restricted in solution. Unfortunately the NOESY spectrum of **52** did not provide any further information.

Cyclic voltammetry of **52** (Figure 2-24a) revealed a one electron reduction wave at -849 mV (vs. Ag/Ag^+). This is more negative than that of the parent $[Mo_6O_{19}]^{2-}$ ($E_{1/2}$ = -707 mV) and is typical for a mono-substituted system of this type.[5-9]

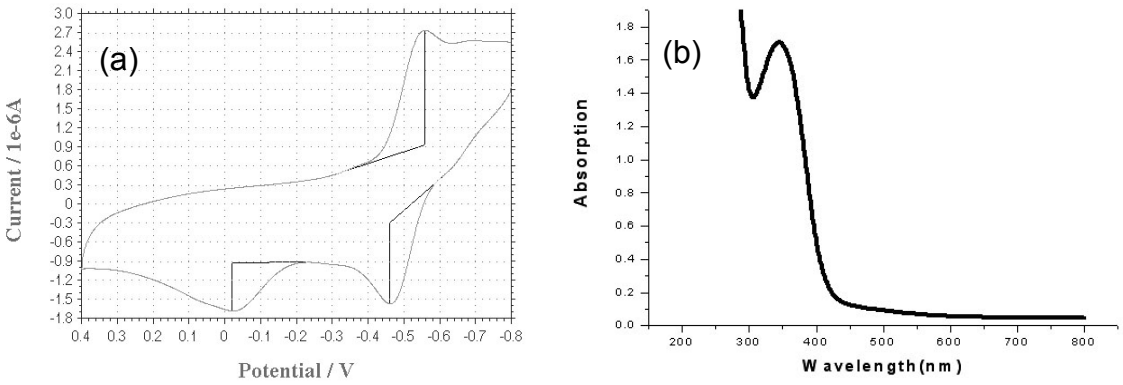

Figure 2-25: (a) Cyclic Voltammogram and (b) UV-Vis spectrum of **52**.
(CV: Ag/Ag^+ ,1 mM of 52 in CD_3CN, 100 mV/s, 0.1 M $TBA(BF_4)$;
UV-Vis: 1 mM of 52 in CD_3CN).

The electronic spectrum of **52** (in acetonitrile) was found to have its lowest energy absorption maximum at 346 nm ($\varepsilon = 1.7 \times 10^4\ M^{-1}cm^{-1}$) (Figure 2-24b). This is also consistent with observations on related systems such as $[Mo_5O_{18}Mo{\equiv}N\text{-}(2,6\text{-}\ (^iPr)_2C_6H_3)]^{2-}$ and $[Mo_5O_{18}Mo{\equiv}N\text{-}(2,6\text{-}(CH_3)_2\text{-}4\text{-}BrC_6H_2)]^{2-}$ with absorptions at 351 nm ($\varepsilon = 1.9 \times 10^4\ M^{-1}cm^{-1}$)[5] and 360 nm ($\varepsilon = 2.2 \times 10^4\ M^{-1}cm^{-1}$)[13], respectively. Corresponding data for the parent $[Mo_6O_{19}]^{2-}$ system are λ_{max} = 325 nm; $\varepsilon = 0.63 \times 10^3\ M^{-1}cm^{-1}$.[5] The observed red shift in the electronic spectrum indicates the presence of Mo-N charge transfer, while the more negative reduction potential of **52** reflects the superior ability of the organoimido ligand to furnish the cluster with electron density compared to the terminal oxo that was replaced.[5]

The desired increase in distance between the σ-donor function and the cluster was successfully achieved with the synthesis of **52** and perhaps in the impure sample of **51**. The 3-(pyridin-3-yl)phenylimido hexamolybdate **52,** at this time is the only hexamolybdate of its type, i.e. covalently functionalized with a biaryl ligand containing a remote σ-donor group. The combination of the observed 'twisted' configuration of **52** along with the extension provided by the biarylimido unit may both tend to reduce the electron withdrawing influence of the cluster. The metal coordination abilities of **52** will be demonstrated and discussed in the next section.

2.2.4 Novel metalloligand behavior of 3-(pyridin-3-yl)phenylimido hexamolybdate, 52.

The successful synthesis and isolation of **52** prompted trials to determine the metal coordination capabilities of this novel hybrid POM. Preliminary attempts at metal coordination initially focused on suitable silver (I) salts. Since linear, two coordinate complexes dominate Ag(I) chemistry,[21] two equivalents of **52** were added to an equivalent of silver triflate (CF_3SO_3Ag) in acetonitrile at room temperature. Changes in the ^1H NMR spectrum of the organoimido POM were to be expected upon successful coordination. However after 2 days at room temperature, no such changes were observed. The experiment was repeated at reflux temperatures for 2 days. Unfortunately, no changes were seen in the ^1H NMR spectrum of the mixture even at elevated temperatures.

Another transition metal complex capable of pyridyl coordination is bis(dibenzoylmethanato)nickel(II), $[Ni(DBM)_2]$.[38] Again two equivalents of **52** were added to a solution of $Ni(DBM)_2$ in acetonitrile. The resulting green solution, **62b**, was analyzed by ^1H NMR (Figure 2-25). The paramagnetic nature of Ni(II) rendered the ^1H NMR spectrum inconclusive and crystals suitable for single x-ray crystal diffraction were not obtained.

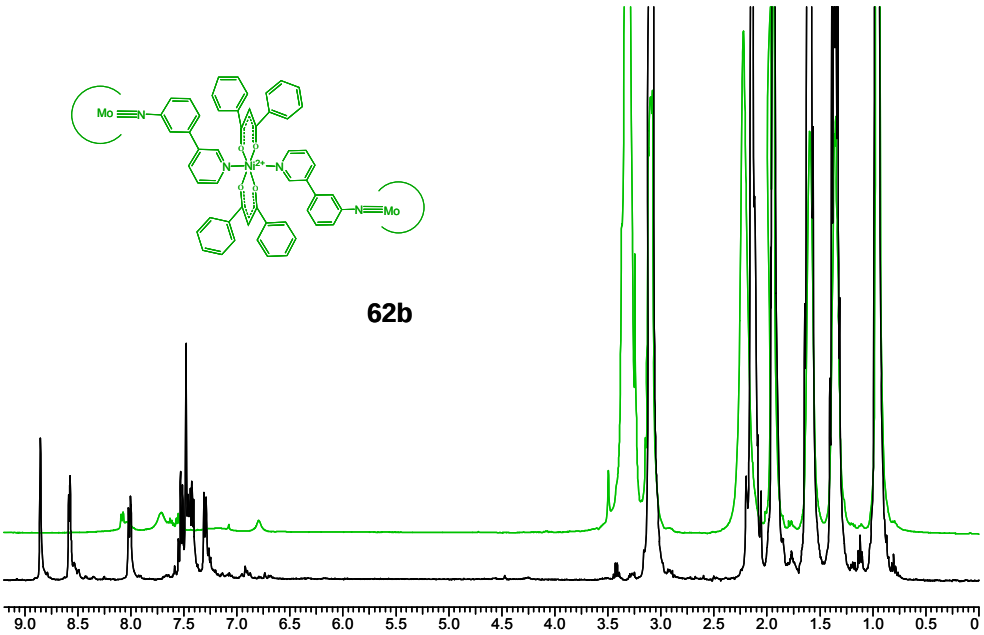

Figure 2-26: 400 MHz ^1H NMR spectra of **62b** (top) and **52** (bottom) (CD_3CN).

An alternative transition metal complex capable of pyridyl ligand coordination is bisbenzonitrile-dichloro palladium (II), **[Pd(II)]**. Gouzerh *et al.*[39] reported that the pyridyl substituents in the bis-alkoxy functionalized Anderson-Evans POM, **67** readily displaced the benzonitrile molecules of **[Pd(II)]** to form the adduct, $MnMo_6O_{18}\{(OCH_2)_3CNHCO\text{-}(4\text{-}C_5H_4N)\}_2PdCl_2$ **[Pd(II)-67].**[39] The single crystal structure of the adduct **[Pd(II)]-67** was not reported but its formation was confirmed by FT-IR and ^{1}H NMR methods.[39] In a similar fashion, two equivalents of **52** were added to a solution of **[Pd(II)]** in acetonitrile at room temperature. The reaction solution was monitored by ^{1}H NMR. After 2 days no changes in the spectrum was observed.

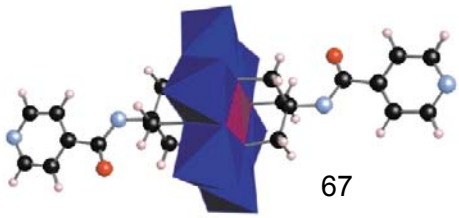

Figure 2-27: Molecular structure of **67**, a bis-alkoxy Anderson-Evans hexamolybdate. (Blue octahedra = Mo, Purple octahedra = Mn; black spheres C, red spheres O, light blue spheres N, white spheres H).[39]

Another metal complex known to favor pyridyl coordination was found is *meso*-(5,10,15,20-tetraphenyl- porphyrinato)carbonyl ethanolate ruthenium (II) **68**[40] (Figure 2-27). Such metalloporphyrins represent an interesting class of molecules utilized in a variety of fields.[41a-c] Most relevant to this discussion are its applications in supramolecular devices (nanocars),[41a] molecular chromophores (photovoltaic supramolecules)[41b] and NMR shift reagents (cis-trans motif of bis-substituted porphyrins).[41c]

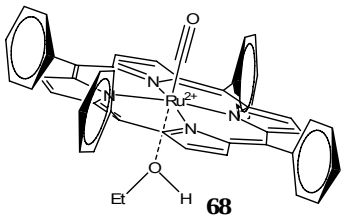

Figure 2-28 *Meso*-(5,10,15,20-tetraphenylporphyrinato)-carbonyl ruthenium (II) ethanolate complex **68**.[40]

The axial ethanol ligand of **68** is labile and can be displaced readily by pyridyl-type ligands.[42c] This capability has been exploited by various groups,[42a-d] and most recently by Hasenknopf *et al*.[43,44] They demonstrated that the pyridyl nitrogen of **67** was capable of displacing the axial ethanolate of **68** at room temperature to yield the adduct **69** (Figure 2-28).

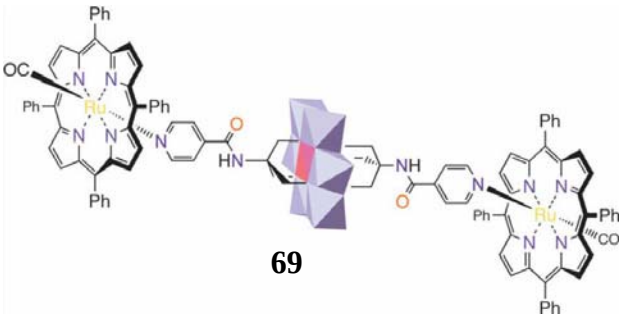

69

Figure 2-29: Molecular representation of the adduct **69**, $[(TBA)_3MnMo_6O_{18}\{(OCH_2)_3CR\}][RuTPP(CO)]$.[44]

With this knowledge, an equivalent of **52** was added to a red suspension of **68** in anhydrous chloroform at room temperature under argon (Figure 2-29). As observed in this study and also reported by Gianferrara *et al.,*[41c] **68** was only partially soluble in pure anhydrous chloroform and the coordination of **52** aided dissolution. The resultant dark red suspension was stirred and after 10 minutes a dark red solution formed. The dark red solution was analyzed by different spectroscopic methods in search of the coordination complex **70,** [(3(pyridin-3-yl)phenylimido-hexamolybate : *meso*-(5,10,15,20 tetraphenylporphyrinato)carbonyl ruthenium (II)] (Figure 2-30).

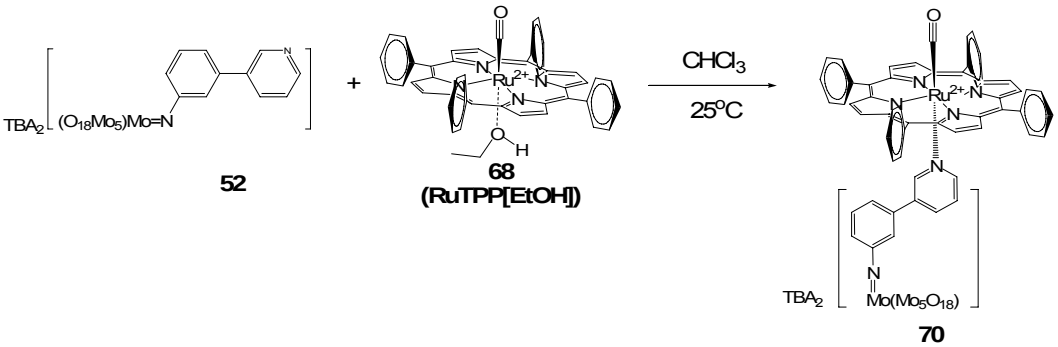

Figure 2-30: Coordination of the hexamolybdate **52** with **68** at room temperature.

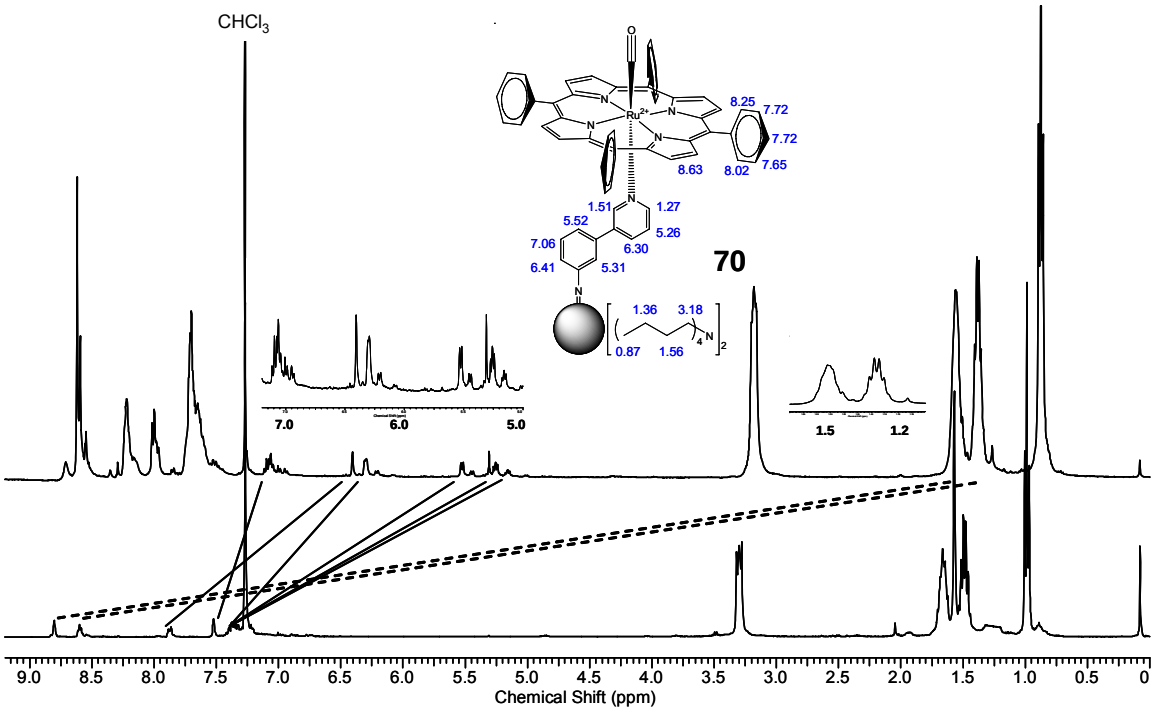

Figure 2-31: ^{1}H NMR spectra (400 MHz, $CDCl_3$) of **70** (top) vs. **52** (bottom). (Black sphere = $[Mo_6O_{18}]^{2-}$; dashed lines = pyridyl protons; solid lines = phenylimido).

Gianferrara[41d] and Hasenknopf[43] noted that once formed, the Ru-N coordinate bond was strong and resistant to displacement by coordinating solvents such as acetonitrile. This was confirmed from cyclic voltammetry and UV-Vis studies conducted in acetonitrile. However, it should be noted that the effects of other coordinating solvents (σ-donors) such as pyridine, N,N'-dimethylsulfoxide[45] and tetrahydrofuran were not studied.

Compound **70** was characterized by means of 1D and 2D ^{1}H NMR spectroscopy. Signal integration established ligand, macrocycle and countercation stoichiometry while a combination of ^{1}H-^{1}H COSY, NOESY, CycleNOE and NOE irradiation experiments permitted and confirmed proton assignments. The absence of the amino protons in the ^{1}H NMR of **70** suggested that if the decomposition of **52** had occurred during coordination, it was not detectable. This is a very strong indication that the observed spectrum of **70** (NMR) is due to the coordination adduct **70**. However, since the imidohexamolybdate ligand **52** might hydrolyze back to biarylamine **47** (especially in solution) adduct **71** was also synthesized, as a model compound for **70**.

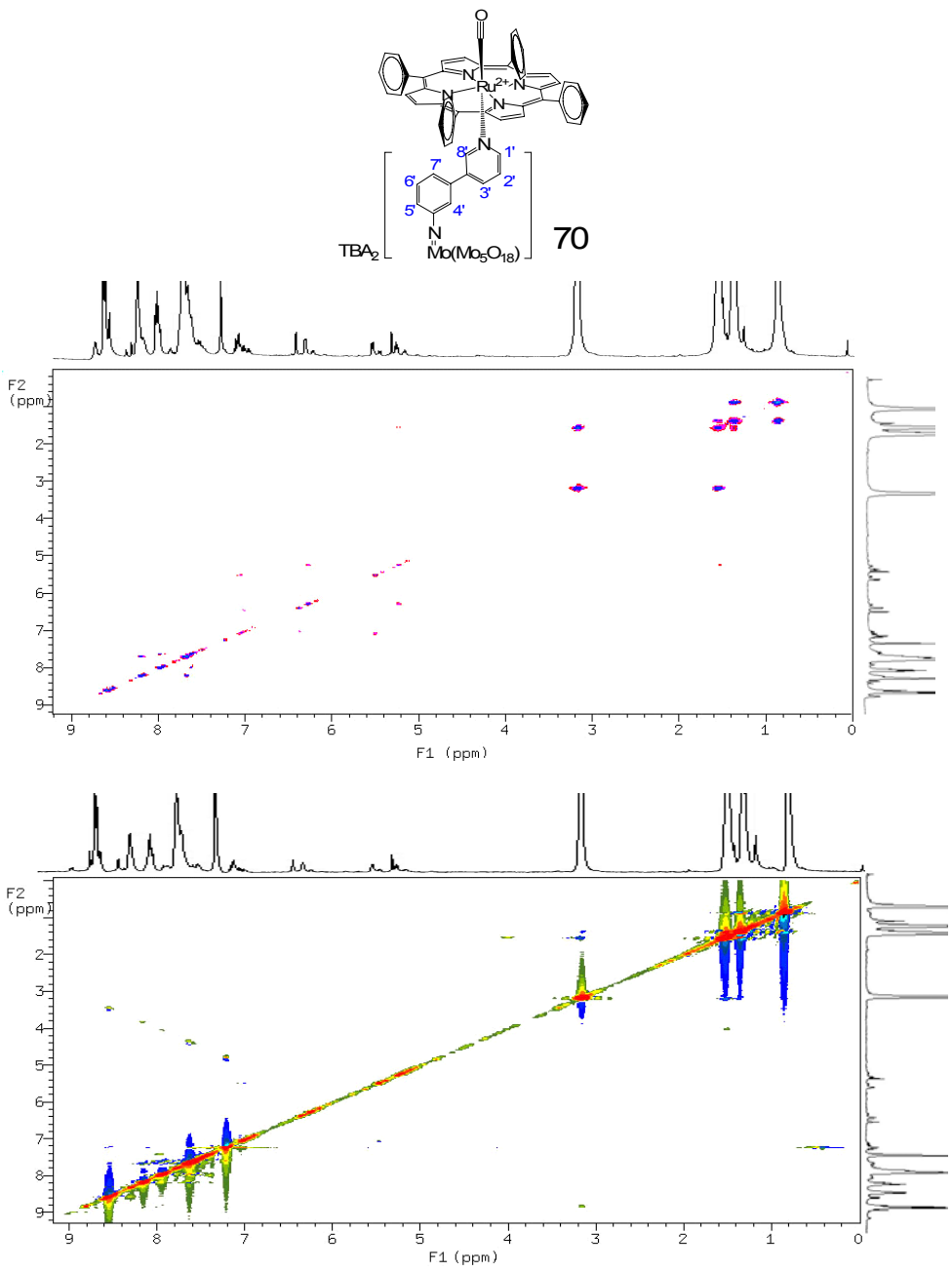

Figure 2-32: 400 MHz NMR, COSY (top) and NOESY (bottom) spectra of **70** in $CDCl_3$.

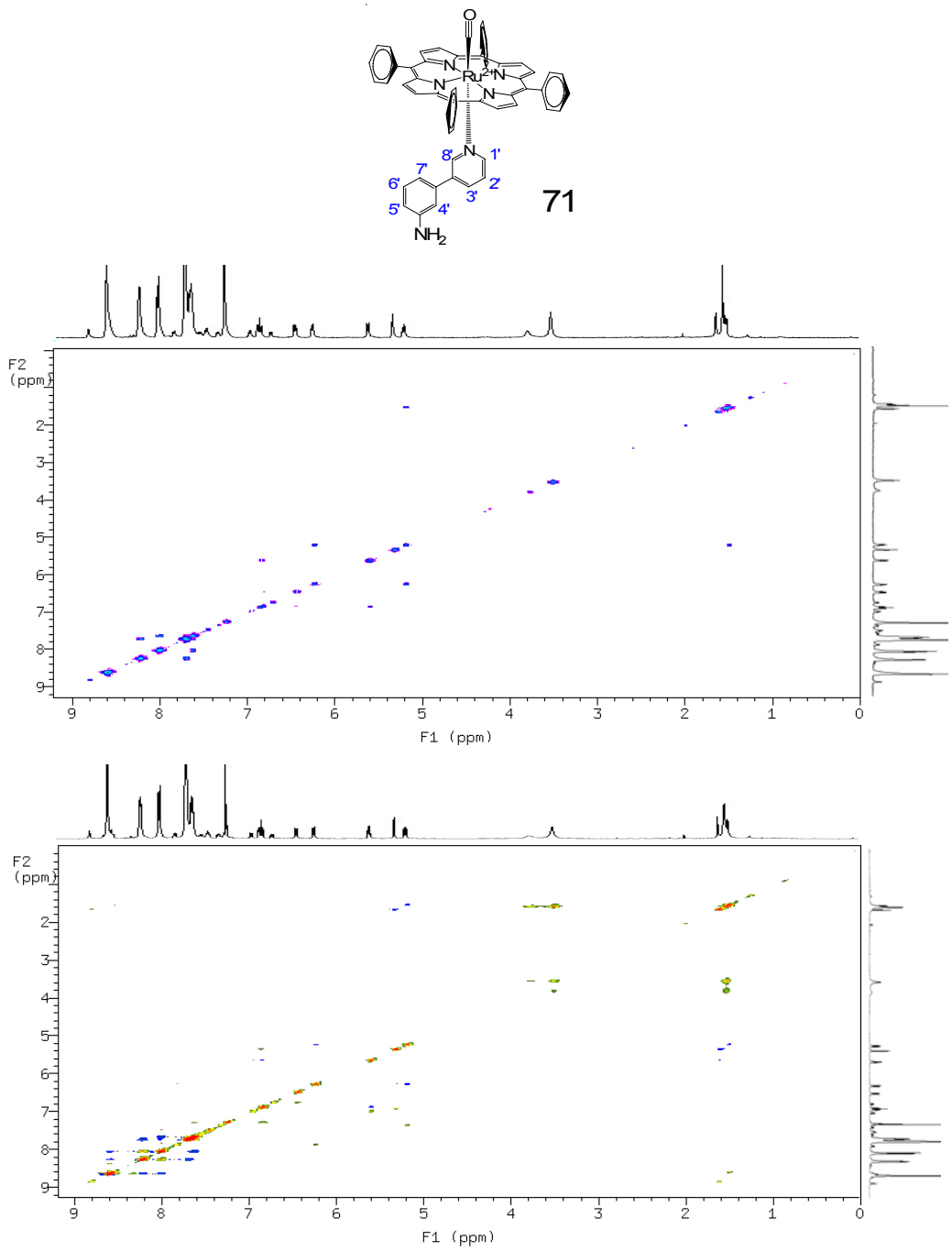

Figure 2-33: 400 MHz NMR COSY (top) and NOESY (bottom) spectra of **71** in $CDCl_3$.

A characteristic feature of successful coordination is the drastic upfield shifts (^{1}H NMR) of the pyridyl ring protons. This phenomenon has precedence and is attributable to the anisotropic (additive) shielding cone of the aromatic macrocycle.[44-45] This is a feature common to metallo-porphyrins bearing axially-coordinated pyridyl ligands (Figure 2-31 and 32).[43-44] The 2D COSY NMR spectra of adducts **70** and **71** confirmed the upfield shift in the ^{1}H NMR spectra, in

particular, that of proton 1' of **70** and its appearance as a complex multiplet within the TBA^+ cation signal at 1.53 ppm (Figure 2-31 and 2-32). Unfortunately, as was the case with **52**, the NOESY spectrum of **70** did not provide any new information regarding the interactions between protons 3' – 4' and 7' – 8'.

Table 2-5 ^{1}H NMR (400 MHz, $CDCl_3$) chemical shifts and Δδ values (in brackets) from ligands **47** and **52** and their adducts **70** and **71**.

	δ of the ligand protons / ppm							
Compound	1'	2'	3'	4'	5'	6'	7'	8'
47	8.58	7.35	7.85	6.89	6.98	7.27	6.74	8.82
52	8.60	7.48	7.88	7.54	7.48	7.48	7.21	8.85
70	1.27	5.26	6.30	5.31	6.41	7.06	5.52	1.51
70*	(-7.09)	(-2.22)	(-1.58)	(-2.23)	(-1.07)	(-0.42)	(-1.69)	(-7.58)
71	1.52	5.21	6.27	5.34	6.47	6.86	5.64	1.63
71**	(-7.06)	(-2.14)	(-1.58)	(-1.55)	(-0.51)	(-0.41)	(-1.14)	(-7.19)

(70* = δ{52 – 70}ppm; 71** = δ{47 – 71}ppm)

The extent of shielding experienced by the biaryl protons of both adducts (**70** and **71**) are highlighted by the changes in chemical shift (Δδ) values before and after coordination (**70*** and **71****) as shown in Table 2-5. Protons 1' and 8' (closest to the Ru-N (pyridyl) bond) of adduct **70** were shifted upfield by 7.09 and 7.58 ppm, respectively. In comparison, 6' only shifted by 0.42 ppm (confirmed by COSY NMR). These drastic shifts by the bound pyridyl protons are consistent with those reported in literature.[44 -45]

Although the NOESY spectrum of **70** did not provide correlation between protons 7' and 8', their spatial proximity to each other permitted the use of cycleNOE (1D ^{1}H NMR $CDCl_3$; relaxation time = 25 s; mix = 0.05s) experiments. The resonance assigned to 7' was irradiated causing the signal from any neighboring protons with NOE to 7' -in this case 6' and 8' -to change in intensity (Figure 2-34). Protons 6' and 8' were further distinguished by their distinct multiplicities in the ^{1}H NMR spectrum (i.e., 6' = doublet of doublets; 8' = singlet). This method of selective irradiation proved valuable for confirming the assignments of the biaryl protons in the adducts (Figure 2-34 and 2-35). These cycleNOE NMR experiments also confirmed the presence of shifted pyridyl protons in the ^{1}H NMR spectra of **70** and **71**. It was especially

important in confirming the peak assigned as 8' of **70**, which was initially shown by COSY NMR to be concealed within the resonance at 1.51 ppm from the TBA^+ cation.

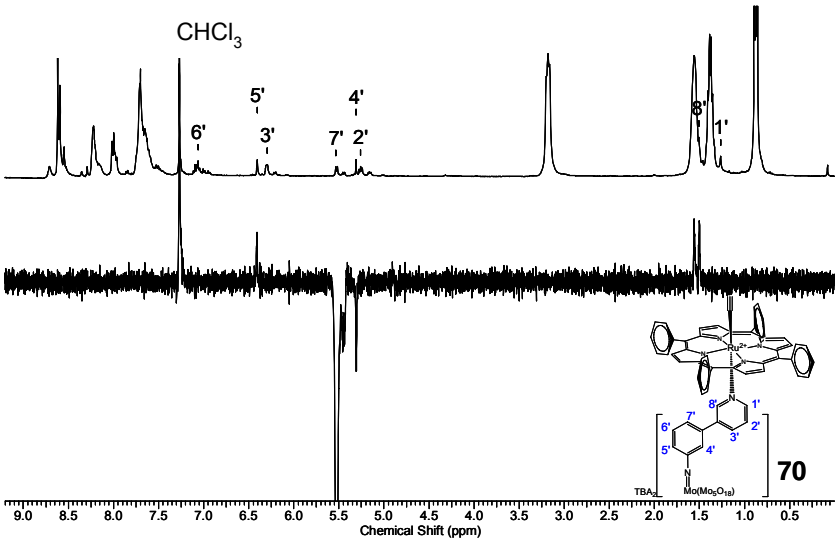

Figure 2-34: ^{1}H NMR spectrum(top; 400 MHz, $CDCl_3$) and CycleNOE NMR (bottom) spectrum as a result of irradiating proton 7' (5.53 ppm) of **70**.

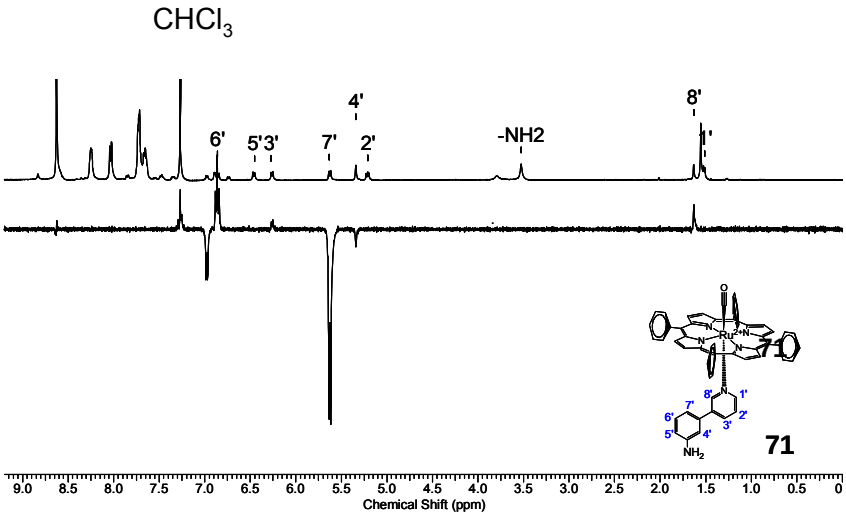

Figure 2-35: ^{1}H NMR spectrum (400 MHz, $CDCl_3$) and CycleNOE NMR (bottom) spectrum as a result of irradiating proton 7' (5.64 ppm) of **71**.

As mentioned previously, the crystal structure of **52** showed that the pyridyl nitrogen is oriented away from the imidohexamolybdate. This orientation was not expected to change upon

coordination to the metallo-macrocyle. Indeed, cycleNOE NMR experiments confirmed that the 'twisted and locked' orientation was preserved in **70**. Similar changes were observed for the same protons of the model adduct **71** (Table 2-5).

As noted in the literature[44-46] and as demonstrated here, the shielding effect on the pyridyl-phenyl protons progressively diminishes as their distance from the Ru coordination site increases. The upfield shifts of the pyridyl protons in **70** indicate successful coordination of the ruthenium porphyrin macrocycle by the pyridylimido-hexamolybdate, thus achieving the primary goal of this thesis.

Further evidence of successful coordination was found through UV-Vis spectrophotometry in acetonitrile (Table 2-6). The electronic spectrum of **70** bears a striking resemblance to that of **71** and **68** (ruthenium (II) porphyrin ethanolate). This was expected since the adduct **[68-pyridine]**,[46a] as reported by Ibers, was also found to display a UV-Vis spectrum very similar to that of **68**. Upon displacement of the ethanolate with pyridine, the band of **68** at 528 nm was red-shifted to 532 nm.[45a] Adduct **70** was found to exhibit an identical red-shift to 533 nm. These observations also confirm that formation of **70** was successful.

Table 2-6: UV-Vis data of **52**, **68**, **70**, **71** and **[68-pyridine]**.

	λ_{max}, nm(log ε)				
Compound	**52**	**70**	**71**	**68**[a]	**[68-pyridine]**[a]
	-	585 (4.0)	565 (2.85)	563 (3.4)	566 (3.6)
	-	533 (4.3)	531 (3.07)	528 (4.3)	532 (4.2)
	-	495 *sh* (4.0)		490 (3.6)	495 *sh* (3.7)
	-	486 (4.0)		-	-
	-	410 (5.2)	410 (3.91)	412 (5.4)	413 (5.4)
	346 (4.2)	349 (4.2)	-	-	-
	-	-	313 (3.04) 286 (2.96	-	-
	-	-	239 (3.09)	-	-

(a = Ref.[46a]: Conditions: 5.53×10^{-6} M in anhydrous acetonitrile)

In contrast, no evidence for the intact adduct **70** or **71** was found by mass spectrometry (MALDI-ToF/ToF-MS). Instead only fragmnts at 714.023 and 714.141 m/z were observed; these are assignable as [Ru(TPP)]+, indicating that both carbonyl and pyridyl-hexamolybdate ligands were detached in the mass spectrometer. Similar results were reported by Ibers,[42a] who noted that

in the mass spectrum of **[68-pyridine]** both axially bound ligands (C≡O and pyridine) became separated from the metalloporphyrin.

The υ(C=O) stretching frequencies of adducts **70** and **71** were observed at 1938 cm^{-1} in their IR spectra. These are comparable to values for the RuTPP(CO)[pyridine] and ethanolate adduct **68**, as reported by Ibers[42b] and Cenini[42c]. The reported C=O stretch for other RuTPP(CO)[L] compounds, where L is an axially coordinated pyridyl, aqua, or alcoholic ligand, were found to occur between 1940-1955 cm^{-1} in the IR, (error margin of approximately 5-10 cm^{-1})[45 c] compared to **68**.

Table 2-7: Selected FT-IR data for various RuTPP(CO)[L] adducts.

	υ / cm^{-1}	
Compound	$(C=O)_{terminal}$	$(Ru\text{-}N)^{a}_{porphyrin}$
RuTPP(CO) [a]	1952	459[e]
RuTPP(CO)[EtOH]	1942[e]	463[e]
RuTPP(CO)[MeOH] [42c]	1949	n/r
RuTPP(CO)[H_2O] [42c]	1949	n/r
RuTPP(CO)[pyridine] [b]	1939	n/r
69 [c]	1951	462
70	1938	460
71	1938	457

(a = Ref[47]; b = Ref[42a]; c = Ref[44] ; n/r = not reported; e = this study)

Cenini[45c] also noted that although the RuTPP(CO) complexes are widely used as precursors for most ruthenium tetraphenylporphyrin chemistry and are available commercially, they have not been characterized as thoroughly as would be expected. This includes the lack of reported IR assignments for the Ru-N(porphyrin) stretch when coordinated with various ligands. Table 2-7 shows assignments of the υ(Ru-N) vibrational frequency, assigned at 460 and 457 cm^{-1} for **70** and **71**, respectively.[47] Analogous to the υ(C=O) values, the Ru-N stretching frequencies also remain virtually constant (± 6 cm^{-1}) with various axially coordinated ligands, L.

Although the reasons for the lack of changes in the υ(C=O) and υ(Ru-N) stretching frequencies are unclear, the observed similarities between the UV-Vis and IR spectra of **70**, **71** and those of the other complexes in Tables 2-7 and 2-6 serves to reinforce the observed NMR data, *i.e.* we can conclude that successful coordination to the Ru-macrocycle was achieved with

52. Thus the hexamolybdate POM has been transformed successfully and demonstrated capable of metalloligand behavior via an appended pyridyl-phenylimido moiety.

2.2.5 - Functionalization of hexamolybdate with ligands containing modified extended spacer and σ-donors groups.

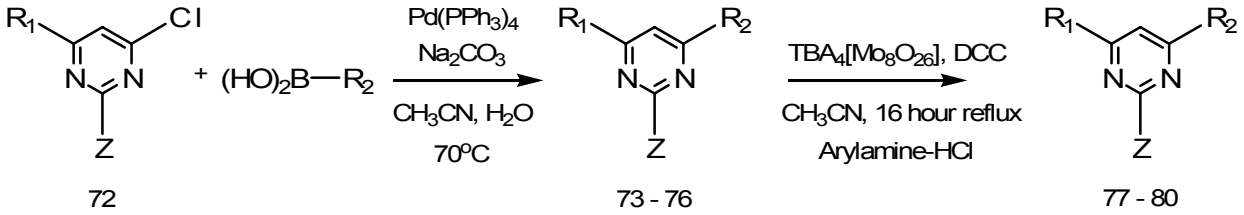

Figure 2-36: Planned functionalization of hexamolybdate with pyrimidyl groups adapted from Wei's method[13] (DCC = dicyclohexylcarbodiimide; Z = $-NH_2$ or imido-$[Mo_6O_{18}]^{2-}$).

Encouraged by the successful syntheses and characterization of **52** and its metal coordination ability, other biarylamine compounds containing pyrimidine heterocycles were targeted (Figure 2-36). Several 'pyrimidyl-phenylamine' compounds have been reported by Aäkeroy.[48] These possess functionalities analogous to those of **73 - 76** and **47**.[48]

The incorporation of electron donating substituents at the R_1 position may further tend to favor metal coordination (Figure 2-36). The proximity of the pyrimidyl nitrogens to the hexamolybdate, in compounds **77 - 80**, may offset the influence of the hexamolybdate through increased electron density of the ligand (compared to the biaryls **46** and **47**). The functionality at R_1 was altered easily and readily by simply varying the starting materials **72** (R_1 = $-CH_3$, $-OCH_3$; Z = $-NH_2$) which are commercially available.[48] The R_2- boronic acids were synthesized from their corresponding arylbromide compounds according to the literature.[48] (Figure 2-6) Compounds **73 - 76** were synthesized via Suzuki C-C coupling protocols modified from the literature (Table 2-8).[32,48] Hexamolybdate functionalization was attempted using the phosphinimine derivatives of **73 - 76** (obtained by methods described earlier)[15,21] but without success.

Table 2-8: Series of *m*-amino-pyrimidyl biaryl ligands and the *m*-pyrimidylimido functionalized hexamolybdates.

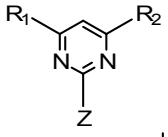

	Z	R_1	R_2		Z	R_1	R_2
73[a]	$-NH_2$	$-CH_3$		77[b]	$[-N-Mo(Mo_5O_{18})]^{2-}$	$-CH_3$	
74[a]	$-NH_2$	$-CH_3$	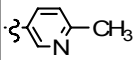	78[b]	$[-N-Mo(Mo_5O_{18})]^{2-}$	$-CH_3$	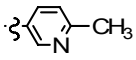
75[a]	$-NH_2$	$-CH_3$	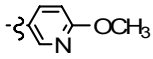	79[b]	$[-N-Mo(Mo_5O_{18})]^{2-}$	$-CH_3$	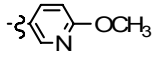
76[a]	$-NH_2$	$-OCH_3$	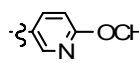	80[b]	$[-N-Mo(Mo_5O_{18})]^{2-}$	$-OCH_3$	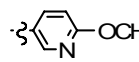

(a = synthesized according to literature[48]; b = TBA^+ salts)

Unfortunately, only **77** was found to show any evidence of the characteristic shoulder at 950cm^{-1} in the IR spectrum. Attempted purification from recrystallization (acetonitrile: diethylether) and column chromatography (silica gel) yielded only the biarylamine and the parent hexamolybdate $[Mo_6O_{19}]^{2-}$ with some urea byproduct. Since **77** was not isolated, metal coordination with **68** was not attempted. So far, crystals suitable for single crystal structure determination of **77** have to yet to be obtained.

2.3 - Conclusions and Future Work

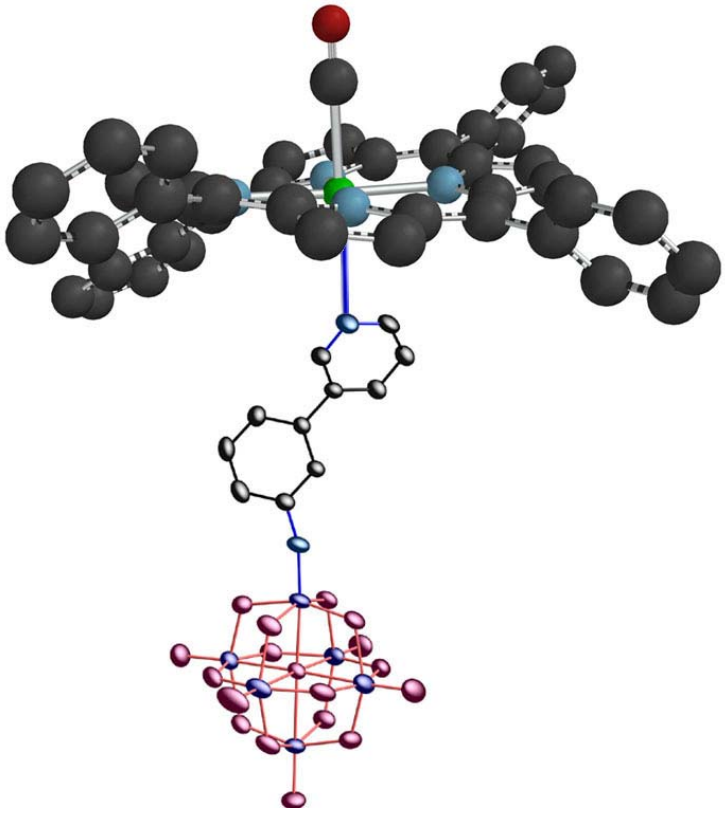

Figure 2-37: Proposed structure of 3-(pyridin-3-yl)phenylimido-hexamolybdate:porphyrin ruthenium(II) carbonyl adduct, **70**.

A new and exciting avenue of polyoxometalate chemistry has been demonstrated. The successful synthesis and characterization of the biarylimidohexamolybdate species has further extended the family of known organoimido appended POMs. This new hybrid POM demonstrated and fulfilled the main goal of this project by achieving metal coordination with a ruthenium-porphyrin macrocyle (Figure 2-37). This also brings the hexamolybdate POM one step closer to being capable of forming the supramolecular architectures mentioned earlier. Further work will be needed in order to determine why the other synthesized biarylamine compounds were incapable of functionalizing the hexamolybdate POM. The biarylamine compounds might also be further extended via the incorporation of an 'ethylnyl' bridge via Sonogashira coupling reactions (Figure 2-38).

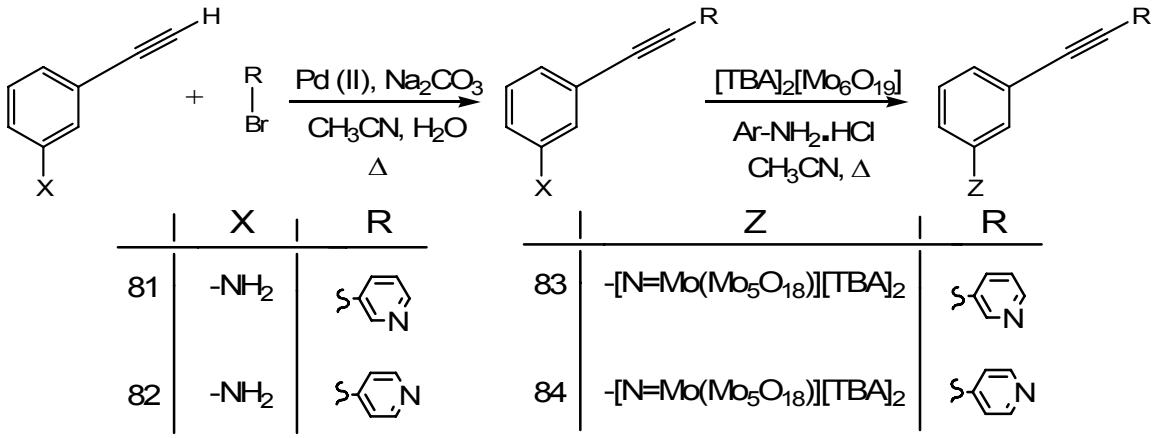

	X	R
81	-NH_2	
82	-NH_2	

	Z	R
83	-[N=Mo(Mo_5O_{18})][TBA]$_2$	
84	-[N=Mo(Mo_5O_{18})][TBA]$_2$	

Figure 2-38: Future target molecules with 'extended' biaryl ligands (Sonogashira coupling protocol).[49]

2.4 - Experimental

$TBA_2[Mo_6O_{18}]$[20] and $TBA_4[Mo_8O_{26}]$[20] were prepared according to literature methods. All manipulations were done under an inert atmosphere of argon, unless otherwise stated. THF was distilled over sodium, ditheylether and CH_3CN were dried over CaH_2 and distilled as needed. The boronic acids were purchased from Frontier Scientific and dried at 40°C for 24 hours prior to use, unless otherwise stated. Compounds **28**,[32] **29**,[32] **46**,[32] **47**[32] and **73** - **76**[48] were synthesized following literature methods.

All other starting materials and Pd(II) catalysts were purchased from Aldrich or Fisher Scientific; solids were dried under vacuum at 40°C for 24 hours prior to use. Oily and liquid reagents were purged of oxygen via the 'freeze-pump thaw' method (5 cycles) prior to use. NMR 1D and 2D NMR spectra were recorded on a Varian Unity Inova 400 MHz spectrometer and processed with vNMRj. ^1H NMR spectras were referenced to residual protonated solvent peaks ($CDCl_3$ = 7.27 ppm, CD_3CN = 1.94 ppm and DMSO-d_6 = 2.50 ppm). Electrochemical (CV) data were collected in acetonitrile, with sample concentrations of 10^{-3} M and 0.1 M $[TBA]BF_4$ as the supporting electrolyte. A standard three-electrode cell was used, consisting of a carbon electrode, a polished auxiliary platinum electrode and aqueous (Ag-AgCl) reference electrode equipped on a CHI 720C instrument and Electrochemical Analyzer/Workstation V.501. Electronic (UV-Vis) spectra and data were collected on a Varian Cary 500 Scan with quartz glass cell with a path length of 1 cm at room temperature in anhydrous acetonitrile. FT-IR spectra were recorded on a Nicolet Protégé 460 instrument as KBr pellets. Mass spectra (MALDI-ToF/ToF-MS) were collected on a Bruker Daltronics Ultraflex ToF/ToF mass spectrometer. Silica gel was purchased from AnalTech (150 Å pore).

*2.4.1 N-(3,5-dimethylphenyl)acetamide[22] (**5a**)*

To a stirred solution of 3,5-dimethylaniline (10.0 g, 82.52 mmol) and pyridine (6.53g, 82.52 mmol) in $CHCl_3$, was added a solution of acetyl chloride (6.48g, 84.54 mmol) in 5 mL of

$CHCl_3$ dropwise over 20 minutes at 0°C under argon. The resulting yellow solution formed a white precipitate upon warming to room temperature. The suspension was stirred at room temperature for 2 hours. Removal of the solvent (under reduced pressure) produced a yellow residue which was redissolved into ethyl acetate and washed with saturated $NaHCO_3$ solution (2 x 15 mL) and distilled water (3 x 10 mL). The combined organic layers were dried over anhydrous $MgSO_4$. Removal of the solvent yielded an off-white solid. Dissolution in acetic acid and cooling to -5°C precipitated the pure product as a white crystalline solid. The solid was washed with ice-cold water and dried under vacuum for 24 hours. Yield (8.26g, 62 %) ^{1}H NMR ($CDCl_3$): δ 2.16 (s, 3H), 2.39 (s, 6H), 7.17 (s, 1H), 7.25 (s, 2H) ppm. ^{13}C NMR ($CDCl_3$): δ 20.9, 25.4, 118.5, 120.6, 139.4, 140.3, 172.9 ppm. FT-IR (KBr): υ 3546, 3304, 3264, 1637 cm^{-1}.

*2.4.2 t-Butyl-3,5-dimethylphenylcarbamate[22] (**5b**)*

To a stirred solution of 3,5-dimethylaniline (5.00 g, 0.0413 mmol) in 1,4-dioxane (50 mL) was added a solution of NaOH (1.65g, 0.0413 mmol) in 25 mL of water. The resulting suspension was cooled to 0°C and di-^{t}butyl dicarbonate (9.91g, 0.045 mmol) was added dropwise over 10 minutes. The resulting mixture was maintained at 0°C for another 30 minutes, after which the mixture was allowed to warm to room temperature and was stirred overnight. The product was extracted with ethyl acetate (3 x 20 mL) and the combined organic phases were washed with water (3 x 30 mL) and dried over anhydrous $MgSO_4$. Removal of the solvent yielded an off-white solid. The product was recrystallized from CH_2Cl_2 as fine white needles that were dried under vacuum. Yield (7.21g, 79%) ^{1}H NMR ($CDCl_3$): δ 1.48 (s, 9H), 2.24 (s, 3H), 6.36 (s, 1H), 6.64, (s, 1H), 6.96 (s, 2H) ppm. ^{13}C NMR ($CDCl_3$): δ 25.2, 27.8, 81.2, 118.2, 122.3, 128.3, 139.1, 169.4 ppm. FT-IR (KBr): υ 3360, 2968, 1694 cm^{-1}.

*2.4.3 N-(4-bromo-3,5-dimethylphenyl)acetamide[22] (**6a**)*

To a stirred solution of **5a** (1.0g, 6.16 mmol) was added bromine (0.99g, 6.19 mmol) dropwise over 10 minutes. The resulting yellow mixture was stirred at room temperature. After 14 hours, the white suspension was poured into 100g of ice. The pure product was collected on a

glass frit as a white solid. The product was dried overnight at 50°C under high vacuum. Yield (1.16g, 78 %) ^{1}H NMR ($CDCl_3$): δ 2.16 (s, 3H), 2.38 (s, 6H), 7.25 (s, 2H) ppm. ^{13}C NMR ($CDCl_3$): δ 20.6, 24.4, 121.5, 120.4, 138.4, 140.3, 171.0 ppm. FT-IR (KBr): *υ* 3546, 3304, 3264, 1637, 903 cm^{-1}.

2.4.4 *t-Butyl-4-bromo-3,5-dimethylphenylcarbamate*[22] ***(6b)***

To a stirred solution of **5b** (0.25g, 1.206 mmol) and glacial acetic acid (2 mL) was added a solution of bromine (0.19g, 1.206 mmol) in glacial acetic acid (2 mL) dropwise over 10 minutes. The resulting brown suspension was stirred at room temperature until a white suspension formed (approx. 4 hours). The product was extracted with ethyl acetate (3 x 5mL). The combined organic phases were washed with water (3 x 30 mL) and dried over anhydrous $MgSO_4$. Removal of the solvent yielded the pure product as a white solid. Yield (0.18g, 53%) ^{1}H NMR ($CDCl_3$): δ 1.44 (s, 9H), 2.30 (s, 6H), 6.38 (s, 1H), 7.03, (s, 1H) ppm. ^{13}C NMR ($CDCl_3$): 20.2, 29.8, 79.2, 121.2, 125.3, 138.3, 136.2, 155.7 ppm. FT-IR (KBr) *υ* 3353.35, 2978.32, 1694.31, 905.4 cm^{-1}.

2.4.5 *4-Bromo-3,5-dimethylaniline*[22] ***(7)***

To a stirred of solution of **6b** (0.75g, 2.862 mmol) in CH_2Cl_2 (2 mL) was added trifluoroacetic acid (2 mL). The resulting brown solution was stirred at room temperature. After 3 hours, the dark brown solution was carefully basified (pH 11) with a 30% solution of NaOH in water. The product was extracted with CH_2Cl_2 (3 x 3 mL). The combined organic phases were washed with water (3 x 15mL), 5% citric acid solution (2 x 5 mL) and water again (3 x 5 mL). The organic layer was dried over anhydrous $MgSO_4$ and filtered. After removal of the solvent, the desired product was isolated as a brown oil. (Yield = 0.23g, 52 %) ^{1}H NMR ($CDCl_3$): δ 2.33 (s, 6H), 3.54 (s, 2H), 6.45 (s, 2H) ppm. ^{13}C NMR ($CDCl_3$): δ 20.6, 118.2, 125.3, 138.3, 145.7 ppm. FT-IR (KBr) *υ* 3353, 2978, 905 cm^{-1}.

2.4.6 4-Cyano-3,5-dimethylaniline[25] (8)

To a stirred of solution of **7** (0.23g, 1.15 mmol) in 2-pyrrolidinone (3 mL) was added Cu(I)CN (0.10g, 1.15 mmol). The resulting suspension was heated to 135^{o}C. After 4 days, the black suspension was allowed to cool to room temperature and cooled further to 0^{o}C. To the cooled suspension was added concentrated NH_4OH (40 mL) followed by water (40mL) and the resulting suspension stirred for 3 hours. The brown solid was collected and washed with cold water (3 x 15mL) and dried overnight under vaccum. (Yield = 0.05g, 30 %) ^{1}H NMR ($CDCl_3$) δ 2.63 (s, 6H), 6.52 (s, 2H), 7.65 (s, 2H) ppm. ^{13}C NMR ($CDCl_3$): 21.6, 115.2, 117.5, 144.9 ppm. FT-IR (KBr): υ 3450, 3002, 2999, 2210 cm^{-1}.

2.4.7 Iodo-2,3,5,6-tetramethylbenzene[25] (16)

To a stirred suspension of 2,3,5,6-tetramethylbenzene (5.0 g, 37.30 mmol), iodine (3.78g, 14.70 mmol) and periodic acid (1.70g, 7.45 mmol) was added a solution of sulfuric acid (1.10 mL), water (7.50 mL) and glacial acetic acid (37.5 mL). The resulting purple solution was stirred and heated to 70^{o}C. After an hour, the off-white suspension was filtered and the white solid recrystallized from acetone. The desired product was obtained as white crystalline needles. Yield (3.50g, 36%) ^{1}H NMR ($CDCl_3$): δ 2.33 (s, 6H), 2.463 (s, 6H), 6.910 (s, 1H) ppm. ^{13}C NMR ($CDCl_3$): 21.85, 26.81, 11.79, 131.66, 134.31, 137.79 ppm. FT-IR (KBr): υ 3001, 2919, 1466 cm^{-1}.

2.4.8 Cyano-2,3,5,6-tetramethylbenzene[26] (17)

To a stirred suspension of Cu(I)CN (0.89g, 9.92 mmol) in hexamethylphosphoric triamide (2.65g, 14.76 mmol) was added **16** (2.0g, 7.69 mmol). The green suspension was stirred and heated to 100^{o}C. After 5 hours, the black solution was allowed to cool temperature. To the black solution was added an aqueous solution of $FeCl_3$ (15 mL, 1M). The resulting black precipitate was collected and washed with 0.5M solution of sodium bisulfite (3 x 15 mL)

followed by water (3 x 20 mL). The tan solid was air-dried and transferred into a Soxhlet thimble. The product was extracted with light petroleum ether (b.p. 38-53^{o}C) using a Soxhlet extractor (17 hours). Removal of the solvent under reduced pressure yielded **17** as a white crystalline solid. Yield (0.43g, 21%). ^{1}H NMR ($CDCl_3$): δ 2.24 (s, 6H), 2.43 (s, 6H), 7.12(s, 1H) ppm. ^{13}C NMR ($CDCl_3$): δ 18.09, 19.74, 114.13, 118.57, 134.68, 135.50, 137.90 ppm. FT-IR (KBr): *υ* 3002, 2923, 2213 cm^{-1}.

2.4.9 *1,4-Dibromo-2,3,5,6-tetramethylbenzene*[25] ***(18)***

To a stirred solution of 2,3,5,6-tetramethylbenzene (15.0 g, 111.7 mmol) in 45 mL of CH_2Cl_2 was added iodine (0.233 g, 0.916 mmol). The dark brown solution was stirred for 10 minutes and bromine (86.18 g, 539 mmol) was added slowly over an hour in the dark. After the addition, the red-brown solution was heated to reflux and stirred for 20 hours. The dark red-brown solution was allowed to cool to room temperature and 240 mL of 5M NaOH solution was added slowly. The yellow mixture was extracted with CH_2Cl_2 (3 x 40 mL). The combined organic layers were washed with distilled water (3 x 20 mL). The product was recrystallized from CH_2Cl_2 to leave fine white needles that were dried under vacuum. Yield (27.0 g, 83%) ^{1}H NMR ($CDCl_3$): δ 2.49 (s, 12H) ppm. ^{13}C NMR ($CDCl_3$): δ 135.25, 128.36, 22.53 ppm. FT-IR (KBr): *υ* 2999, 2853 (C-H, s), 1414, 1381 (C-H, b), 1170 (C-Br, s) cm^{-1}.

2.4.10 *4-Cyano-2,3,5,6-tetramethyl-bromobenzene*[28] ***(19)***

To a stirred suspension of CuCN (1.29 g, 14.38 mmol) in 30 mL of dimethylformamide was added **18** (3.00 g, 10.37 mmol). The green suspension was stirred and held at reflux temperature. After 15 hours, the orange colored mixture was cooled to room temperature and a solution of $FeCl_3$ (55.7 g, 0.34 mmol) in concentrated HCl (17 mL) and distilled water (68.5 mL) was added slowly over a period of 30 minutes. The product was extracted with $CHCl_3$ (3 x 40 mL) and washed with brine (3 x 30 mL) followed by distilled water (3 x 20 mL). The organic layer was dried over anhydrous sodium sulfate and the solvent removed under reduced pressure to yield an off-white crystalline solid. Pure product was obtained by column chromatography

(9:1 ; petroleum ether:ethyl acetate) as white needles. Yield (0.78 g, 32%). ^{1}H NMR ($CDCl_3$): δ 2.55 (s, 6H), 2.43 (s, 6H) ppm. ^{13}C NMR ($CDCl_3$): δ 138.59, 135.61, 134.49, 118.31, 113.59, 21.16, 20.04 ppm. FT-IR (KBr): υ 2988 (C-H, s), 2221 (C≡N, s) 1219 (C-Br, s) cm^{-1}.

2.4.11 *4-Bromo-2,3,5,6-tetramethylbenzaldehyde[28] **(20)***

To a stirred solution of **19** (0.50g, 2.10 mmol) in anhydrous CH_2Cl_2 (20 mL) was slowly added diisobutylaluminium hydride (0.36 g, 2.56 mmol) as a 1M solution in toluene over 20 minutes via syringe at 0^{o}C under argon. After addition was completed, the solution was allowed to warm to room temperature overnight under argon. The reaction mixture was quenched with 1M HCl (10 mL) and refluxed for 30 minutes. The organic layer was washed with distilled water (3 x 10 mL) and dried over anhydrous sodium sulfate. The solvent was removed under reduced pressure to leave a white crystalline solid. Pure product was obtained by column chromatography (9:1; petroleum ether:ethyl actetate) as white needles. Yield (0.50 g, 99%) ^{1}H NMR ($CDCl_3$): δ 10.61 (s, 1H), 2.46 (s, 6H), 2.45 (s, 6H) ppm. ^{13}C NMR ($CDCl_3$): δ 20.03, 21.15, 113.58, 118.30, 134.49, 135.60, 138.58 ppm. FT-IR (KBr): υ 2955 (C-H, s), 1639 (C=O, s), 1127 (C-Br, s) cm^{-1}.

2.4.12 *4-Cyano-2,3,5,6-tetramethylbenzaldehyde[28] **(21)***

To a stirred solution of CuCN (0.104 g, 1.16 mmol) in dimethylformamide (10 mL) was added **20** (0.20 g, 0.829 mmol). The resulting green solution was purged with argon and heated to 165^{o}C. After 14 hours, the orange-brown solution was allowed to cool to room temperature and an aqueous solution of $FeCl_3$ (0.74 g, 4.56 mmol) in concentrated HCl (0.27 mL) and distilled water (0.9 mL) was added carefully. The mixture was stirred at 75^{o}C for 20 minutes and allowed to cool back to room temperature. The mixture was diluted with $CHCl_3$ (40 mL) and washed with brine (2 x 15 mL) followed by distilled water (2 x 15 mL). The organic layer was dried over anhydrous $NaSO_4$. Filtration and removal of the solvent under reduced pressure afforded the pure product as a pale yellow solid. Yield (0.06 g, 6%) ^{1}H NMR ($CDCl_3$): δ 10.62

(s, 1H), 2.52 (s, 6H), 2.38 (s, 6H) ppm. ^{13}C NMR ($CDCl_3$): δ 15.79, 18.67, 117.85, 134.81, 139.00, 141.56, 196.24 ppm. FT-IR (KBr): *υ* 2963 (s), 2225 (s), 1702 (m) cm^{-1}.

2.4.13 *4-cyano-2,3,5,6-tetramethylbenzoic acid*[29] ***(14)***

To a cooled (0^oC) solution of H_5IO_6 (0.107 g, 0.470 mmol) in CH_3CN (5 mL) was added a solution of **21** in CH_3CN and a solution of pyridinium chlorochromate in CH_3CN (2 mL). The orange solution was stirred at 0^oC for 3 hours. The reaction solution was then diluted with EtOAc (25 mL) and washed with brine-water (as a 1:1 mix by volume; 3 x 10 mL) followed by sat. aq. $NaHSO_3$ solution (2 x 5 mL) and brine (3 x 10 mL). The organic later was dried over anhydrous Na_2SO_4 and concentrated. Repeated attempts at purification by acid-base extraction and column chromatography were not successful presumably due to decomposition or unsuccessful elution of the product.

2.4.14 *4'-cyano-2',3',5',6'-tetramethylbiphenyl-4-carboxylic acid*[32] ***(27)***

To a stirred suspension of **19** (0.69g, 2.41 mmol) and 4-carboxyphenylboronic acid (0.40g, 2.41 mmol) in CH_3CN (30 mL) was added an aqueous solution of Na_2CO_3 (0.51g, 4.82 mmol). Argon was bubbled through the resulting colorless solution. After 15 minutes, tetrakis(triphenylphosphine) palladium (0) (0.070g, 0.06 mmol) was added and the flask was fitted with a condenser. The orange suspension was heated to reflux under argon with constant stirring. The reaction was monitored by TLC (hexane/ethyl acetate; 3/1). After 48 hours at reflux, a white solid precipitated from the orange solution. The solids were collected and washed with water and cold ether. The desired product was collected as a white crystalline solid and dried under vaccum for 24 hours. Yield = 0.52g, 77%. ^1H NMR ($CDCl_3$): δ 1.92 (s, 6H), 2.53 (s, 6H), 7.21 (d, 2H, J=7.97), 8.23 (d, 2H, J=7.97) ppm. ^{13}C NMR (DMSO-d_6): δ 15.43, 18.54, 112.66, 118.04, 128.79, 129.73, 132.67, 137.27, 145.02, 145.16, 167.07, 194.59 ppm. FT-IR (KBr): υ (*s* strong, *m* medium, *w* weak) 3206 s, 3104 *m*, 3032 *w*, 2930 *w*, 2238 *s*, 1735 *s*, 1209 *s*, 1090 *s*, 1017 *m*, 864 *m*, 811 *m*, 698 *m*, 652 *m* cm^{-1}. MALDI-MS ($m/z + H^+$) 251.39 (calculated m/z 250.34).

2.4.15 4'-cyano-2',3',5',6'-tetramethylbiphenyl-4-isocyanate[31] (30)

To a stirred suspension of **27** (0.40g, 1.43 mmol) in 15 mL of THF was added diphenylphosphoryl azide (DPPA) (0.309 mL, 1.43 mmol) followed quickly by 1,8-bis(dimethylamino)naphthalene (0.61g, 2.86 mmol). The vigorously stirred pale yellow solution was heated slowly to reflux under argon. After 48 hours the dark yellow solution was cooled to room temperature and filtered under argon. The solvent was removed from the dark yellow filtrate to leave a yellow/orange oil which was analyzed by ^{1}H NMR, IR and MALDI-ToF mass spectroscopy. Unfortunately no trace of the desired isocyanate was observed.

2.4.16 4-(pyridine-4-yl)phenylisocyanate[31] (31)

To a stirred suspension of **28** (0.40g, 2.01 mmol) in 15 mL of THF was added DPPA (0.55g, 2.01 mmol) followed quickly by 1,8-bis(dimethylamino)naphthalene (0.86g, 4.02 mmol). The vigorously stirred brown suspension was heated slowly to reflux and held at reflux temperature under argon. After 48 hours the yellow solution (with white precipitate) was cooled to room temperature and filtered under argon. The solvent was removed from the yellow filtrate. Unfortunately no evidence for the formation of the desired isocyanate was seen by FT-IR or MALDI-ToF mass spectroscopy.

2.4.17 4-(pyridin-3-yl)phenylisocyanate[31] (32)

To a stirred suspension of **29** (0.40g, 2.01 mmol) in 15 mL of THF was added DPPA (0.55g, 2.01 mmol) followed quickly by 1,8-bis(dimethylamino)naphthalene (0.86g, 4.02 mmol). The vigorously stirred brown suspension was heated slowly to reflux and held at reflux temperature under argon. After 48 hours the yellow solution (with white precipitate) was cooled to room temperature and filtered under argon. The solvent was removed from the yellow filtrate. The yellow residue still contained unreacted carboxylic acid, **1** (20%). ^{1}H NMR (DMSO-d_6): δ 7.62-7.69 (dd, 1H, J1=8.06, J2=5.04), 7.88-8.09 (dd, 4H, J1=24.64, J2=8.39) 8.31 (d, 1H, J=8.06), 8.69 (d, 1H, J=4.03), 9.04 (s, 1H) ppm. ^{13}C NMR (DMSO-d_6): δ 125.34, 135.82, 139.95, 145.02, 146.17, 155.61, 160.39, 163.25, 175.04, 188.26, 190.64 ppm.

2.4.18 3'-amino-2,3,5,6-tetramethylbiphenyl-4-carbonitrile[32] (45)

To a stirred suspension of **22** (0.20g, 0.840 mmol) and 3-aminophenylboronic acid, **44** (0.115g, 0.840 mmol) in CH_3CN (5 mL) was added an aqueous solution of Na_2CO_3 (0.178g, 1.68 mmol). Argon was bubbled through the resulting white suspension. After 15 minutes, tetrakis(triphenylphosphine) palladium (0) (0.0200g, 0.021 mmol) catalyst was added and the flask was fitted with a condenser. The orange suspension was heated to reflux under argon with constant stirring. The reaction was monitored by TLC (hexane:ethyl acetate; 3:1). After 36 hours at reflux, a white solid precipitated from the orange solution. The solids were collected and washed with water and cold acetonitrile. The white solid was the desired product and proved to have very poor solubility in both polar and non-polar solvents. (Yield = 0.14g, 64%) ^{1}H NMR ($CDCl_3$): δ 1.95 (s, 6H), 2.50 (s, 6H), 3.73 (s, br, 2H), 6.45 (s, 1H), 6.49 (d, 1H, J=7.42 Hz), 6.77 (d, 1H, J=10.15 Hz), 7.25 (t, 1H, J=8 Hz) ppm. ^{13}C NMR ($CDCl_3$): δ 17.86, 19.07, 113.30, 114.68, 115.95, 118.85, 119.94, 129.91, 133.37, 134.78, 137.68, 142.55, 146.57 ppm. FT-IR (KBr): υ (*s* strong, *m* medium, *w* weak) 3445 *m*, 3335 *m*, 3234 *m*, 3097 *w*, 3053 *m*, 2991 *m*, 2922 *m*, 2219 *s*, 1640 *s*, 1492 *s*, 1453 *s*, 1384 *m*, 1329 *s*, 1244 *s*, 1019 *s*, 995 *s*, 874 *m*, 787 *s*, 707 *s*, 656 *w*, 593 *w* cm^{-1}. MALDI-MS ($m/z + H^+$) 251.39 (calculated m/z 250.34).

2.4.19 3-(pyridin-3-yl)phenylamine[32] (47)

To a 200 mL round bottom flask was added 3-aminophenylboronic acid (2.000 g, 12.91 mmol), 3-bromopyridine (2.039g, 12.91 mmol), Na_2CO_3 (2.736g, 25.81 mmol) and tetrakis(triphenylphosphine) palladium (0) (0.373g, 0.00323 mmol), followed by CH_3CN (40 mL) and H_2O (40 mL). Argon was bubbled through the resulting orange suspension for 15 minutes. A condenser was attached and the mixture was maintained at 75^{o}C with stirring under argon. The reaction was monitored by TLC, and was allowed to cool to room temperature upon completion (48 hours). The orange solution was then diluted with ethyl acetate (50 mL) and washed with distilled water (3 x 30 mL), and saturated aqueous sodium chloride (2 x 20 mL). The organic phase was separated and dried over anhydrous $MgSO_4$. The solvent was removed under reduced pressure and the orange oil chromatographed on silica with petroleum ether:ethyl

acetate (2:1) as eluant. The product was isolated as an off-white solid. Yield = 1.93g (88%) ^{1}H NMR (400 MHz, $CDCl_3$): δ 5.22 (br. s., 2H) 6.73 (d, *J*=7.87 Hz, 1H) 6.88 (s, 1H) 6.96 (d, *J*=7.69 Hz, 1H) 7.23 - 7.26 (m, 1H) 7.35 - 7.39 (m, 1H) 7.87 (d, *J*=7.87 Hz, 1H) 8.57 (d, *J*=4.94 Hz, 1H) 8.83 (s, 1H) ppm. ^{1}H NMR (400 MHz, CD_3CN): δ 4.27 (br. s., 2H) 6.69 (d, *J*=7.81 Hz, 1H) 6.89 - 6.93 (m, 2H) 7.20 (t, *J*=8.00 Hz, 1H) 7.38 (dd, *J*=7.81, 4.69 Hz, 1H) 7.91 (d, *J*=7.81 Hz, 1H) 8.52 (d, *J*=4.69 Hz, 1H) 8.79 (s, 1H) ppm. ^{13}C NMR (101 MHz, $CDCl_3$): δ 113.80, 114.97, 117.66, 123.63, 130.22, 134.48, 137.00, 139.21, 147.24, 148.52, 148.63 ppm. FT-IR (KBr): *υ* 3334, 3116, 1609, 1481, 1409, 1322, 1235, 1169, 1023, 864, 777, 698 cm^{-1}. MALDI-ToF/ToF-MS: *m/z* 171.23 ([**47** + H^+]) (calculated m/z 170.043).

2.4.20 *3-(pyridin-3-yl)phenylamino hydrochloride salt (**47.HCl**)*

To a solution of **47** (1.14g, 6.693 mmol) in anhydrous THF (5 mL) was added a solution of 2N HCl in ether (3.35 mL, 6.693 mmol) via syringe. A pale yellow precipitate formed immediately upon addition of the HCl solution. The yellow suspension was stirred for another 20 minutes. The solvent was removed under reduced pressure and the precipitate washed with a several times with a minimal amount of chloroform. The pale yellow solid was dried under reduced pressure for 24 hours at 45^{o}C. The pure product was isolated as a pale yellow solid. Yield (1.03g, 74%). ^{1}H NMR (400 MHz, D_2O): δ 7.60 (d, *J*=7.81 Hz, 1H), 7.73 - 7.81 (m, 1H), 7.88 (d, *J*=8.20 Hz, 1H), 8.19 (dd, *J*=8.20, 5.86 Hz, 1H), 8.83 (d, *J*=5.86 Hz, 1H), 8.90 (d, 1H), 9.12 (s, 1H) ppm.

2.4.21 *3'-(triphenylphosphine)imine-2,3,5,6-tetramethylbiphenyl-4-carbonitrile[21] (**48**)*

To a suspension of PPh_3Br_2 (0.27g, 639 mmol) in benzene (15 mL) was added a solution of **45** (0.16g, 639 mmol) in benzene (5 mL) followed by triethylamine (0.178 mL, 1.28 mmol). The flask was maintained under argon and fitted with a condenser. The mixture was then heated to reflux and stirred overnight. After 16 hours, a pale yellow suspension was filtered. The colorless oil was dried under vacuum for 30 hours to yield the desired product as a off-white

solid. (Yield = 0.11g, 0.34%) ^{1}H NMR ($CDCl_3$): δ 2.46 (s, 6H), 2.49 (s, 6H), 6.81 (d, 1H), 6.91 (d, 1H), 7.10 (t, 1H), 7.47-7.67 (m, 15H) ppm. ^{13}C NMR ($CDCl_3$): δ 19.09, 25.48, 50.21, 74.52, 106.32,111.98, 113.10, 118.72, 128.68, 128.79, 132.17, 132.20, 132.37, 133.20, 146.71, 157.46, 159.32 ppm. ^{31}P NMR (($CDCl_3$; external reference = H_3PO_4): δ 11.43 ppm. MALDI-MS (m/z + H^+) 511.56 (calculated m/z 510.60).

*2.4.22 3-(triphenylphosphine)imine-(4-pyridyl)-benzene[21] (**49**)*

To a suspension of PPh_3Br_2 (0.74g, 1.76 mmol) in benzene (15 mL) was added a solution of **46** (0.30g, 1.76 mmol) in benzene (5 mL) followed by triethylamine (0.49 mL, 3.53 mmol). The flask was maintained under argon and fitted with a condenser. The mixture was then heated to reflux and stirred overnight. After 16 hours, a yellow suspension was filtered. The yellow oil was dried under vacuum for 36 hours to yield the desired product as a pale yellow solid. (Yield = 0.27g, 76%) ^{1}H NMR ($CDCl_3$): δ 6.84 (d, 1H, J = 7.81), 6.93 (d, 1H, J = 7.81), 7.08 (s, 1H), 7.30 (m, 1H), 7.49-7.65 (m, 15H), 7.77 (d, 1H), 8.52 (d, 1H) ppm. ^{13}C NMR ($CDCl_3$): δ 121.72, 122.31, 123.88, 124.05, 128.52, 128.62, 128.75, 128.95, 129.47, 132.12, 132.34, 132.85, 132.94 ppm. ^{31}P NMR ($CDCl_3$; external reference = H_3PO_4): δ 16.41 ppm. FT-IR (KBr): *υ* (*s* strong, *m* medium, *w* weak) 3402 *s*, 3234 *m*, 3059 *m*, 2930 *s*, 1633 *s*, 1479 *m*, 1434 *s*, 1194 *m*, 1105 *m*, 902 *m*, 749 *m* cm^{-1}. MALDI-MS (m/z + H^+) 431.40 (calculated m/z 430.49).

*2.4.23 3-(triphenylphosphine)imine-(3-pyridyl)-benzene[21] (**50**)*

To a suspension of PPh_3Br_2 (0.55g, 1.29 mmol) in benzene (10 mL) was added a solution of **47** (0.22g, 1.29 mmol) in benzene (5 mL) followed by triethylamine (0.36 mL, 2.59 mmol). The flask was maintained under argon and fitted with a condenser. The mixture was then heated to reflux and stirred overnight. After 16 hours, a yellow suspension was filtered. The pale yellow residue was dried under vacuum for 36 hours to yield the desired product as a pale yellow solid. (Yield = 0.35g, 56%) ^{1}H NMR ($CDCl_3$): δ 6.80 (t, 1H), 6.86 (s, 1H), 7.05 (t, 1H), 7.27 (d, 1H), 7.60 (d, 1H), 7.76 (multiplet, 1H) 8.46 (d, 1H), 8.61 (s, 1H) ppm.^{13}C NMR ($CDCl_3$): δ 121.72,

122.13, 122.31, 123.88, 124.05, 128.52, 128.62, 128.75, 128.95, 129.06, 129.47, 132.12, 132.34, 132.85, 132.94 ppm. ^{31}P NMR ($CDCl_3$; external reference = H_3PO_4): δ 13.68 ppm. FT-IR (KBr): *υ* (*s* strong, *m* medium, *w* weak) 3402 *s*, 3234 *m*, 3059 *m*, 2930 *s*, 1633 *s*, 1479 *m*, 1434 *s*, 1194 *m*, 1105 *m*, 902 *m*, 749 *m* cm^{-1} MALDI-MS ($m/z + H^+$) 431.44 (calculated m/z 430.49).

*2.4.24 3-(pyridin-4-yl)phenylimido hexamolybdate (**51**)*

To a 25 mL round bottom flask was added $[N(C_4H_9)_4]_4[\alpha\text{-}Mo_8O_{26}]$ (0.62 g, 0.287 mmol), DCC (0.20 g, 0.977 mmol), **46** (0.066 g, 0.385 mmol) and CH_3CN. The resulting off-white suspension was stirred for 10 minutes and allowed to settle before **46.HCl** was added (0.081 g, 0.385 mmol). The flask was fitted with a condenser and purged with argon for 15 minutes. A light red color developed upon stirring and the mixture was heated to reflux (75^{o}C). After 17 hours, a dark red solution with a suspension had formed and the reaction was allowed to cool to room temperature. The white precipitate (dicyclohexylurea by-product) was filtered and the filtrate concentrated. The product was recrystallized twice from the dark red filtrate by slow vapor diffusion of diethyl ether. Pure product was obtained as dark red crystals (Yield (based on initial amount of **46**) = 0.16g, 27.5 %). ^{1}H NMR (400 MHz, CD_3CN) δ 0.97 (s, 24H) 1.35 (s, 17H) 1.61 (br. s., 17H) 3.08 (s, 16H) 7.33 (br. s., 1H) 7.53 (br. s., 3H) 7.61 (br. s., 4H) 8.63 (br. s., 2H) ppm. FT-IR (KBr): *υ* (*s* strong, *m* medium, *w* weak) 2960 *s*, 2868 *m*, 1654 *m*, 1465 *m*, 1373 *m*, 1342 *m*, 974 *sh*, 953 s, 906 *w*, 794 *m*, 651 *m* cm^{-1}

*2.4.25 3-(pyridin-3-yl)phenylimido hexamolybdate (**52**)*

To a 50 mL round bottom flask was added $[N(C_4H_9)_4]_4[\alpha\text{-}Mo_8O_{26}]$ (0.54g, 0.251 mmol), DCC (0.18g, 0.855 mmol), **47** (0.057g, 0.337 mmol) and CH_3CN (10 mL). The resulting off-white suspension was stirred for 10 minutes and allowed to settle before **47.HCl** was added (0.07g, 0.337 mmol). The flask was fitted with a condenser and purged with argon for 15 minutes. A light red color developed upon stirring and the mixture was heated to reflux (75^{o}C). After 18 hours, a dark red suspension had formed and the reaction was allowed to cool to room

temperature. The white precipitate (dicyclohexylurea by-product) was filtered and the filtrate concentrated. The product was recrystallized twice from the dark red filtrate by slow vapor diffusion of diethyl ether. Pure product was obtained as dark red crystals. (Yield (based on initial amount of **47**) = 0.175g, 46%) ^{1}H NMR (400 MHz, $CDCl_3$) δ 0.98 (t, *J*=7.22 Hz, 24H, TBA) 1.46 - 1.53 (m, 16H, TBA) 1.63 - 1.69 (m, 16H, TBA) 3.23 - 3.31 (m, 16H, TBA) 7.21 (d, *J*=7.81 Hz, 1H) 7.32 - 7.40 (m, 3H) 7.54 (br. s., 1H) 7.88 (d, *J*=7.81 Hz, 1H) 8.60 (t, *J*=4.69 Hz, 1H) 8.81 (br. s., 1H) ppm. ^{1}H NMR (400 MHz, CD_3CN) δ 0.96 (t, *J*=7.42 Hz, 24H, TBA) 1.32 - 1.40 (m, 16H, TBA) 1.60 (quin, *J*=8.00 Hz, 16H, TBA) 3.06 - 3.12 (m, 16H, TBA) 7.30 (d, *J*=7.81 Hz, 1H) 7.40 - 7.56 (m, 4H) 8.01 (d, *J*=7.81 Hz, 1H) 8.58 (d, *J*=4.69 Hz, 1H) 8.85 (s, 1H) ppm. ^{13}C NMR (101 MHz, CD_3CN) δ 13.90 (TBA), 20.42 (TBA), 24.42 (TBA), 34.44, 59.40 (TBA), 124.76, 126.82, 127.83, 130.59, 130.49, 135.48, 149.14, 150.05, 195.65 ppm. FT-IR (*KBr*): *υ* (*s* strong, *m* medium, *w* weak, *sh* shoulder) 2959 *m*, 2933 *m*, 2873 *m*, 1481 *m*, 1465 *m*, 1375 *w*, 1345 *w*, 975 (*sh*), 950 *s*, 785 *s*, 712 (*sh*), 606 *w*, 446 *w* cm^{-1}. Elemental Analysis Observed (Calculated): %C 36.91 (34.05), %H 5.61 (5.32), %N 3.92 (3.69).

2.4.26 *[3-(pyridin-3-yl)phenylimidohexamolybdate][meso-(5,10,15,20-tetraphenylporphyrinato)carbonyl ruthenium-(II)] (**70**)*

To a red suspension of **68** (4.0 mg, 0.00508 mmol) in $CHCl_3$ (3 mL) was added **52** (7.7 mg, 0.00508 mmol) with stirring at room temperature under argon. A dark red solution formed within 5 minutes which was stirred for a further 30 minutes. The solvent was removed under reduced pressure to leave a dark red solid. Yield assumed to be quantitative. ^{1}H NMR (400 MHz, $CDCl_3$) δ 0.87 (t, *J*=7.22 Hz, 24H, TBA), 1.27 (br. s., 1H, pyr), 1.33 - 1.43 (m, 16H, TBA), 1.56 (d, *J*=3.12 Hz, 17H, TBA + 1H pyr), 3.18 (br. s., 16H, TBA), 5.26 (m, 1H, pyr), 5.34 (s, 1H, pyr), 5.53 (d, *J*=7.03 Hz, 1H, pyr), 6.27 (d, *J*=4.69 Hz, 1H, pyr), 6.47 (s, 1H, pyr) 7.06 (m, 1H, pyr), 7.72 (br. s., 8H, RuTPP), 7.65 (br. s., 4H, RuTPP) 8.02 (br. s., 4H, RuTPP), 8.25 (br. s., 4H, RuTPP), 8.63 (m, 8H, RuTPP) ppm. ^{13}C NMR (101 MHz, $CDCl_3$) δ 13.92 (TBA), 19.88 (TBA), 24.30 (TBA), 58.93 (TBA), 121.73, 124.52, 126.49, 126.53, 126.67 (RuTPP), 126.74, 127.39, 127.48 (RuTPP), 128.39, 131.95, 131.99 (RuTPP), 134.36 (RuTPP), 134.53, 134.60, 142.82,

142.93 (RuTPP), 143.84 (RuTPP), 182.36 (C≡O) ppm. FT-IR (KBr): υ (*s* strong, *m* medium, *w* weak, *sh* shoulder) 2959 *m*, 2920 *m*, 2871 *m*, 1938 w, 1650 *m*, 1459 *m*, 1384 *m*, 1009 *m*, 963 (*sh*), 951 *s*, 789 *s*, 811 *m*, 599 *m* cm^{-1}. UV-Vis ($CDCl_3$) λ (log ε): 585 (3.97), 533 (4.25), 495 *sh* (4.00), 410 (5.24), 315 (4.34), 291 (4.37) nm. MALDI-ToF/ToF-MS: 714.023 m/z (calculated as $^{12}C_{44}{}^{1}H_{28}{}^{14}N_4{}^{102}Ru_{1;}$ $[RuTPP]^+$ = 714.1353 m/z).

*2.4.27 [3-(pyridin-3-yl)phenylamine][meso-(5,10,15,20-tetraphenyl-porphyrinato) carbonyl ruthenium-(II)] (**71**)*

To a 10 mL round bottom flask was added a dark red suspension of **68** (5.0 mg, 0.00635 mmol) in 1 mL of $CHCl_3$ followed by a colorless solution of **47** (1.2 mg, 0.00635 mmol) also in 1 mL of $CDCl_3$ under argon at room temperature. Immediately upon addition, a dark red suspension formed which was stirred for a further 10 minutes. The solvent was removed under reduced pressure to leave a dark red solid. Yield assumed to be quantitative. ^{1}H NMR (400 MHz, $CDCl_3$) δ 1.52 (dd, *J*=5.66, 1.37 Hz, 1H, pyr) 1.63 (d, *J*=1.95 Hz, 1H, pyr) 3.53 (br. s., 2H, -NH_2) 5.21 (dd, *J*=7.61, 5.66 Hz, 1H, pyr) 5.34 (t, *J*=1.95 Hz, 1H, pyr) 5.63 (d, *J*=7.42 Hz, 1H, pyr) 6.26 (ddd, *J*=8.00, 1.76, 1.56 Hz, 1H, pyr) 6.46 (dd, *J*=7.81, 1.95 Hz, 1H, pyr) 6.86 (t, *J*=7.81 Hz, 1H pyr) 7.65 (br. s., 5H, RuTPP) 7.72 (br. s., 8H, RuTPP) 8.03 (d, *J*=7.42 Hz, 4H, RuTPP) 8.25 (br. s., 4H, RuTPP) 8.63 (s, 9H, RuTPP) ppm. ^{13}C NMR (101 MHz, $CDCl_3$) δ 114.90, 116.15, 121.78, 126.50 (RuTPP), 126.77, 127.44 (RuTPP), 131.97 (RuTPP), 132.16, 132.27, 134.27 (RuTPP), 134.57, 142.86, 143.86 (RuTPP) ppm. FT-IR (KBr): υ (*s* strong, *m* medium, *w* weak, *sh* shoulder) 2965 *s*, 2931 *m*, 2874 *m*, 1938 *w*, 1637 *m*,1482 *m*, 1382 *m*, 1192 *w*, 944 (*sh*), 923 m, 904 *s*, 851 *w*, 712 *w*, 665 *m* cm^{-1}. UV-Vis ($CDCl_3$) λ (log ε): 531 (3.07), 410 (3.91), 313 (3.04), 239 (3.09) (4.37) nm. MALDI-ToF/ToF-MS: 714.141 m/z (calculated as $^{12}C_{44}{}^{1}H_{28}{}^{14}N_4{}^{102}Ru_1$: $[RuTPP]^+$ = 714.1353 m/z).

---

[1] (a) Proust, A., Thouvenot, R., Gouzerh, P., *Chem. Commun.* **2008**, 1837.

(b) Pope, M.T., Müller A., *Angew. Chem., Int. Ed. Engl.* **1991**, *30*, 34.
[2] Hill, C.L (Guest Editor), *Chem. Rev.* **1998**, *98*, 8.
[3] Zeng, H., Newkome, G.R., Hill, C.L., *Angew. Chem. Int. Ed.* **2000**, *39*, 1772.
[4] Special edition print, *Chem. Rev.*, **1998**, *98*, 77.
[5] Strong, J., Yap, G., Ostrander, R., Liable-Sands, Rheingold, A., Thouvenot, R., Gouzerh, P., Maatta, E.A., *J. Am. Chem. Soc.* **2000**, *122*, 639.
[6] Strong, J.B., Haggerty, B.S., Rheingold, A.L., Maatta, E.A., *Chem. Commun.*, **1997**, 1137.
[7] Moore, A., Kwen, H., Beatty, A., Maatta, E.A, *Chem. Comm.* **2000**, 1793.
[8] Stark, J., Young, V., Maatta, E.A., *Angew. Chem. Int. Ed. Engl.* **1995**, *34*, 2547.
[9] Stark, J., Rheingold, A., Maatta, E.A., *Chem. Comm.*, **1995**, 1165.
[10] Xu, B, Lu, M., Kang, J., Wang, D., Brown, J, Peng, Z., *Chem. Mater.* **2005**, *17*, 2841.
[11] Wu, P., Li, Q., Ge, N., Wei, Y., Wang, Y., Wang, P., Guo, H., *Eur. J. Inorg. Chem.* **2004**, 2819.
[12] Li, Q., Wei, Y., Hao, J., Zhu, Y., Wang, L., *J. Am. Chem. Soc.* **2007**, *129*, 5810.
[13] Li, Q., Zhu, L., Meng, X., Zhu, Y., Hao, J., Wei, Y., *Inorganica Chimica Acta* **2007,** *360*, 2558.
[14] Li, Q., Wu. P, Wei, Y., Xia, Y., Wang, Y., Guo, H., *Z. Anorg. Allg. Chem.* **2005**, *631*, 773.
[15] Moore, A., PhD Thesis, Kansas State University, **1998**.
[16] (a) Xu, B., Peng, Z., Wei, Y., Powell, D., *Chem. Comm.* **2003**, 2562.
(b) Kang, J., Xu, B., Peng, Z., Zhu, X., Wei, Y., Powell, D.R., *Angew. Chem. Int. Ed. Engl.* **2005**, *44*, 6902.
[17] Karcher J., *PhD Thesis, Kansas State University*, **2000**.
[18] Fuchs, J., Jarh, F.Z., *Naturfoch. B* **1968**, 1380.
[19] Che, M., Fournier M., Launay, J.P., *J. Chem. Phys.*, **1979**, *71*, 1954.
[20] Hur, N.H., Klemperer, W.G., Wang, R.C., *Inorg. Synth.* **1990**, *27*, 77.
[21] Kwen, H., PhD Thesis, Kansas State University, **2000**.
[22] T. W. Green, P. G. M. Wuts, *Protective Groups in Organic Synthesis*, Wiley-Interscience, New York, **1999**, 550-555, 740-743.
[23] T. W. Green, P. G. M. Wuts, *Protective Groups in Organic Synthesis*, Wiley-Interscience, New York, **1999**, 278.
[24] Rusanova, J, Pilkington, M., Decurtins, S., *Chem. Comm*. **2002**, 2236.
[25] Suzuki, H., *Org. Synth.* **1971**, *51*, 94.
[26] Suzuki, H., Koge, M., Hanafusa, T., *Bull. Chem. Soc. Jap.* **1978**, *51(4)*, 1168.
[27] Myung, B.Y., Kim, J.J., *J. Polymer Science: A, Polymer Chemistry* **2002**, *40*, 4217.
[28] Moorthy J.N., Mal, P., Singhal, N., Venkatarishnana, P., Malik, R., Venugopalan, P., *J. Org. Chem.* **2004**, *69*, 8459
[29] Hunsen, M., *Syntheses* **2005**, *15*, 2487.
[30] M. Ohashi, H. Kudo, S. Yamada, *J. Am. Chem. Soc.* **1979**, *101*, 2201.
[31] Gilman, J.W., Otonari, Y.A., *Synthetic Communications* **1993**, *23*(3), 335.
[32] Sekiya, R., Nishikiori, S., Ogura, K., *Inorg. Chem.* **2006**, *45*, 9233.
[33] (a)Li, W., Nelson, D.P., Jensen, M.S., Hoerrner, R.S., Cai, D., Larsen, R.D., Redier,

P.J., *J. Org. Chem.* **2002**, *67*, 5394.
(b) www.kinbester.com (CAS: 25487-66-5).

[34] Frontier Scientific Inc, P.O. Box 31 Logan, UT 84323-0031.

[35] Krishnamurthy, S.S., Ramabrahmam, A.R., Murthy, A.R.V., *Z. Anorg. Allg. Chem.* **1985**, *522*, 226.

[36] (a) Li, Q., Wu. P, Wei, Y., Xia, Y., Wang, Y., Guo, H., *Z. Anorg. Allg. Chem.* **2005**, *631*, 773.
(b) Qui, Y., Xu, L., Gao, G., Wang, W.,Li, F, *Inorg. CHim. Acta* **2006**, 451.

[37] (a) Li, Q., Wu. P, Wei, Y., Xia, Y., Wang, Y., Guo, H., *Z. Anorg. Allg. Chem.* **2005**, *631*, 773.
(b) Qui, Y., Xu, L., Gao, G., Wang, W.,Li, F, *Inorg. CHim. Acta* **2006**, 451.

[38] Soldatov, D., Ripmeester, J.A, *Chem. Eur. J.* **2001**, *7* (14), 2979.

[39] Favette, S., Hasenknopf, B., Vaissermann, J., Gouzerh, P., Roux, C., *Chem. Commun.* **2003**, 2664.

[40] Chow, B.C, Cohen, I.A., *Bioinorganic Chemistry* **1971**, *1*, 57.

[41] (a) Sasaki, T., Osgood, A.J., Kiappes, J.L., Kelly, K.F., Tour, J.M., *Organic Letters* **2008**, 10 (*7*), 1377.
(b) Da Ros, T., Prato, M., Guldi, D.M., Ruzzi, M., Pasimeni, L., *Chem. Eur. J.* **2001**, 7 (*4*), 816.
(c) Gianferrara, T., Giust, D., Bratsos, I., Alessio, E., *Tetrahedron*, **2007**, *63*, 5006.

[42] (a) Bonnet, J.J., Eaton, S.S., Eaton, G.R., Holm, R.H., Ibers, J.A., *J. Am. Chem. Soc.* **1973**, 95(*7*), 2141.
(b) Ball, R.G., Domazetis, G., Dolphin, D., James, B.R., Trotter, J., *Inorg. Chem.* **1981**, *20*, 1556.
(c) Gallo, E., Caselli, A., Ragaini, F., Fantauzzi, S., Masciocchi, N., Sironi, A., Cenini, S., *Inorg. Chem.* **2005**, *44*, 2039.
(d) Prodi, A., Indelli, M.T., Kleverlaan, C.J., Scandola, F., Alessio, E., Gianferrara T., Marzilli, L.G., *Chem. Eur. J.* **1999**, 5(*9*), 2668.

[43] Allain, C., Favette, S., Chamoreau, L.M., Vaissermann, J., Ruhlman, L., Hasenknopf, *Eur. J. Inorg. Chem.* DOI:10.1002/ejic.200701331.

[44] Allain, C., Favette, S., Chamoreau, L.M., Vaissermann, J., Ruhlman, L., Hasenknopf, B., *Polymer Preprints* **2007**, 48(*2*), 663.

[45] Gallo, E., Caselli, A., Ragaini, F., Fanauzzi, S., Masciocchi, N., Sironi, A., Cenini, S., *Inorganic Chemistry* **2005**, 44 (*6*), 2039.

[46] Little, R.G., Ibers, J.A., *J. Am. Chem. Soc.* **1973**, 95 (*26*), 8583.

[47] Allen, A.D., Senoff, C.V., *Canadian Journal of Chemistry* **1967**, *45*, 1337.

[48] Aäkeroy, C.B., Schultheiss, N., Desper, J., *Inorganic Chemistry* **2005,** 44*(14),* 4983.

[49] (a) Ruiz, J., Cutillas, N., López, F., Bautista, D., *Organometallics*, **2006**, *25*, 5768.
(b) Corbet, J.P., Mignani, G., *Chem. Rev.* **2006**, *106*, 2651.

CHAPTER 3 - A Chromium(V) Nitrido-Keggin Polyoxometalate, $[(Cr^{V}N)PW_{11}O_{39}]^{5-}$

3.1 Introduction

3.1.1 Transition metal nitrido complexes.

Transition metal nitrido complexes, $[L_nM{\equiv}N]$, are those which contain the $[N]^{3-}$ ligand. The nitrido ligand is isoelectronic[1] with the oxo $[O]^{2-}$ and organoimido $[N\text{-}R]^{2-}$ ligands prominent in the first two chapters of this thesis. As with oxo and organoimido systems, nitrido complexes are most prevalent for transition metals in their higher oxidation states. The field has been reviewed.[2,3,4,5] Although nitrido complexes are predominantly terminal or linearly bridging, other bonding modes have been identified (Figure 3.1).[6]

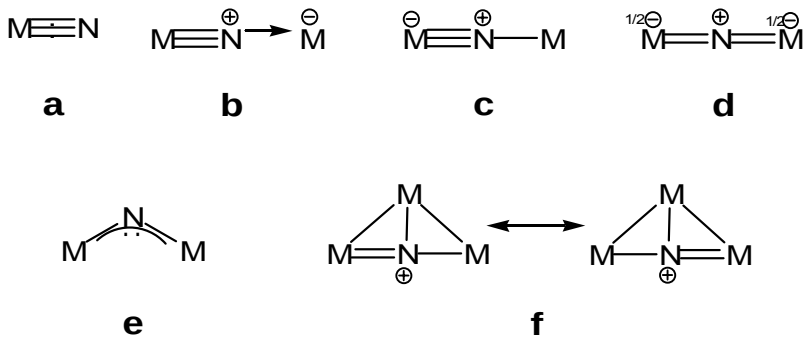

Figure 3-1: Known bonding modes of the nitrido ligand.[6] (a = linear; b = asymmetric; c = asymmetric, linear bridge of the donor acceptor type; c = asymmetric, linear bridge with covalent bond; d = symmetric, linear bridge; e = bent bridge; f = T-shaped)

Current interest in nitrido complexes stems in large part from their demonstrated ability to serve as N-atom transfer reagents following treatment with a suitable electrophile. An early example of such reactivity was reported by Groves and Takahashi[7] who showed that the Mn(V) nitrido-porphyrin complex [MnN(TMP)] (TMP = 5, 10, 15, 20- tetra-mesitylporphyrinato(2-)),

when treated with trifluoroacetic anhydride (TFAA), could transfer the [N-CO-CF_3] unit to the C=C double bond of cyclooctene; such an "aziridination" reaction is the nitrogen analogue of the well-known epoxidation reaction of olefins (Figure 3-2). More recently, Carreira has demonstrated similar nitrogen transfers utilizing nitrido-manganese complexes of salen-type ligands.[8,9]

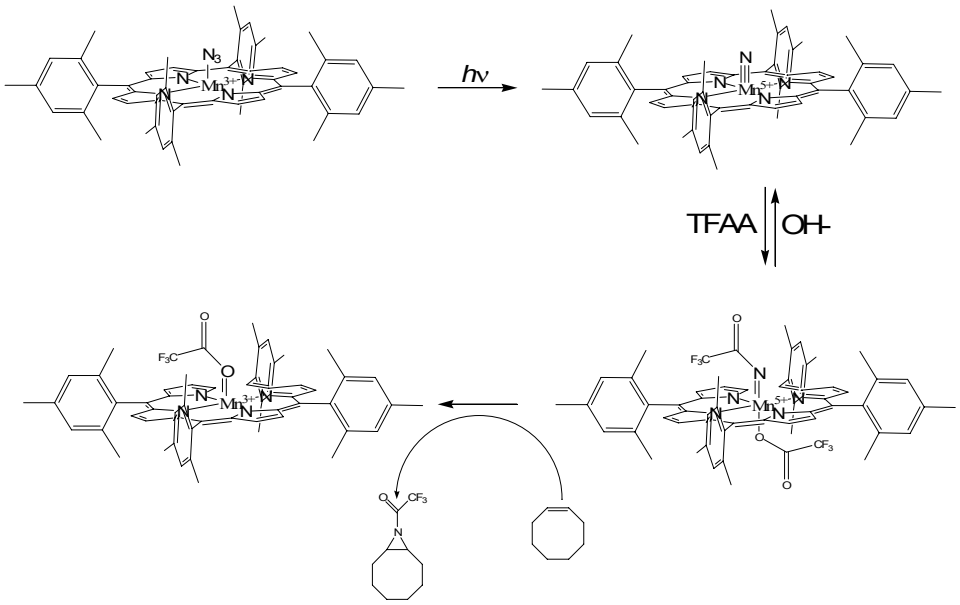

Figure 3-2: Groves reaction, [N-CO-CF_3] transfer onto cyclooctene from [$Mn^{V}N$(TMP)].[7](TFAA = trifluoroacetic anhydride)

Analogies between lacunary POM fragments and porphyrin (or salen-type) ligands have been recognized for some time.[10,11] Both of these ligand types are capable of stabilizing high oxidation state metal systems, and they generally display considerable thermal and oxidative stability (with POM systems typically being less prone to deterioration under harsh conditions).

Unlike the situation for the Lindqvist dianion $[Mo_6O_{19}]^{2-}$, only a few examples of nitrogenous derivatives of Keggin-type anions $[XM_{12}O_{40}]^{n-}$ species have been reported.[12,13] Many of the methods commonly used for direct functionalization of $[Mo_6O_{19}]^{2-}$ fail in the case of the corresponding Keggin systems (either through unwanted redox reactions or simple inertness to substitution); the main route to nitrogenous Keggin systems involve the reaction of a lacunary polyanion with a preformed metal-nitrogenous ligand.[12,13]

3.1.2 Metal Nitrides incorporated into Keggin Type POMs.

The parent Keggin POMs are denoted by the general formula, $[XM_{12}O_{40}]^{(n-)}$ (where X typically = P or Si; M = W or Mo). Removal of one $[M^{VI}O]^{4+}$ unit from the parent produces the lacunary structure, $[XM_{11}O_{39}]^{(n+4)-}$ (Figure 3-3). The lacunary structure can then be utilized as a pentadentate ligand through the five exposed oxygen atoms (Figure 3-3).[13a] In such 'insertion' reactions, the tungsten cluster framework has been found more stable and less likely to undergo reduction or structural transformations compared to the molybdenum analogue.[14]

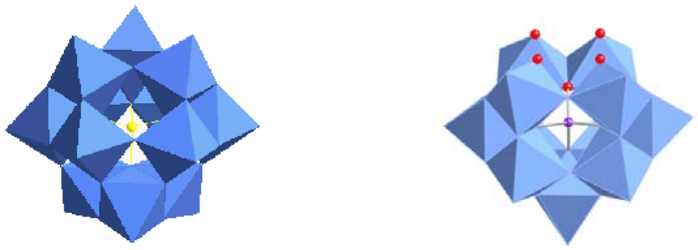

(a) (b)

Figure 3-3: Polyhedral models of (a) the parent Keggin ($[XM_{12}O_{40}]^{(n-)}$) and (b) the pentadentatelacunary Keggin ($[XM_{11}O_{39}]^{(n+4)-}$, red balls = exposed oxygen atoms).

Zubieta[15] reported the first nitrido-POM complex, $[Mo_6O_{18}\{N\}]^{3-}$ synthesized via cluster-assembly from dimolybdate instead of metal insertion into the lacunary Keggin (Figure 3-4). Zubieta also reported a nitrido-POM, $TBA_4[PW_{11}O_{39}\{TcN\}]$,[16] obtained via metal insertion into the lacunary Keggin system $[PW_{11}O_{39}]^{7-}$.

$$2\,[MoCl_4\{N\}]^- + 5\,[Mo_2O_7]^{2-} \xrightarrow{H_2O} 2\,[Mo_6O_{18}\{N\}]^{3-} + 6\,Cl^- + 2\,HCl$$

Figure 3-4: Cluster assembly reported by Zubieta, the first nitrido-POM.[15]

However, neither of these early nitrido-POM complexes were thoroughly characterized. More recently, Maatta and Proust synthesized and fully characterized $TBA_4[PW_{11}O_{39}\{Os^{VI}N\}]$[12] and $TBA_4[PW_{11}O_{39}\{Re^{V}N\}]$[13(a)] (Figure 3-5) as well as the Dawson-Wells analogue, $TBA_7[P_2W_{17}O_{61}\{OsN\}]$[17], the latter of which will be discussed further in the next chapter. These

[OsN] and [ReN] species were synthesized through insertion of a metal-nitrido fragment into the appropriate lacunary Keggin or Dawson-Wells POM.

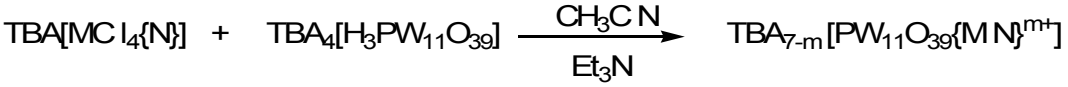

Figure 3-5: Synthesis of lacunary Keggin metal nitride complexes reported by Maatta and Proust. (M = Os[12], Re[13(a)]; TBA = $[^{n}Bu_4N]^+$)

Herein will be described a reproducible synthetic route to the titled, $Cr^{V}N$ Keggin, complex, as well as results from preliminary attempts at nitrogen atom transfer. These results, as a collaborative effort with our colleagues at the University of Paris, have been accepted for publication in the European Journal of Inorganic Chemistry.[18]

3.2 Results and Discussion

3.2.1 $TBA_4H[PW_{11}O_{39}\{CrN\}]$

As part of a series of metal Keggin type POMs, the title compound was synthesized in a similar manner to those mentioned earlier *i.e.* via insertion of **2,** the $\{Cr^{V}N\}$ moiety, into the lacunary Keggin, **1**. (Figure 3-6)

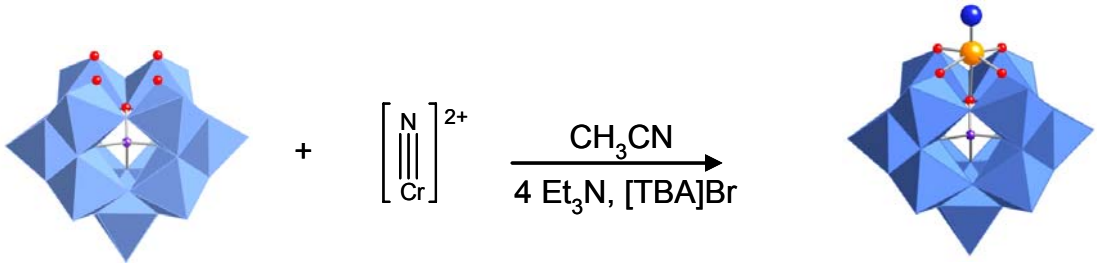

1 **2** **3**

Figure 3-6: Reaction scheme for the insertion of the $Cr^{V}N$ **2** into the lacunary Keggin **1**.[18]

The previous {OsN}-Keggin[12] **5** and {ReN}-Keggin[13] **7** syntheses, relied upon the pentadentate lacunary Keggin **1**, displacing either the chloride[12] or the chloride and phosphine[13] ligands of a preformed metal complex such as **4** and **6**, respectively (Figure 3-7).

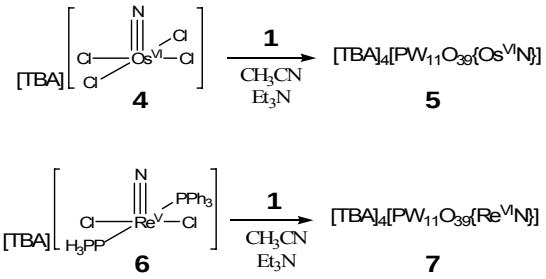

Figure 3-7: Delivery reagents **4** and **6** employed for the synthesis of the {OsN}-Keggin[12] **5** and {ReN}-Keggin[13] **7** Keggin POMs.

The synthetic method reported herein is similar but differs in the nature of the metal delivery reagent. The $Cr^{V}N$[19] precursor $[THF_x\{Cr^{V}N\}]^{2+}$ **2** was prepared via inter-metal N-atom transfer[20] between $[\{Mn^{V}N\}salen]$[20b] **8** and $[\{Cr^{III}Cl_3\}.THF_x]$[21] **9** (Figure 3-8), all of which were synthesized according to literature methods.[19a-21] A Mn(III) chloride salen **10** by-product was precipitated during the reaction and removed from the solution leaving the $Cr^{V}N$ reagent in the filtrate.

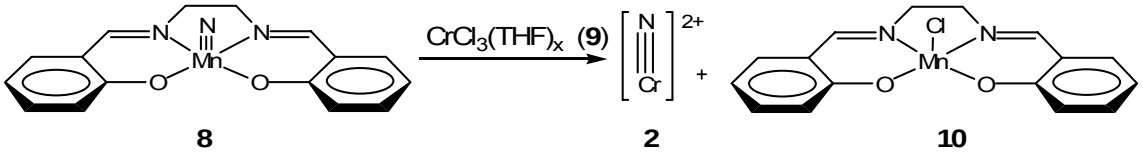

Figure 3-8: Formation of the $[Cr^{V}N]^{2+}$ delivery reagent **2**.[20b]

The introduction of the solvated $[Cr^{V}N]^{2+}$ species **2**, to a solution of $TBA_4[H_3PW_{11}O_{39}]$[22] **1** in the presence of excess triethylamine, TBABr and acetonitrile resulted in the rapid (within 30 seconds) formation of an orange mixture.[23] The formed polyanion **3a** (Figure 3-6), was isolated from the dark orange-brown reaction solution by slow diffusion of diethyl ether as orange crystals (yield 55%). The excess triethylamine, was added in order to quench the HCl by-product with the TBABr providing the necessary counter-cation to the desired Keggin complex (Figure 3-6). The paramagnetic nature of the Cr^{V} (d^1) limited the characterization of the CrN-Keggin **3a**

to infra-red (FT-IR), mass spectrometry, ^{31}P NMR and elemental analysis. The ^{31}P NMR spectrum (161.83 Hz, CD_3CN) revealed a broad signal at -11.85 ppm ($\Delta_{1/2}$ = 16 Hz); such a broadened signal is consistent with the presence of a paramagnetic Cr(V) center.

Initial mass spectrometry studies (MALDI-ToF/ToF MS) of **3a** suggested the presence of five $[TBA]^+$ counter-cations (Figure 3-9) as illustrated by the peak at 3956.02 m/z (calculated = 3956.65 m/z; as $^{12}C_{80}{}^{1}H_{181}{}^{14}N_6{}^{32}P_1{}^{134}W_{11}{}^{16}O_{39}{}^{52}Cr_1$, $[TBA]_5[PW_{11}O_{39}\text{-}\{CrN\}] + {}^{1}H$) and another at 3700.11 m/z. The latter corresponds to the loss of 256 m/z from the former, consistent with the loss of one nitrogen [N] atom and one $[TBA]^+$ cation. Another interesting feature was the extra peak of lower intensity at 3942.45 m/z, which strongly suggested the presence of $[TBA]_5[PW_{11}O_{39}\{Cr\}]$ (calculated = 3941.65 m/z) formed by the loss of a nitrogen atom (i.e. 14 m/z). These initial observations suggested the possible loss of a nitrogen atom, albeit in an unknown manner.

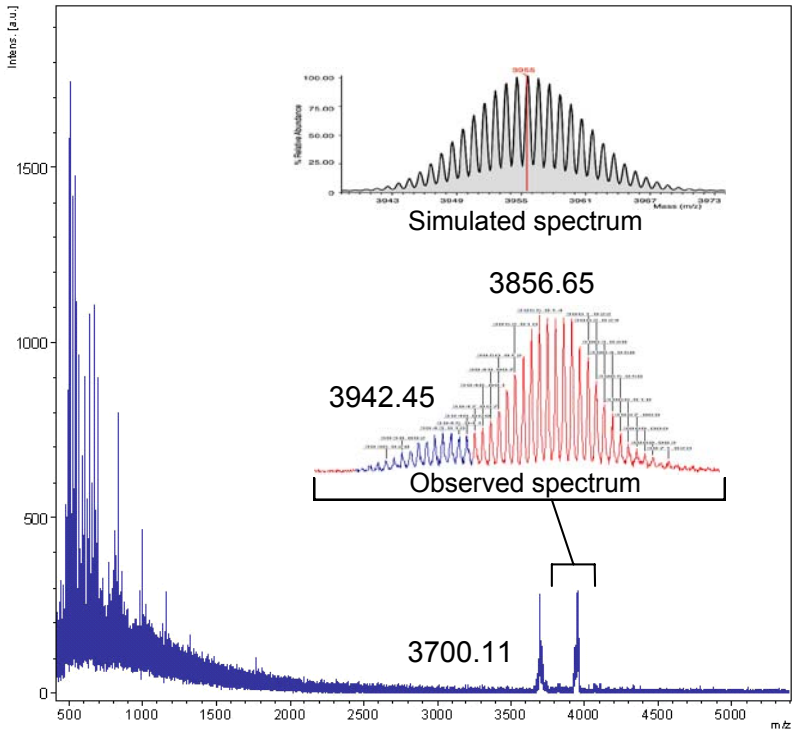

Figure 3-9: Observed Mass spectrum (Maldi-ToF/ToF) for $TBA_5[PW_{11}O_{39}\{CrN\}]$, **3a**.
(Inset top: simulated spectrum; Inset bottom: Expansion of 3925-4000 m/z)

Further analysis revealed the mass spectrum of the initial precipitate from the reaction mixture was almost identical to those of the purified orange crystals obtained after several

recrystallizations, with the exception of decreased intensity at 3956 m/z accompanied by increased intensity of 3942 and 3700 m/z in the mass spectra. Product decomposition occurred during attempted purification via column chromatography using silica gel. Furthermore, the CrN-Keggin **3a** was found to decompose after multiple recrystallizations in the presence of air as evidenced by the increased intensity of 3942 m/z along with a decreased intensity of 3956 m/z (mass spectrum).

An unexpected result came from the elemental analysis of the CrN-Keggin; instead of the expected five $[TBA]^+$ cations, elemental analysis strongly suggested the presence of only four $[TBA]^+$ units with one proton, which will now be called $[TBA_4H][PW_{11}O_{39}\{CrN\}]$ **3b** (Table 3-1 and Figure 3-10).

Table 3-1: Elemental Analysis of 3a from acetonitrile recrystallization.

	%C	% H	% N	% Cr
Experimental results for **3a**[(a)]	20.78	3.79	1.98	1.17
Calculated for $TBA_5[PW_{11}O_{39}]$[(b)]	24.29	4.59	2.12	1.31
Calculated for $TBA_4H[PW_{11}O_{39}]$[(b)]	20.70	3.93	1.89	1.40

(a = Analysis by Desert Analytics, Tucson, AZ, USA; b = Calculated using Jasper V2.0)

These results suggested that the addition of excess triethylamine and TBABr are not necessary in order to produce the desired Cr^VN Keggin POM. It is often observed that the protons will remain coordinated to POM fragments even in the presence of available $[TBA]^+$ cations, and the reaction scheme in Figure 3-10 (*i.e.* for **3a**) was followed.

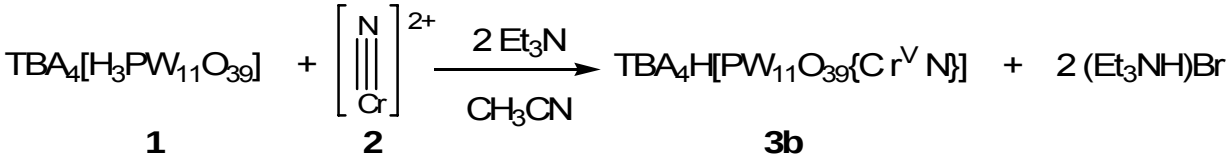

Figure 3-10: Reaction scheme for the stoichiometric formation of the chromium (V) nitrido Keggin complex, **3b**.

The FT-IR spectra of **3a** and **3b** showed the expected characteristic features of **1** (Table 3-2). The parent Keggin $[TBA]_3[PW_{12}O_{40}]$ shows only one P-O stretch at 1081 cm^{-1} in the IR spectrum, since it has ideal tetrahedral (T_d; Figure 3) symmetry.

Table 3-2: Selected FT-IR (cm^{-1}) data for $TBA_4[\alpha\text{-}PW_{11}O_{39}Os^{VI}(N)]$,[13a] $TBA_4[\alpha\text{-}PW_{11}O_{39}Re^{VI}(N)]$,[13a] **3a** and **3b**.

	$\upsilon(P\text{-}O)^a$	$\upsilon(W\text{-}O_t)^a$	$\upsilon(W\text{-}O_c\text{-}W)^a$	$\upsilon(W\text{-}O_e\text{-}W)^a$	$\upsilon(M\text{-}N)^a$
$TBA_3[PW_{12}O_{40}]$	1081	973	893	811	-
$TBA_4[\alpha\text{-}H_3PW_{11}O_{39}]$	1106, 1054	971	894	816	-
$TBA_4[\alpha\text{-}PW_{11}O_{39}Os(N)]$	1072, 1053	963	884	811	-
$TBA_4[\alpha\text{-}PW_{11}O_{39}Re(N)]$	1072, 1072	961	881	802	-
3a	1096,1059	951	884	811	996
3b	1098, 1060	954	881	809	997

(a = wavenumber in cm^{-1}; O_t = terminal oxygen; O_c = corner bridging oxygen; O_e = edge bridging oxygen)

Upon formation of the mono-vacant Keggin **1**, the P-O bands are observed at 1108 and 1055 cm^{-1} (IR spectrum). This large separation ($\Delta\upsilon$ = 53 cm^{-1}) is attributed to the lower symmetry of **1** since one of the P-O bonds is so different to the other three. This separation in the IR spectrum decreases upon metal insertion, as observed for both the {OsN} (1072 and 1053 cm^{-1})[13a] and {ReN} (1096 and 1072 cm^{-1})[13a] with $\Delta\upsilon$ values of 19 and 24 cm^{-1}, respectively (Table 3-2). This is in very good agreement with the observed IR spectrum of **3a** (1096 and 1059 with $\Delta\upsilon$ = 37cm^{-1}) and **3b** (1095 and 1058 with $\Delta\upsilon$ = 37 cm^{-1}) (Table3-2). Another notable feature in the IR spectrum of **3a** and **3b** is the presence of a new weak signal at 996 cm^{-1}, assigned to υ(Cr-N) stretch.[20b,24] Based on the above results, we can conclude that **3a** and **3b** are the same compound (*i.e.* "**3**") with no distinction between them.

The CrN-Keggin was also characterized electronically (in acetonitrile) in collaboration with our colleagues in Paris, Proust *et al.*[18] It was found to have its lowest energy absorption maximum at 467 nm (log ε = 2.1).[18] This is consistent with the $\{Re^{V}N\}$[13a] analogue, with its lowest energy absorption maximum at 500 nm (log ε = 3.06). The presence of the Cr(V) metal center was confirmed by the presence of the a reversible wave (cyclic voltammetry at a glassy carbon in acetonitrile) at 0.87 V (vs SCE)[18] credited to the oxidation of Cr(V) to Cr(VI).[18]

Unfortunately, as with the {OsN}- and {ReN}- Keggin complexes, crystals of the CrN-Keggin belong to the cubic crystallographic system (cubic I a = 17.7 Å, V = 5500 $Å^3$),[18] which rendered analysis by X-ray diffraction ineffective. Therefore the complex should display only one metallic center composed of 11/12 W and 1/12 Cr, one disordered terminal, one doubly

bridging oxygen and one quadruply bridging oxygen linked to the phosphorus,[18] as reported previously by Proust and Maatta.[13a]

The orange CrN-Keggin polyanion was determined to be stable over 12 months, provided it was stored as a solid at room temperature under argon. However the compound was observed to decompose in solution as noted by the increased intensity (Mass spectrometry) of the signal at 3942 m/z (fragment = $[TBA]_5[PW_{11}O_{39}\{Cr\}] + {}^1H$) coupled with the decrease in intensity of 3956 m/z (fragment = $[TBA]_5[PW_{11}O_{39}\{CrN\}] + {}^1H$).

3.2.2 Reactivity of $[TBA]_4H[PW_{11}O_{39}\{CrN\}]$ 3.

The reactivity of the nitrido complex was tested for nitrogen transfer capability toward *cis*-cyclooctene, following conditions outlined by Groves.[20a] A slight excess of trifluoroacetic anhydride (TFAA) was introduced to an orange solution of **3** in acetonitrile followed by *cis*-cyclooctene (Figure 3-11).

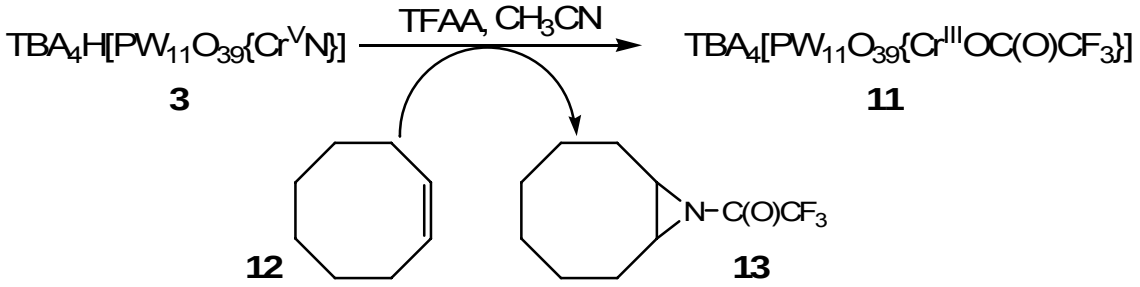

Figure 3-11: Attempted nitrogen transfer reaction scheme of **3** (Groves protocol).[20a]

The addition of *cis*-cyclooctene and TFAA to the orange solution of **3** resulted in rapid (~30 seconds) formation of a green solution. The color change from orange to green was a promising indication of Cr^V reduction to Cr^{III} (commonly green in color). The crude green solution was analyzed by various spectroscopic methods in search of **13,** the aziridine 9-(trifluoroacetyl)-9-azabicyclo[6.1.0]nonane. Unfortunately, residual para-magnetic Cr^V species made analysis by ^1H NMR ineffective. Attempted removal of the Cr^V species through recrystallization or column chromatography proved unfruitful. The crude green solution was analyzed by mass spectroscopy (MALDI-ToF) and a fragment at 242 m/z was attributed to a

$[TBA]^+$ unit. However, no fragments corresponding to the acylimido derivative **11** was observed in the mass spectrum (MALDI-ToF).

HPLC studies of the green solution confirmed the results previously reported by Karcher.[23] The presence of a new peak with a retention time of ~12.3 minutes (*c.f. cis*-cyclooctene ~8.5 minutes). This new peak could not be assigned to any of the starting materials and might be indicative of the presence of the aziridine **13**.[23] These observations were found to be reproducible but only with careful omission of oxygen and water during the synthesis.

As reported by our colleagues,[18] the IR spectrum of **11** showed the formation of two new bands at 1203 and 1682 cm^{-1}, assignable to υ(C-F) and υ(C=O) vibrational frequencies,[20b] respectively, along with disappearance of the band at 996 cm^{-1} assigned to υ(C-N). Further support came from the ^{19}F NMR spectrum ($CH_3CN/CDCl_3$) data of **11**: two peaks, a broad peak at -76.3 ppm ($\Delta_{1/2}$ = 40 Hz) and a sharp peak at -77.4 ppm (5% impurity from TFAA). As well as the presence of the broad peak at -11.85ppm ($\Delta_{1/2}$ = 16 Hz) in the ^{31}P NMR spectrum of **11**. The broad peaks in the NMR spectra maybe consistent with a "$NC(O)CF_3$" group bound to a paramagnetic chromium center and parallels that of some chromium nitrido porphyrin systems.[25]

Considering the inconsistencies in the above results, and given that our Paris collaborators were also unable to detect aziridine formation using a very similar protocol,[18] we conclude that no significant aziridination has taken place under the above set of conditions.

3.3 Conclusions and Future Work

A new chromium(V) nitrido Keggin complex has been synthesized and characterized by FT-IR, mass spectroscopy and elemental analysis in $[TBA]_4H[PW_{11}O_{39}\{CrN\}]$ **3**.[18] Synthetic reproducibility was achieved by working under stringently anhydrous conditions.

Further experiments should examine the reactivity of 3 as an N-atom transfer reagent toward other alkenes such as styrene[26] and cyclohexene[27,28]. (Figure 3-12) Reactions with alkylating agents other than TFAA (such as methyl iodide should also be investigated to better screen for nucleophilic reactivity at the chromium nitrido function.

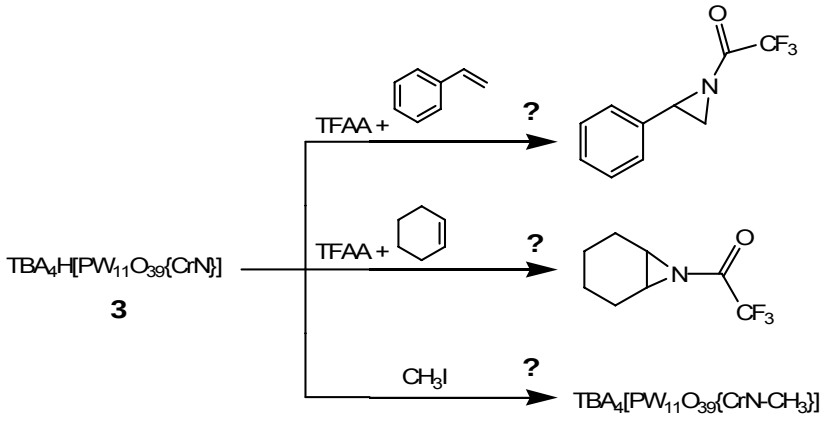

Figure 3-12: Future reaction schemes for the {CrN} Keggin, **3**.

3.4 Experimental

$TBA_4[\alpha\text{-}H_3PW_{11}O_{39}]$,[22] $[Cr^{V}N(THF)_x]$,[19] [Mn(N)Salen],[20b] and $[CrCl_3(THF)_x]$[21] were prepared according to literature methods. All manipulations, including recrystallizations, were done under an inert atmosphere of argon, unless otherwise stated. THF was distilled over sodium and CH_3CN was dried over CaH_2. All glassware was thoroughly dried by flame under reduced pressure. Starting materials were purchased from Aldrich and the solids dried under vacuum at 40°C for 24 hours prior to use. *Cis*-cyclooctene and anhydrous triethylamine was purged of oxygen via the 'freeze-pump thaw' method (5 cycles). ^{31}P NMR spectra were recorded on a Varian Unity Inova 400 MHz spectrometer and referenced to an externally to a solution of 85% $\sigma\text{-}H_3PO_4$ (0 ppm) in deuterated water. FT-IR spectra were recorded on a Nicolet Protégé 460 instrument as KBr pellets. Mass spectra (MALDI-ToF/ToF-MS) were collected on a Bruker Daltonics Ultraflex ToF/ToF-MS instrument.

The chromatographic system employed consisted of a HP1090 high-performance liquid chromatography unit with a HP3396 Series III integrator using a 10 mL injection loop. Detection was done at 254 nm. The stationary phase was a Zorbax ODS column (DuPont Instruments) 4.6mm x 25 cm packed with C_{18} (5 micron particle size) with a mobile phase of acetonitrile/water mixture and a flow rate of 1 mL/min. The mobile phase was run as a gradient of increasing acetonitrile content (30 minutes per analysis). The mobile phase began as a 70/30 mix of CH_3CN/H_2O for the first 10 minutes and was increased to 90% CH_3CN over another 10 minutes at a rate of 2%/min and held constant for the last 10 minutes.

3.4.1 TBA_4 $[\alpha\text{-}H_3PW_{11}O_{39}]$ Keggin[22] (1)

$$Na_2WO_4.2H_2O + Na_2HPO_4.7H_2O \xrightarrow[(ii)\ TBABr]{(i)\ 13.5\ M\ HCl} TBA_4[H_3PW_{11}O_{39}]$$
1

A 200 mL Erlenmeyer flask was charged with $Na_2HPO_4.7H_2O$ (1.48 g, 5.5 mmol) and $Na_2WO_4.2H_2O$ (20.0 g, 60.6 mmol) and dissolved in 40 mL of distilled water. To this colorless solution was cautiously added 4 mL of concentrated HCl over 20 minutes. If a white precipitate formed on addition, it was allowed to dissolve before any more HCl was added. After complete addition, the solution was stirred and maintained at room temperature for one hour until a white precipitate formed. The pH of the suspension was adjusted to 5.0 - 5.5 by careful dropwise addition of concentrated HCl causing dissolution. The pH of the solution was kept at this range for the next 30 minutes by further dropwise addition of dilute aqueous HCl. A solution of TBABr (8.0 g, 25 mmol) in 60 mL of distilled water was added causing the product to precipitate as a white solid. More of the desired product was isolated from the filtrate after the pH was adjusted to 1.1 – 1.2 with dilute HCl. The white product was collected on a glass frit and washed with water (3 x 30 mL) and diethyl ether (3 x 20 mL). The desired product was dried under high vacuum at 50°C for 24 hours. Yield (18.5 g, 92%). ^{31}P NMR (161.83 MHz, CD_3CN; external reference to H_3PO_4 at 0 ppm): δ -11.91 ppm.. FT-IR (KBr; *s* = strong, *m* = medium, *w* = weak): υ 957 *s*, 886 *s* cm^{-1}.

3.4.2 $[Cr^VN]^{2+}$ solution[19] (2)

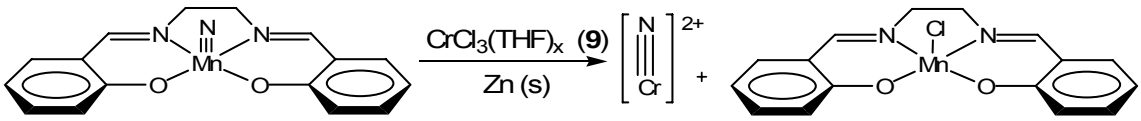

8 **2** **10**

To a flask charged with **8** (0.81 g, 2.42 mmol) were added **9** (0.91g, 2.42 mmol), zinc dust (0.02 g, 3 mmol) followed by CH_3CN (20 mL) under agron. Upon addition of CH_3CN, a dark brown solution developed which was stirred at room temperature. After 30 minutes, an insoluble brown precipitate formed and was filtered off to leave **2** in the yellow-brown filtrate. Yield assumed to be quantitative.

3.4.3 [TBA]$_5$[PW$_{11}$O$_{39}${Cr^{V}N}] (3a)

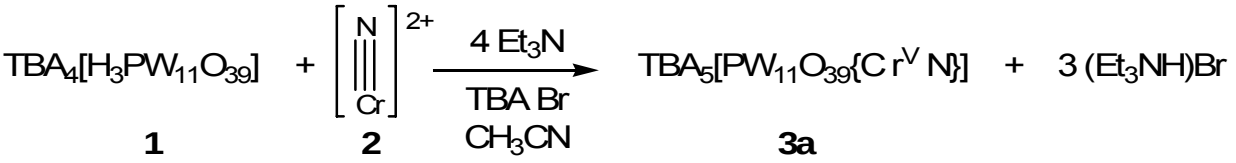

To a solution of **1** (2.94 g, 0.8067 mmol) in CH_3CN (40 mL) was added Et_3N (0.163 g, 1.613 mmol) and a solution of **2** under argon. The resultant orange mixture became dark brown within 30 seconds of addition. The dark-brown mixture was stirred at room temperature under argon. After 10 hours, a white precipitate was removed by filtration to leave a brown-orange solution which was concentrated under reduced pressure. Slow vapor diffusion of diethyl ether into the concentrated dark brown-orange solution yielded orange crystals of **3a**. Yield (0.10 g, 31% based on **1**) ^{31}P NMR (161.83 MHz, CD_3CN; external reference to H_3PO_4 at 0 ppm): δ -11.85 ppm ($\Delta_{1/2}$ = 16 Hz). FT-IR (Nujol): υ (*s* strong, *m* medium, *w* weak) 2960 *s*, 2870 *s*, 1096 *m*, 1059 *m*, 996 *w*, 951 *s*, 884 *s*, 811 *s* cm^{-1}. MS (MALDI-ToF/ToF-MS): 3956.02 m/z for ((C$_{80}$H$_{180}$N$_6$PW$_{11}$O$_{39}$Cr; [TBA]$_5$[PW$_{11}$O$_{39}${CrN}] + ^{1}H = 3956.65 m/z), 3942.45 m/z for ((C$_{80}$H$_{180}$N$_5$PW$_{11}$O$_{39}$Cr; [TBA]$_5$[PW$_{11}$O$_{39}${Cr}] + ^{1}H = 3942.65 m/z) and 3700.11 m/z for (C$_{64}$H$_{144}$N$_4$PW$_{11}$O$_{39}$Cr; [TBA]$_4$[PW$_{11}$O$_{39}$Cr] + 1H = 3700.18 m/z).

3.4.4 [TBA]$_4$H[PW$_{11}$O$_{39}${Cr^{V}N}] (3b)

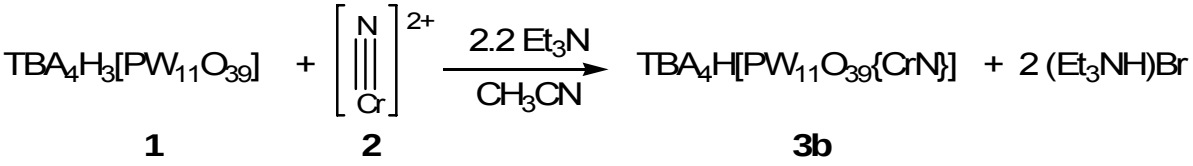

To a solution of **1** (0.1597 g, 0.0437 mmol) in CH_3CN (40 mL) was added Et_3N (0.0097 g, 0.00963 mmol) and **2** (0.00289g, 0.0437) under argon. The dark brown mixture was stirred at room temperature. After 15 hours, a white precipitate was removed by filtration to leave a

brown-orange solution which was concentrated under reduced pressure. Slow vapor diffusion of diethyl ether into the concentrated brown-orange solution yielded white crystals, later determined to be **1** and an oily orange residue.The residue was washed repeatedly with diethylether and yielded the CrN-Keggin product as an orange powder. (Yield 0.03g, 16 %) FT-IR (Nujol): υ (*s* strong, *m* medium, *w* weak) 2962 *m*, 2874 *m*, 1098 *m*, 1060 *m*, 997 *w*, 954 *s*, 881 *s*, 809 *s* cm^{-1}.

3.4.5 $Mn^{V}N(salen)$[20b] (8)

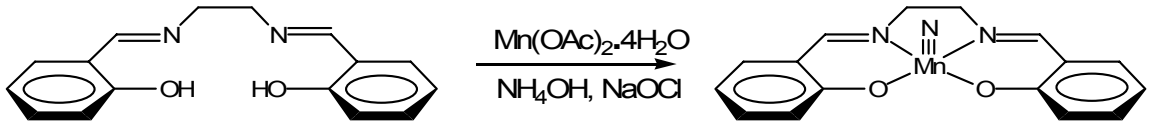

8

To a suspension of *N,N′*-ethylenebis(salicylimine) (salen; 8.26 g, 30.8 mmol) in methanol (400 mL) at 55°C was slowly added $Mn(OAc)_2$ (7.9 g, 32.4 mmol) in small portions. The brown solution was refluxed for 1 hour and allowed to cool to room temperature. Next, concentrated NH_4OH (31 mL) was added dropwise over 5 minutes, followed by 0.7M $NaOCl_{(aq)}$ (280 mL) dropwise over 40 minutes. After addition was complete, the dark green solution was cooled to 4°C and diluted slowly with dichloromethane (400 mL). The mixture was allowed to warm to room temperature with stirring and water was added (200 mL). The organic layer was collected and the aqueous layer further extracted with dichloromethane (3 x 20 mL). The organic layers were combined and washed with water (3 x 30 mL). Removal of the solvent under reduced pressure gave the crude green product. Pure **2** was isolated as a dark green solid after column chromatography with dichloromethane as the eluent. Yield (5.50 g, 82%). ^{1}H NMR (400 MHz, $CDCl_3$) δ 3.77 (s, 2H), 3.91 (s, 2H), 6.69 (s, 2H), 7.17 (m, 4H), 7.39 (s, 2H), 8.06 (s, 2H) ppm.

3.4.6 Chromium Trichloride Tetrahydrofuranate[21] (9)

Under inert atmosphere of argon, a Soxhlet thimble was charged with anhydrous $CrCl_3$ (12.21 g, 77.1 mmol) and zinc dust (0.15 g, 2.29 mmol). The thimble was placed in a Sohxlet

extractor connected to a 250 mL flask charged with anhydrous THF (140 mL) The solvent was heated to reflux under argon. After 16 hours, a dark purple solution had formed in the flask. Removal of solvent under reduced pressure yielded **3** as a purple solid. Yield (9.30g, 76%) FT-IR (Nujol): *υ* (*s* strong, *m* medium, *w* weak) 1010 *s*, 880 *s* cm^{-1}.

3.4.7 Reactivity of $[TBA]_4H[PW_{11}O_{39}\{CrN\}]$ with cis-cyclooctene.[20a]

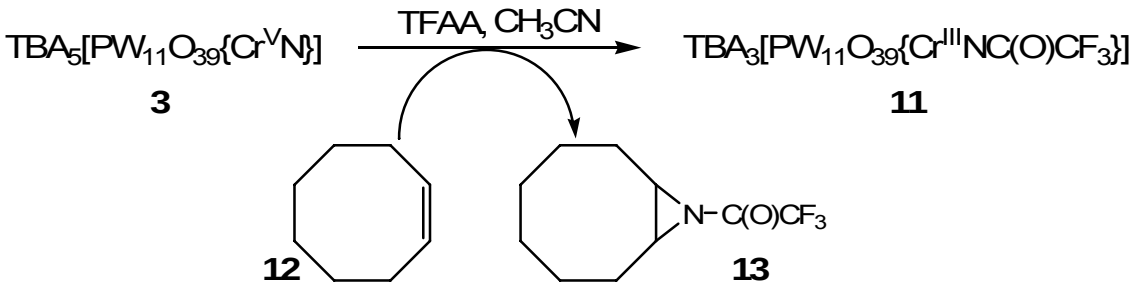

To a stirred orange solution **3** (0.1 g, 0.02528 mmol) in CH_3CN (5 mL) under argon was added a solution of TFAA (trifluoroacetic anhydride) (3.86 μL, 0.02781 mmol) in CH_3CN (2 mL) dropwise at room temperature, followed by *cis*-cyclooctene (32.9 μL, 02528 mmol). The orange solution rapidly (within 30 seconds) turned green upon complete addition of the cyclooctene. After 8 hours at room temperature, an aliquot of the green crude reaction solution was analyzed by mass spectrometry (MALDI-ToF) and liquid chromatography (HPLC). MS (MALDI-ToF/ToF-MS): 244 m/z (calculated for $[(C_{10}H_{14}NOF_3)Na]$ = 244.41 m/z). HPLC ~ 12.3 minutes.

[1] Nugent, W. A., Mayer, J. M., *Metal-Ligand Multiple Bonds*, Wiley, New York, 1988.
[2] Griffith, W. P., *Coord. Chem. Rev.* **1972**, *8*, 369.
[3] Dehnicke, K., Strahle, J., *Angew. Chem. Int. Ed. Engl.* **1981**, *20*, 413.
[4] Dehnicke, K., Strahle, J., *Angew. Chem. Int. Ed. Engl.* **1992**, *31*, 413.
[5] Eikey, R. A., Abu-Omar, M. M., *Coord. Chem. Rev.* **2003**, *243*, 83.
[6] (a) Karcher J., *PhD Thesis, Kansas State University*, **2000**.
(b) Dehicke, K., Strahle, J., *Angew. Chem.* **1981**, *93*, 451.
(c) Dehicke, K., Strahle, J., *Angew. Chem. Int. Ed.* **1981**, *20*, 413.
(d) Dehicke, K., Strahle, J., *Angew. Chem. Int. Ed.* **1992**, *31*, 955.
[7] Groves, J. T., Takahashi, T., *J. Am. Chem. Soc.* **1983**, *105, 2073.*
[8] Du Bois, J., Hong, J., Carreira, E. M., Day, M. W., J. Am. Chem. Soc. **1996**, 118, 915.
[9] Du Bois, J., Tomooka, C. S., Hong, J.,Carreira, E. M., Acc. Chem. Res. **1997**, 30, 364.
[10] Katsoulis, D. E., Pope, M. T., *J. Chem. Soc., Chem. Commun.* **1986**, 1186.
[11] Hill, C. L., Brown, R. B., Jr., *J. Am. Chem. Soc.* **1986**, *108*, 536.
[12] Dablemont, C., Hamaker, C.G., Thouvenot, R., Zbigniew, S., Che., M., Maatta, E.A., Proust, A., *Chem. Eur. J.* **2006**, *12*, 9150.
[13] (a) Kwen, H., Tomlinson, S., Maatta, E.A., Dablemont, C., Thouvenot, R., Proust, A., Gouzerh, P., *Chem. Commun.* **2002**, 2970.
(b) Dablemont, C., Proust, A., Thouvenot, R., Afonso, C., Fournier, F., Tabet, J.C., Dalton Trans. 2005, 1831.
(c) Proust, A., Thouvenot, R., Robert, F., Gouzerh, P., *Inorg. Chem.* **1993**, *32*, 5299.
(d) Proust, A., Thouvenot, R., Roh, S.G., Yoo, J.K., Gouzerh, P., *Inorg. Chem.* **1995**, *34*, 4106.
(e) Bustos, C., Hasenknopf, B., Thouvenot, R., Vaissermann, J., Proust, A., Gouzerh, P., *Eur. J. Inorg. Chem.* **2003**, 2757.
(f) Kang, H., Zubieta, J., *J. Chem. Soc., Chem. Commun.* **1988**, 1192.
[14] Pope, M.T., *"Heteropoly and Isopoly Oxometalates" Springer-Verlag: New York,* **1983**.
[15] Kang, H., Zubieta, J., *Chem. Commun.* **1988**, *8*, 707.
[16] Abrams, M., Costello, C., Shaikla, S., Zubieta, J., *Inorg. Chim. Acta.* **1991**, *180*, 9.
[17] Dablemont, C., Hamaker, C.G., Thouvenot, R., Sojka, Z., Che, M., Maatta, E.A., Proust, A., *Chem. Eur. J.* **2006**, *12*, 9150.
[18] Lahootun, V., Karcher, J., Courillon, C., Launay, F., Mijare, K., Maatta, E.A., Proust, A., *Eur. J. Inorg. Chem.*, accepted for publication, June 6, **2009**.
[19] Birk, J., Bendix, J., *Inorg. Chem.*, **2003**, *42*, 7608.
[20] (a) Groves, J. Takahashi, T., *J. Am. Chem. Soc.* **1983**, *105*, 2073.
(b) Bottomley, L., Neely, F., *Inorg. Chem.* **1997**, *36*, 5435.
[21] Herwig, W., Zeiss, H., *J. Org. Chem.*, **1958**, *23*, 1404.
[22] Klemperer, W.G., *Inorg. Synth.*, *27*, 105.
[23] Karcher, J.D., PhD Thesis, Kansas State University, **2007**.
[24] Hori, A, Ozawa, T., Yoshida, H., Imori, Y., Kuribayashi, Y., Nakano, E., Azuma, N., *Inorganica Chimica Acta* **1998**, 207.

[25] Bottomley, L.A., Neely, F.L., *Inorg. Chem.* **1990**, *29*, 1860.
[26] Pérez, F., Belmar, J., Moreno, Y., Baggio, R., Peña, O. *New. J. Chem.* **2005**, *29*, 283.
[27] Caiazzo, A., Dalili, S., Picard, C., Sasaki, M., Siu, T., Yudin, A.K. *Pure Applied Chemistry* **2004**, *76* (3), 603.
[28] Caselli, A., Gallo, E., Fantauzzi, S., Morlacchi, S., F. Ragaini F., Cenini, S. *Eur. J. Inorg. Chem.* **2008**, 3009.

CHAPTER 4 - An Osmium Nitrido Dawson-Wells Polyoxometalate

4.1 Introduction

4.1.1 Synthesis of nitrido Dawson-Wells type complexes.

Unfortunately the successful functionalization protocols discussed earlier for the hexamolybdate POM are not applicable to the Keggin $[PM_{11}O_{39}]^{7-}$ nor the Dawson-Wells $[P_2M_{18}O_{62}]^{6-}$ type POMs (i.e. M = W, Mo, V). An example illustrating such incompatibility is the reaction of $[TBA]_3[\alpha\text{-}PMo_{12}O_{40}]$ with an organic isocyanate ((*p*-MeC_6H_4NCO) in pyridine leading to the neutral $[Mo_{10}(NC_6H_4Me\text{-}p)_{12}(C_5H_5N)_2O_{18}]$ complex instead of the desired covalently functionalized hybrid material (Figure 4-1).[1]

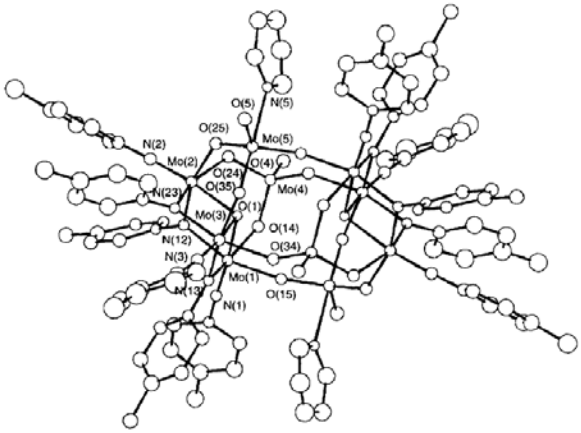

Figure 4-1: Molecular drawing of $[Mo_{10}(NC_6H_4Me\text{-}p)_{12}(C_5H_5N)_2O_{18}]$: unexpected product of direct functionalization of $[\alpha\text{-}PMo_{12}O_{40}]^{3-}$ with *p*-MeC_6H_4NCO.[1]

Thus far, the most effective route has employed a preformed metallo-organoimido complex such as **1** to fill the vacant site of the lacunary (Keggin or Dawson-Wells) POM[2] (Figure 4-3). However, this route also produces the corresponding $[TBA]_4[\alpha\text{-}PW_{11}O_{39}\{ReO\}]$ species which cannot be separated from the desired {Re(NPh)} complex, **3** (Figure 4-2).[3]

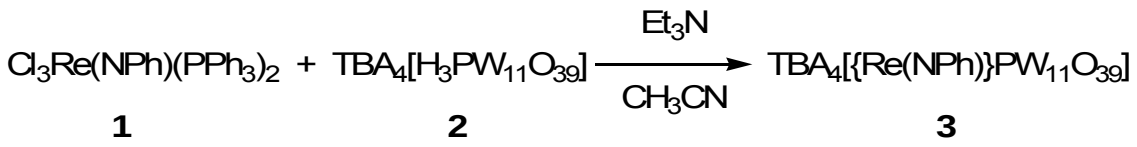

Figure 4-2: Functionalization of the lacunary Keggin $[H_3PW_{11}O_{39}]^{4-}$ POM with $\{Re(NPh)\}^{2}$ (TBA = $[^{n}Bu_4N]^{+}$).[3]

Metal nitrido-POM derivatives offer another possible route to hybrid materials such as **3** (Figure 4-2) through reactions with electrophiles (e.g., alkylating agents) and nucleophiles (e.g. organophosphines) to yield organoimido or phosphoraniminato POMs;[4] They may also be relevant to nitrogen fixation as outlined by Schrock and Yandulov[5] in their studies on high oxidation state nitrido Mo(VI) complexes.

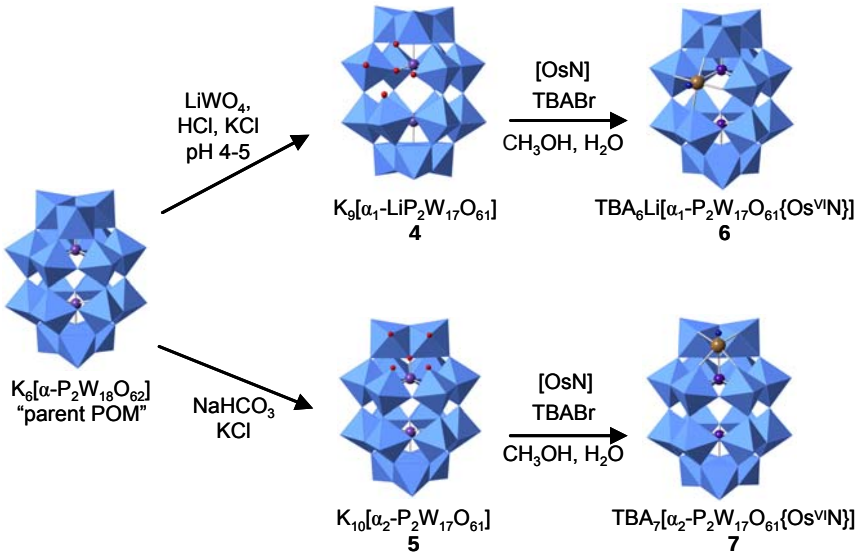

Figure 4-3: Synthetic reactions outlined by Maatta and Proust for $TBA_6Li[\alpha_1\text{-}P_2W_{17}O_{61}\{OsN\}]$ **6** (C_1 symmetric) and $TBA_7[\alpha_2\text{-}P_2W_{17}O_{61}\{OsN\}]$ **7** (C_S symmetric).[2,3]
(red ball = oxygen, purple = tungsten, brown = osmium and green = nitrogen)

The lacunary systems $K_9[\alpha_1\text{-}LiP_2W_{17}O_{61}]$ **4** and $K_{10}[\alpha_2\text{-}P_2W_{17}O_{61}]$ **5** are air-stable and were synthesized following methods reported in literature.[2] The $TBA_6Li[\alpha_1\text{-}P_2W_{17}O_{61}\{OsN\}]$[3] complex **6** was synthesized via the reaction of ([TBA][$OsNCl_4$]) with **4** in a mixture (1:1) of methanol and water (Figure 4-3). Since the (equatorial) α_1-isomer is known to be unstable in

organic media the (polar) α_2-isomer, **5** will be used to determine the possibility of synthesizing **7** under anhydrous conditions as well as studying its electrochemical properties. Herein, will be described the synthesis and characterization of **7** in organic media (acetonitrile) through the reaction of the $[TBA]^+$ derivative of **5** instead of aqueous methanolic media.[3]

4.2 Results and Discussion

The $Os^{VI}N$- Daswon-Wells complexes **6** and **7** were obtained in an analogous manner to that used for $[TBA]_4[PW_{11}O_{39}\{Os^{VI}N\}]$ **8** and $[TBA]_4[PW_{11}O_{39}\{Re^{VI}N\}]$ **9**.[3] The metal-nitrido delivery reagent $[TBA][OsNCl_4]$[9] **10** was obtained from methods adapted from the literature: the reaction of potassium osmate with sodium azide in the presence of excess acid, followed by treatment with [TBA]OH precipitated **10** as a pink solid which was dried under vacuum (Figure 4-4).[6,9]

$$K_2OsO_4 + NaN_3 + [TBA]OH \xrightarrow[H_2O]{13.5\ M\ HCl} \underset{\mathbf{10}}{[TBA][OsNCl_4]}$$

Figure 4-4: Synthesis of the osmium (VI) nitrido delivery reagent, **10**.[9]

The lacunary system $K_{10}[\alpha_2\text{-}P_2W_{17}O_{61}]$[8] **5** was synthesized by the abstraction of one $[WO]^{4-}$ unit from the parent Dawson-Wells POM, $K_6[P_2W_{18}O_{62}]$[8] with an equivalent of the mild base sodium bicarbonate, according to the literature.[8] The $[TBA]^+$ salt of POM derivative **11** was precipitated as a white solid from an aqueous solution of **5** by the addition of [TBA]Br (Figure 4-5).

$$\underset{\mathbf{5}}{K_{10}[\alpha_2\text{-}P_2W_{17}O_{61}]} + 10\,[TBA]Br \xrightarrow{H_2O} \underset{\mathbf{11}}{[TBA]_{10}[\alpha_2\text{-}P_2W_{17}O_{61}]}$$

Figure 4-5: Scheme for cation exchange reaction to yield, **11**.

Purification was achieved by washing **11** with distilled water and recrystallization from a concentrated acetonitrile solution. The formation of the lacunary species $[TBA]_{10}[\alpha_2\text{-}P_2W_{17}O_{61}]$ was confirmed by its ^{31}P NMR (CD_3CN) spectrum. Two distinct phosphorus environments are

seen as is typical for a lacunary Dawson-Wells POM: a peak at -7.0 ppm is assignable to the -PW_8 fragment (*i.e.* that with the abstracted vertex) and another at -13.8 ppm is assignable to the -PW_9 fragment (Figure 4-6).

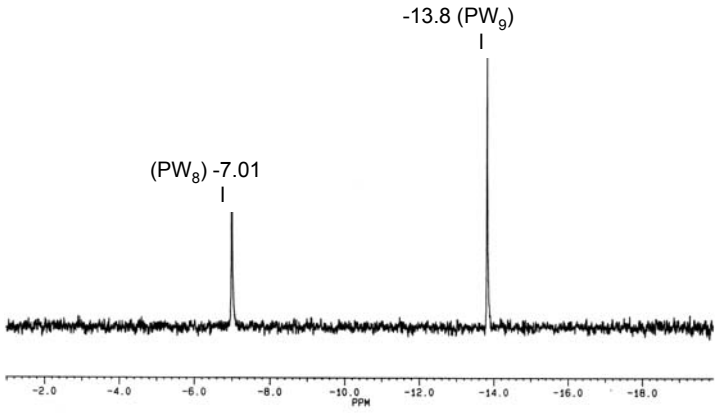

Figure 4-6: ^{31}P NMR spectrum (CD_3CN) of the Lacunary species $TBA_{10}[\alpha_2\text{-}P_2W_{17}O_{61}]$, **11**.

Introduction of $[TBA][OsNCl_4]$ **6** in CH_3CN to a colorless solution of **11** (also in CH_3CN) resulted in the immediate formation of a dark purple-black solution (Figure 4-7). The observed color change is analogous to that reported[2] for the same reaction in methanol and water and is indicative of metal nitrido insertion into the cavity of **11**. Successful metal insertion induces a change in the metal coordination environment of the osmium, from a pentacoordinated species **6** to the hexacoordinated species **12** (Figure 4-7). The [TBA]Cl by-product was never isolated as a precipitate from the reaction.

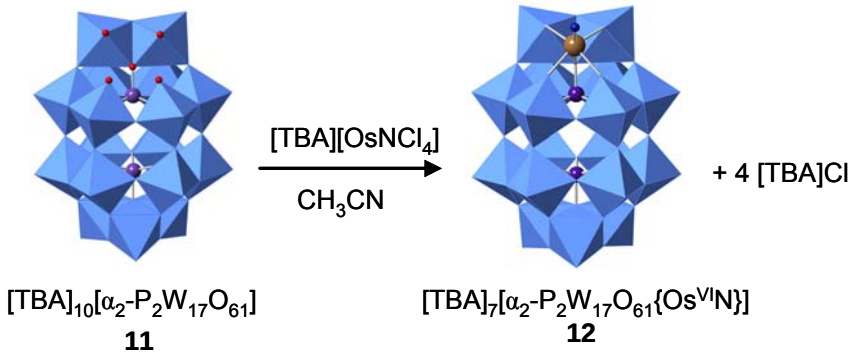

Figure 4-7: Synthesis of $[TBA]_7[\alpha_2\text{-}P_2W_{17}O_{61}\{OsN\}]$ **12** in anhydrous acetonitrile.

Successful metal insertion induces a change in the metal coordination environment of the osmium, from a pentacoordinated species **6** to the hexacoordinated species **12** (Figure 4-7). The [TBA]Cl by-product was never isolated as a precipitate from the reaction.

Repeated attempts at purification by diffusion of diethylether into a concentrated acetonitrile solution of **12** were unfruitful. Removal of acetonitrile under reduced pressure yielded **12** as a dark purple powder, which was analyzed by ^{31}P NMR, FT-IR (Fourier Transform Infra Red) and CV (Cyclic Voltammetry). Unfortunately, mass spectroscopy (ESI-MS: ElectroSpray Ionization Mass Spectroscopy) proved unsuccessful at characterizing the desired OsN-Dawson species **12**.

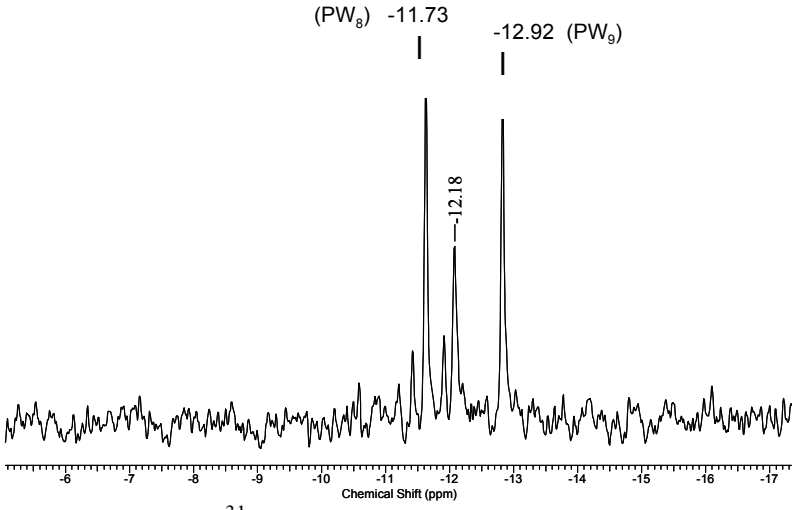

Figure 4-8: ^{31}P NMR (161.85 MHz, CD_3CN) of **12**.
(Referenced externally to H_3PO_4 in D_2O; Chemical shift at -12.18 ppm due to [TBA][α-$P_2W_{18}O_{62}$])

The ^{31}P NMR spectrum of **12,** matches that reported by Maatta and Proust,[2] *i.e.* -11.73 ppm for the –PW_8{OsN} fragment and -12.92 ppm for the –PW_9 fragment. The upfield shift of the signal assigned to the –PW_8 fragment, from -7.0 ppm (in **11**) to -11.73 ppm (in **12**), is consistent with literature[2] values and filling of the empty-vertex on the lacunary Dawson. Unfortunately as reported in literature,[2] the final product is also contaminated by the parent [TBA]$_6$[α-$P_2W_{18}O_{62}$] (~25%, as judged from ^{31}P NMR spectrum) as evident by the peak at -12.18 ppm (Figure 4-8). Unfortunately the source of the parent POM contaminant is yet to be determined. Since the ^{31}P NMR spectrum of the lacunary POM **11** showed no signals at -12.18

ppm, it must be re-formed during the metal insertion reaction. Attempts at removing the parent POM by chromatography on silica gel resulted in either product decomposition or it was never eluted from the column.

The IR spectrum of **12** was also consistent with that reported by Proust and Maatta,[2] with the characteristic features of a Dawson-Wells type structure: four strong bands at 1089, 953, 915 and 794 cm^{-1}, which correspond to the υ(P-O), υ(W=$O_{terminal}$) and υ(W-O-$W_{bridging}$) stretching modes, respectively.[2]

Cyclic voltammetry studies (reduction cycle) revealed two reversible one electron processes, attributed to the reduction of $Os^{6+} \rightarrow Os^{5+}$ (-0.97 V) and $Os^{5+} \rightarrow Os^{4+}$ (-1.35 V), consistent with literature[7] values (Figure 4-9).

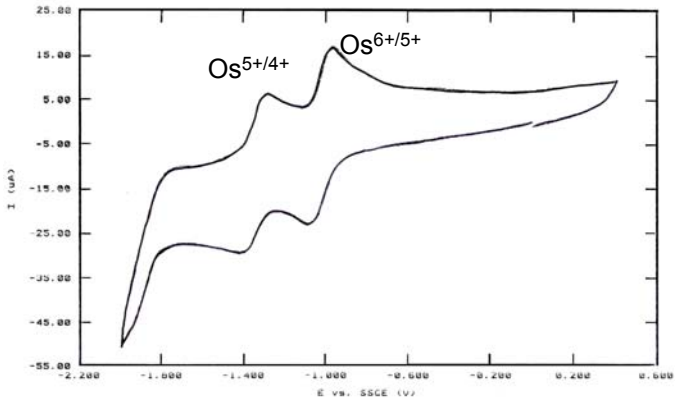

Figure 4-9: Cyclic voltammogram (reduction cycle) of **12** in CD_3CN.
(0.1 M [TBA][BF_4]; scan rate=100 ms/V; Pt electrode vs. SCE).

The oxidation cycle of **12** also showed two reversible waves, neither of which corresponded to the parent $[TBA]_6[P_2W_{18}O_{62}]$ or lacunary POM **11** or the [TBA][$OsNCl_4$] moieties (Figure 4-10). These processes may correspond to the $Os^{6+} \rightarrow Os^{7+}$ and $Os^{7+} \rightarrow Os^{8+}$ oxidations respectively, but further work will be needed to establish that conclusively. The combination of ^{31}P NMR, FT-IR and the electrochemical (CV) data strongly suggest that the desired OsN-Dawson complex was successfully synthesized in organic media.

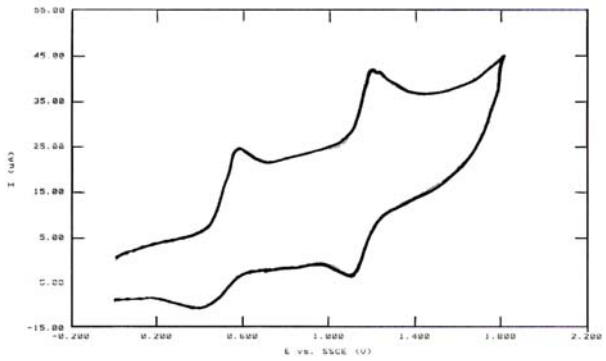

Figure 4-10: Cylic voltammograms (oxidation cycle) of **12** acetonitrile.

(0.1 M $TBABF_4$; scan rate=100 ms/V; Pt electrode vs. SCE).

4.3 Conclusions and Future work:

An alternative synthetic route to $[TBA]_7[\alpha_2\text{-}P_2W_{17}O_{61}\{OsN\}]$ **12** in organic media was demonstrated and confirmed by IR, ^{31}P NMR and cyclic voltammetry studies. Unfortunately, the method outlined here also showed the presence of the parent POM, $[TBA_6][P_2W_{18}O_{62}]$ in the final product. It is clear that further experiments are needed to determine the source of the parent Dawson or to least devise ways to remove the parent POM from the product. Ultimately the reactivity of the osmium-nitrido should be tested in a similar manner as those outlined in an earlier chapter for $[TBA]_4H[PW_{11}O_{39}\{CrN\}]$ (*i.e.* Groves protocol) to determine if the these metal-nitrido complexes are capable of nitrogen atom transfer reactions.

4.4 Experimental

The syntheses of the following POM precursors, $K_6[\alpha/\beta\text{-}P_2W_{18}O_{62}].10H_2O$,[10] $K_6[\alpha\text{-}P_2W_{18}O_{62}].14H_2O$,[11] $K_9Li[\alpha_1\text{-}P_2W_{17}O_{61}].20H_2O$,[8] $K_{10}[\alpha_2\text{-}P_2W_{17}O_{61}].15H_2O$,[8] $TBA_{10}[\alpha_2\text{-}P_2W_{17}O_{61}]$,[10] $TBA[OsNCl_4]$,[9] using slight literature modifications are reported here. The following reagents were purchased from Sigma-Aldrich and were used as received: $Na_2SO_4.2H_2O$, NaN_3, $LiWO_4$, TBA(OH), TBA(Br), K_2OsO_4. Acetonitrile was purchased from Fisher Scientific and distilled from CaH_2 prior to use. All other solvents were purchased as ACS Reagent grade and used as received from the manufacturer. ^{31}P NMR (146.21 MHz) spectra were recorded on a Varian Unity Plus and Inova 400 MHz spectrometer or a Bruker AC 300 spectrometer (121.5 MHz) in CD_3CN and CH_3CN. Compounds were prepared for infrared (FT-IR) analysis on a Nicolet Protégé 460 instrument as KBr pellets, unless otherwise stated. Mass spectra, MALDI-ToF/ToF-MS instrument, were recorded on a Bruker Daltonics Ultraflex ToF/ToF. Electrochemical (CV) data were collected in acetonitrile, with sample concentrations of 10^{-3} M and 0.1 M $[TBA]BF_4$ as the supporting electrolyte. A standard three-electrode cell was used, comprising a carbon electrode, a polished auxiliary platinum electrode and an aqueous saturated calomel electrode (SCE) equipped with a double junction on a PAR model 273 instrument.

4.4.1 ($K_9Li[\alpha_1\text{-}P_2W_{17}O_{61}].20H_2O$)[8] (4)

A solution of LiCl (13.45 g, 317 mmol) in H_2O (250mL) was acidified with 1M HCl (5 mL) and allowed to cool to room temperature. To this solution was added solid $K_{12}[H_2P_2W_{12}O_{48}].24H_2O$[8] (20 g, 50 mmol) with vigorous stirring. A white insoluble solid was filtered away and a 1M Li_2WO_4 solution (25 mL, 25 mmol) was added to the filtrate over 20 seconds. Immediately after addition was complete, a 1M HCl solution (55 mL, 55 mmol) was added dropwise over a 3 minute period while carefully maintaining pH between 4 and 5, followed immediately by a saturated KCl aqueous solution (100 mL). A white precipitate formed and was collected on a glass frit. The product was air-dried under suction filtration for 4 hours

and washed by stirring in ethanol (125 mL) for 15 minutes. The white product was collected and air-dried in an open container for 3 days. Yield 12.7 g (41%). ^{31}P NMR (146.21 MHz; in 1/1 mix of D_2O/H_2O; external reference to 85% σ-H_3PO_4): δ -8.70, -13.85 ppm. FT-IR (Nujol): υ (*s* strong, *m* medium, *w* weak) 1621 *s*, 1120 *s*, 1085 *s*, 1012 *s*, 944 *s*, 730 *s* cm^{-1}.

4.4.2 ($K_{10}[\alpha_2$-$P_2W_{17}O_{61}].15H_2O)^8$ (5)

$$K_6[\alpha\text{–}P_2W_{18}O_{62}].14H_2O + KHCO_3 \xrightarrow{H_2O} K_{10}[\alpha_2\text{-}P_2W_{17}O_{61}].15H_2O$$

To a solution of $K_6[\alpha$-$P_2W_{18}O_{62}].14H_2O$ (13.5 g, 2.78 mmol) in H_2O (50 mL) at 40°C was added a solution of 1M $KHCO_3$ (47.3 mL, 47.3 mmol) with vigorous stirring. Upon addition, a white precipitate formed. The mixture was stirred and maintained at 40°C for another 30 minutes. The white solid was collected and was recrystallized from boiling H_2O (50 mL). The product was isolated as white crystals and dried under vacuum at room temperature for 24 hours. Yield 8.31g (62%). ^{31}P NMR (146.21 MHz; in 1/1 mix of D_2O/H_2O; external reference to σ-H_3PO_4): δ -7.01, -13.84 ppm. FT-IR (Nujol): υ (*s* strong, *m* medium, *w* weak) 1636 *m*, 1082 *s*, 1049 *m*, 1015 *m*, 939 *s*, 887 *s*, 812 *s*, 740 *s*, 522 *m*, 462 *w* cm^{-1}.

4.4.3 [Tetra-^{n}butylammonium Tetrachloronitrido-osmium (VI)]^9 (10)

$$K_2OsO_4 + NaN_3 + TBA(OH) \xrightarrow[H_2O]{13.5\ M\ HCl} TBA[OsNCl_4]$$
6

In a concentrated solution of HCl (50 mL) was dissolved $K_2OsO_4.2H_2O$ (1.10 g, 3.09 mmol) and a solution of NaN_3 (0.44 g, 6.81 mmol) was then added. The dark purple-black solution was stirred at room temperature for 1 hour, after which, the product was precipitated as a red solid by addition of a 1M solution of [TBA]OH (1.11 g, 1.11 mL). The red suspension was stirred for another 30 minutes and the solid was collected on a frit and washed with cold diethyl

ether. Yield 0.56 g (37%). FT-IR (Nujol): υ (*s* strong, *m* medium, *w* weak) 2964 *s*, 2876 *s*, 1625 *m*, 1471 *s*, 1382 *m*, 1169 *w*, 1126 *w*, 1099 *m*, 1060 *m*, 925 *m*, 884 *m*, 830 *w*, 796 *w* cm^{-1}.

4.4.5 ($[TBA]_{10}[\alpha_2\text{-}P_2W_{17}O_{61}]$)[10] (11)

$$K_{10}[\alpha_2\text{-}P_2W_{17}O_{61}].15H_2O + 10TBABr \xrightarrow{H_2O} TBA_{10}[\alpha_2\text{-}P_2W_{17}O_{61}]$$

To a solution of **5** (1.70 g, 0.354 mmol) in H_2O (70 mL) was added a solution of TBABr (1.14 g, 3.54 mmol) in CH_3CN (40 mL) followed by CH_2Cl_2 (40 mL). The bi-phasic mixture was stirred at room temperature for 45 minutes, after which, the layers were separated and the organic phase was dried over anhydrous Na_2CO_3. Removal of the solvent afforded a white residue which was washed with diethyl ether (2 x 15 mL) leaving the desired product as white solid. Yield 0.84 g (37%). ^{31}P NMR (146.21 MHz; in 1/1 mix of CH_3CN/CD_3CN; external reference to σ-H_3PO_4): δ -7.20, -13.54 ppm. FT-IR (Nujol): υ (*s* strong, *m* medium, *w* weak) 2940 *s*, 1090 *s*, 1045 *s*, 1010 *s*, 958 *s*, 886 *m*, 805 *s*, 715 *s* cm^{-1}.

4.4.6 ($[TBA]_7[\alpha_2\text{-}P_2W_{17}O_{61}\{OsN\}]$) (12)

$$TBA_{10}[\alpha_2\text{-}P_2W_{17}O_{61}] + TBA[OsNCl_4] \xrightarrow{CH_3CN} TBA_7[\alpha_2\text{-}P_2W_{17}O_{61}\{Os^{VI}N\}]$$

To a stirred solution of **11** (0.044 g, 0.0759 mmol) in CH_3CN (3 mL) was added a solution of **6** (0.50 g, 0.0759 mmol) in CH_3CN (5 mL) with vigorous stirring. The dark purple-black solution was stirred overnight under argon. After 21 hours, the solvent was removed under reduced pressure to leave a dark purple-black solid which was washed with cold diethyl ether and dried under vacuum. Yield 0.43 g (96%). ^{31}P NMR (146.21 MHz; in 1/1 mix of CH_3CN/CD_3CN; external reference to σ-H_3PO_4): δ -11.32, -12.27, -13.02 ppm. FT-IR (Nujol): υ (*s* strong, *m* medium, *w* weak) 2956 *s*, 2872 *s*,1645 *m*, 1474 *s*, 1380 *m*, 1169 *w*, 1109 *sh*, 1089 *m*, 1030 *w*, 953 *s*, 915 *m*, 991 *w,* 794 *s*, 737 *sh,* 628 *w* cm^{-1}.

4.4.7 ($K_6[\alpha/\beta\text{-}P_2W_{18}O_{62}].10H_2O$)[10]

To a suspension of $Na_2WO_4.2H_2O$ (50g, 0.1515 mol) in H_2O (175 mL) was added 85% σ-H_3PO_4 (75 mL, 0.3860 mol) dropwise over 30 minutes. The pale green solution was stirred and refluxed. After 8 hours, the crude product (mix of α and β) was precipitated by the addition of solid KCl (50g, 0.67 mmol) and recrystallized from boiling water (200 mL) after being cooled to 5°C overnight. The product was collected on a fine glass frit where it was washed with H_2O (3 x 25 mL), 95 % Ethanol (3 x 25 mL) and diethyl ether (3 x 25 mL). The white solid was dried under vacuum at room temperature for 24 hours. Yield 68 g (84%). ^{31}P NMR (146.21 MHz; $LiClO_4/KClO_4$ in 1/1 mix of D_2O/H_2O): δ -10.80 (β PW_8), -11.57 (β PW_9), -12.29 (α) ppm. FT-IR (Nujol): υ (*s* strong, *m* medium, *w* weak) 1090 *s* , 1045 *m*, 1010 *m*, 930 *w*, 870 *m*, 805 *s*, 750 *m* cm^{-1}.

4.4.8 ($K_6[\alpha\text{-}P_2W_{18}O_{62}].14H_2O$)[11]

To a solution of $K_6[\alpha/\beta\text{-}P_2W_{18}O_{62}]$**.**$10H_2O$ (35 g, 7.5 mmol) in water (125 mL at 80°C) was added a drop (0.1 mL) of bromine (to oxidize the small amount of reduced POM which caused the light green solution). To the colorless solution was added a solution of 1M $KHCO_3$ (200 mL, 400 mmol) over 5 minutes. A white precipitate formed during addition. The mixture was allowed to stir for 30 minutes after which more of the precipitate had formed. The solution was reformed by the addition of a 6M HCl (75 mL, 900 mmol) over 10 minutes. Some insoluble impurities was filtered away through a Celite pad. To the stirred pale yellow solution was added solid KCl (50 g, 670 mmol) and it was cooled to 5°C overnight. The white crystals obtained were recrystallized from water (200 mL) at 5°C overnight. Yield (27 g, (81%). ^{31}P NMR (146.21 MHz; in 1/1 mix of D_2O/H_2O): δ -12.0 ppm. FT-IR (Nujol): υ (*s* strong, *m* medium, *w* weak) 1010 *s*, 880 *s* cm^{-1}.

[1] Proust, A., Taunier, S., Artero, V., Robert, F., Thouvenot, R., Gouzerh, P., *J. Chem. Soc., Chem. Commun.*, **1996**, 2195.
[2] Dablemont, C., Hamaker, C.G., Thouvenot, R., Sojka, Z., Che, M., Maatta, E.A., Proust, A., *Chem. Eur. J.* **2006**, *12*, 9150.
[3] Dablemont, C., Proust, A., Thouvenot, R., Afonso, C., Fournier, F., Tabet, J.C., *Dalton, Trans.* **2005**, 1831.
[4] Eikey, R.A., Abu-Omar, M.M., *Coord. Chem. Rev.* **2003**, *243*, 83.
[5] (a) Yandulov, D.V., Schrock, R.R., *Science* **2003**, *310*, 76.
(b) Schrock, R.R., *Chem. Commun.* **2003**, 2389.
[6] Wu, A., Dehestani, A., Crevier, T.J., Kaminsky, W., Cohen, D.E., Mayer, J.M., *Inorganica Chimica Acta*, **2006**, *359*, 2842.
[7] Huynh, M.H.V., White, P.S., John, K.D., Meyer, T.J., *Angew. Chem.* **2001**, 113 (*21*), 4173.
[8] Contant, R., Klemperer, W.G., Yaghi, O., *Inorg. Synth.* **1998**, 27, 109.
[9] Griffith, W.P., Pawson, D., *J. Chem. Soc. Dalton Trans.* **1973**, 1315.
[10] Lyon, D.K., Miller, W.K., Novet, T., Domaille, P.J., Evitt, E., Johnson, D.C., Finke, R.G., J. Am. Chem. Soc. **1991**, 113, 7209.
[11] Randall, W.J., Lyon, D.K., Domaille, P.J., Finke, R.G., Khenkin, A.M., Hill, C., *Inorg. Synth.* **1998**, *32*, 242.

Appendix A - Chapter 2

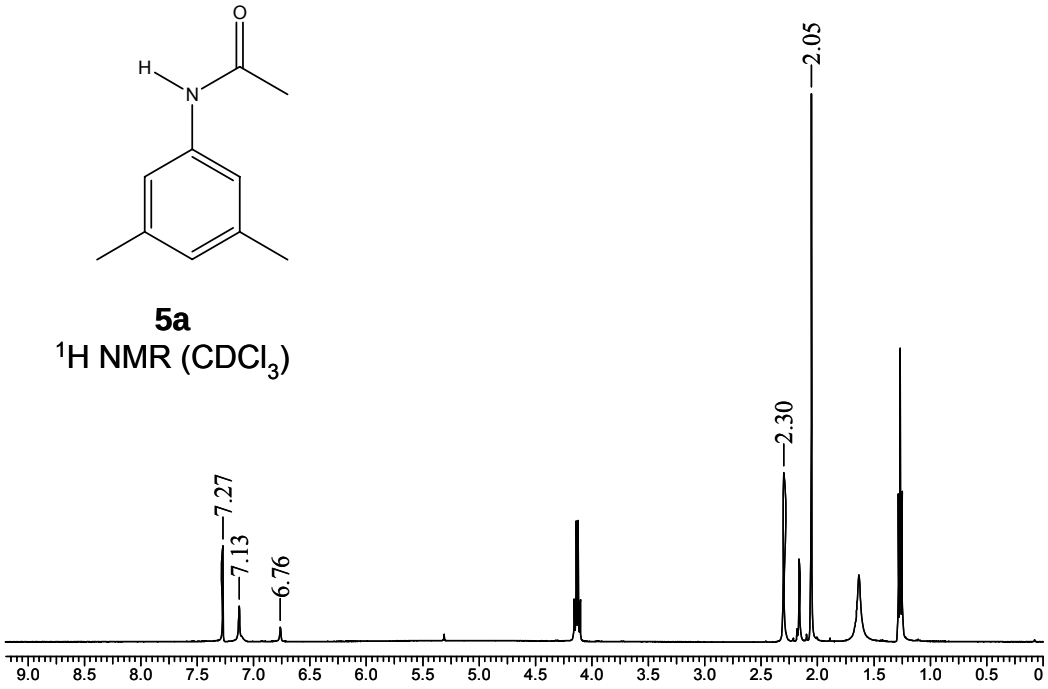

Figure A-1: ^{1}H NMR spectrum (400 MHz, $CDCl_3$) of **5a**.

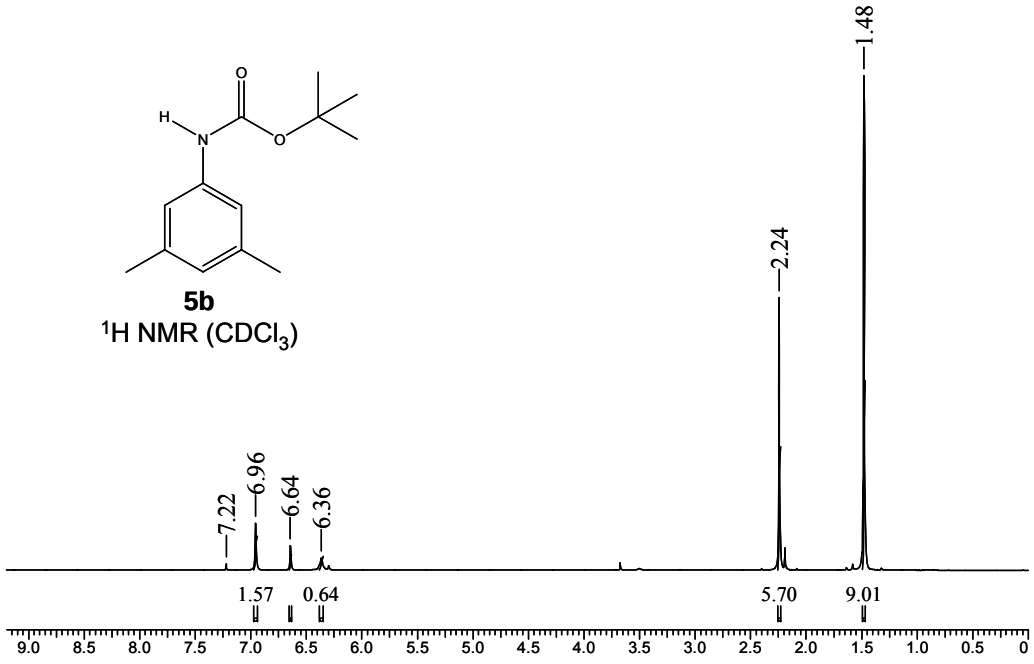

Figure A-2^{1}H NMR spectrum (400 MHz, $CDCl_3$) of **5b**.

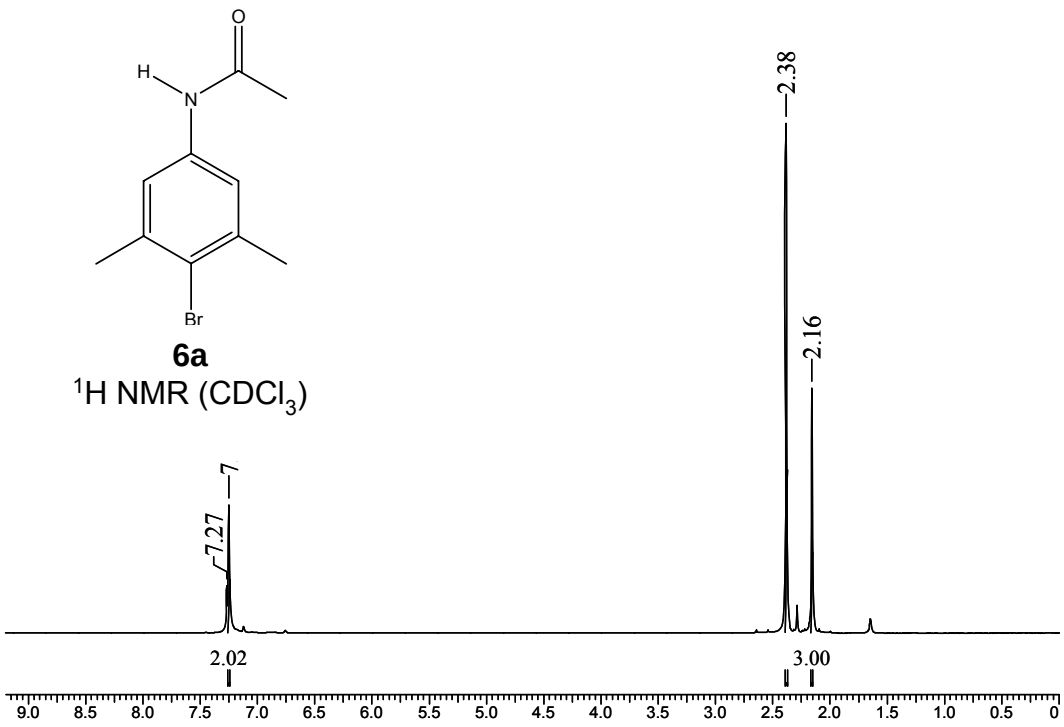

Figure A-3: ^{1}H NMR spectrum (400 MHz, $CDCl_3$) of **6a.**

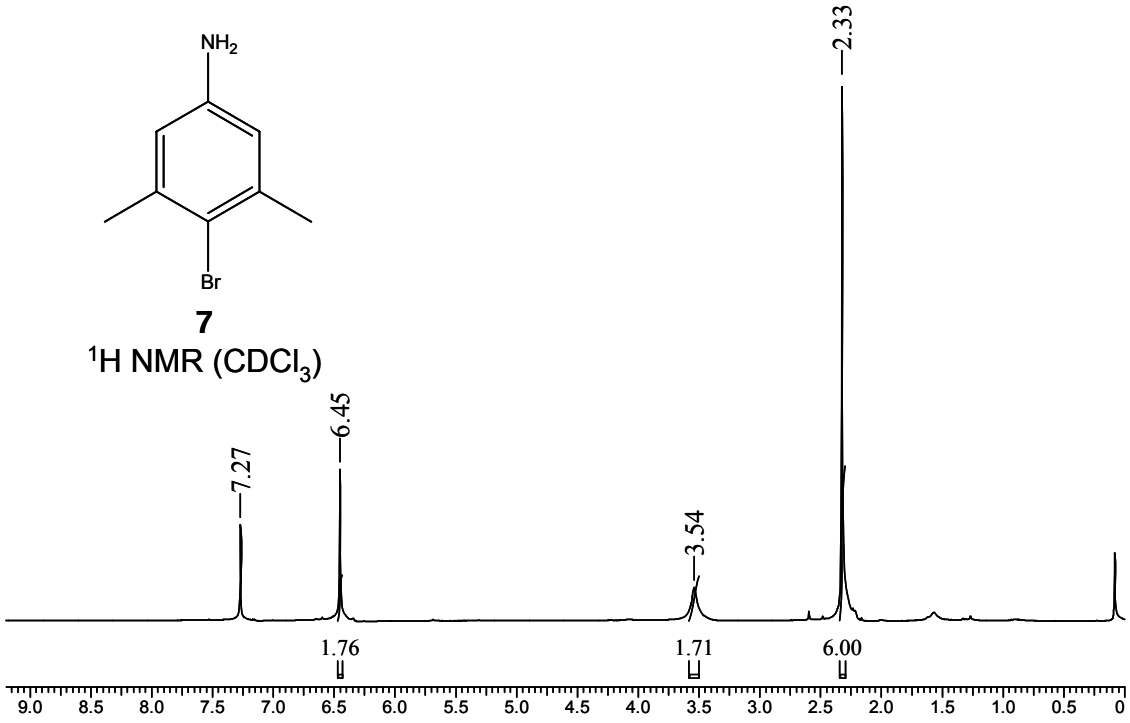

Figure A-4: ^{1}H NMR spectrum (400 MHz, $CDCl_3$) of **7**.

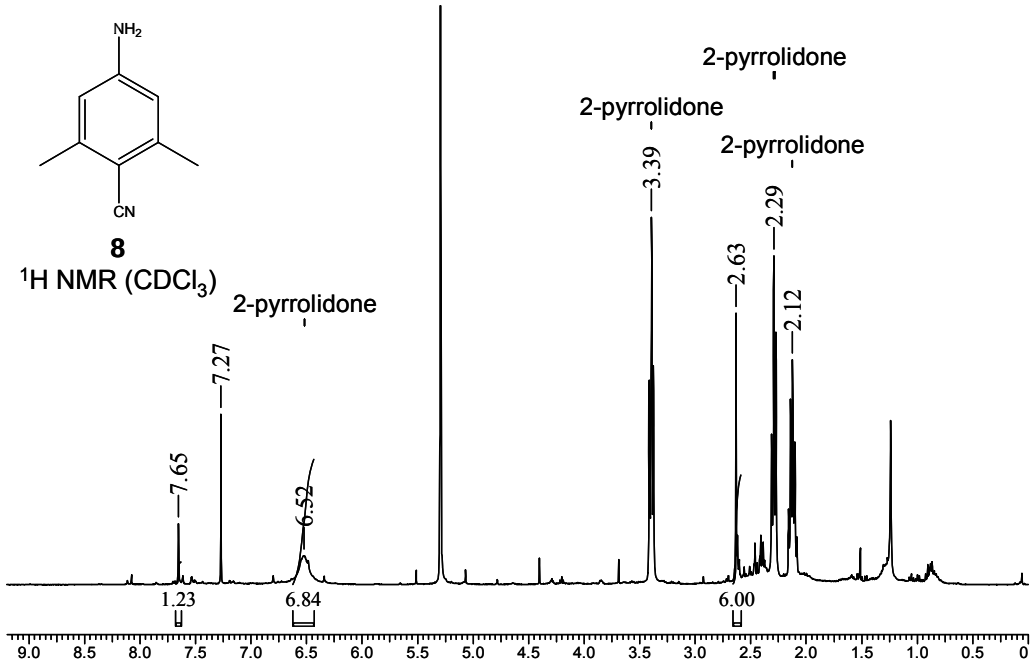

Figure A-5: ^{1}H NMR spectrum (400 MHz, $CDCl_3$) of **8**.

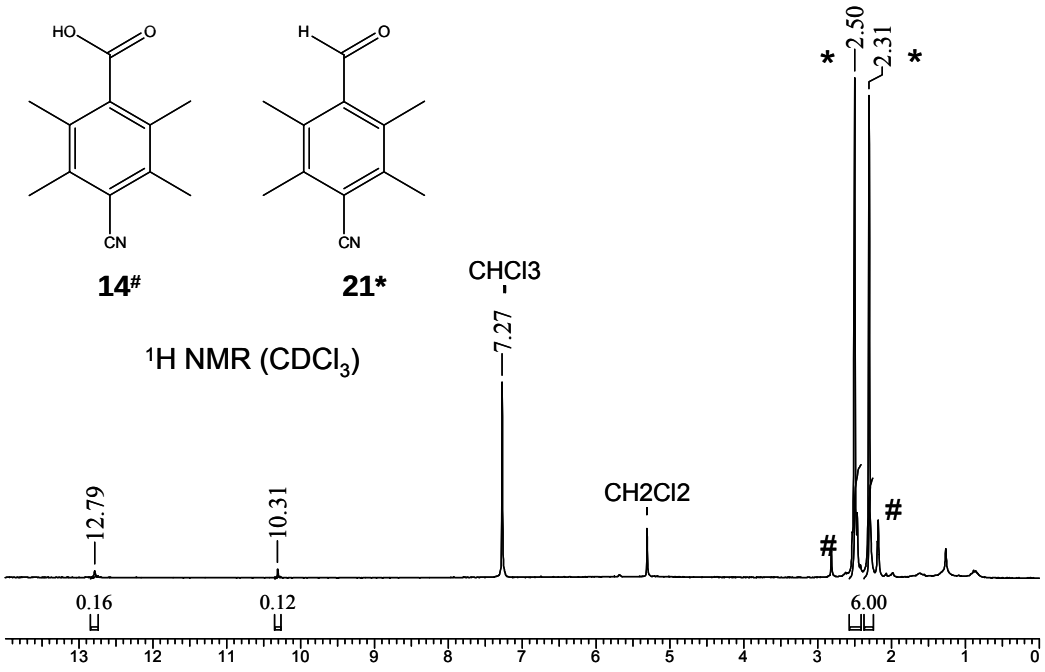

Figure A-6: ^{1}H NMR spectrum (400 MHz, $CDCl_3$) of **14** contaminated with **21**.

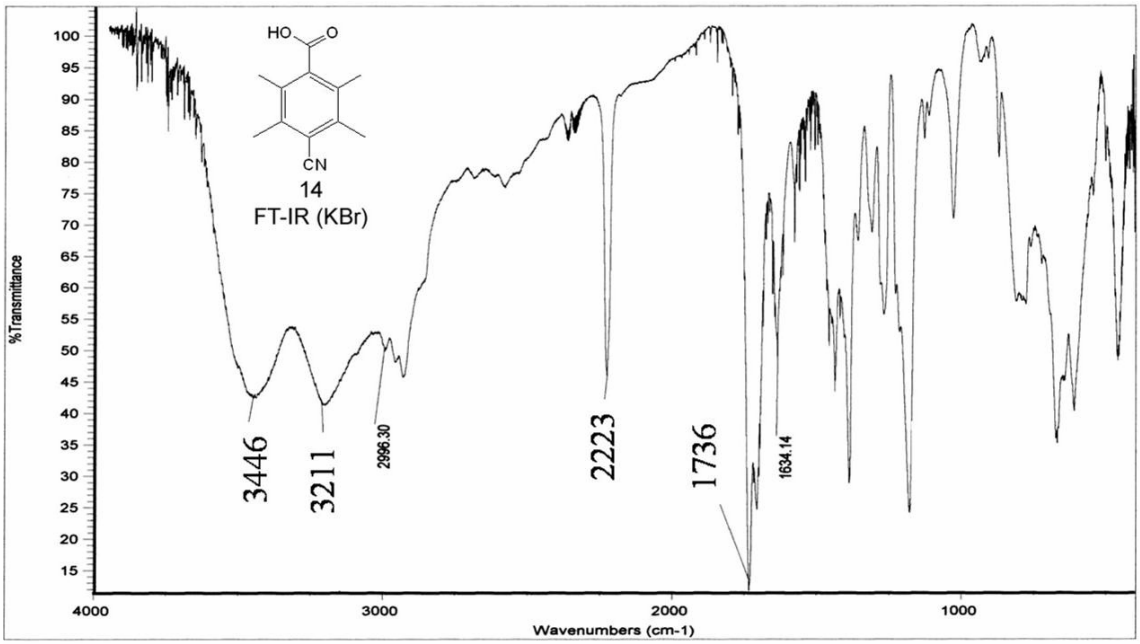

Figure A-7: FT-IR spectrum (KBr) of **14** contaminated with **21**.

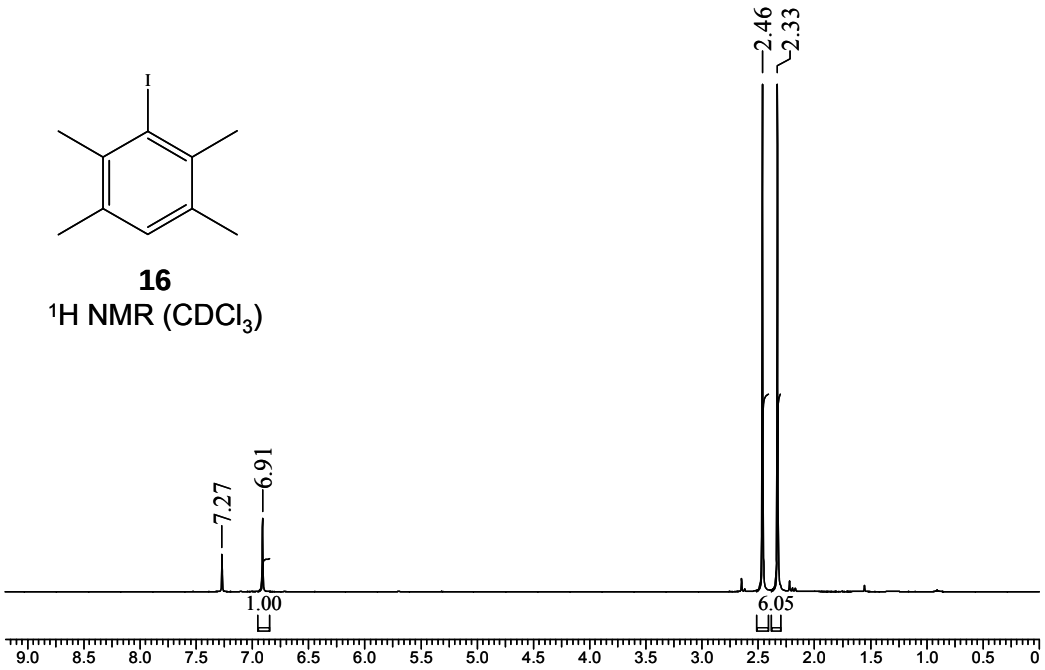

Figure A-8: ^{1}H NMR spectrum (400 MHz, $CDCl_3$) of **16**.

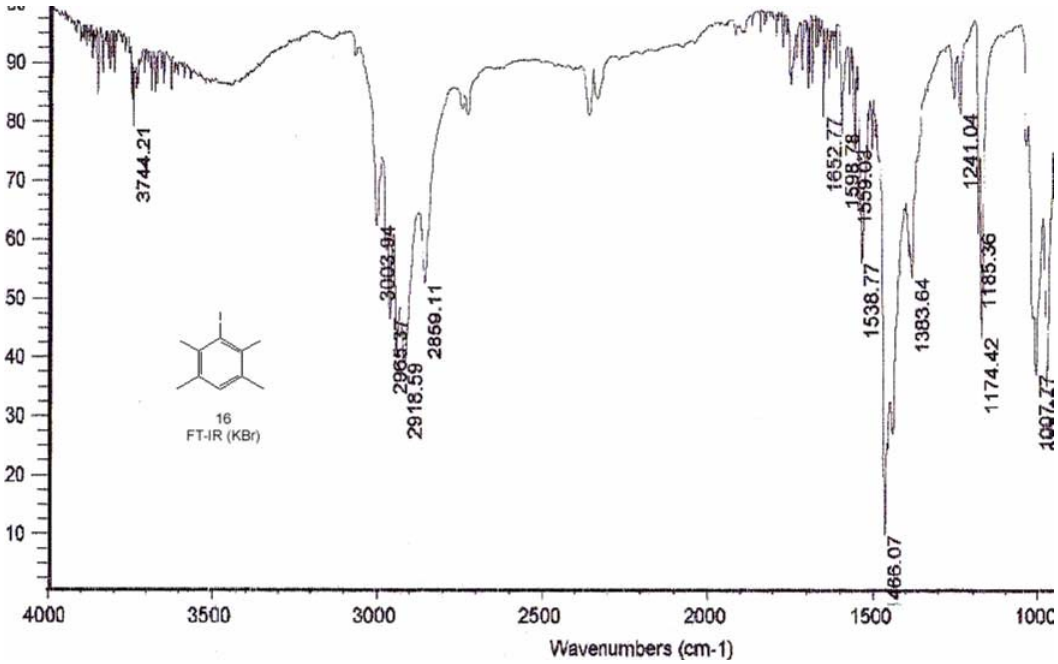

Figure A-9: FT-IR spectrum (KBr) of **16**.

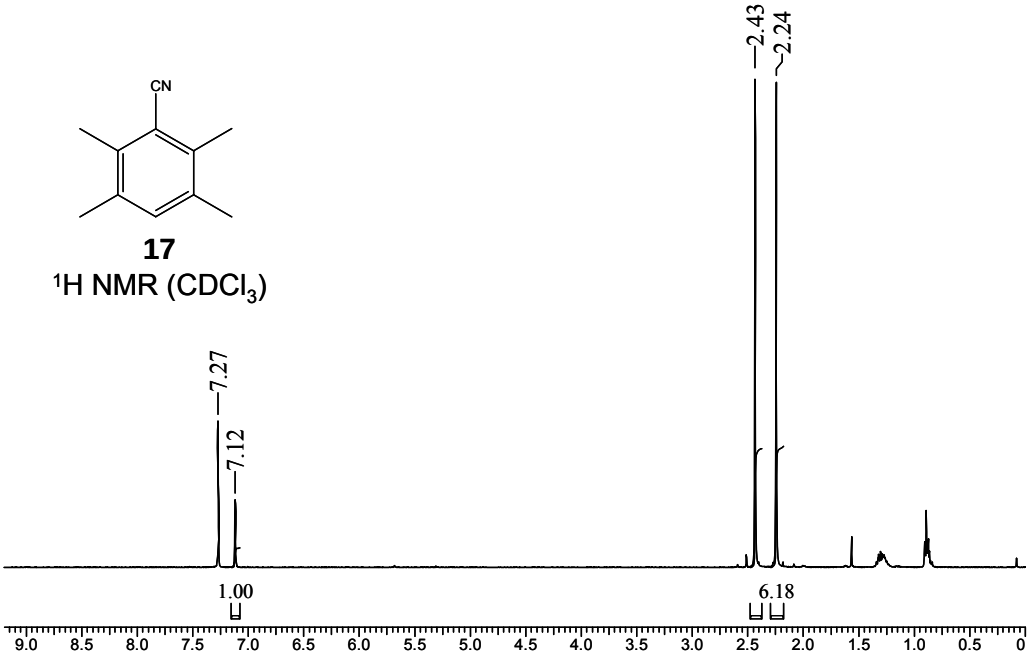

Figure A-10: ^{1}H NMR spectrum (400 MHz, $CDCl_3$) of **17**.

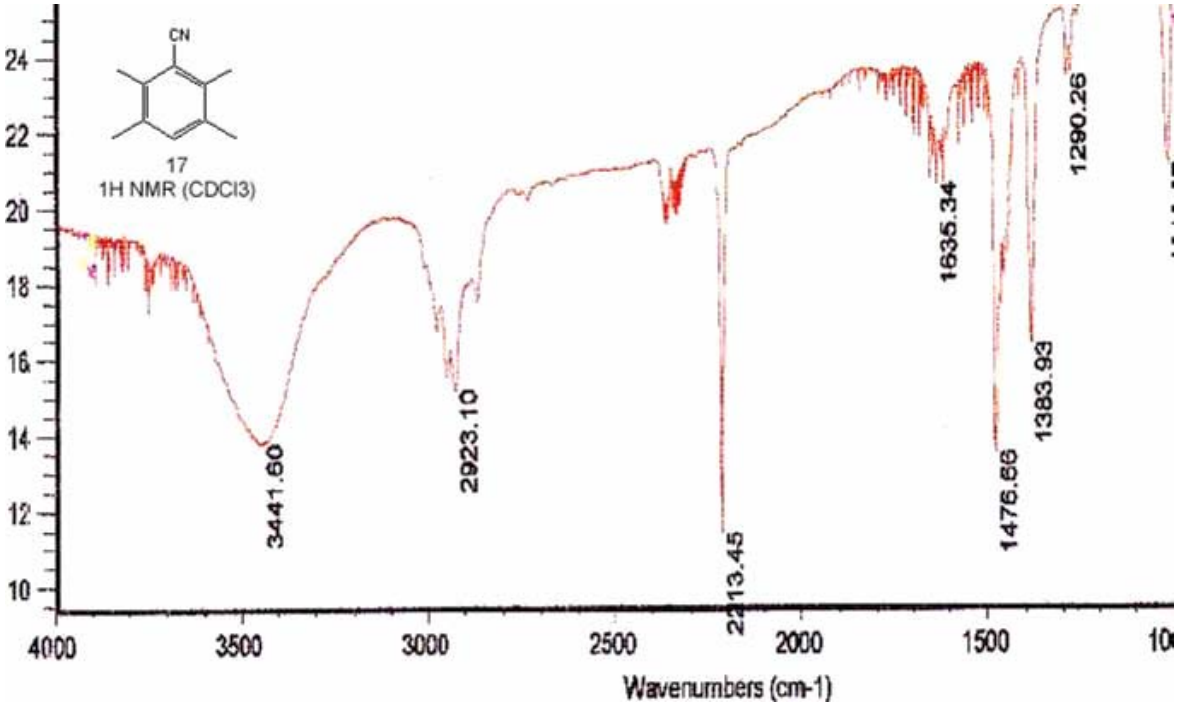

Figure A-11: FT-IR spectrum (KBr) of **17**.

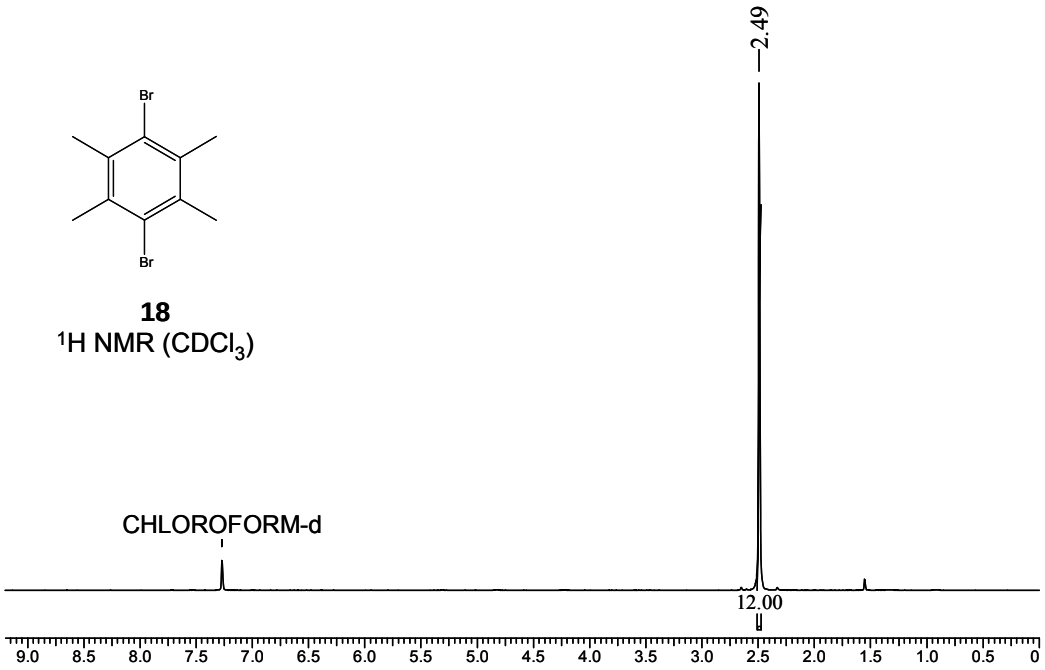

Figure A-12: ^{1}H NMR spectrum (400 MHz, $CDCl_3$) of **18**.

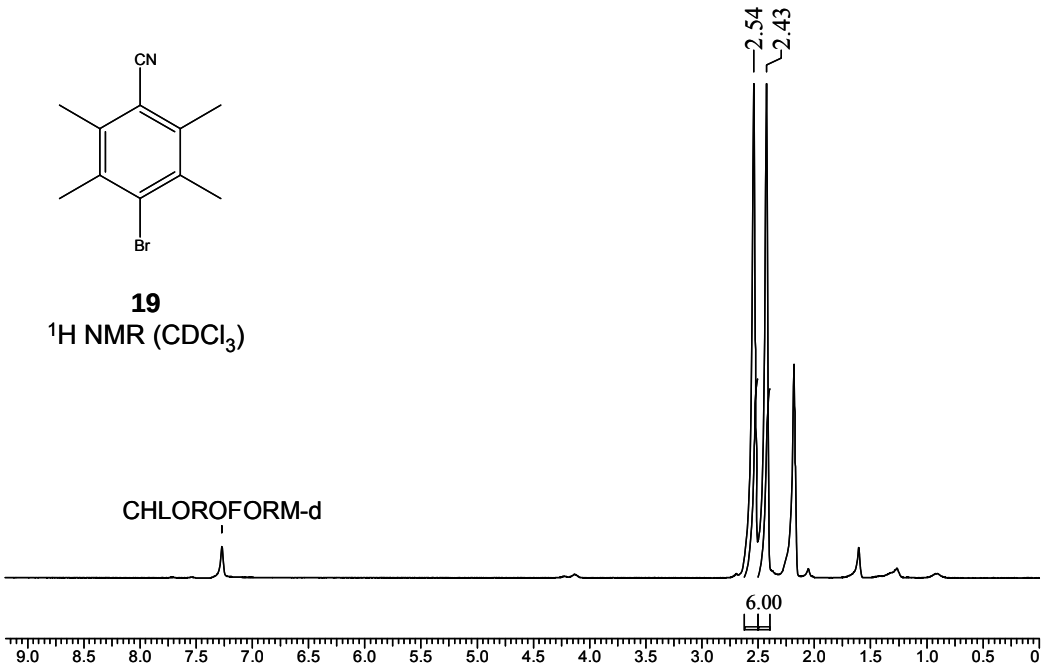

Figure A-13: ^{1}H NMR spectrum (400 MHz, $CDCl_3$) of **19**.

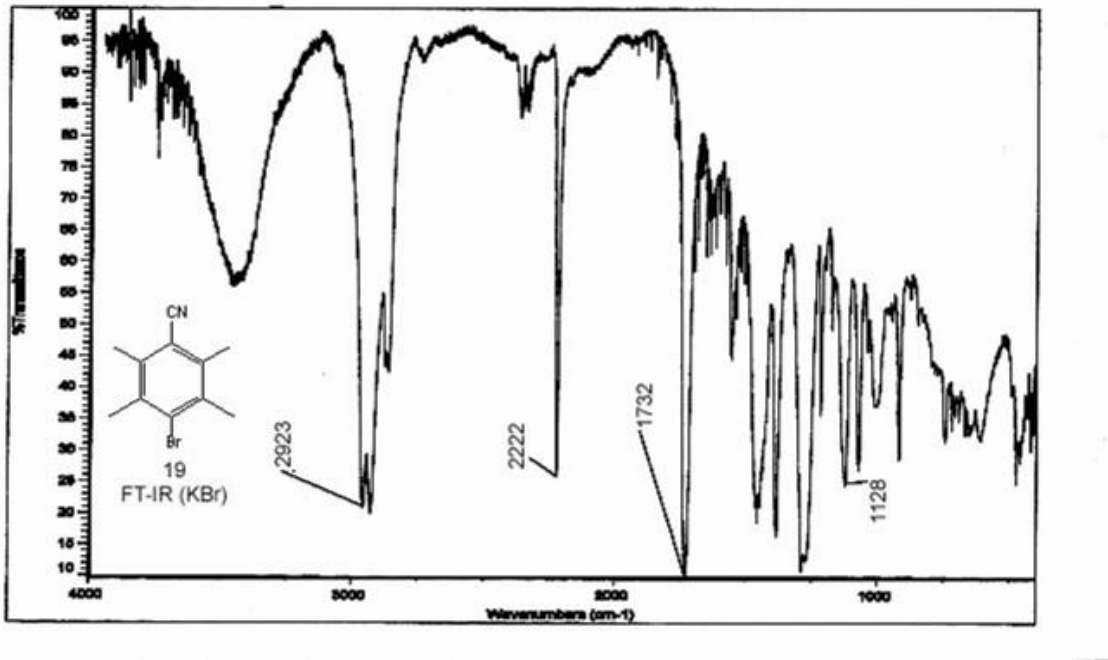

Figure A-14: FT-IR spectrum (KBr) of **19**.

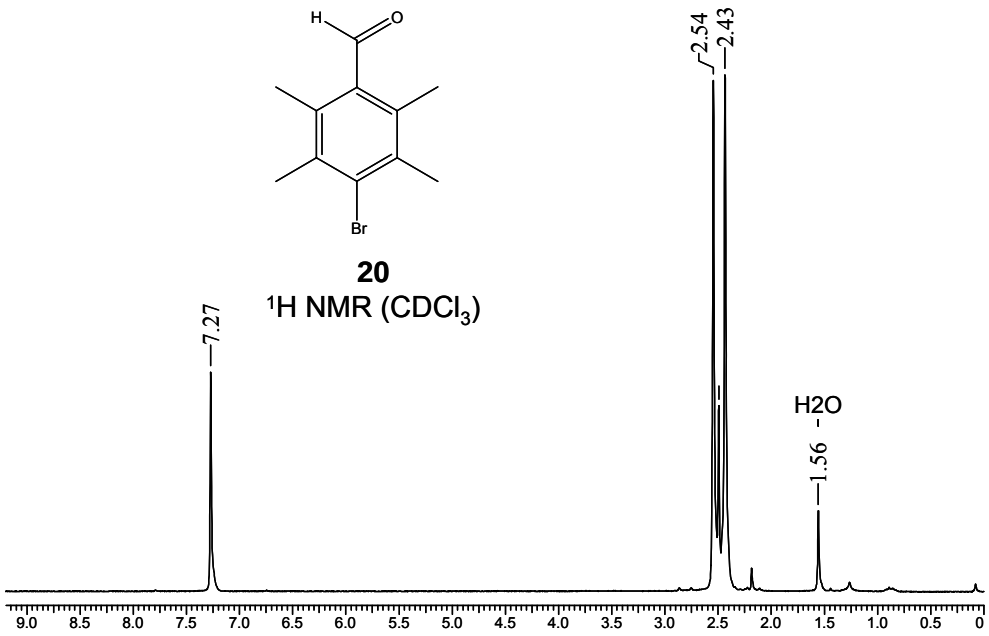

Figure A-15: ^{1}H NMR spectrum (400 MHz, $CDCl_3$) of **20**.

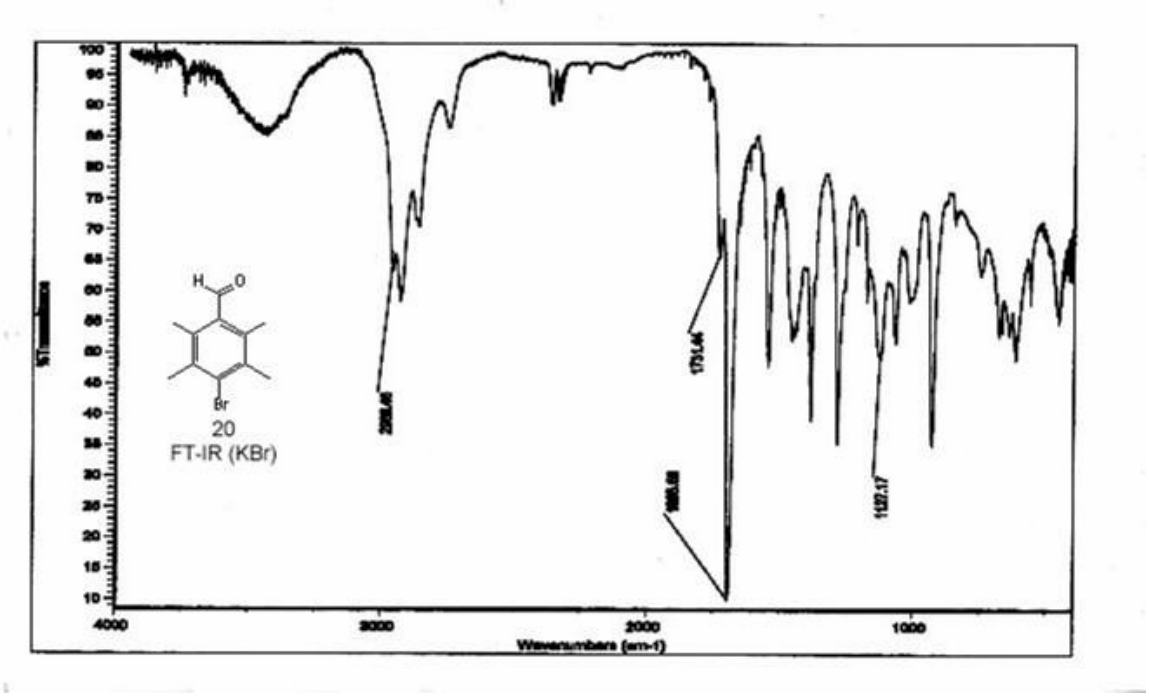

Figure A-16: FT-IR spectrum (KBr) of **20**.

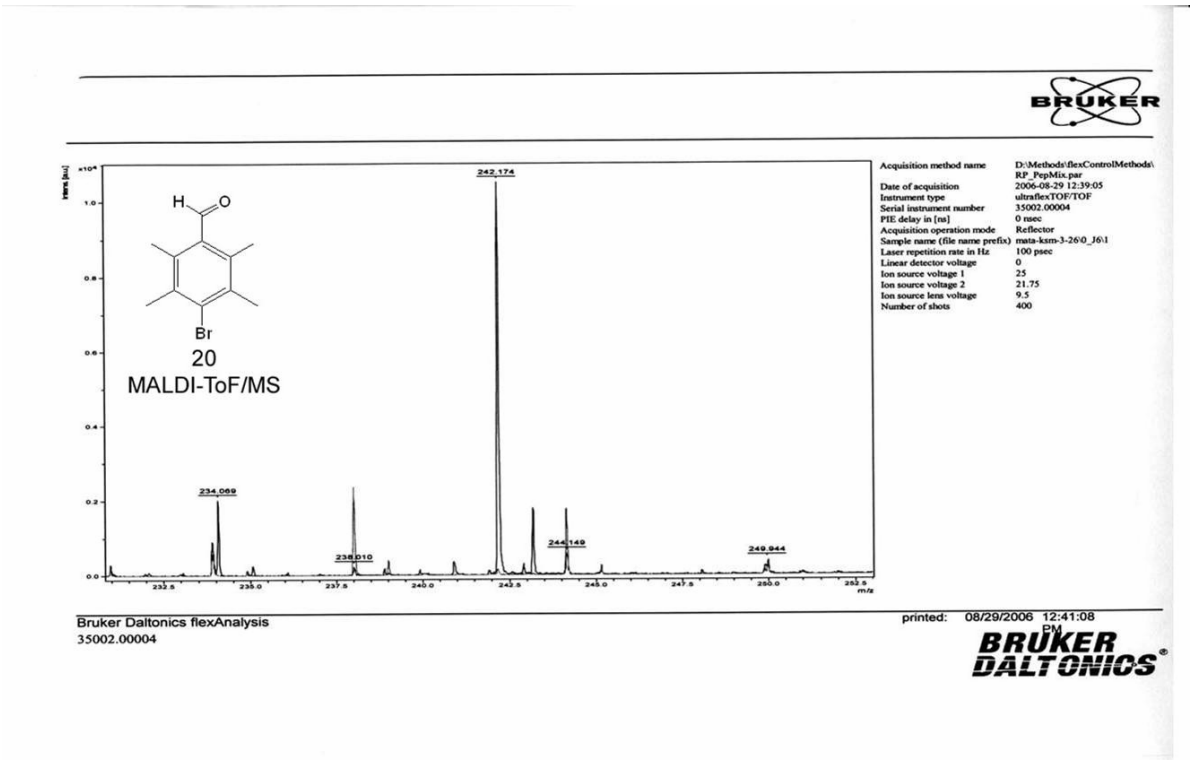

Figure A-17: MALDI-ToF/MS-ToF spectrum of **20**.

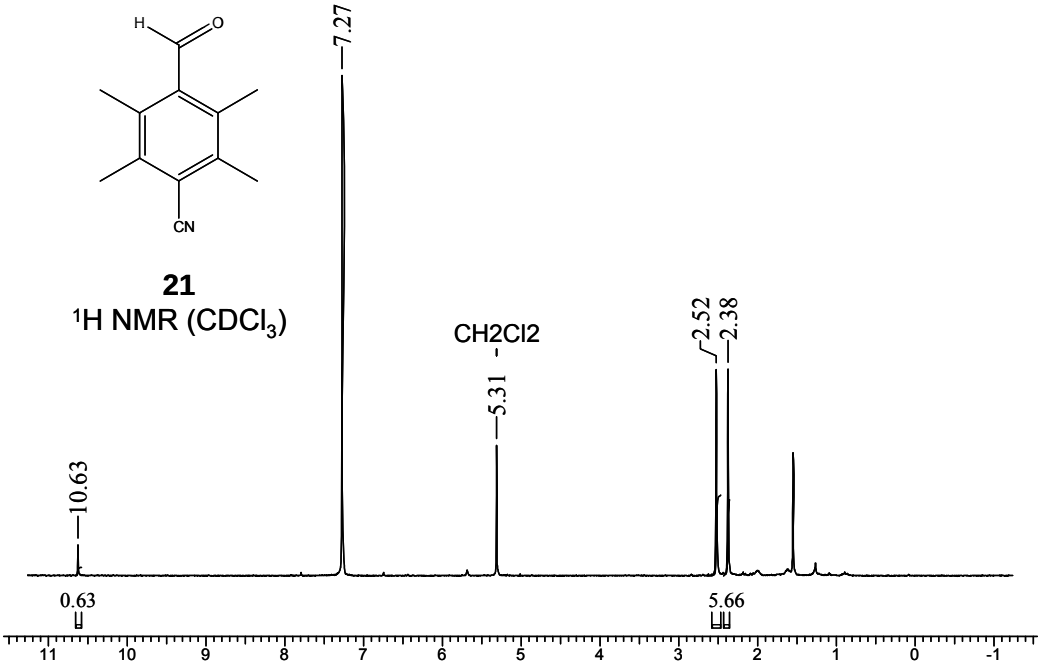

Figure A-18: ^{1}H NMR spectrum (400 MHz, $CDCl_3$) of **21**.

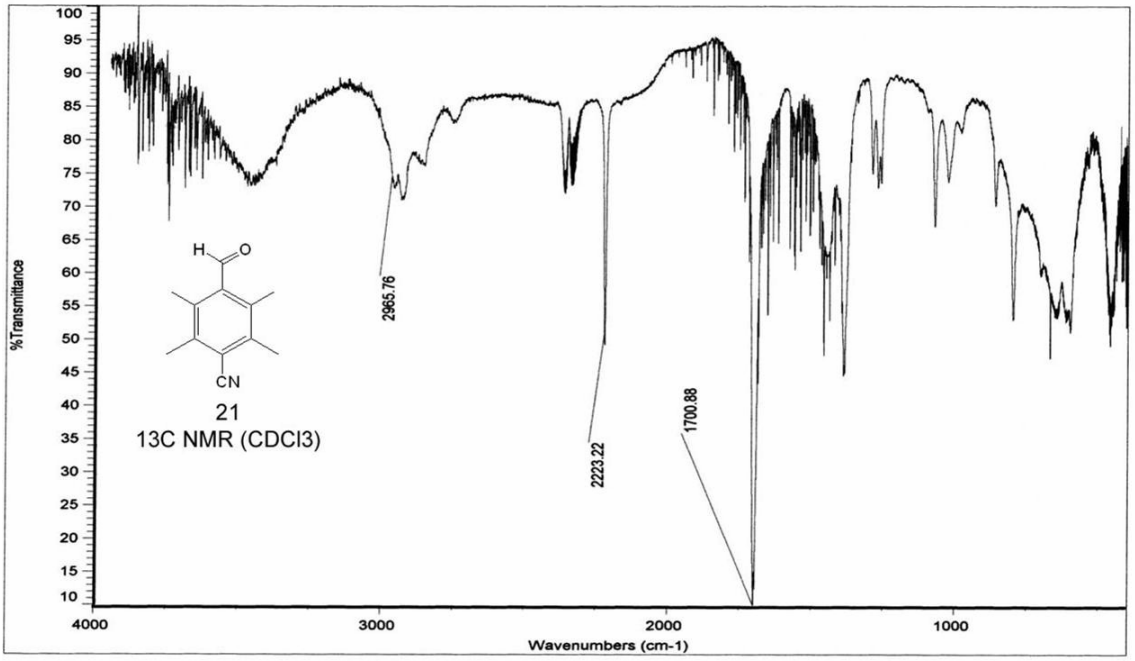

Figure A-19: FT-IR spectrum (KBr) of **21**.

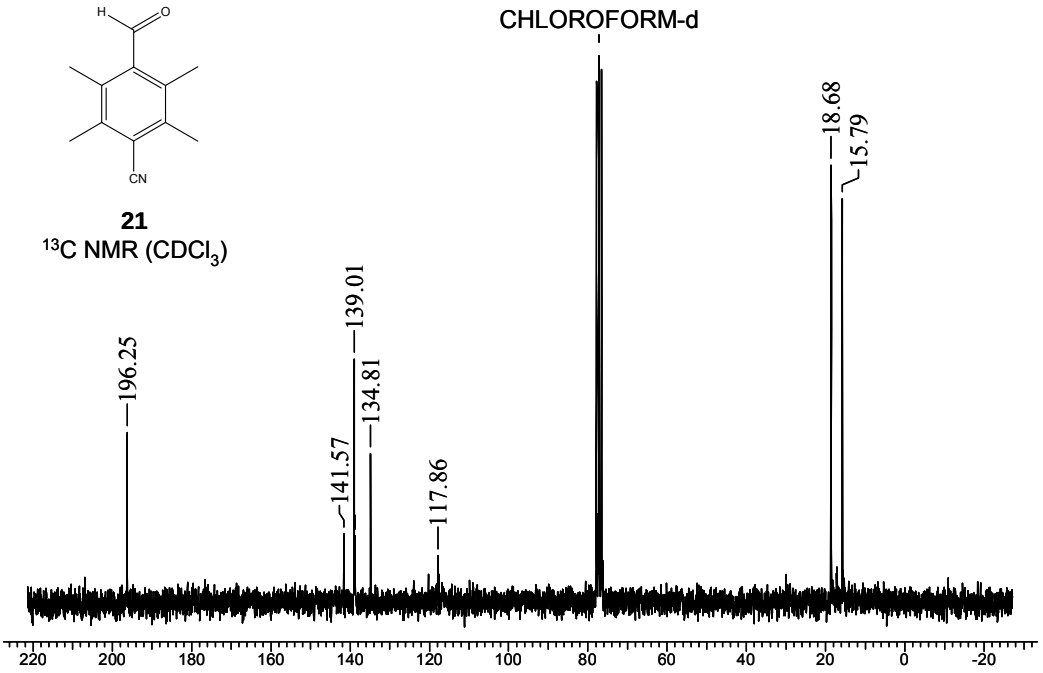

Figure A-20: ^{13}C NMR spectrum (400 MHz, $CDCl_3$) of **21**.

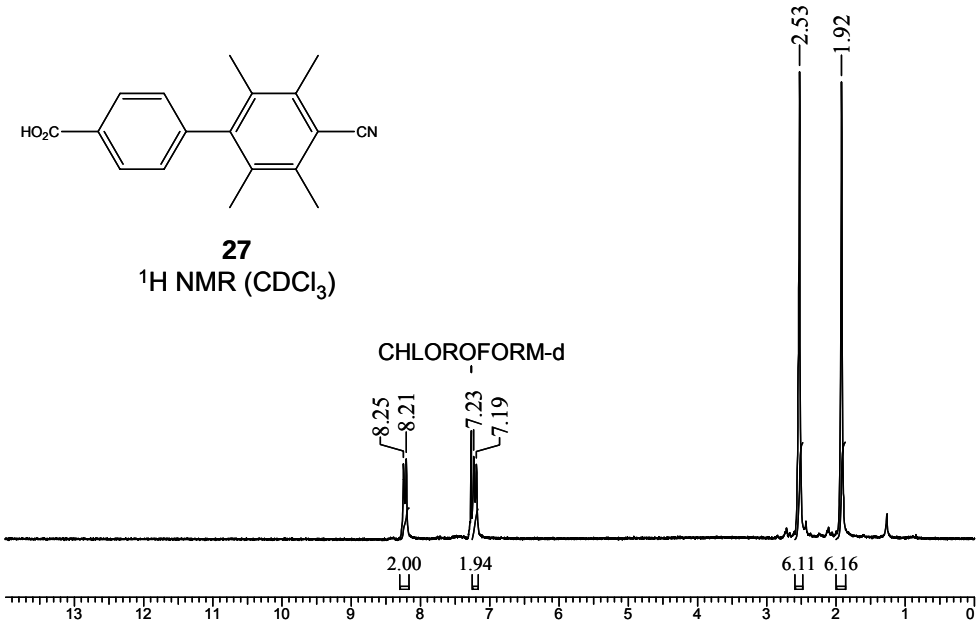

Figure A-21: ^{1}H NMR spectrum (400 MHz, $CDCl_3$) of **27**.

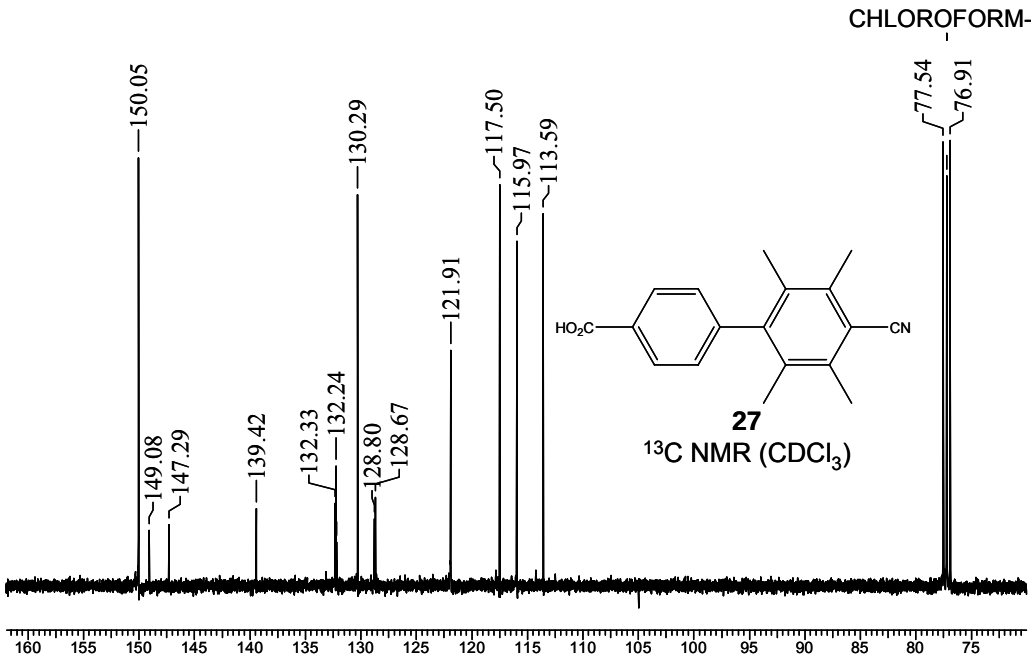

Figure A-22: ^{13}C NMR spectrum (400 MHz, $CDCl_3$) of **27**.

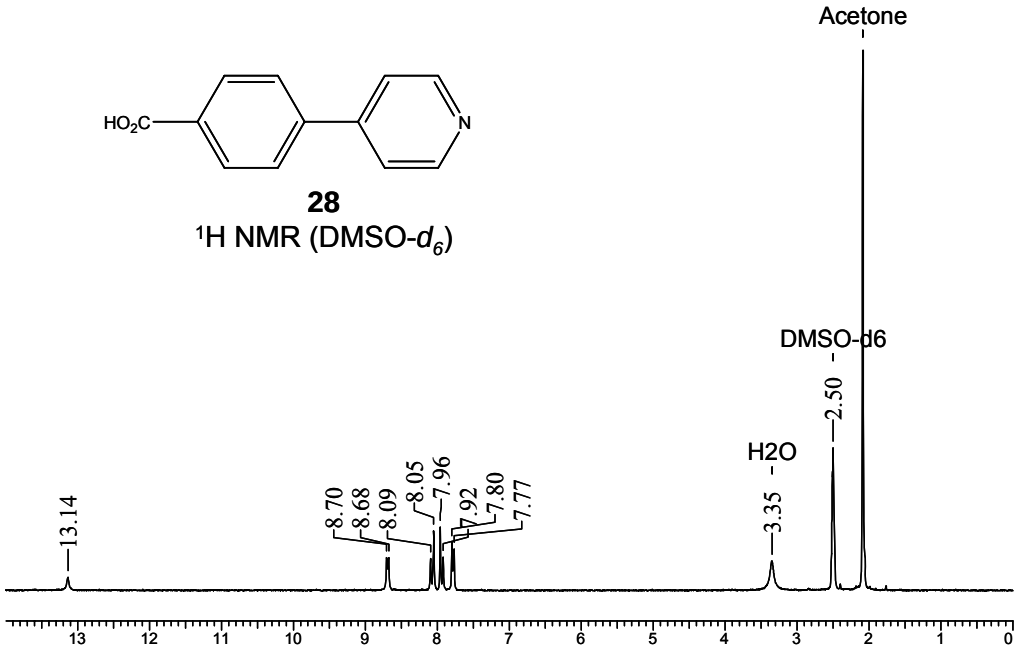

Figure A-23: ^{1}H NMR spectrum (400 MHz, DMSO-d_6) of **28**.

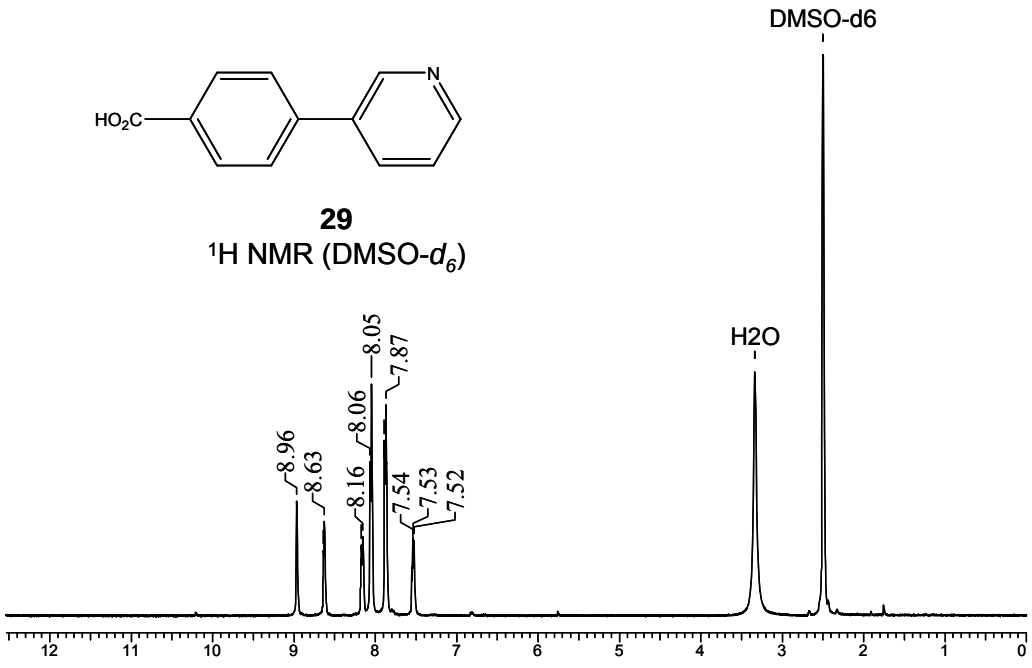

Figure A-24: ^{1}H NMR spectrum (400 MHz, DMSO-d_6) of **29**.

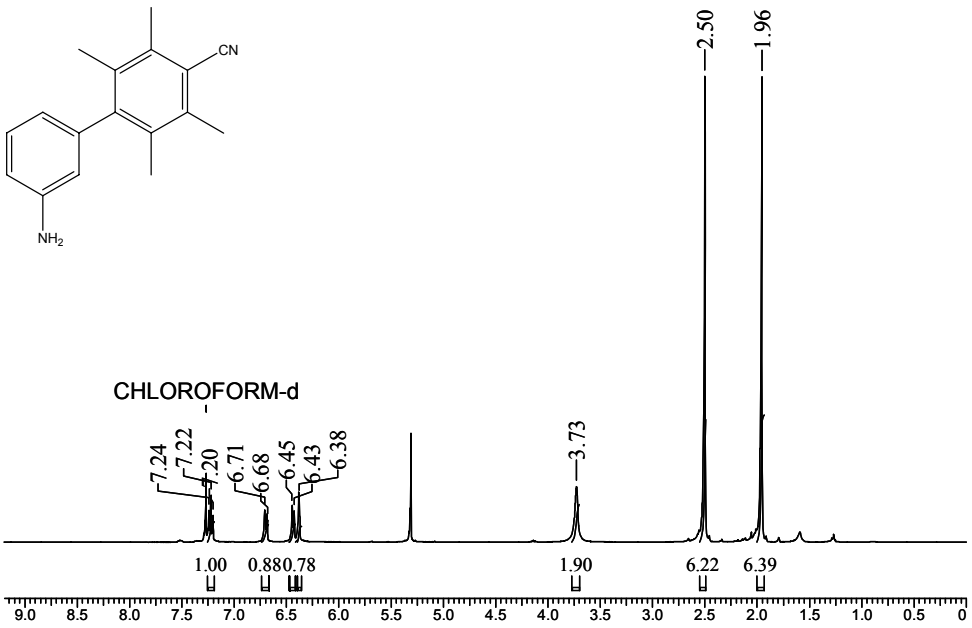

Figure A-25: ^{1}H NMR spectrum (400 MHz, $CDCl_3$) of **45**.

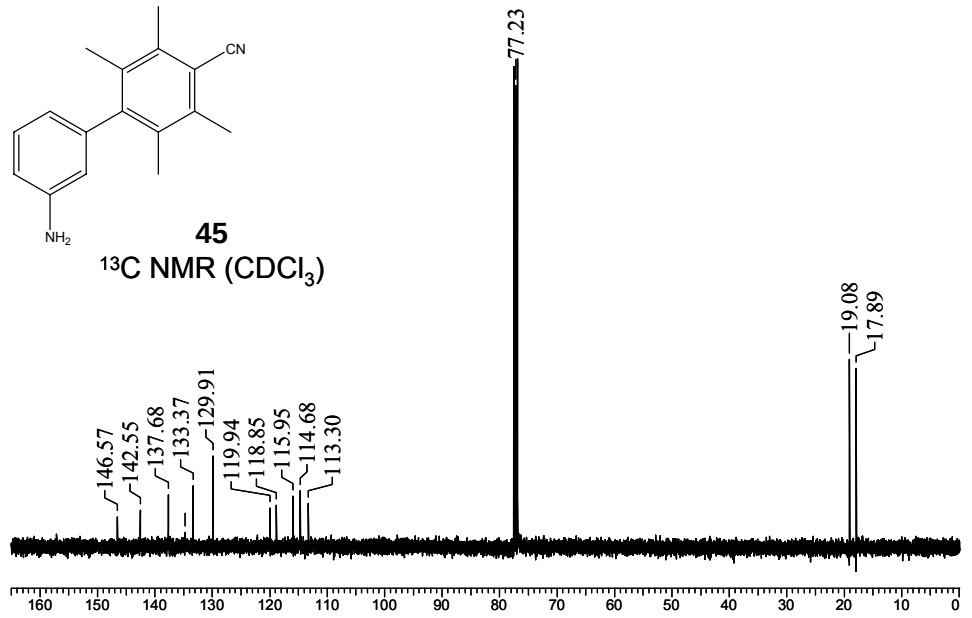

Figure A-26: ^{13}C NMR spectrum (400 MHz, $CDCl_3$) of **45**.

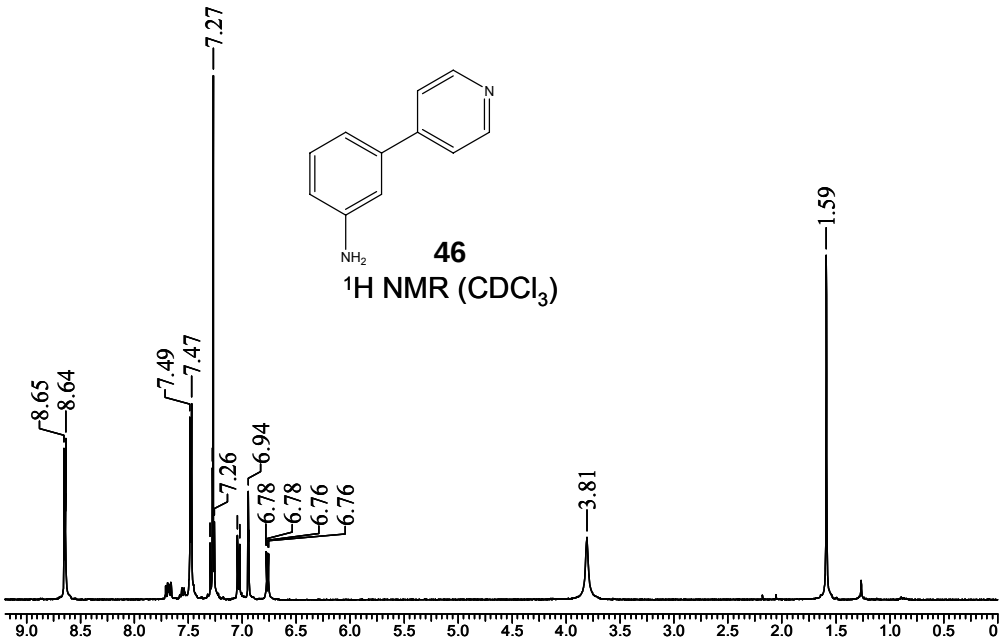

Figure A-27: ^{1}H NMR spectrum (400 MHz, $CDCl_3$) of **46**.

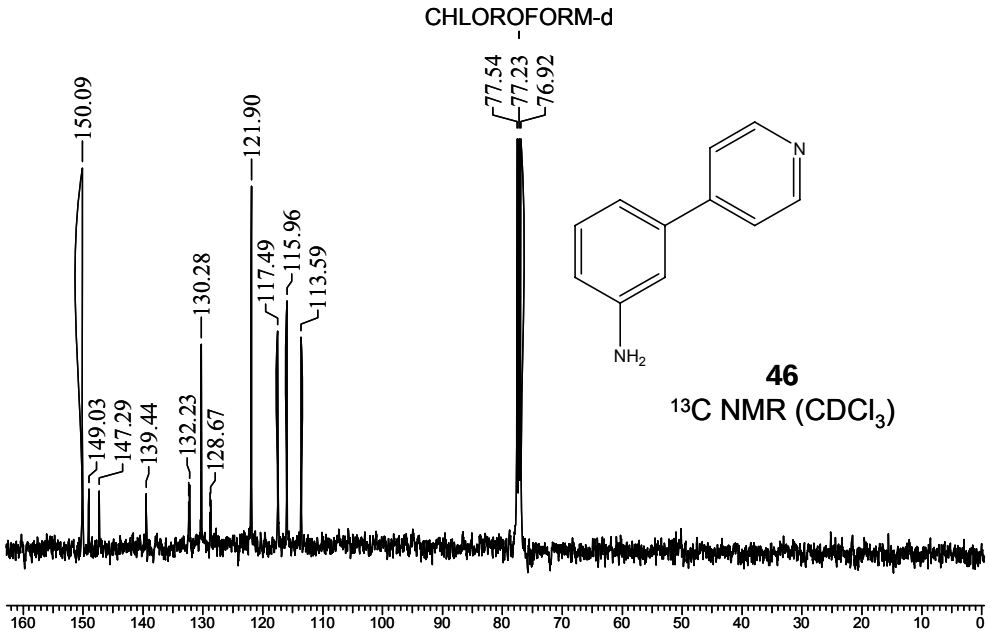

Figure A-28: ^{13}C NMR spectrum (400 MHz, $CDCl_3$) of **46**.

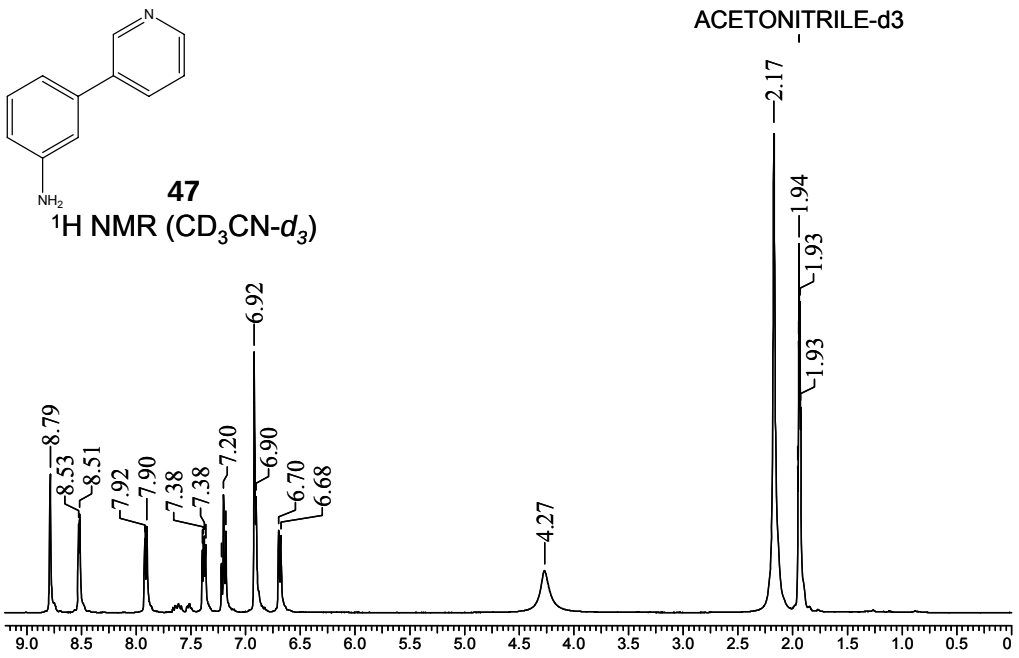

Figure A-29: ^{1}H NMR spectrum (400 MHz, CD_3CN) of **47**.

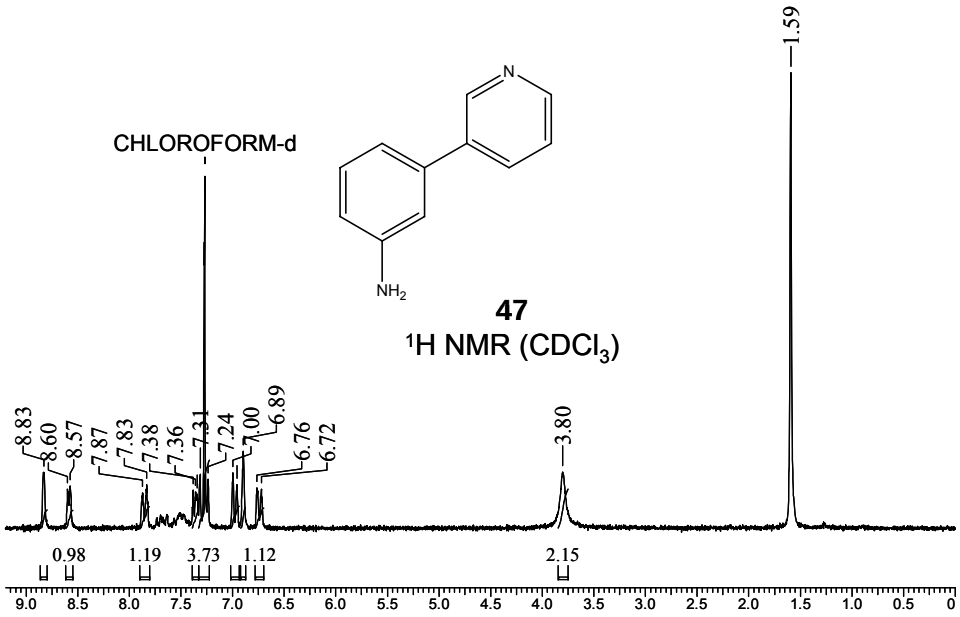

Figure A-30: ^{1}H NMR spectrum (400 MHz, $CDCl_3$) of **47**.

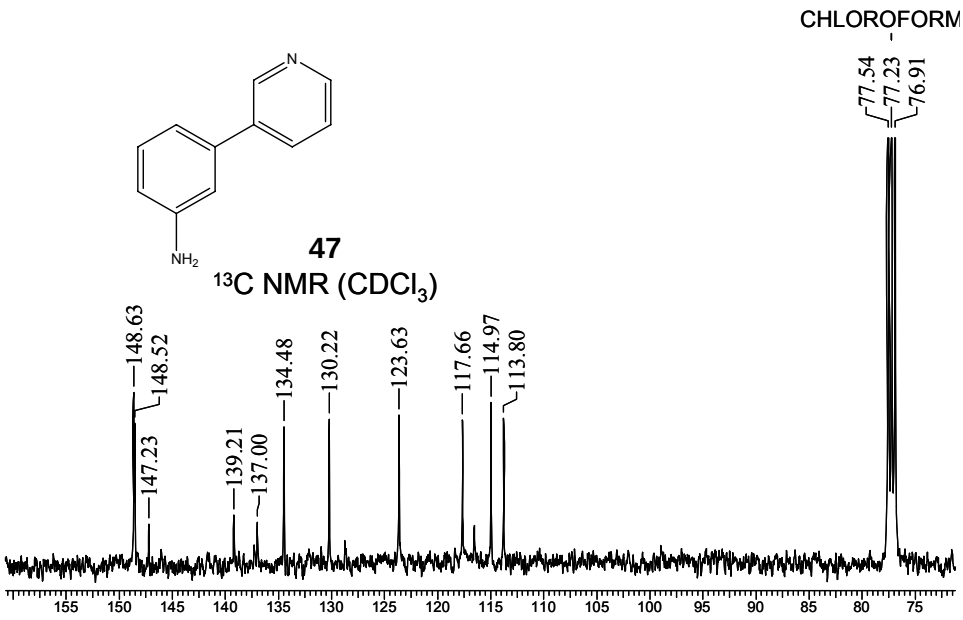

Figure A-31: ^{13}C NMR spectrum (400 MHz, $CDCl_3$) of **47**.

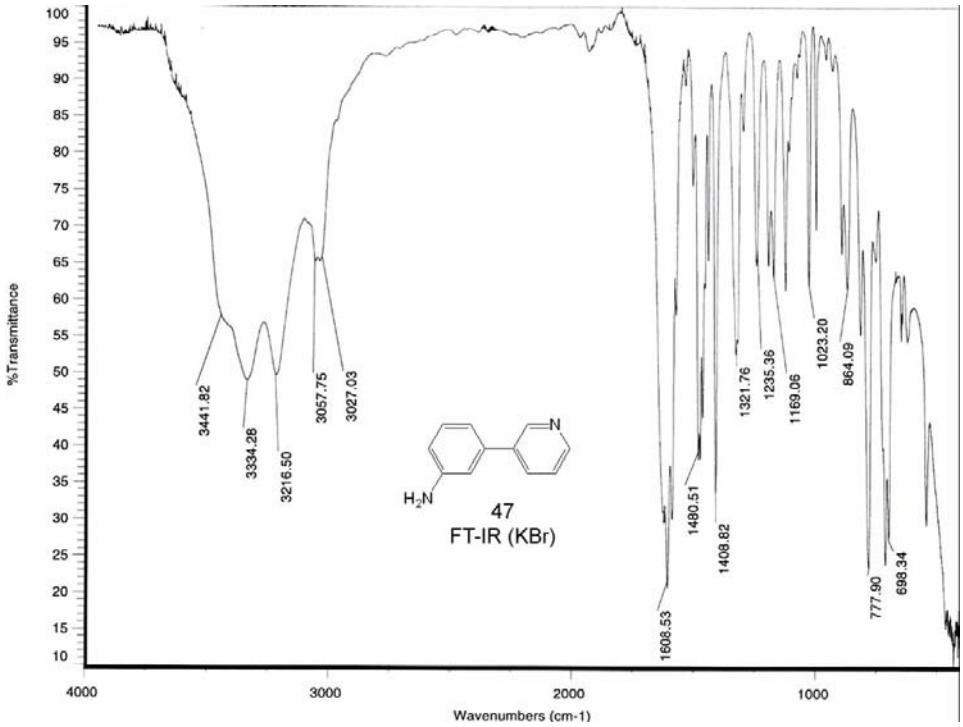

Figure A-32: FT-IR spectrum (KBr) of **47**.

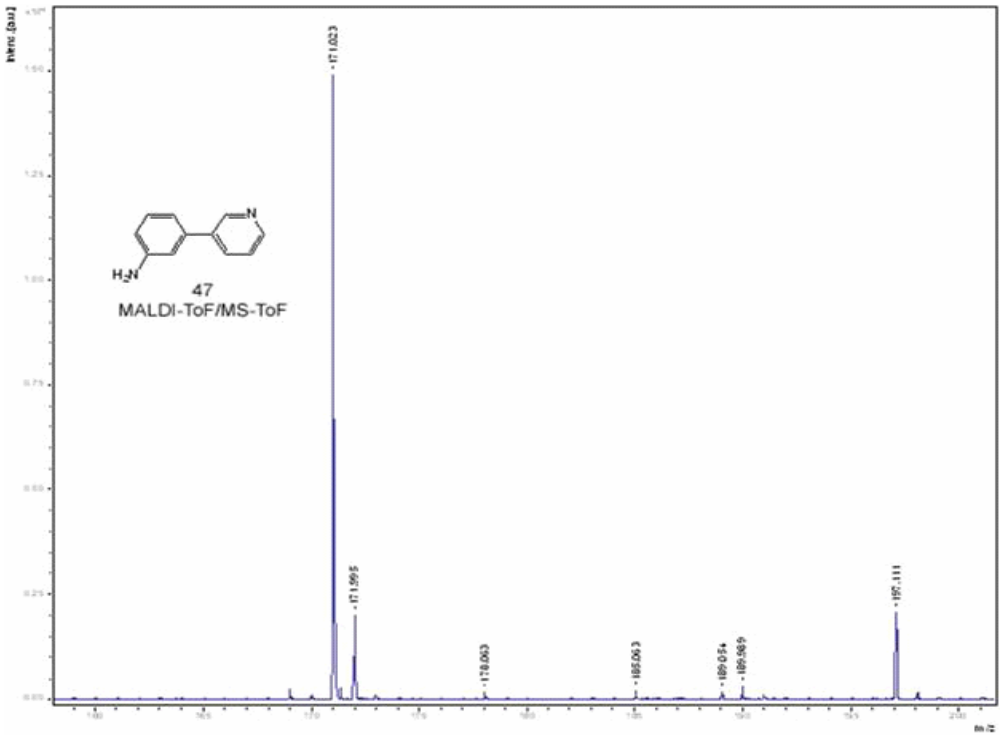

Figure A-33: MALDI-ToF/MS-ToF spectrum of **47**.

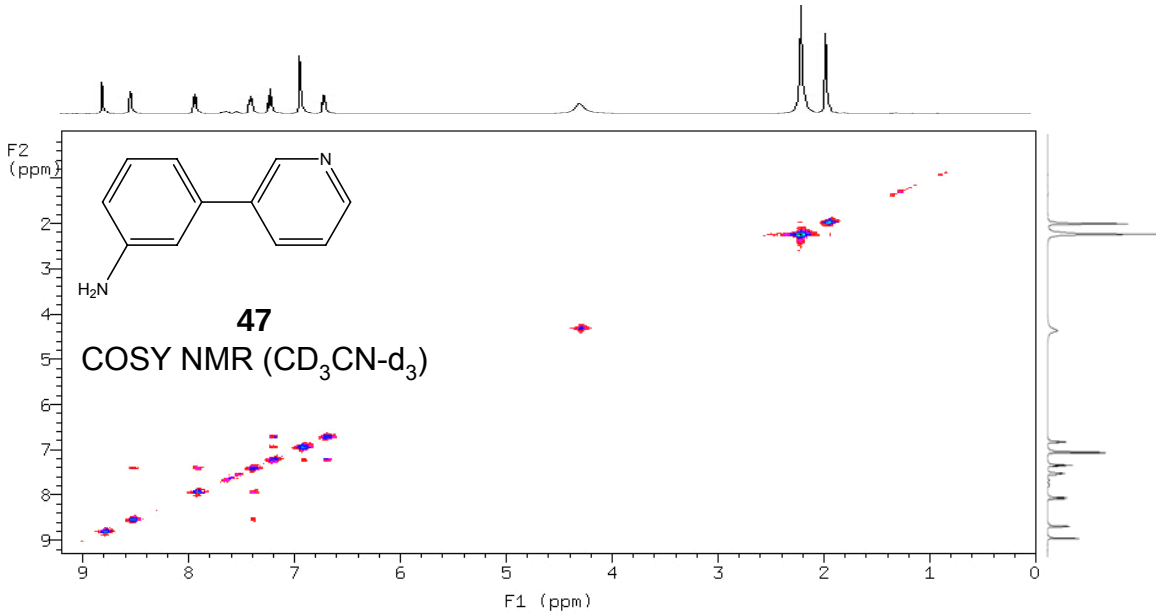

Figure A-34: 2D COSY NMR spectrum (400 MHz, CD_3CN) of **47**.

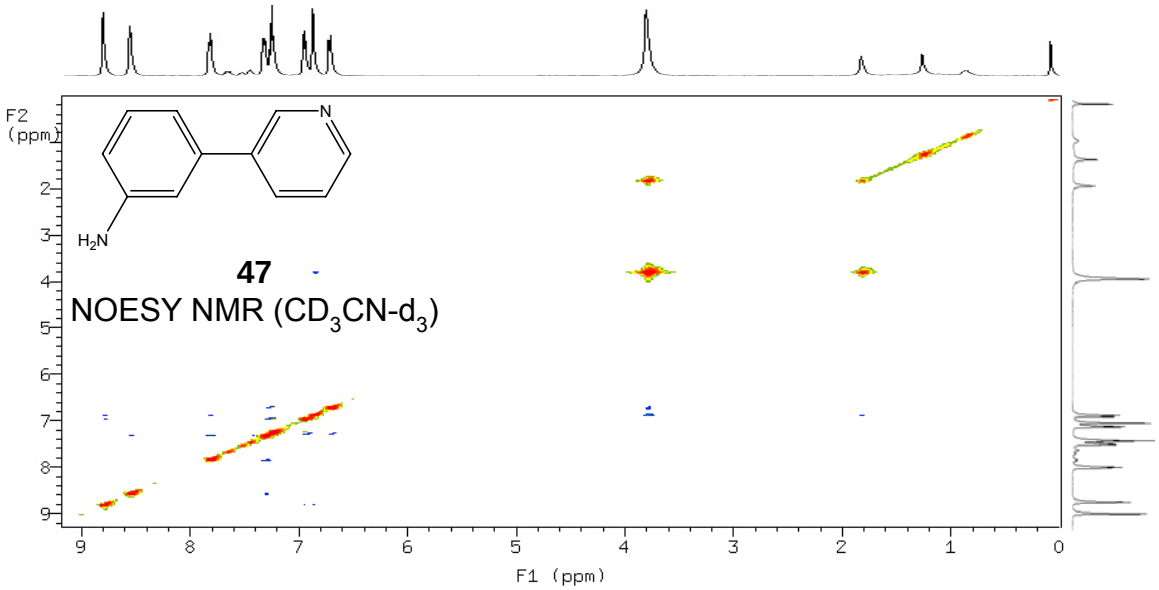

Figure A-35: 2D NOESY NMR spectrum (400 MHz, CD_3CN) of **47**.

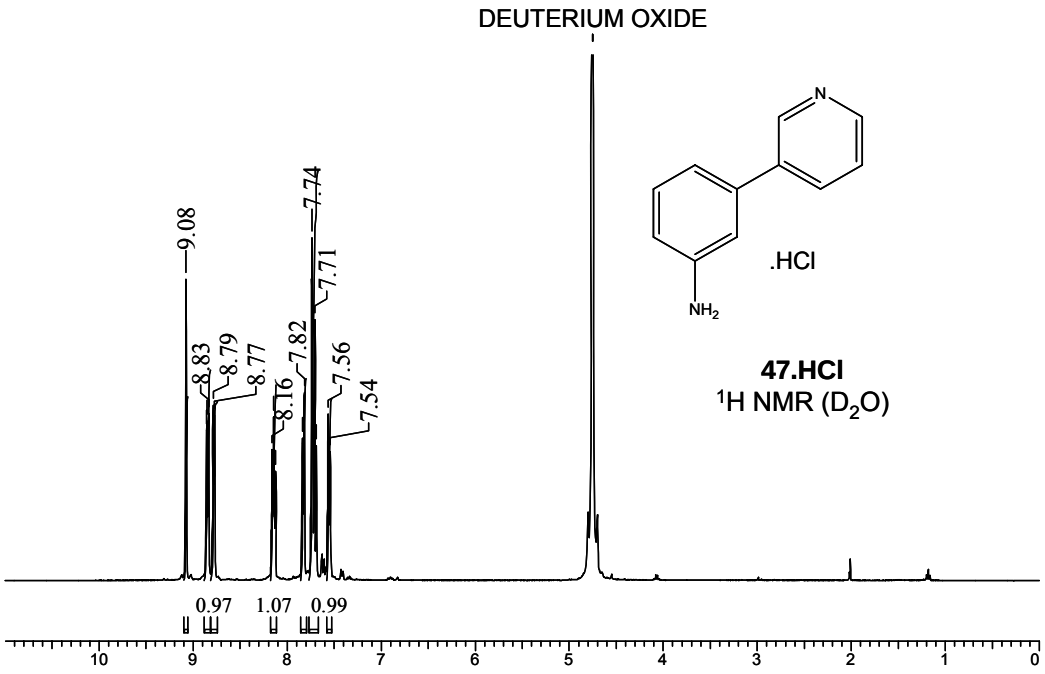

Figure A-36: ^{1}H NMR spectrum (400 MHz, D_2O) of **47.HCl**.

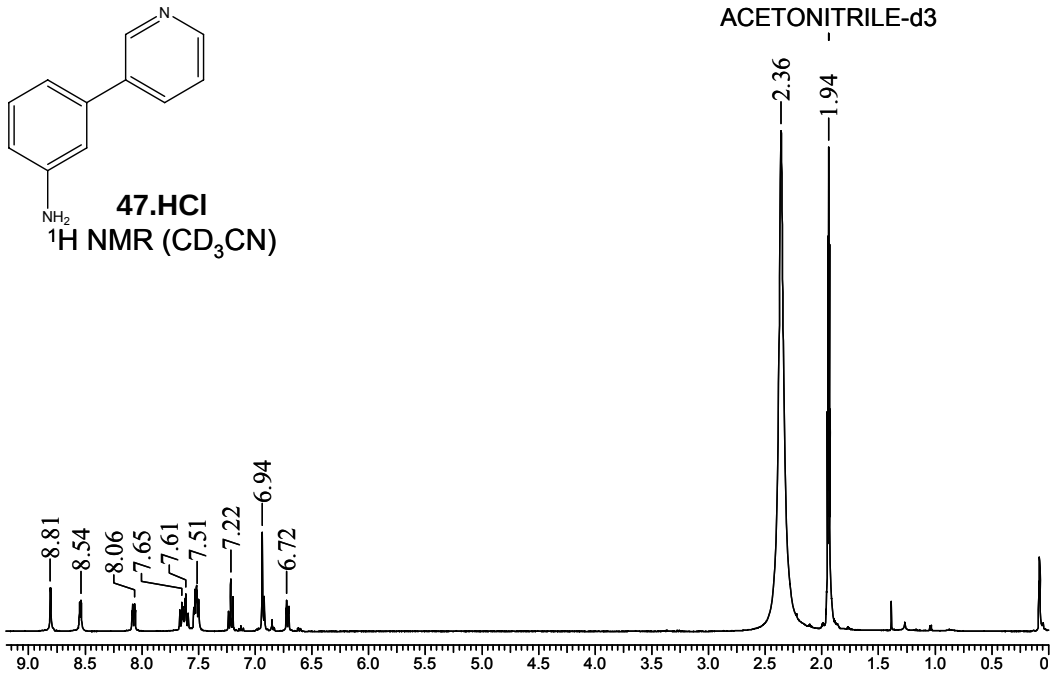

Figure A-37: ^{1}H NMR spectrum (400 MHz, CD_3CN) of **47.HCl**.

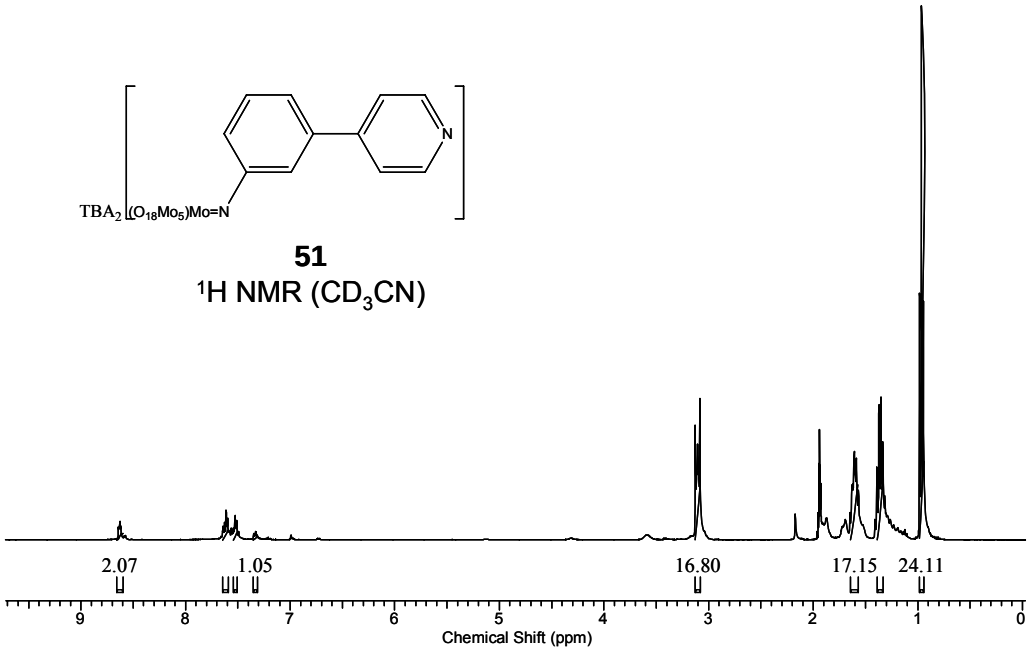

Figure A-38: ^{1}H NMR spectrum (400 MHz, CD_3CN) of **51**.

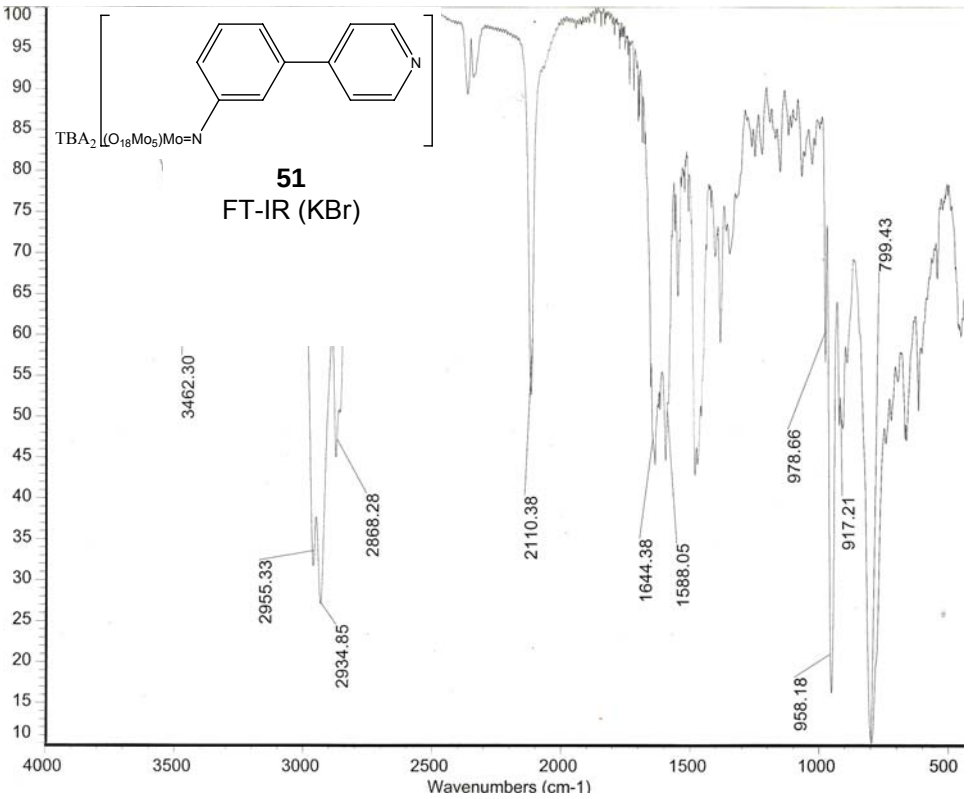

Figure A-39: FT-IR spectrum (KBr) of **51**.

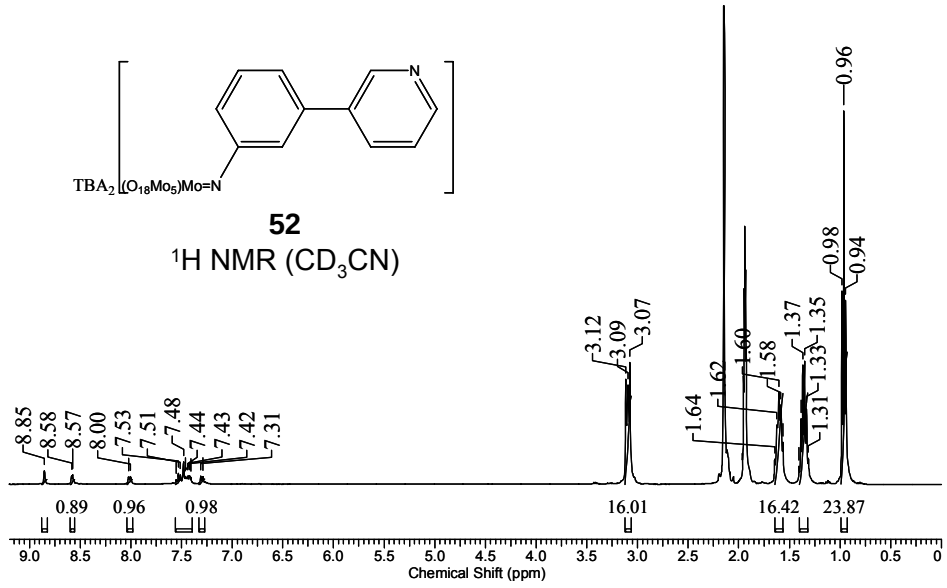

Figure A-40: ^{1}H NMR spectrum (400 MHz, CD_3CN) of **52**.

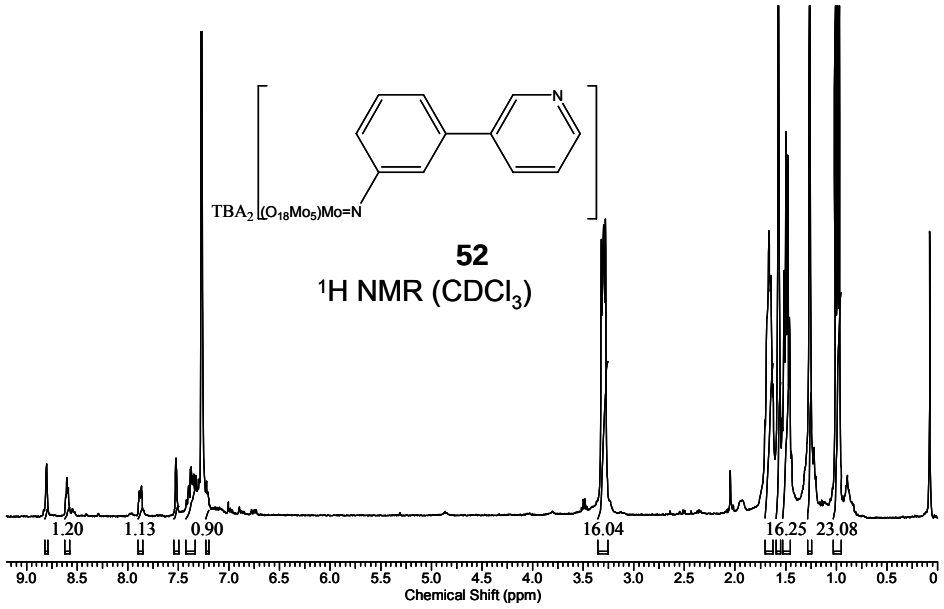

Figure A-41: ^{1}H NMR spectrum (400 MHz, $CDCl_3$) of **52**.

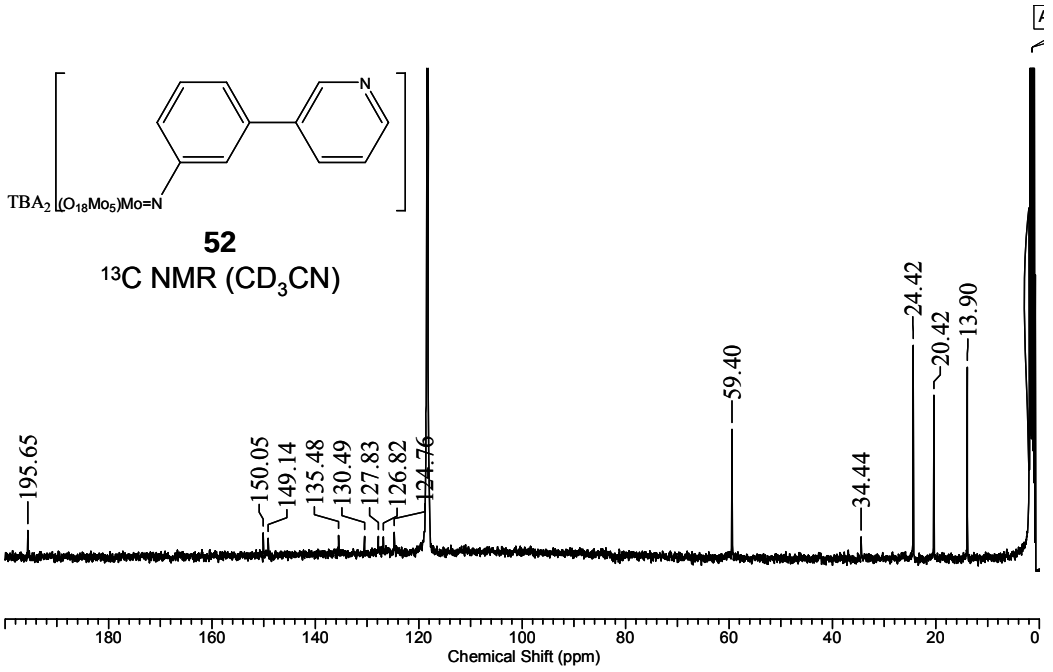

Figure A-42: ^{13}C NMR spectrum (400 MHz, CD_3CN) of **52**.

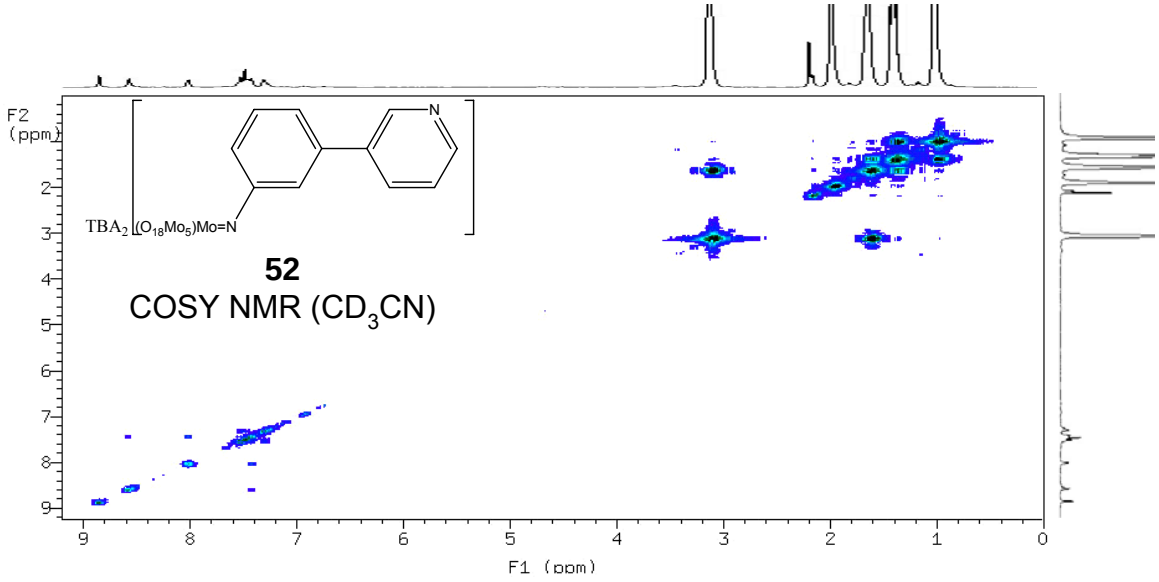

Figure A-43: 2D COSY NMR spectrum (400 MHz, CD_3CN) of **52**.

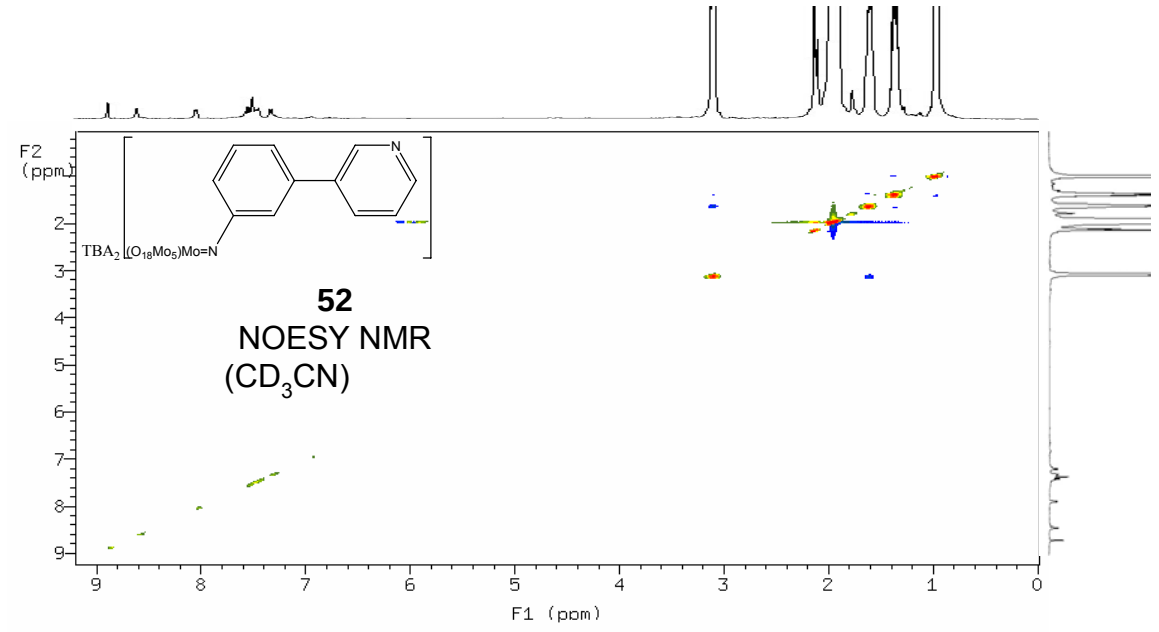

Figure A-44: 2D NOESY NMR spectrum (400 MHz, CD_3CN) of **52**.

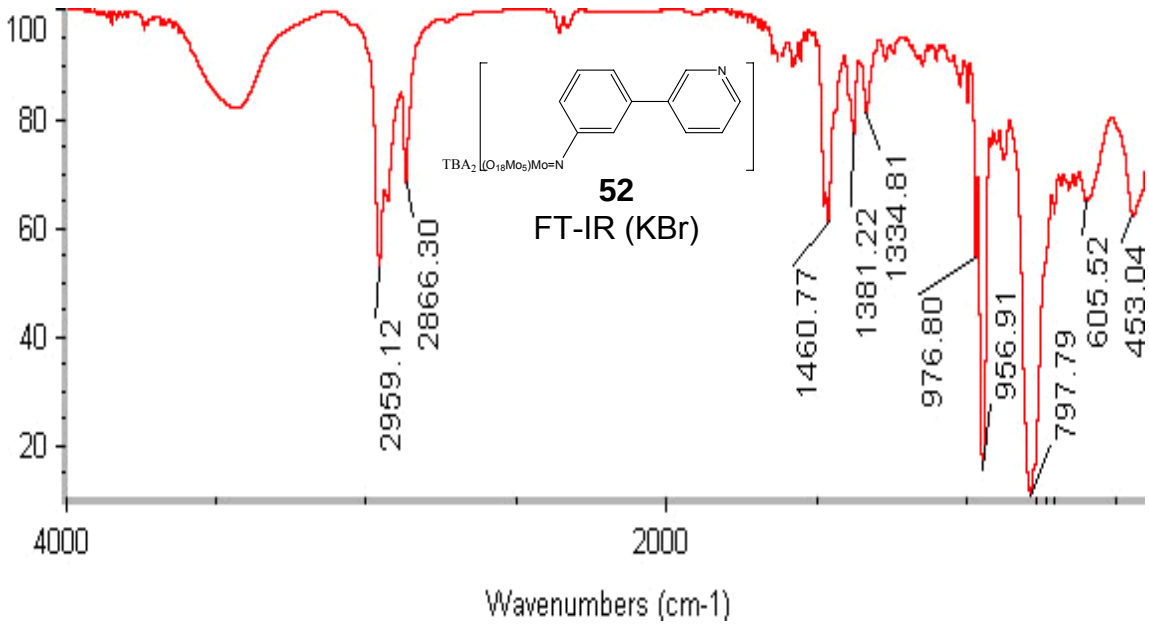

Figure A-45: FT-IR spectrum (KBr) of **52**.

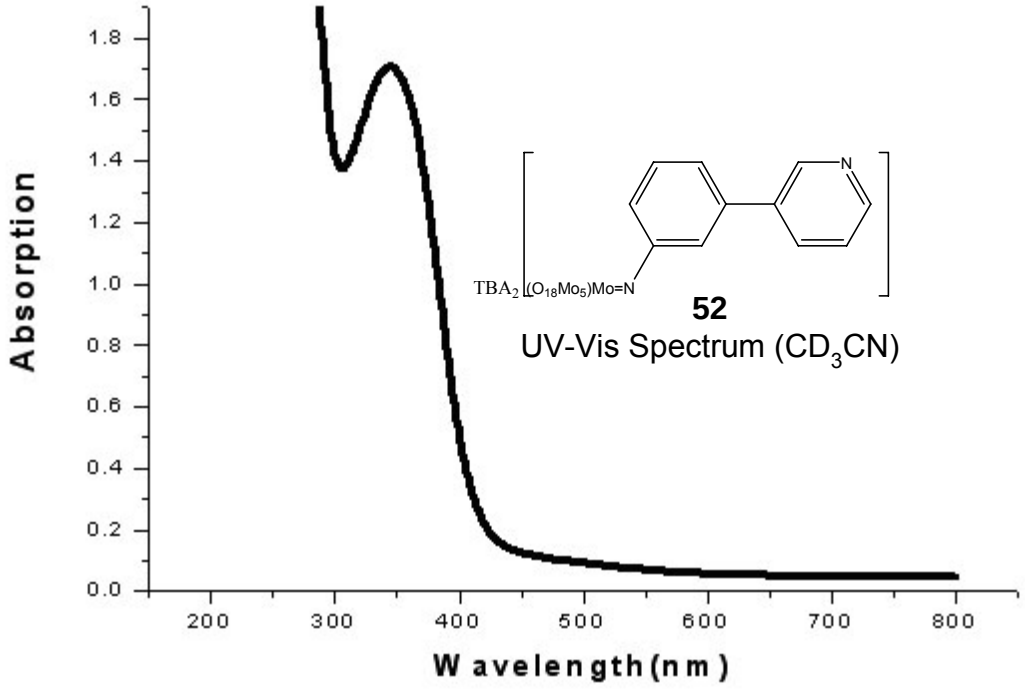

Figure A-46: UV-Vis spectrum (CD_3CN) of **52**.

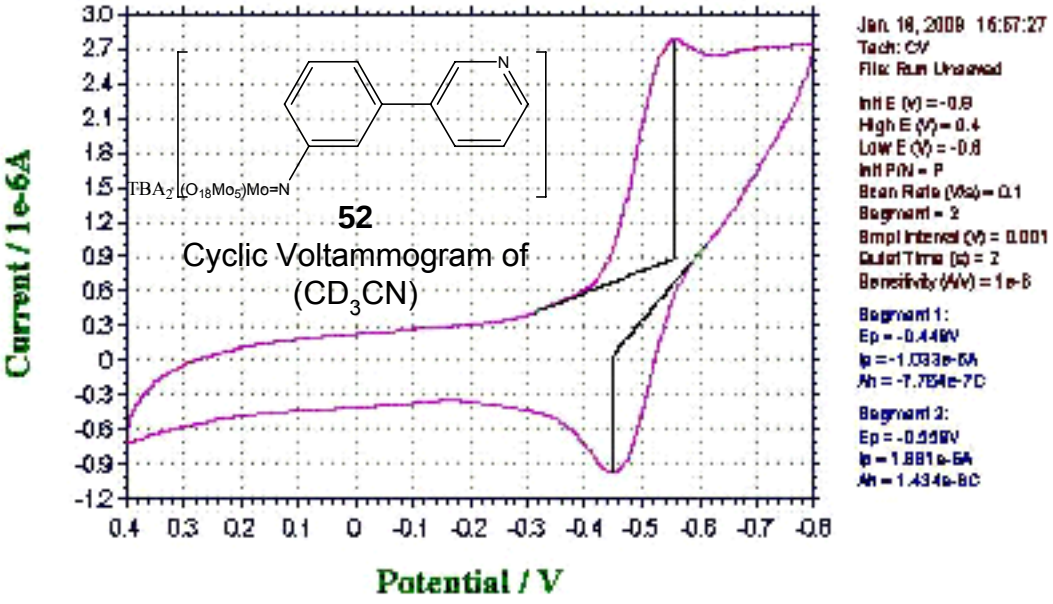

Figure A-47: Cyclic Voltammogram (CD_3CN) of **52**.

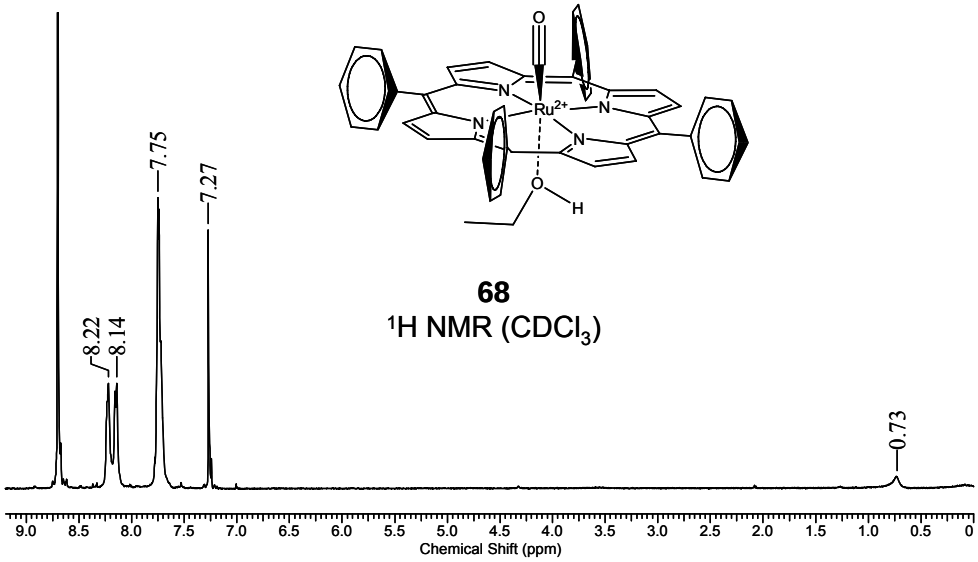

Figure A-48: ^1H NMR spectrum (400 MHz, $CDCl_3$) of **68**.

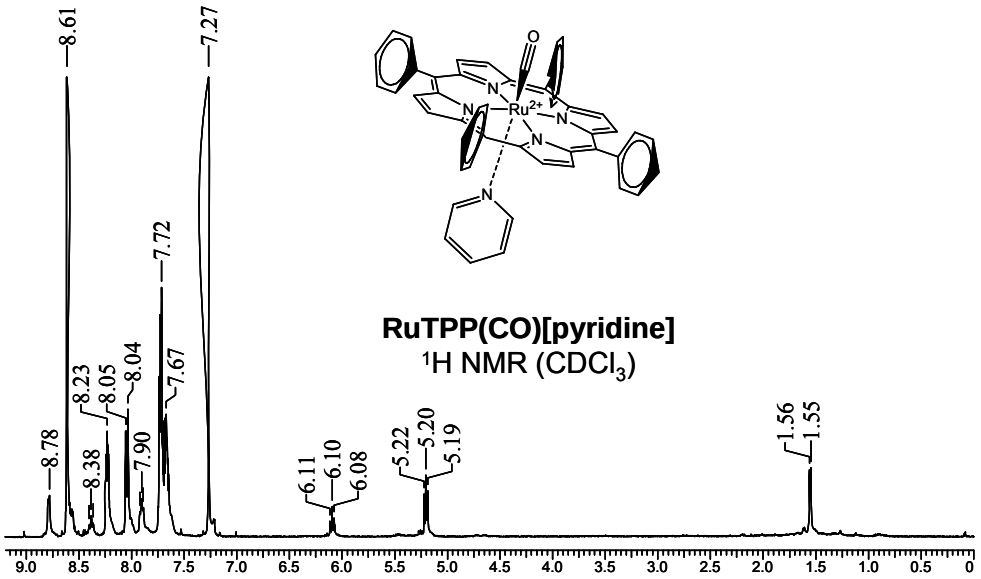

Figure A-49: ^{1}H NMR spectrum (400 MHz, $CDCl_3$) of **RuTPP(CO)[pyridine]**.

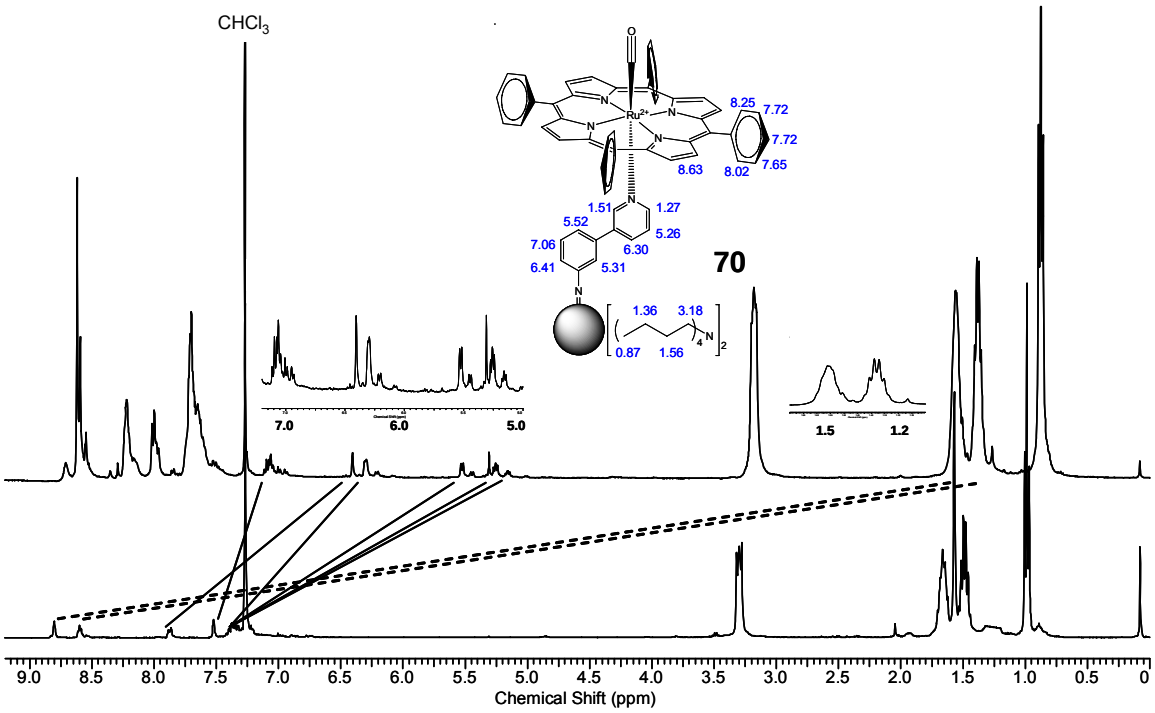

Figure A-50: ^{1}H NMR spectrum (400 MHz, $CDCl_3$) of **70**.

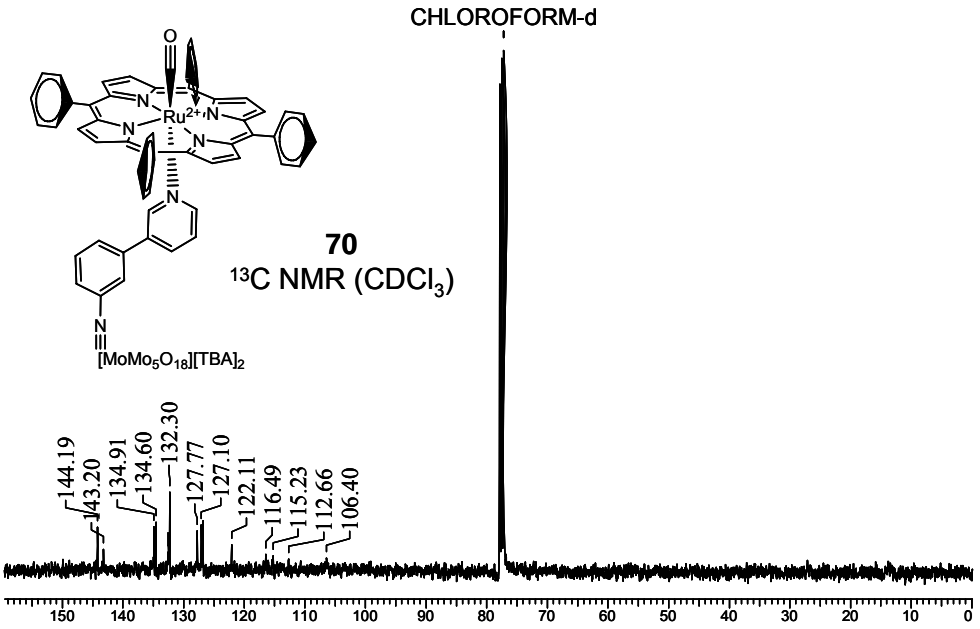

Figure A-51: ^{13}C NMR spectrum (400 MHz, $CDCl_3$) of **70**.

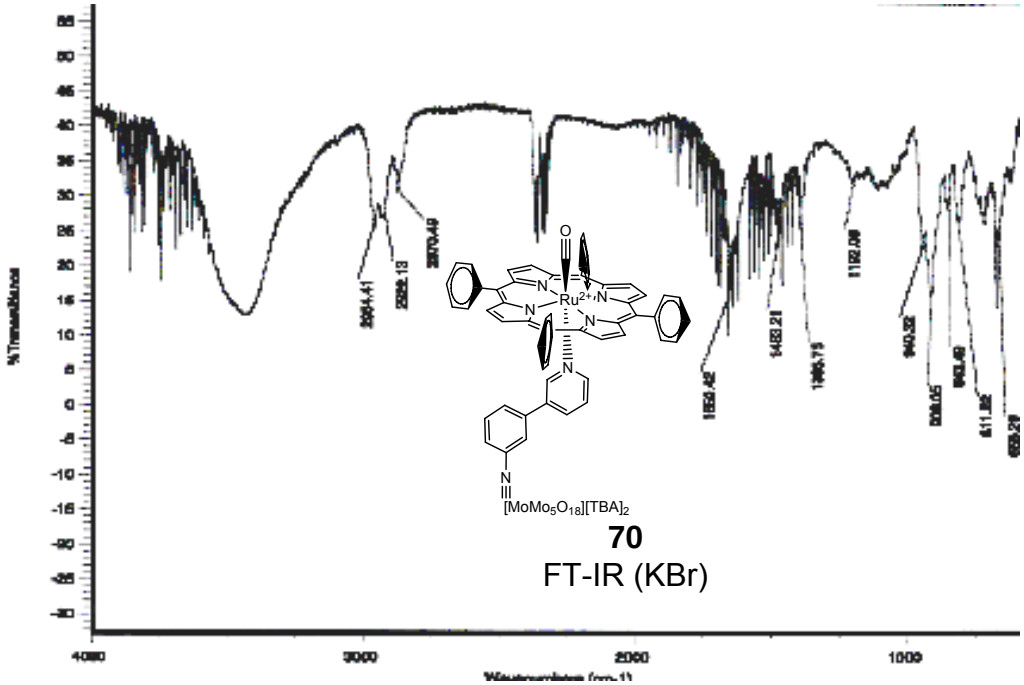

Figure A-52: FT-IR spectrum (KBr) of **70**.

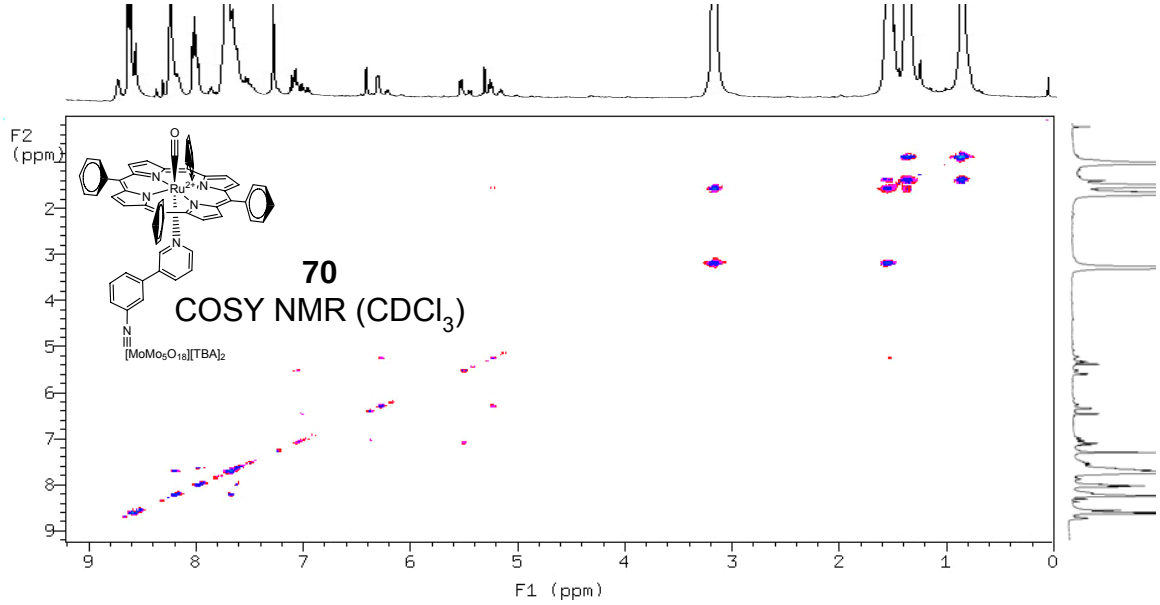

Figure A-53: 2D COSY NMR spectrum (400 MHz, $CDCl_3$) of **70**.

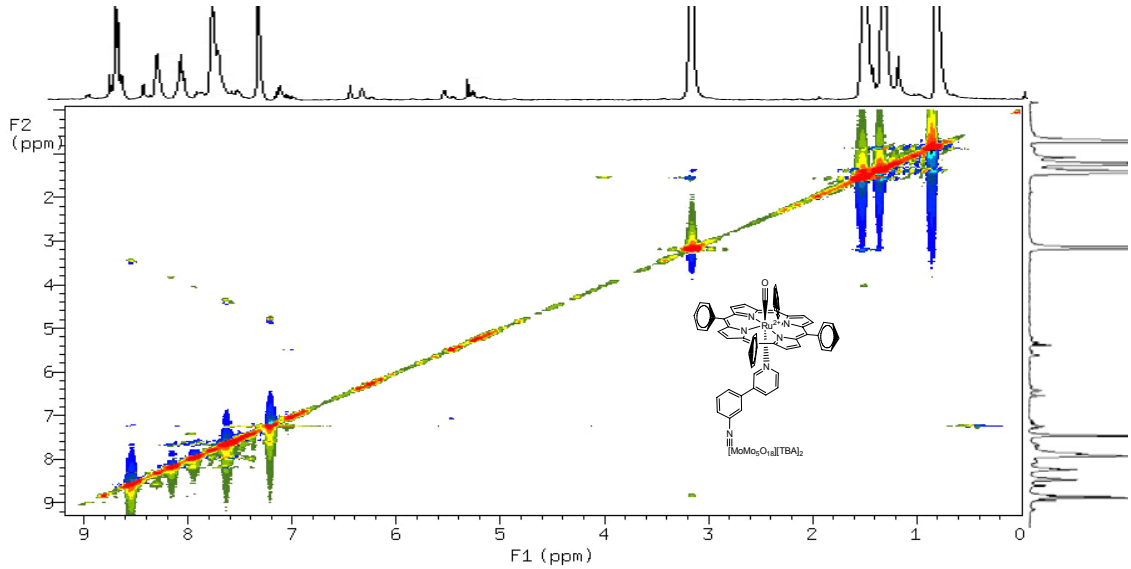

Figure A-54: 2D NOESY NMR spectrum (400 MHz, $CDCl_3$) of **70**.

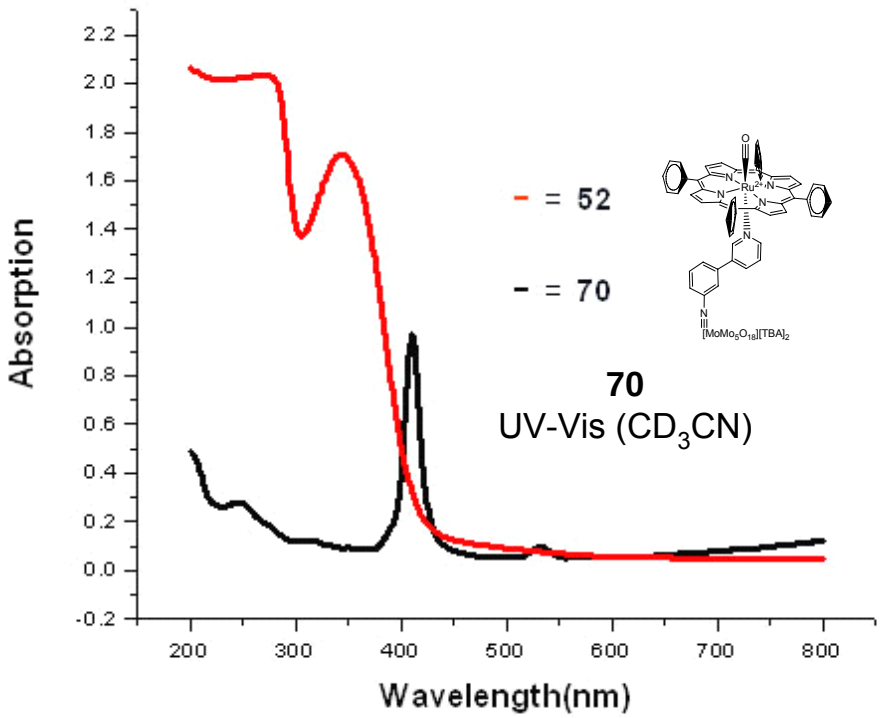

Figure A-55: UV-Vis spectrum (CD_3CN) of **70**.

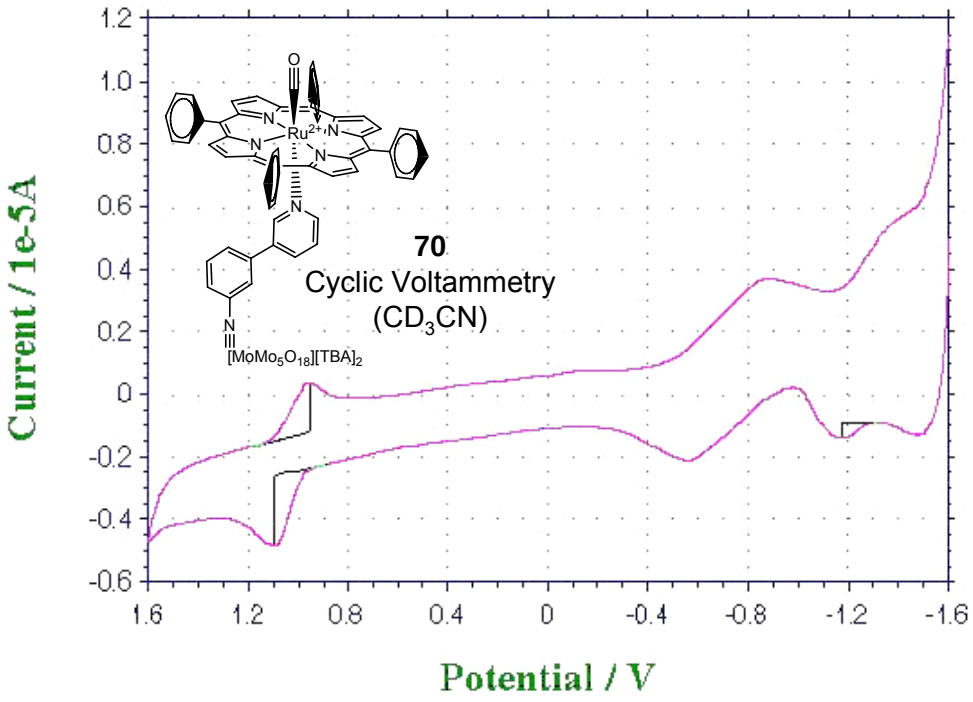

Figure A-56: Cyvlic Voltammogram (CD_3CN) of **70**.

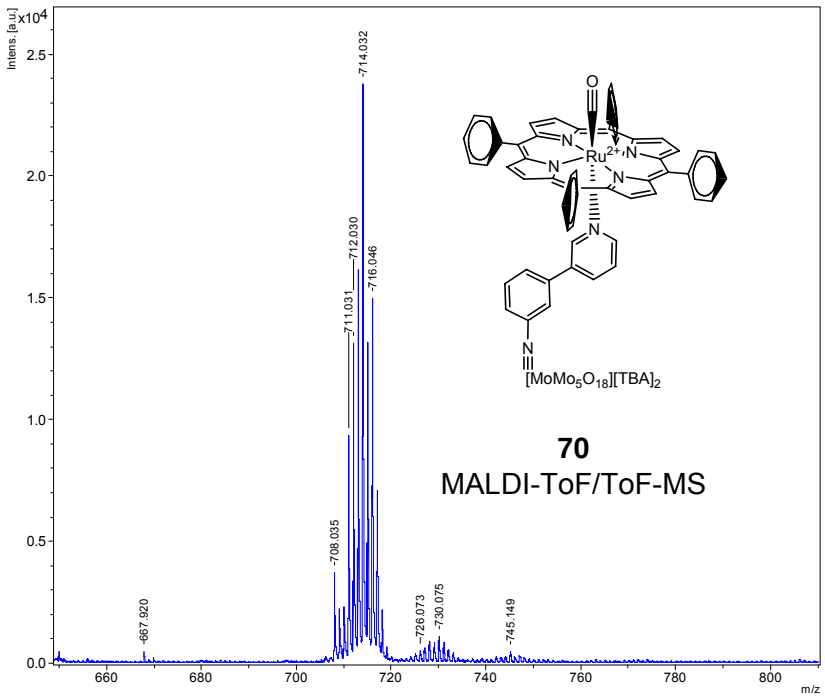

Figure A-57: MALDI-ToF/MS-ToF spectrum of 70 showing only the [RuTPP]+ fragment. (Only detected the $[RuTPP]^+$ peak)

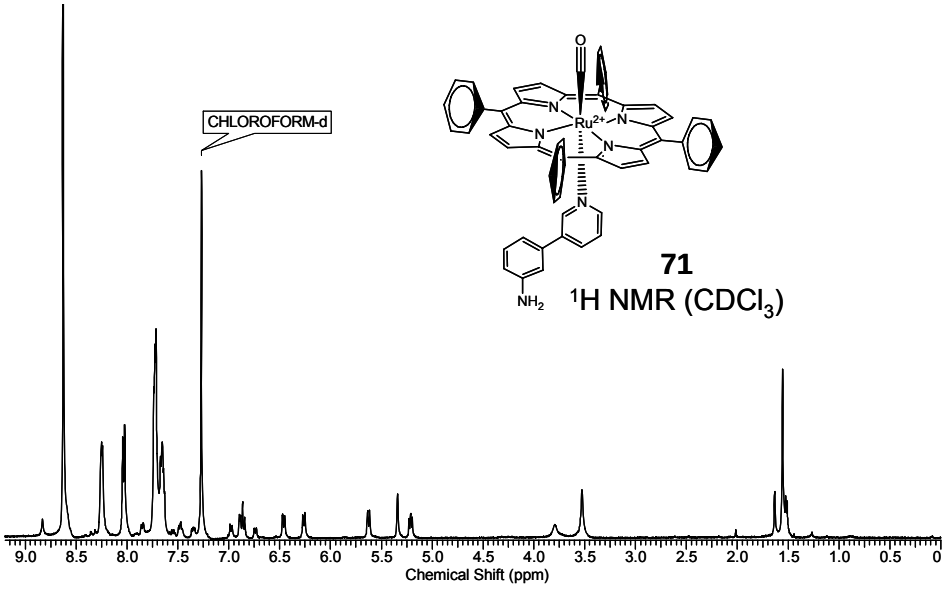

Figure A-58: ^1H NMR spectrum (400 MHz, $CDCl_3$) of **71**.

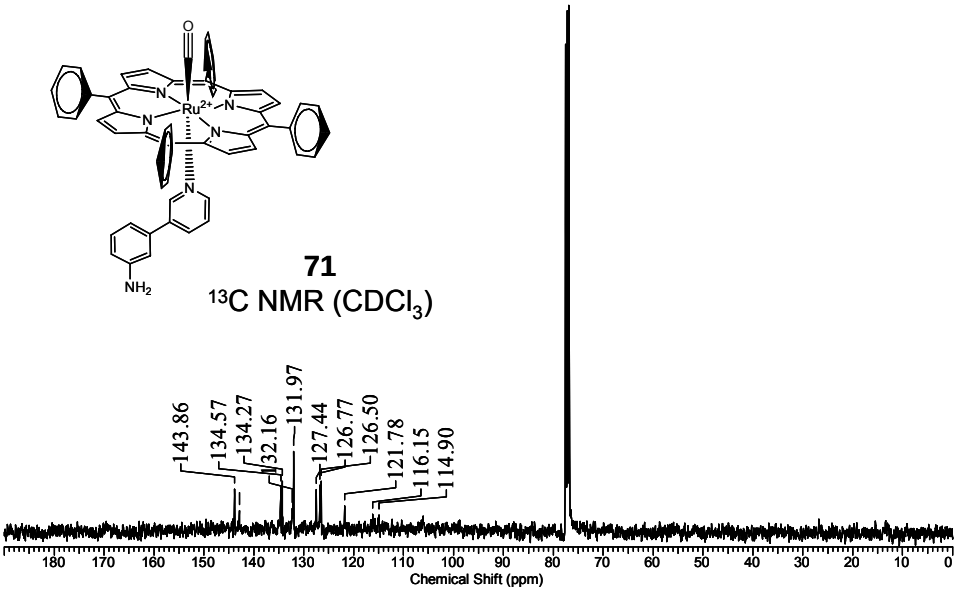

Figure A-59: ^{13}C NMR spectrum (400 MHz, $CDCl_3$) of **71**.

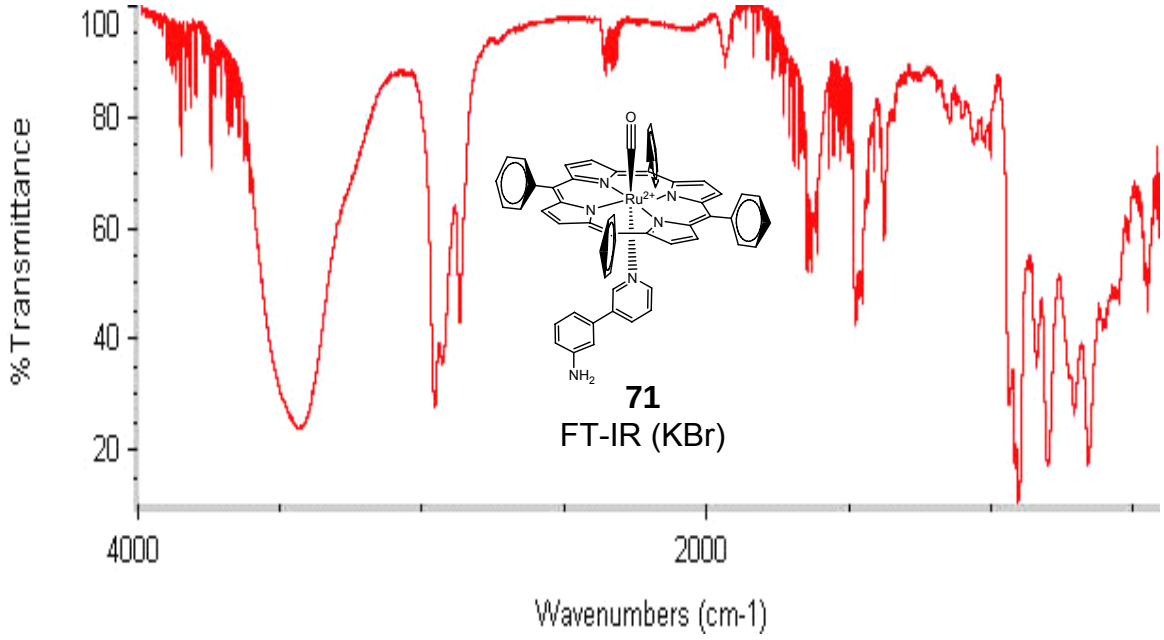

Figure A-60: FT-IR spectrum (KBr) of **71**.

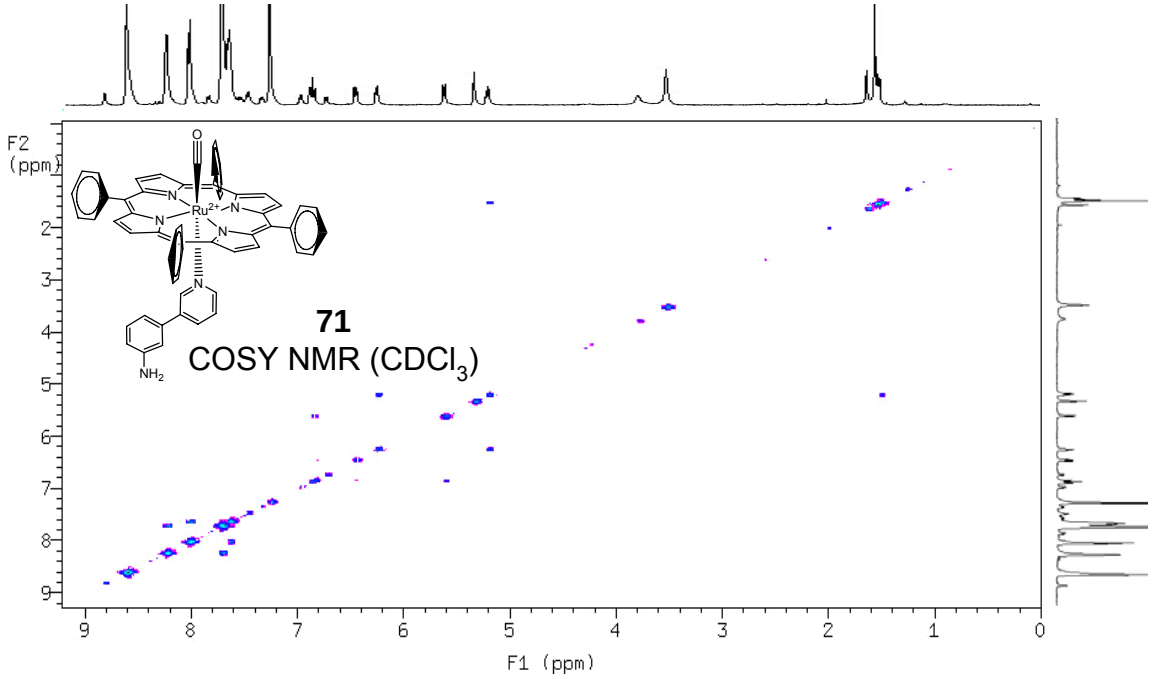

Figure A-61: 2D COSY NMR spectrum (400 MHz, $CDCl_3$) of **71**.

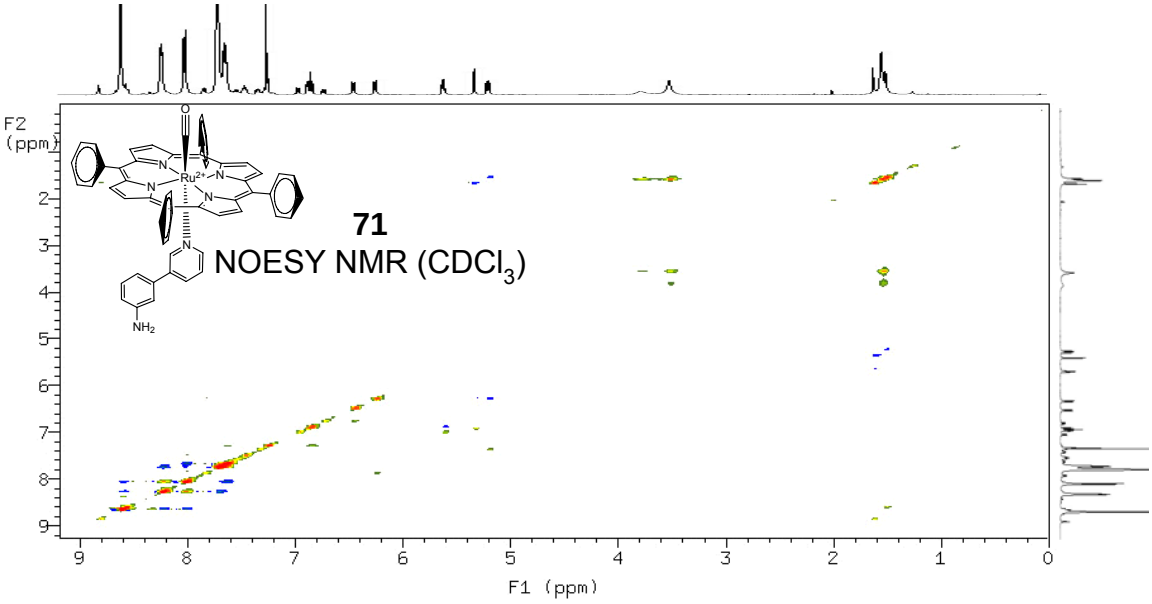

Figure A-62: 2D NOESY NMR spectrum (400 MHz, $CDCl_3$) of **71**.

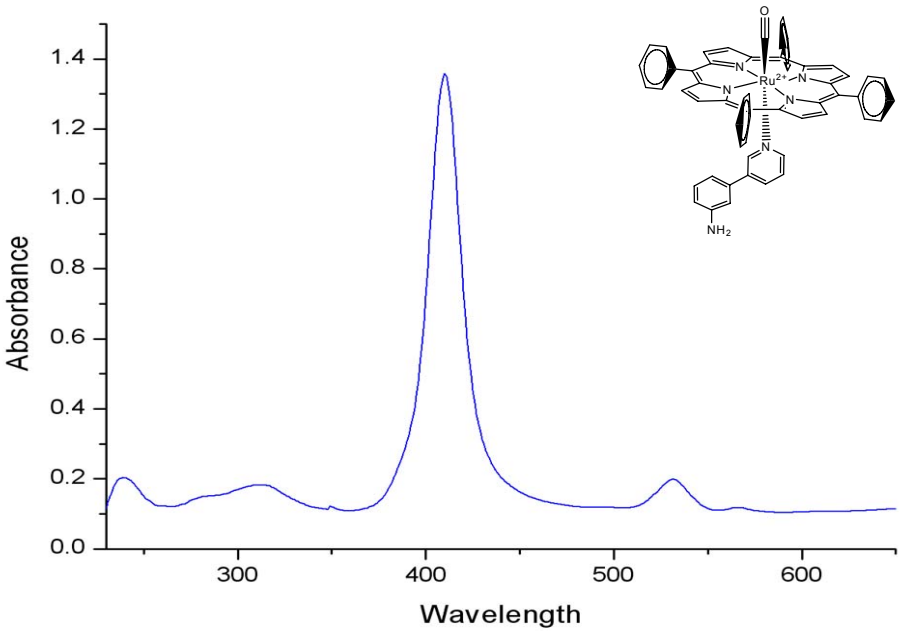

Figure A-63: UV-Vis spectrum (CD_3CN) of **71**.

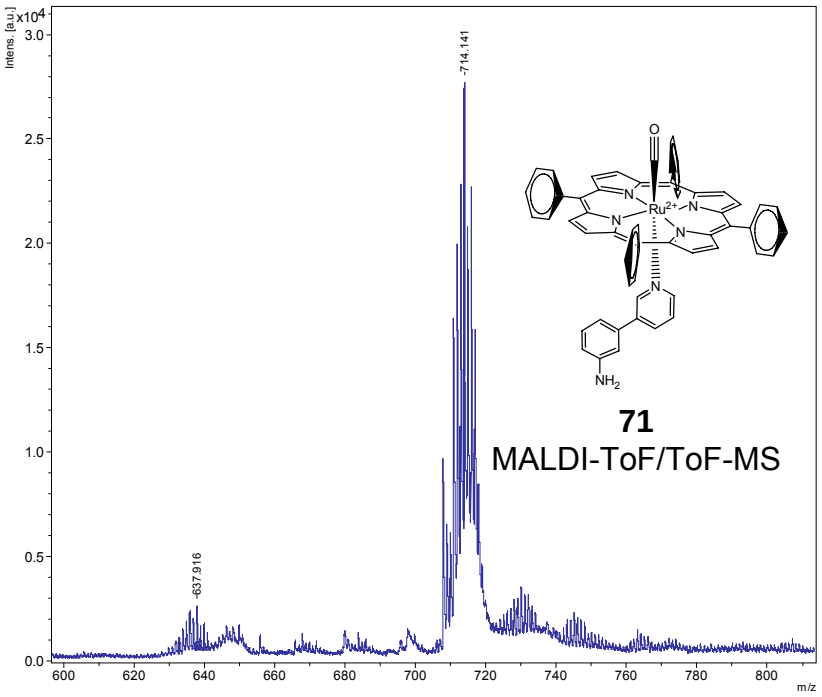

Figure A-64: MALDI-ToF/MS-ToF spectrum of **71**.

(Only found $[RuTPP]^+$ peak)

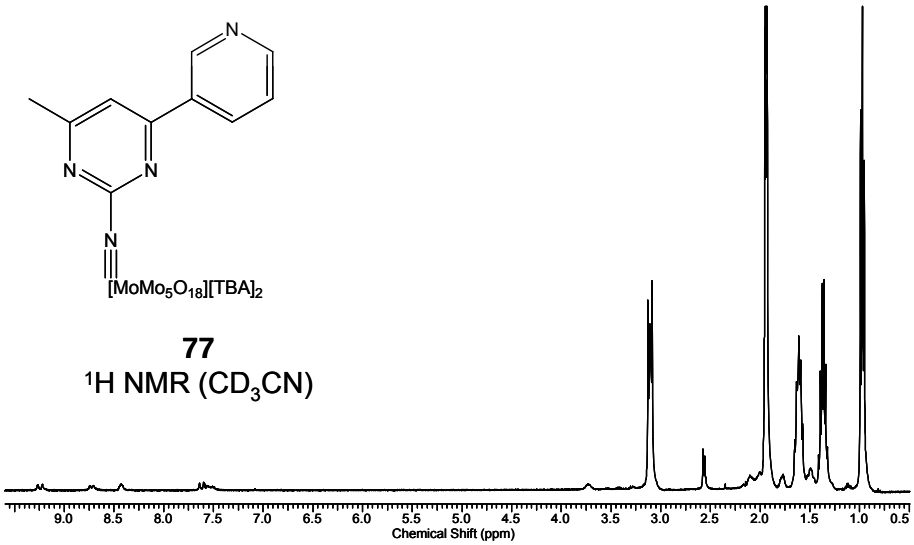

Figure A-65: ^{1}H NMR spectrum (400 MHz, $CDCl_3$) of **77**.

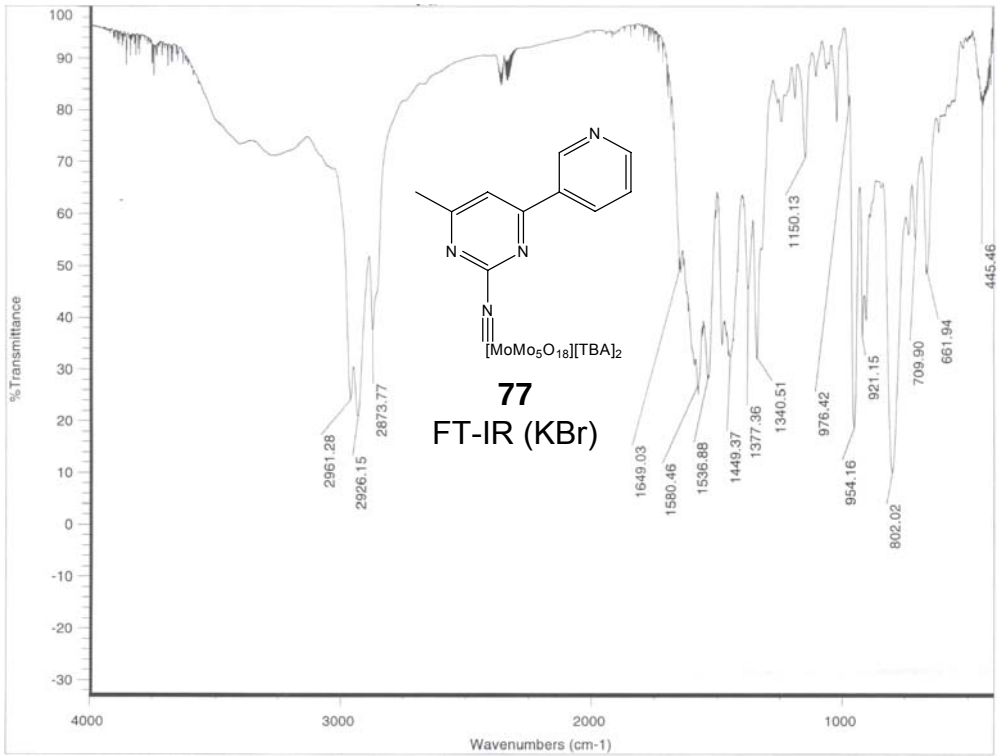

Figure A-66: FT-IR spectrum (KBr) of **77**.

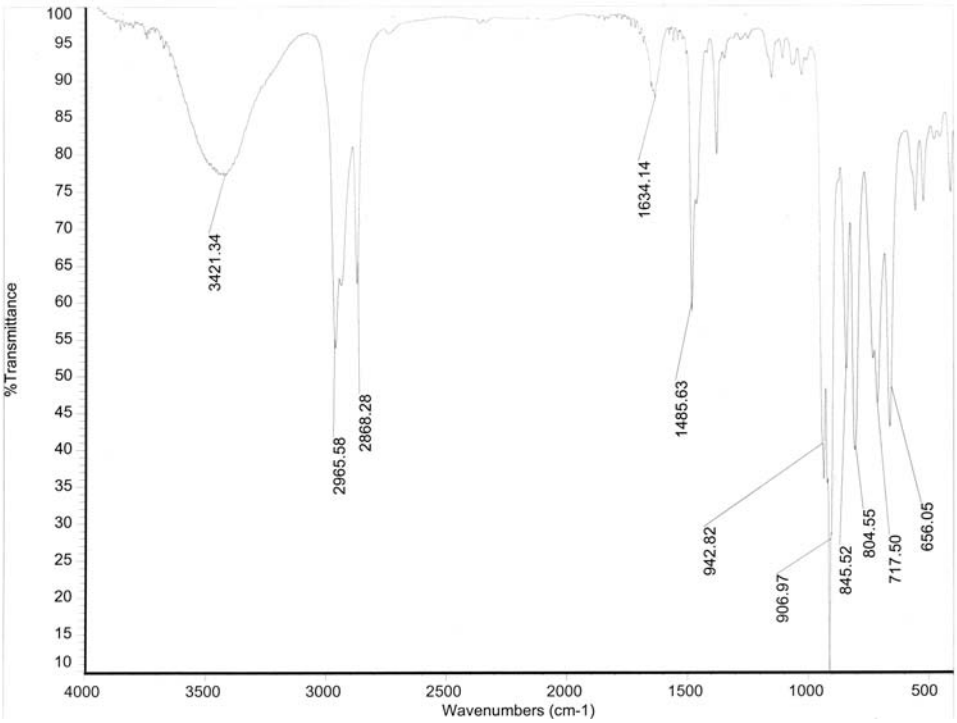

Figure A-67: FT-IR spectrum (KBr) of $TBA_4[Mo_8O_{26}]$.

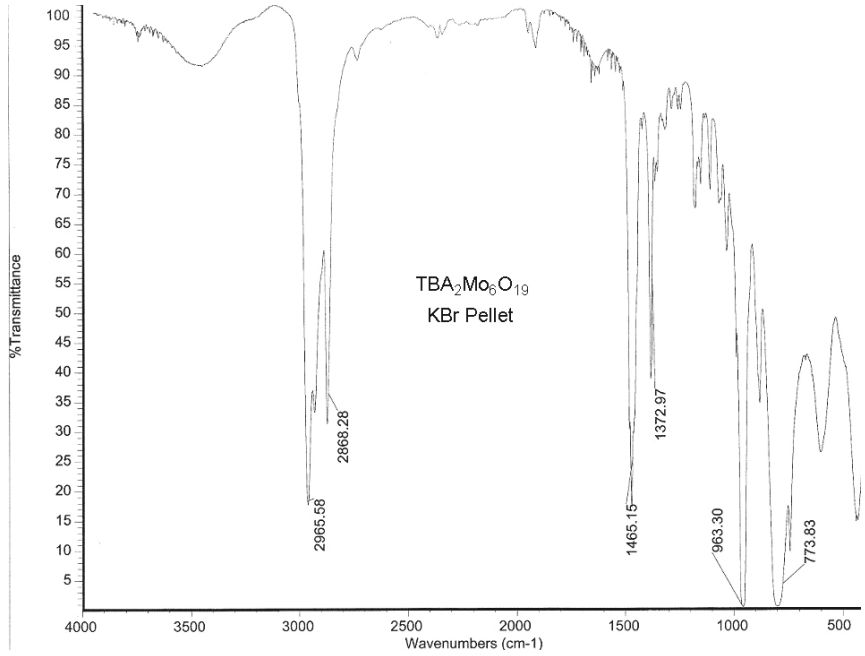

Figure A-68: FT-IR spectrum (KBr) of $TBA_2[Mo_6O_{19}]$.

Appendix B - Chapter 3

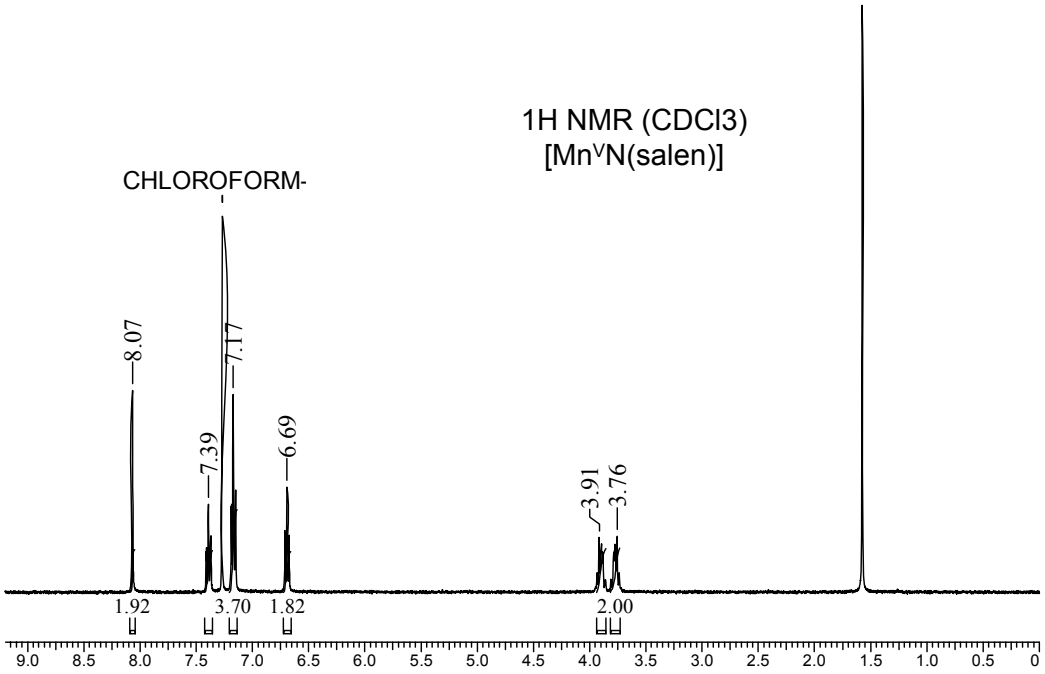

Figure B-1: ^{1}H NMR spectrum (400 MHz, $CDCl_3$) [$Mn^{V}N$(salen)] complex, **8**.

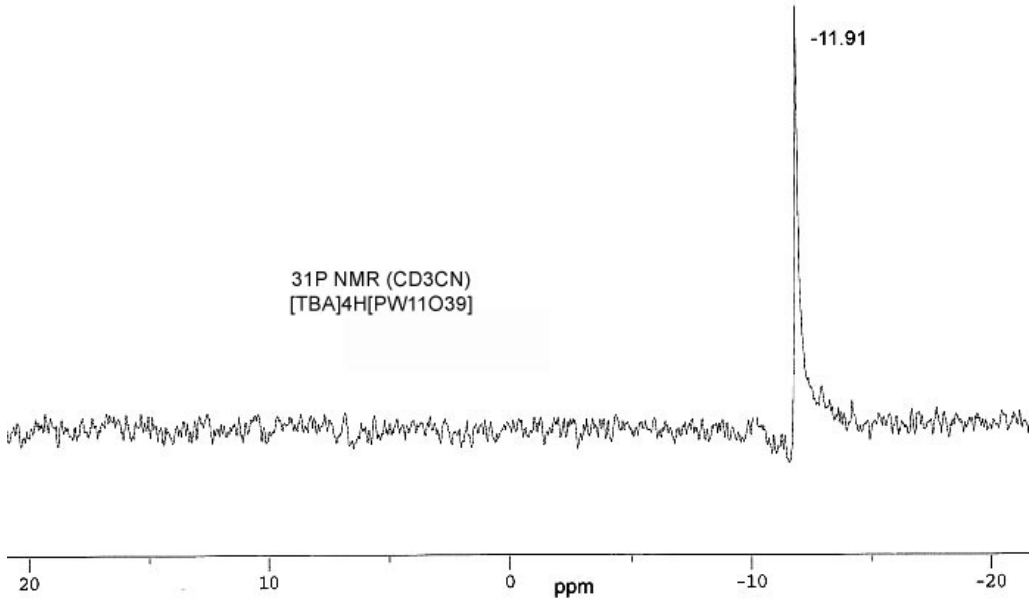

Figure B-2: ^{31}P NMR spectrum (161.83 MHz, CD_3CN; external reference H_3PO_4) of $TBA_4H_3[PW_{11}O_{39}]$ **1.**

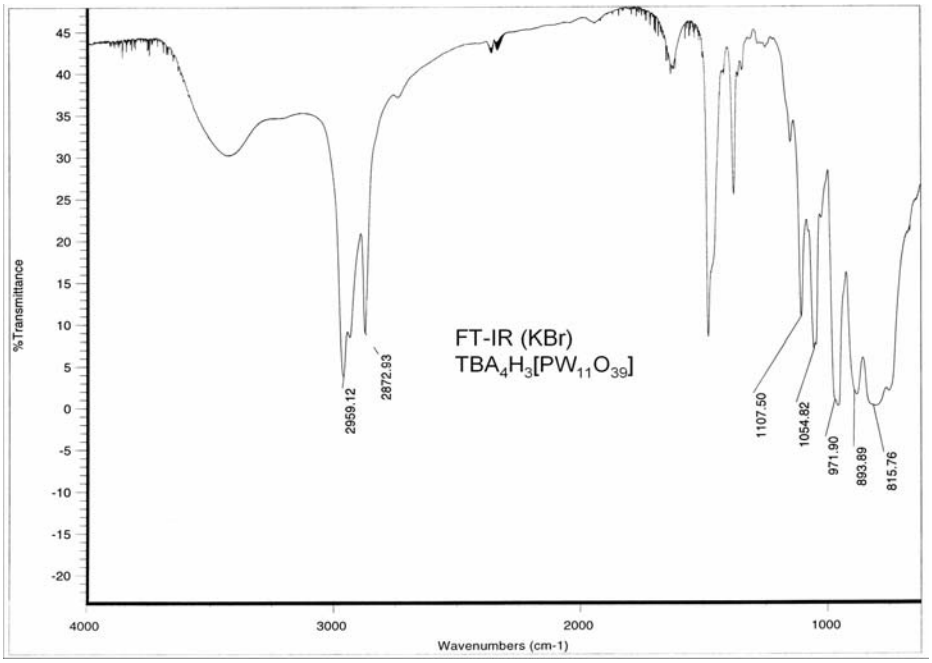

Figure B-3: FT-IR spectrum (KBr) of $TBA_4H_3[PW_{11}O_{39}]$ **1**.

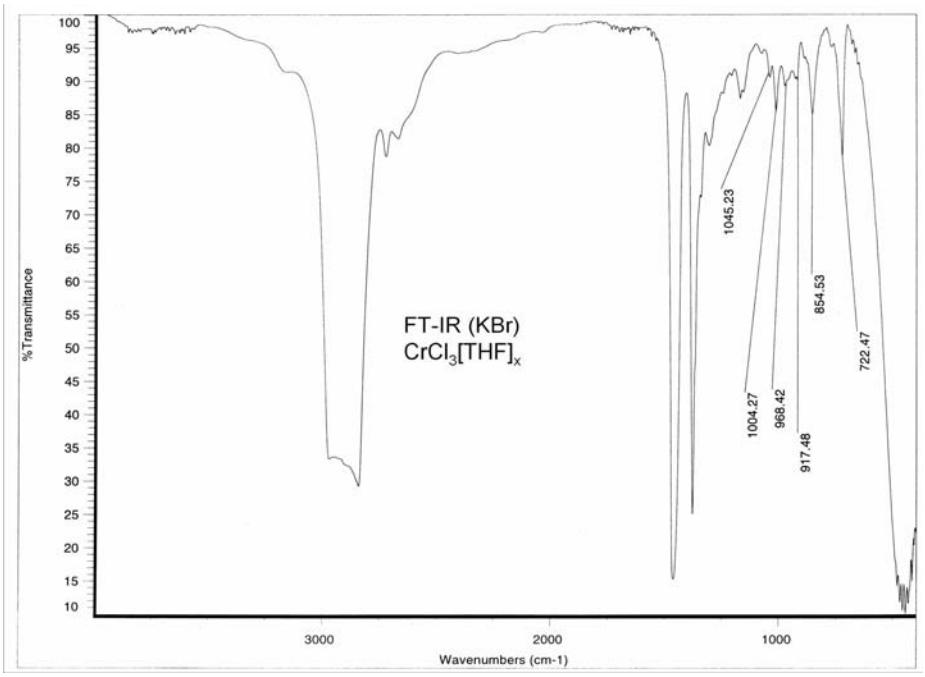

Figure B-4: FT-IR spectrum (KBr) of $Cr^{III}Cl_3.THF_x$ complex, **9**.

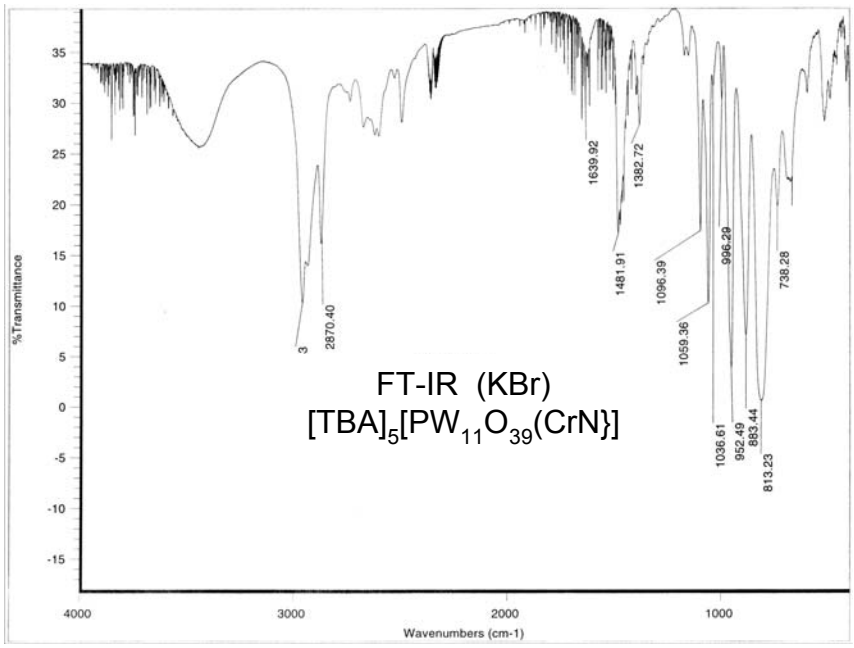

Figure B-5: FT-IR spectrum (KBr) of $TBA_5[PW_{11}O_{39}\{CrN\}]$, **3a**.
(Stored under argon for 12 months)

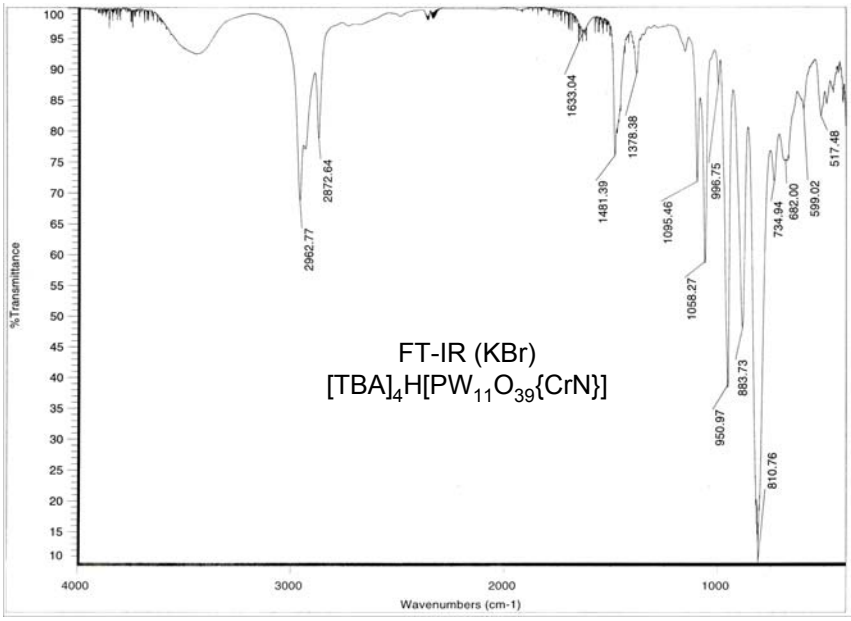

Figure B-6: FT-IR spectrum (KBr) of $TBA_4H[PW_{11}O_{39}\{CrN\}]$, **3b**.
(Orange powder stored in the presence of oxygen and water for 6 months).

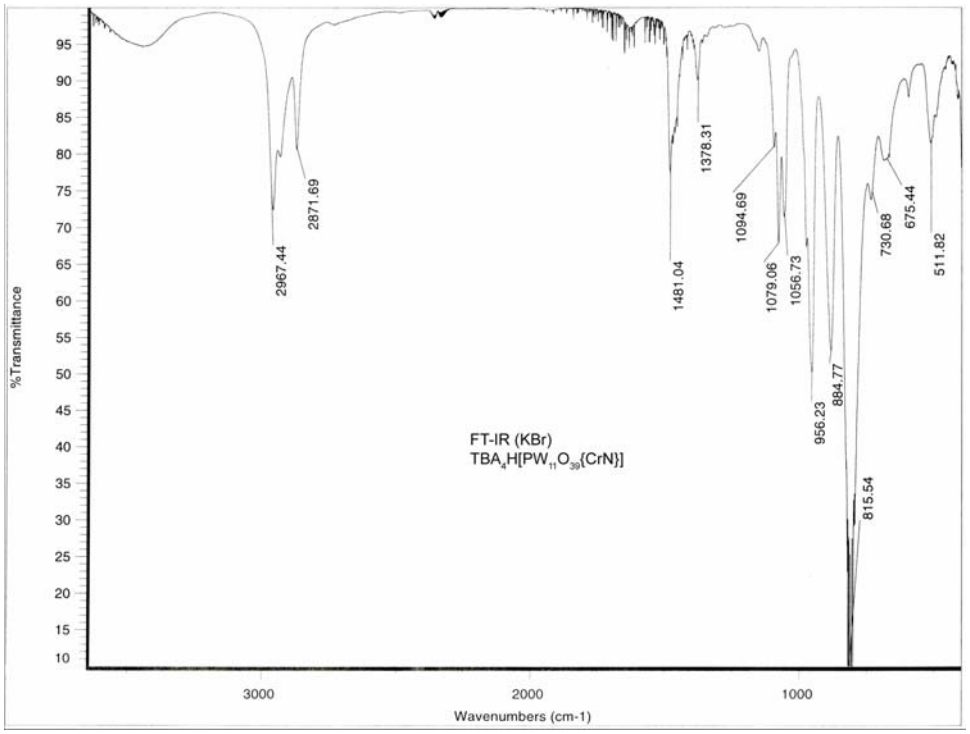

Figure B-7: FT-IR spectrum (KBr) of $TBA_4H[PW_{11}O_{39}\{CrN\}]$, **3b**.

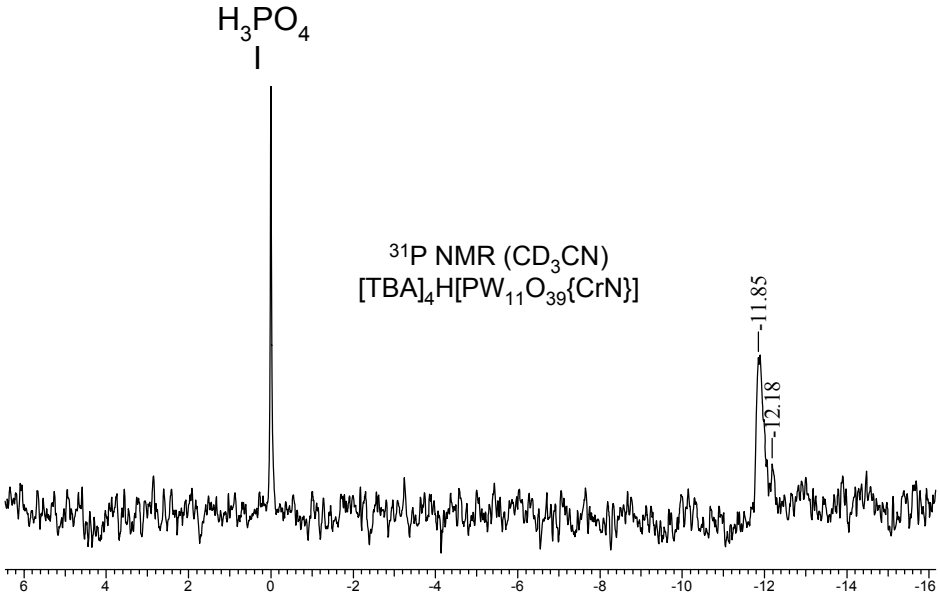

Figure B-8: ^{31}P NMR spectrum (161.85 MHz, CD_3CN, externally referenced to σ-H_3PO_4) of $TBA_4H[PW_{11}O_{39}\{CrN\}]$, **3**.

Appendix C - Chapter 4

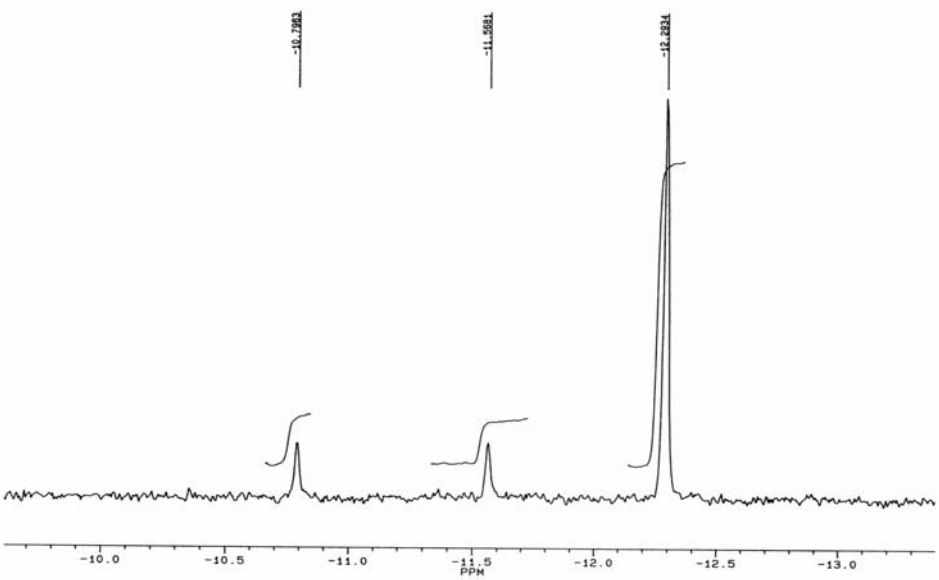

Figure C-1: ^{31}P NMR spectrum of $K_6[\alpha/\beta\text{-}P_2W_{18}O_{62}]$.

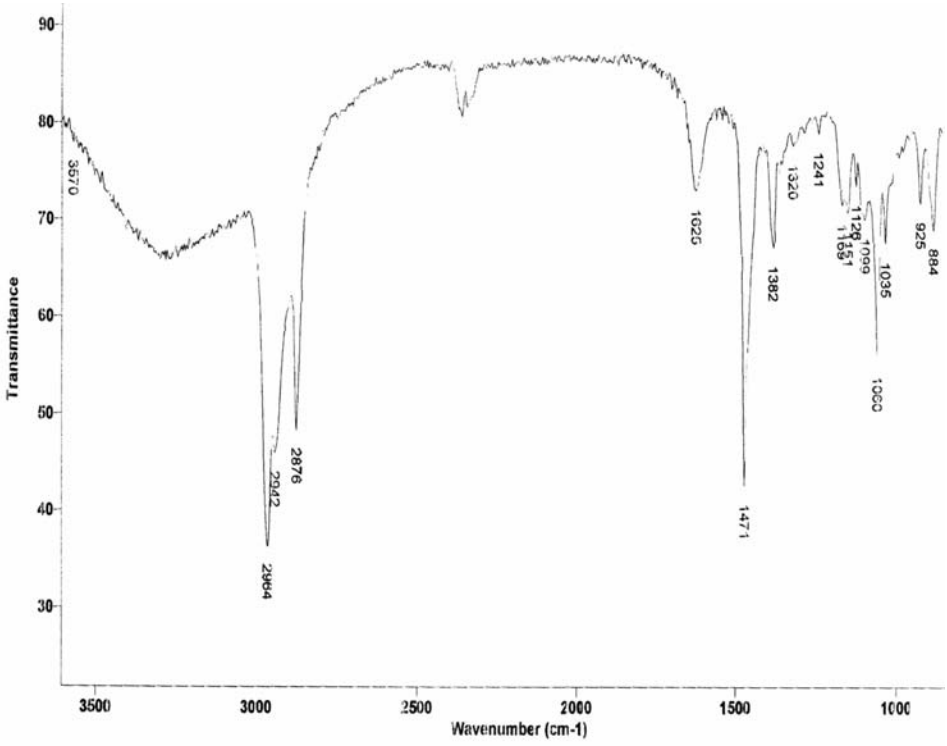

Figure C-2: FT-IR (KBr) spectrum [TBA][$OsNCl_4$] **10**.

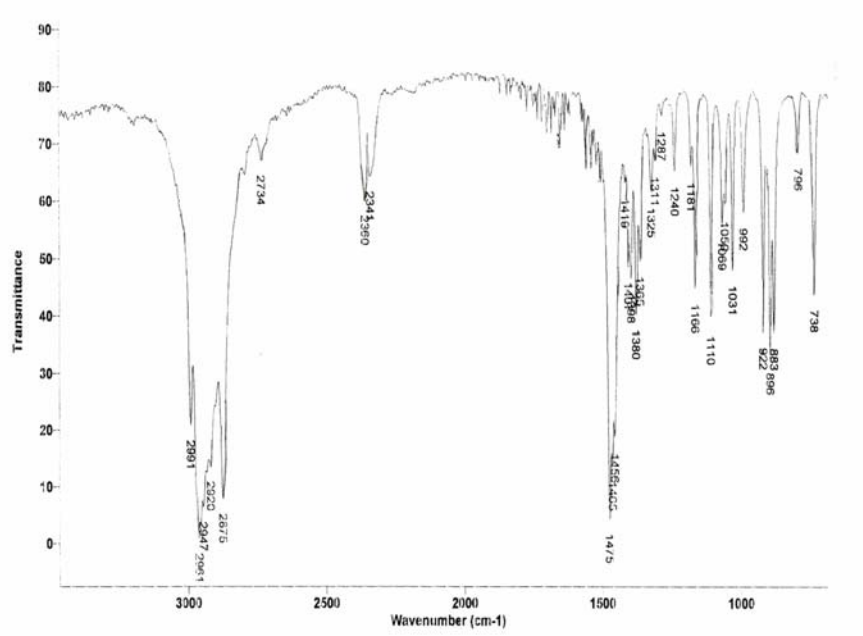

Figure C-3: FT-IR (KBr) spectrum of TBABr.

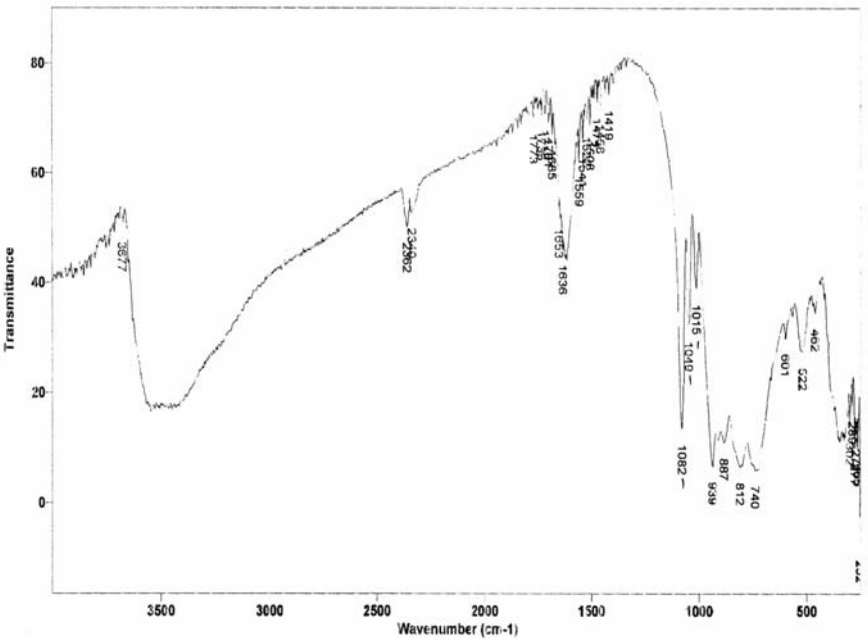

Figure C-4: FT-IR spectrum (KBr) of $TBA_{10}[\alpha_2\text{-}P_2W_{17}O_{61}]$.

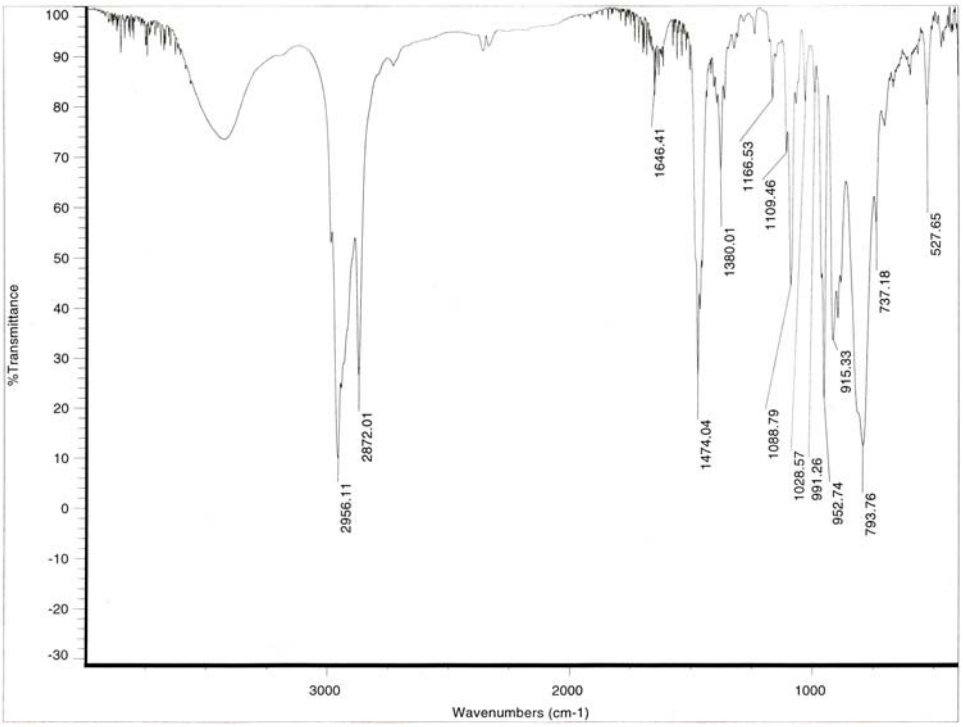

Figure C-5: FT-IR spectrum (KBr) of $[TBA]_7[\alpha_2\text{-}P_2W_{17}O_{61}\{OsN\}]$ **12**.

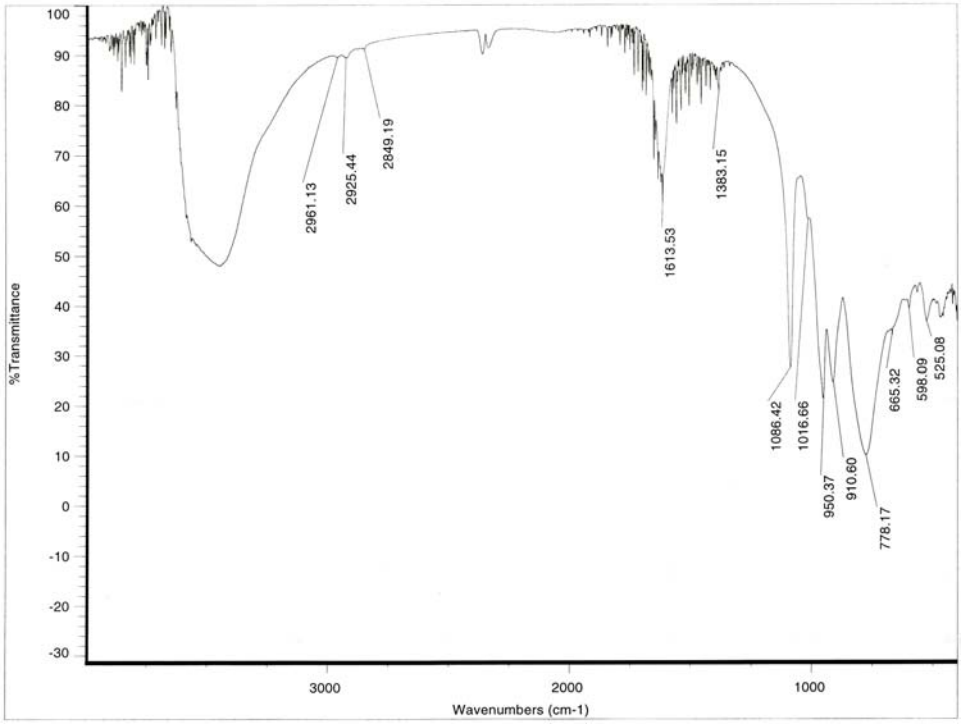

Figure C-6: FT-IR spectrum (KBr) of $[TBA]_7[\alpha_2\text{-}P_2W_{17}O_{61}\{OsN\}]$ synthesized from literature methods. (Maatta E.A., Proust. A., *Chem.Eur.J.*, 2006, *12*, 9150)

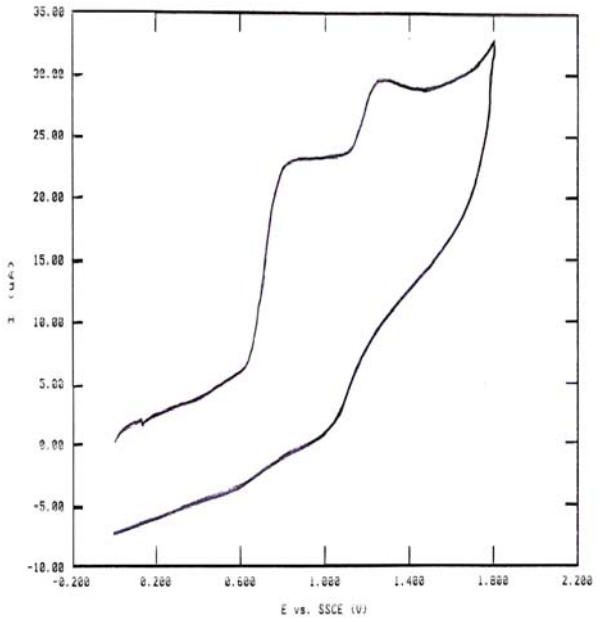

Figure C-7: Voltammogram (Oxidation cycle) of parent POM, $TBA_6[\alpha\text{-}P_2W_{18}O_{62}]$. (0.1 M $TBABF_4$; scan rate=100 ms/V; Pt electrode vs. SSCE).

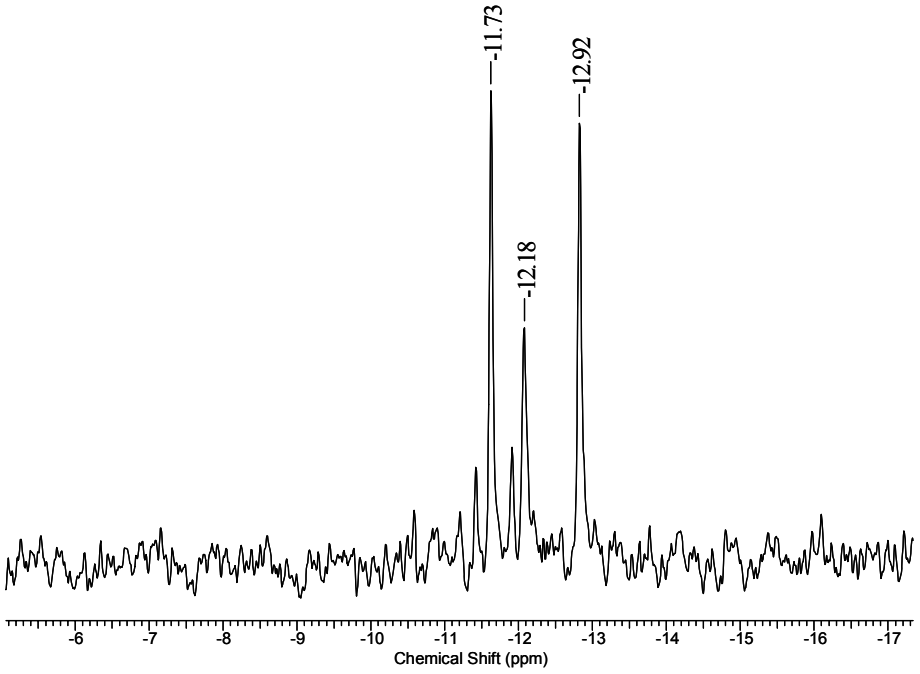

Figure C-8: ^{31}P NMR spectrum of $TBA_7[\alpha_2\text{-}P_2W_{17}O_{61}\{OsN\}]$ (CD_3CN).

Appendix D - Crystallographic Data

3-(pyridin-3-yl)phenylimido hexamolybdate

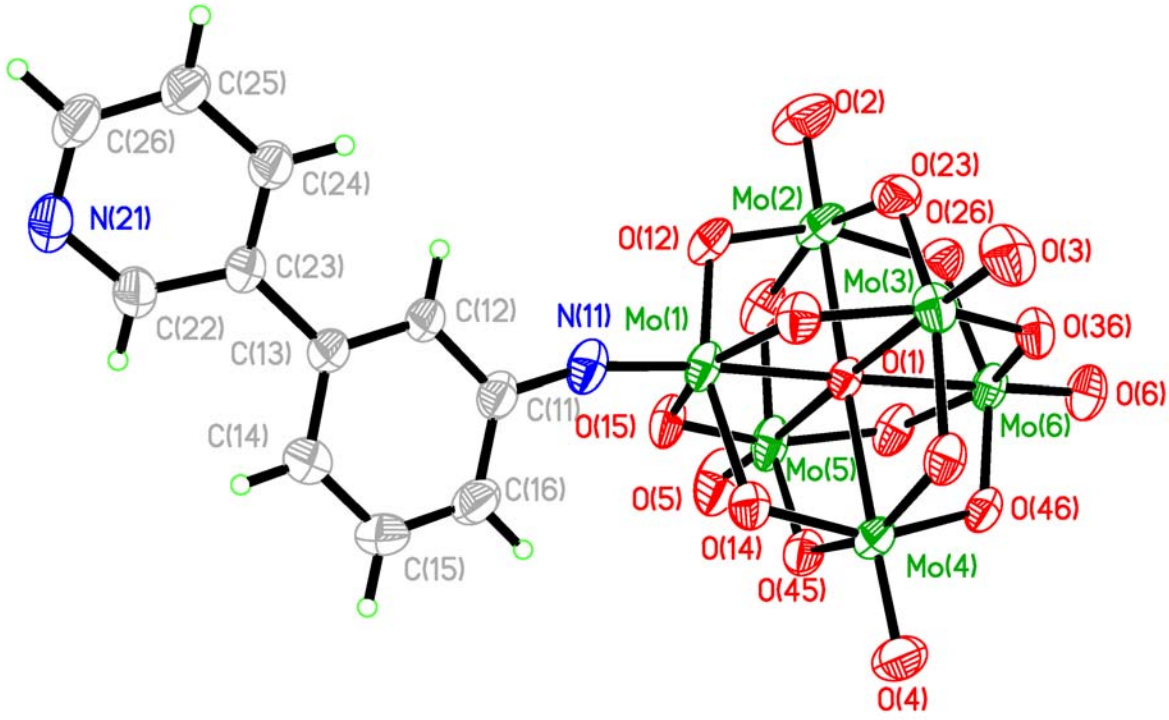

Table 1. Crystal data and structure refinement for km0801m.

Identification code	km0801m	
Empirical formula	C43 H80 Mo6 N4 O18	
Formula weight	1516.75	
Temperature	393(2) K	
Wavelength	0.71073 Å	
Crystal system	Monoclinic	
Space group	P2(1)/n	
Unit cell dimensions	a = 17.0870(6) Å	α= 90°.
	b = 15.9310(6) Å	β= 109.007(2)°.
	c = 22.0320(7) Å	γ = 90°.
Volume	5670.4(3) $Å^3$	
Z	4	
Density (calculated)	1.777 g/cm^3	
Absorption coefficient	1.355 mm^{-1}	
F(000)	3048	
Crystal size	0.25 x 0.20 x 0.10 mm^3	
Theta range for data collection	2.33 to 33.14°.	
Index ranges	-26<=h<=26, -24<=k<=24, -33<=l<=30	
Reflections collected	132285	
Independent reflections	21607 [R(int) = 0.0340]	
Completeness to theta = 33.14°	99.9 %	
Absorption correction	None	
Max. and min. transmission	0.8764 and 0.7282	
Refinement method	Full-matrix least-squares on F^2	
Data / restraints / parameters	21607 / 18 / 625	
Goodness-of-fit on F^2	1.033	
Final R indices [I>2sigma(I)]	R1 = 0.0515, wR2 = 0.1355	
R indices (all data)	R1 = 0.0730, wR2 = 0.1516	
Largest diff. peak and hole	3.544 and -1.527 $e.Å^{-3}$	

Table 2. Atomic coordinates (x 10^4) and equivalent isotropic displacement parameters ($Å^2$x 10^3) for km0801m. U(eq) is defined as one third of the trace of the orthogonalized U^{ij} tensor.

	x	y	z	U(eq)
N(11)	4575(2)	4323(2)	1915(2)	43(1)
C(11)	4406(2)	5154(2)	1762(2)	36(1)
C(12)	4410(2)	5475(2)	1170(2)	33(1)
C(13)	4238(2)	6321(2)	1025(2)	33(1)
C(14)	4056(3)	6833(3)	1476(2)	45(1)
C(15)	4046(3)	6509(3)	2058(2)	49(1)
C(16)	4221(3)	5681(3)	2204(2)	45(1)
N(21)	3598(3)	7648(3)	-463(2)	55(1)
C(22)	3669(3)	7304(3)	104(2)	47(1)
C(23)	4224(2)	6670(2)	397(2)	34(1)
C(24)	4746(2)	6387(2)	71(2)	37(1)
C(25)	4687(2)	6738(3)	-517(2)	41(1)
C(26)	4111(3)	7356(3)	-762(2)	47(1)
Mo(1)	4783(1)	3360(1)	2314(1)	36(1)
Mo(2)	4781(1)	1402(1)	1949(1)	47(1)
Mo(3)	6452(1)	2292(1)	2968(1)	37(1)
Mo(4)	5334(1)	2959(1)	3843(1)	35(1)
Mo(5)	3680(1)	2068(1)	2839(1)	43(1)
Mo(6)	5360(1)	949(1)	3486(1)	34(1)
O(1)	5062(1)	2204(1)	2890(1)	29(1)
O(2)	4620(3)	863(2)	1263(2)	68(1)
O(3)	7469(2)	2363(2)	3046(2)	52(1)
O(4)	5521(2)	3465(2)	4549(1)	51(1)
O(5)	2671(2)	1966(3)	2767(2)	67(1)
O(6)	5545(2)	38(2)	3904(1)	48(1)
O(12)	4662(2)	2566(2)	1652(1)	41(1)
O(13)	5987(2)	3280(2)	2525(1)	37(1)
O(14)	5032(2)	3788(2)	3214(1)	39(1)
O(15)	3707(2)	3066(2)	2352(1)	43(1)
O(23)	5999(2)	1663(2)	2211(1)	43(1)
O(34)	6394(2)	2868(2)	3752(1)	36(1)

O(45)	4138(2)	2680(2)	3597(1)	41(1)
O(52)	3741(2)	1480(2)	2050(1)	47(1)
O(26)	5107(2)	578(2)	2604(1)	46(1)
O(36)	6407(2)	1279(2)	3442(1)	39(1)
O(46)	5464(2)	1776(2)	4118(1)	35(1)
O(56)	4173(2)	1071(2)	3274(1)	42(1)
N11	6760(2)	1010(2)	5985(2)	42(1)
C111	7099(3)	805(3)	6704(2)	50(1)
C121	6502(3)	904(3)	7076(2)	49(1)
C131	6914(4)	573(3)	7761(2)	65(2)
C141	6491(6)	793(5)	8210(3)	99(3)
C211	6183(2)	1752(3)	5857(2)	46(1)
C221	6583(3)	2582(3)	6133(2)	54(1)
C231	5941(4)	3235(3)	6122(2)	64(1)
C241	6319(5)	4093(4)	6338(3)	88(2)
C311	7509(2)	1187(3)	5780(2)	51(1)
C321	7309(2)	1371(3)	5068(2)	51(1)
C331	8065(3)	1730(4)	4926(3)	62(1)
C341	8220(3)	2648(4)	5130(3)	73(2)
C411	6259(2)	274(3)	5618(2)	45(1)
C421	6720(3)	-531(3)	5590(2)	52(1)
C431	6099(3)	-1197(3)	5225(2)	51(1)
C441	6509(4)	-2008(4)	5140(3)	80(2)
N22	7715(3)	10452(3)	1663(2)	71(1)
C112	8152(4)	10041(4)	2300(3)	68(2)
C122	7759(3)	10155(3)	2822(2)	59(1)
C132	8201(3)	9634(4)	3399(3)	61(1)
C142	7836(4)	9702(4)	3940(3)	63(1)
C212	7751(3)	11401(3)	1735(3)	62(1)
C222	8592(4)	11813(4)	1939(4)	83(2)
C232	8502(4)	12768(4)	1930(4)	79(2)
C242	9310(5)	13243(5)	2072(5)	113(3)
C312	8162(5)	10161(5)	1201(3)	99(3)
C32A2	7849(6)	10554(6)	536(4)	116(3)
C33A2	8164(7)	10090(7)	47(5)	84(3)
C34A2	9073(8)	10457(9)	270(7)	99(3)

C32B2	7849(6)	10554(6)	536(4)	116(3)
C33B2	8559(12)	10446(13)	200(8)	84(3)
C34B2	8437(14)	10859(14)	-411(9)	99(3)
C412	6818(4)	10213(4)	1416(3)	80(2)
C422	6627(6)	9290(5)	1319(5)	114(3)
C43A2	5693(7)	9129(8)	1144(6)	151(4)
C44A2	5492(14)	8244(11)	1085(11)	139(5)
C43B2	5693(7)	9129(8)	1144(6)	151(4)
C44B2	5153(12)	9329(15)	439(8)	139(5)

Table 3. Bond lengths [Å] and angles [°] for km0801m.

N(11)-C(11)	1.374(5)
N(11)-Mo(1)	1.746(3)
C(11)-C(16)	1.398(6)
C(11)-C(12)	1.403(5)
C(12)-C(13)	1.394(5)
C(12)-H(12A)	0.9300
C(13)-C(14)	1.397(5)
C(13)-C(23)	1.485(5)
C(14)-C(15)	1.387(6)
C(14)-H(14A)	0.9300
C(15)-C(16)	1.367(6)
C(15)-H(15A)	0.9300
C(16)-H(16A)	0.9300
N(21)-C(22)	1.333(5)
N(21)-C(26)	1.340(6)
C(22)-C(23)	1.393(5)
C(22)-H(22A)	0.9300
C(23)-C(24)	1.389(5)
C(24)-C(25)	1.385(5)
C(24)-H(24A)	0.9300
C(25)-C(26)	1.373(6)
C(25)-H(25A)	0.9300
C(26)-H(26A)	0.9300
Mo(1)-O(12)	1.889(3)
Mo(1)-O(15)	1.926(3)
Mo(1)-O(13)	1.960(3)
Mo(1)-O(14)	2.006(3)
Mo(1)-O(1)	2.199(2)
Mo(2)-O(2)	1.681(3)
Mo(2)-O(52)	1.865(3)
Mo(2)-O(26)	1.895(3)
Mo(2)-O(12)	1.955(3)
Mo(2)-O(23)	2.014(3)
Mo(2)-O(1)	2.348(2)

Mo(3)-O(3)	1.693(3)
Mo(3)-O(23)	1.883(3)
Mo(3)-O(13)	1.886(3)
Mo(3)-O(36)	1.937(3)
Mo(3)-O(34)	1.987(3)
Mo(3)-O(1)	2.329(2)
Mo(4)-O(4)	1.687(3)
Mo(4)-O(14)	1.862(3)
Mo(4)-O(34)	1.890(3)
Mo(4)-O(46)	1.971(3)
Mo(4)-O(45)	1.986(3)
Mo(4)-O(1)	2.332(2)
Mo(5)-O(5)	1.688(3)
Mo(5)-O(45)	1.872(3)
Mo(5)-O(56)	1.904(3)
Mo(5)-O(15)	1.927(3)
Mo(5)-O(52)	2.006(3)
Mo(5)-O(1)	2.336(2)
Mo(6)-O(6)	1.693(3)
Mo(6)-O(46)	1.883(3)
Mo(6)-O(36)	1.896(3)
Mo(6)-O(56)	1.938(3)
Mo(6)-O(26)	1.940(3)
Mo(6)-O(1)	2.354(2)
N11-C211	1.508(6)
N11-C311	1.516(5)
N11-C411	1.519(5)
N11-C111	1.536(5)
C111-C121	1.508(7)
C111-H11A1	0.9700
C111-H11B1	0.9700
C121-C131	1.538(6)
C121-H12A1	0.9700
C121-H12B1	0.9700
C131-C141	1.446(9)
C131-H13A1	0.9700

C131-H13B1	0.9700
C141-H14A1	0.9600
C141-H14B1	0.9600
C141-H14C1	0.9600
C211-C221	1.522(6)
C211-H21A1	0.9700
C211-H21B1	0.9700
C221-C231	1.507(8)
C221-H22A1	0.9700
C221-H22B1	0.9700
C231-C241	1.521(8)
C231-H23A1	0.9700
C231-H23B1	0.9700
C241-H24A1	0.9600
C241-H24B1	0.9600
C241-H24C1	0.9600
C311-C321	1.521(6)
C311-H31A1	0.9700
C311-H31B1	0.9700
C321-C331	1.536(6)
C321-H32A1	0.9700
C321-H32B1	0.9700
C331-C341	1.527(9)
C331-H33A1	0.9700
C331-H33B1	0.9700
C341-H34A1	0.9600
C341-H34B1	0.9600
C341-H34C1	0.9600
C411-C421	1.517(7)
C411-H41A1	0.9700
C411-H41B1	0.9700
C421-C431	1.530(6)
C421-H42A1	0.9700
C421-H42B1	0.9700
C431-C441	1.510(8)
C431-H43A1	0.9700

C431-H43B1	0.9700
C441-H44A1	0.9600
C441-H44B1	0.9600
C441-H44C1	0.9600
N22-C412	1.500(9)
N22-C112	1.508(6)
N22-C212	1.518(7)
N22-C312	1.531(7)
C112-C122	1.520(7)
C112-H11A2	0.9700
C112-H11B2	0.9700
C122-C132	1.500(6)
C122-H12A2	0.9700
C122-H12B2	0.9700
C132-C142	1.519(7)
C132-H13A2	0.9700
C132-H13B2	0.9700
C142-H14A2	0.9600
C142-H14B2	0.9600
C142-H14C2	0.9600
C212-C222	1.509(9)
C212-H21A2	0.9700
C212-H21B2	0.9700
C222-C232	1.530(9)
C222-H22A2	0.9700
C222-H22B2	0.9700
C232-C242	1.515(10)
C232-H23A2	0.9700
C232-H23B2	0.9700
C242-H24A2	0.9600
C242-H24B2	0.9600
C242-H24C2	0.9600
C312-C32A2	1.520(9)
C312-H31A2	0.9700
C312-H31B2	0.9700
C32A2-C33A2	1.541(11)

C32A2-H32A2	0.9700
C32A2-H32B2	0.9700
C33A2-C34A2	1.580(13)
C33A2-H33A2	0.9700
C33A2-H33B2	0.9700
C34A2-H34A2	0.9600
C34A2-H34B2	0.9600
C34A2-H34C2	0.9600
C33B2-C34B2	1.452(16)
C33B2-H33C2	0.9700
C33B2-H33D2	0.9700
C34B2-H34D2	0.9600
C34B2-H34E2	0.9600
C34B2-H34F2	0.9600
C412-C422	1.507(10)
C412-H41A2	0.9700
C412-H41B2	0.9700
C422-C43A2	1.536(10)
C422-H42A2	0.9700
C422-H42B2	0.9700
C43A2-C44A2	1.446(15)
C43A2-H43A2	0.9700
C43A2-H43B2	0.9700
C44A2-H44A2	0.9600
C44A2-H44B2	0.9600
C44A2-H44C2	0.9600
C44B2-H44D2	0.9600
C44B2-H44E2	0.9600
C44B2-H44F2	0.9600

C(11)-N(11)-Mo(1)	164.3(3)
N(11)-C(11)-C(16)	119.0(3)
N(11)-C(11)-C(12)	121.0(3)
C(16)-C(11)-C(12)	119.9(3)
C(13)-C(12)-C(11)	120.0(3)
C(13)-C(12)-H(12A)	120.0

C(11)-C(12)-H(12A)	120.0
C(12)-C(13)-C(14)	118.8(3)
C(12)-C(13)-C(23)	120.9(3)
C(14)-C(13)-C(23)	120.3(3)
C(15)-C(14)-C(13)	120.8(4)
C(15)-C(14)-H(14A)	119.6
C(13)-C(14)-H(14A)	119.6
C(16)-C(15)-C(14)	120.6(4)
C(16)-C(15)-H(15A)	119.7
C(14)-C(15)-H(15A)	119.7
C(15)-C(16)-C(11)	119.9(3)
C(15)-C(16)-H(16A)	120.1
C(11)-C(16)-H(16A)	120.1
C(22)-N(21)-C(26)	116.4(4)
N(21)-C(22)-C(23)	124.9(4)
N(21)-C(22)-H(22A)	117.6
C(23)-C(22)-H(22A)	117.6
C(24)-C(23)-C(22)	116.9(3)
C(24)-C(23)-C(13)	122.8(3)
C(22)-C(23)-C(13)	120.3(3)
C(25)-C(24)-C(23)	119.3(3)
C(25)-C(24)-H(24A)	120.4
C(23)-C(24)-H(24A)	120.4
C(26)-C(25)-C(24)	118.8(4)
C(26)-C(25)-H(25A)	120.6
C(24)-C(25)-H(25A)	120.6
N(21)-C(26)-C(25)	123.8(4)
N(21)-C(26)-H(26A)	118.1
C(25)-C(26)-H(26A)	118.1
N(11)-Mo(1)-O(12)	104.26(14)
N(11)-Mo(1)-O(15)	101.21(14)
O(12)-Mo(1)-O(15)	90.30(13)
N(11)-Mo(1)-O(13)	101.70(13)
O(12)-Mo(1)-O(13)	88.99(12)
O(15)-Mo(1)-O(13)	156.52(10)
N(11)-Mo(1)-O(14)	98.12(14)

O(12)-Mo(1)-O(14)	157.59(11)
O(15)-Mo(1)-O(14)	86.43(12)
O(13)-Mo(1)-O(14)	85.34(11)
N(11)-Mo(1)-O(1)	175.32(13)
O(12)-Mo(1)-O(1)	80.42(10)
O(15)-Mo(1)-O(1)	78.57(10)
O(13)-Mo(1)-O(1)	78.18(9)
O(14)-Mo(1)-O(1)	77.20(9)
O(2)-Mo(2)-O(52)	105.02(18)
O(2)-Mo(2)-O(26)	104.58(16)
O(52)-Mo(2)-O(26)	90.59(13)
O(2)-Mo(2)-O(12)	102.48(15)
O(52)-Mo(2)-O(12)	88.74(13)
O(26)-Mo(2)-O(12)	152.13(12)
O(2)-Mo(2)-O(23)	102.35(18)
O(52)-Mo(2)-O(23)	152.55(12)
O(26)-Mo(2)-O(23)	84.49(12)
O(12)-Mo(2)-O(23)	83.37(12)
O(2)-Mo(2)-O(1)	176.62(15)
O(52)-Mo(2)-O(1)	77.69(10)
O(26)-Mo(2)-O(1)	77.24(10)
O(12)-Mo(2)-O(1)	75.41(9)
O(23)-Mo(2)-O(1)	74.88(10)
O(3)-Mo(3)-O(23)	103.75(15)
O(3)-Mo(3)-O(13)	104.03(13)
O(23)-Mo(3)-O(13)	90.17(12)
O(3)-Mo(3)-O(36)	102.74(13)
O(23)-Mo(3)-O(36)	87.55(12)
O(13)-Mo(3)-O(36)	152.90(11)
O(3)-Mo(3)-O(34)	102.78(14)
O(23)-Mo(3)-O(34)	153.32(11)
O(13)-Mo(3)-O(34)	86.10(11)
O(36)-Mo(3)-O(34)	83.96(11)
O(3)-Mo(3)-O(1)	178.45(14)
O(23)-Mo(3)-O(1)	77.71(10)
O(13)-Mo(3)-O(1)	76.38(9)

O(36)-Mo(3)-O(1)	76.75(9)
O(34)-Mo(3)-O(1)	75.73(9)
O(4)-Mo(4)-O(14)	105.70(14)
O(4)-Mo(4)-O(34)	103.52(14)
O(14)-Mo(4)-O(34)	91.03(11)
O(4)-Mo(4)-O(46)	101.84(13)
O(14)-Mo(4)-O(46)	152.11(11)
O(34)-Mo(4)-O(46)	86.76(11)
O(4)-Mo(4)-O(45)	103.16(14)
O(14)-Mo(4)-O(45)	86.83(11)
O(34)-Mo(4)-O(45)	152.80(12)
O(46)-Mo(4)-O(45)	82.70(11)
O(4)-Mo(4)-O(1)	177.34(12)
O(14)-Mo(4)-O(1)	76.71(10)
O(34)-Mo(4)-O(1)	77.42(10)
O(46)-Mo(4)-O(1)	75.68(9)
O(45)-Mo(4)-O(1)	75.70(10)
O(5)-Mo(5)-O(45)	104.49(17)
O(5)-Mo(5)-O(56)	103.74(15)
O(45)-Mo(5)-O(56)	89.85(12)
O(5)-Mo(5)-O(15)	103.64(15)
O(45)-Mo(5)-O(15)	89.27(12)
O(56)-Mo(5)-O(15)	151.93(11)
O(5)-Mo(5)-O(52)	102.39(17)
O(45)-Mo(5)-O(52)	153.10(11)
O(56)-Mo(5)-O(52)	84.71(12)
O(15)-Mo(5)-O(52)	83.49(12)
O(5)-Mo(5)-O(1)	177.58(14)
O(45)-Mo(5)-O(1)	77.67(10)
O(56)-Mo(5)-O(1)	77.24(9)
O(15)-Mo(5)-O(1)	75.17(9)
O(52)-Mo(5)-O(1)	75.43(10)
O(6)-Mo(6)-O(46)	103.92(13)
O(6)-Mo(6)-O(36)	104.67(13)
O(46)-Mo(6)-O(36)	88.87(12)
O(6)-Mo(6)-O(56)	102.23(13)

O(46)-Mo(6)-O(56)	86.98(12)
O(36)-Mo(6)-O(56)	153.00(11)
O(6)-Mo(6)-O(26)	103.04(14)
O(46)-Mo(6)-O(26)	152.95(11)
O(36)-Mo(6)-O(26)	86.53(13)
O(56)-Mo(6)-O(26)	85.15(13)
O(6)-Mo(6)-O(1)	178.31(12)
O(46)-Mo(6)-O(1)	76.70(9)
O(36)-Mo(6)-O(1)	76.88(9)
O(56)-Mo(6)-O(1)	76.20(9)
O(26)-Mo(6)-O(1)	76.29(10)
Mo(1)-O(1)-Mo(3)	90.92(8)
Mo(1)-O(1)-Mo(4)	91.69(8)
Mo(3)-O(1)-Mo(4)	90.15(8)
Mo(1)-O(1)-Mo(5)	91.38(8)
Mo(3)-O(1)-Mo(5)	177.70(11)
Mo(4)-O(1)-Mo(5)	89.64(8)
Mo(1)-O(1)-Mo(2)	90.12(8)
Mo(3)-O(1)-Mo(2)	90.49(8)
Mo(4)-O(1)-Mo(2)	178.07(10)
Mo(5)-O(1)-Mo(2)	89.65(8)
Mo(1)-O(1)-Mo(6)	178.70(12)
Mo(3)-O(1)-Mo(6)	88.84(7)
Mo(4)-O(1)-Mo(6)	89.59(7)
Mo(5)-O(1)-Mo(6)	88.86(7)
Mo(2)-O(1)-Mo(6)	88.60(8)
Mo(1)-O(12)-Mo(2)	113.83(12)
Mo(3)-O(13)-Mo(1)	114.21(12)
Mo(4)-O(14)-Mo(1)	114.36(13)
Mo(1)-O(15)-Mo(5)	114.87(13)
Mo(3)-O(23)-Mo(2)	116.90(14)
Mo(4)-O(34)-Mo(3)	116.64(12)
Mo(5)-O(45)-Mo(4)	117.00(13)
Mo(2)-O(52)-Mo(5)	117.07(13)
Mo(2)-O(26)-Mo(6)	117.78(15)
Mo(6)-O(36)-Mo(3)	117.50(13)

Mo(6)-O(46)-Mo(4)	117.86(12)
Mo(5)-O(56)-Mo(6)	117.44(12)
C211-N11-C311	111.3(3)
C211-N11-C411	106.6(3)
C311-N11-C411	111.7(3)
C211-N11-C111	111.3(3)
C311-N11-C111	106.1(3)
C411-N11-C111	110.0(3)
C121-C111-N11	116.3(3)
C121-C111-H11A1	108.2
N11-C111-H11A1	108.2
C121-C111-H11B1	108.2
N11-C111-H11B1	108.2
H11A1-C111-H11B1	107.4
C111-C121-C131	108.8(4)
C111-C121-H12A1	109.9
C131-C121-H12A1	109.9
C111-C121-H12B1	109.9
C131-C121-H12B1	109.9
H12A1-C121-H12B1	108.3
C141-C131-C121	114.7(6)
C141-C131-H13A1	108.6
C121-C131-H13A1	108.6
C141-C131-H13B1	108.6
C121-C131-H13B1	108.6
H13A1-C131-H13B1	107.6
C131-C141-H14A1	109.5
C131-C141-H14B1	109.5
H14A1-C141-H14B1	109.5
C131-C141-H14C1	109.5
H14A1-C141-H14C1	109.5
H14B1-C141-H14C1	109.5
N11-C211-C221	115.2(3)
N11-C211-H21A1	108.5
C221-C211-H21A1	108.5
N11-C211-H21B1	108.5

C221-C211-H21B1	108.5
H21A1-C211-H21B1	107.5
C231-C221-C211	111.2(4)
C231-C221-H22A1	109.4
C211-C221-H22A1	109.4
C231-C221-H22B1	109.4
C211-C221-H22B1	109.4
H22A1-C221-H22B1	108.0
C221-C231-C241	112.4(5)
C221-C231-H23A1	109.1
C241-C231-H23A1	109.1
C221-C231-H23B1	109.1
C241-C231-H23B1	109.1
H23A1-C231-H23B1	107.8
C231-C241-H24A1	109.5
C231-C241-H24B1	109.5
H24A1-C241-H24B1	109.5
C231-C241-H24C1	109.5
H24A1-C241-H24C1	109.5
H24B1-C241-H24C1	109.5
N11-C311-C321	114.5(3)
N11-C311-H31A1	108.6
C321-C311-H31A1	108.6
N11-C311-H31B1	108.6
C321-C311-H31B1	108.6
H31A1-C311-H31B1	107.6
C311-C321-C331	111.1(3)
C311-C321-H32A1	109.4
C331-C321-H32A1	109.4
C311-C321-H32B1	109.4
C331-C321-H32B1	109.4
H32A1-C321-H32B1	108.0
C341-C331-C321	111.9(5)
C341-C331-H33A1	109.2
C321-C331-H33A1	109.2
C341-C331-H33B1	109.2

C321-C331-H33B1	109.2
H33A1-C331-H33B1	107.9
C331-C341-H34A1	109.5
C331-C341-H34B1	109.5
H34A1-C341-H34B1	109.5
C331-C341-H34C1	109.5
H34A1-C341-H34C1	109.5
H34B1-C341-H34C1	109.5
C421-C411-N11	117.6(3)
C421-C411-H41A1	107.9
N11-C411-H41A1	107.9
C421-C411-H41B1	107.9
N11-C411-H41B1	107.9
H41A1-C411-H41B1	107.2
C411-C421-C431	109.1(3)
C411-C421-H42A1	109.9
C431-C421-H42A1	109.9
C411-C421-H42B1	109.9
C431-C421-H42B1	109.9
H42A1-C421-H42B1	108.3
C441-C431-C421	112.9(4)
C441-C431-H43A1	109.0
C421-C431-H43A1	109.0
C441-C431-H43B1	109.0
C421-C431-H43B1	109.0
H43A1-C431-H43B1	107.8
C431-C441-H44A1	109.5
C431-C441-H44B1	109.5
H44A1-C441-H44B1	109.5
C431-C441-H44C1	109.5
H44A1-C441-H44C1	109.5
H44B1-C441-H44C1	109.5
C412-N22-C112	111.3(5)
C412-N22-C212	107.0(4)
C112-N22-C212	110.1(5)
C412-N22-C312	110.7(6)

C112-N22-C312	106.6(4)
C212-N22-C312	111.1(5)
N22-C112-C122	116.5(4)
N22-C112-H11A2	108.2
C122-C112-H11A2	108.2
N22-C112-H11B2	108.2
C122-C112-H11B2	108.2
H11A2-C112-H11B2	107.3
C132-C122-C112	110.5(4)
C132-C122-H12A2	109.5
C112-C122-H12A2	109.5
C132-C122-H12B2	109.5
C112-C122-H12B2	109.5
H12A2-C122-H12B2	108.1
C122-C132-C142	113.8(4)
C122-C132-H13A2	108.8
C142-C132-H13A2	108.8
C122-C132-H13B2	108.8
C142-C132-H13B2	108.8
H13A2-C132-H13B2	107.7
C132-C142-H14A2	109.5
C132-C142-H14B2	109.5
H14A2-C142-H14B2	109.5
C132-C142-H14C2	109.5
H14A2-C142-H14C2	109.5
H14B2-C142-H14C2	109.5
C222-C212-N22	117.8(4)
C222-C212-H21A2	107.9
N22-C212-H21A2	107.9
C222-C212-H21B2	107.9
N22-C212-H21B2	107.9
H21A2-C212-H21B2	107.2
C212-C222-C232	110.3(4)
C212-C222-H22A2	109.6
C232-C222-H22A2	109.6
C212-C222-H22B2	109.6

C232-C222-H22B2	109.6
H22A2-C222-H22B2	108.1
C242-C232-C222	114.4(5)
C242-C232-H23A2	108.7
C222-C232-H23A2	108.7
C242-C232-H23B2	108.7
C222-C232-H23B2	108.7
H23A2-C232-H23B2	107.6
C232-C242-H24A2	109.5
C232-C242-H24B2	109.5
H24A2-C242-H24B2	109.5
C232-C242-H24C2	109.5
H24A2-C242-H24C2	109.5
H24B2-C242-H24C2	109.5
C32A2-C312-N22	114.9(5)
C32A2-C312-H31A2	108.5
N22-C312-H31A2	108.5
C32A2-C312-H31B2	108.5
N22-C312-H31B2	108.5
H31A2-C312-H31B2	107.5
C312-C32A2-C33A2	112.5(7)
C312-C32A2-H32A2	109.1
C33A2-C32A2-H32A2	109.1
C312-C32A2-H32B2	109.1
C33A2-C32A2-H32B2	109.1
H32A2-C32A2-H32B2	107.8
C32A2-C33A2-C34A2	97.9(9)
C32A2-C33A2-H33A2	112.2
C34A2-C33A2-H33A2	112.2
C32A2-C33A2-H33B2	112.2
C34A2-C33A2-H33B2	112.2
H33A2-C33A2-H33B2	109.8
C33A2-C34A2-H34A2	109.5
C33A2-C34A2-H34B2	109.5
H34A2-C34A2-H34B2	109.5
C33A2-C34A2-H34C2	109.5

H34A2-C34A2-H34C2	109.5
H34B2-C34A2-H34C2	109.5
C34B2-C33B2-H33C2	107.8
C34B2-C33B2-H33D2	107.8
H33C2-C33B2-H33D2	107.1
C33B2-C34B2-H34D2	109.5
C33B2-C34B2-H34E2	109.5
H34D2-C34B2-H34E2	109.5
C33B2-C34B2-H34F2	109.5
H34D2-C34B2-H34F2	109.5
H34E2-C34B2-H34F2	109.5
N22-C412-C422	116.6(5)
N22-C412-H41A2	108.1
C422-C412-H41A2	108.1
N22-C412-H41B2	108.1
C422-C412-H41B2	108.1
H41A2-C412-H41B2	107.3
C412-C422-C43A2	110.9(7)
C412-C422-H42A2	109.4
C43A2-C422-H42A2	109.4
C412-C422-H42B2	109.4
C43A2-C422-H42B2	109.4
H42A2-C422-H42B2	108.0
C44A2-C43A2-C422	112.5(12)
C44A2-C43A2-H43A2	109.1
C422-C43A2-H43A2	109.1
C44A2-C43A2-H43B2	109.1
C422-C43A2-H43B2	109.1
H43A2-C43A2-H43B2	107.8
C43A2-C44A2-H44A2	109.5
C43A2-C44A2-H44B2	109.5
H44A2-C44A2-H44B2	109.5
C43A2-C44A2-H44C2	109.5
H44A2-C44A2-H44C2	109.5
H44B2-C44A2-H44C2	109.5
H44D2-C44B2-H44E2	109.5

H44D2-C44B2-H44F2	109.5
H44E2-C44B2-H44F2	109.5

Symmetry transformations used to generate equivalent atoms:

Table 4. Anisotropic displacement parameters ($Å^2$x 10^3)for km0801m. The anisotropic displacement factor exponent takes the form: $-2\pi^2[h^2a^{*2}U^{11} + ... + 2 h k a^* b^* U^{12}]$

	U^{11}	U^{22}	U^{33}	U^{23}	U^{13}	U^{12}
N(11)	45(2)	43(2)	38(2)	16(1)	11(1)	2(1)
C(11)	37(2)	40(2)	32(2)	9(1)	11(1)	3(1)
C(12)	36(2)	34(2)	30(2)	7(1)	12(1)	4(1)
C(13)	36(2)	35(2)	30(2)	5(1)	13(1)	4(1)
C(14)	55(2)	42(2)	41(2)	2(2)	21(2)	11(2)
C(15)	56(2)	59(2)	37(2)	-3(2)	23(2)	12(2)
C(16)	46(2)	61(2)	30(2)	7(2)	16(2)	7(2)
N(21)	64(2)	55(2)	50(2)	23(2)	24(2)	22(2)
C(22)	57(2)	43(2)	47(2)	15(2)	27(2)	17(2)
C(23)	40(2)	31(1)	32(2)	7(1)	13(1)	3(1)
C(24)	37(2)	40(2)	36(2)	9(1)	15(1)	6(1)
C(25)	42(2)	49(2)	35(2)	7(2)	16(2)	4(2)
C(26)	55(2)	53(2)	37(2)	17(2)	19(2)	6(2)
Mo(1)	37(1)	38(1)	30(1)	13(1)	7(1)	-1(1)
Mo(2)	65(1)	44(1)	29(1)	1(1)	12(1)	-9(1)
Mo(3)	30(1)	38(1)	47(1)	9(1)	18(1)	1(1)
Mo(4)	39(1)	38(1)	26(1)	3(1)	9(1)	-1(1)
Mo(5)	24(1)	56(1)	43(1)	18(1)	3(1)	-5(1)
Mo(6)	34(1)	33(1)	31(1)	10(1)	6(1)	-3(1)
O(1)	28(1)	32(1)	24(1)	7(1)	7(1)	-1(1)
O(2)	108(3)	57(2)	37(2)	-8(1)	21(2)	-17(2)
O(3)	36(1)	57(2)	71(2)	10(2)	27(1)	1(1)
O(4)	64(2)	53(2)	34(1)	-5(1)	16(1)	-2(1)
O(5)	27(1)	99(3)	68(2)	31(2)	7(1)	-7(2)
O(6)	51(2)	40(1)	47(2)	16(1)	10(1)	-1(1)
O(12)	51(2)	45(1)	25(1)	8(1)	10(1)	-5(1)
O(13)	36(1)	37(1)	41(1)	10(1)	15(1)	-4(1)
O(14)	43(1)	34(1)	38(1)	5(1)	11(1)	4(1)
O(15)	30(1)	55(2)	38(1)	18(1)	3(1)	4(1)
O(23)	56(2)	40(1)	42(1)	6(1)	26(1)	4(1)
O(34)	27(1)	42(1)	35(1)	5(1)	3(1)	-4(1)

O(45)	33(1)	56(2)	37(1)	12(1)	15(1)	7(1)
O(52)	46(2)	51(2)	34(1)	9(1)	-2(1)	-16(1)
O(26)	63(2)	35(1)	39(1)	3(1)	12(1)	-5(1)
O(36)	34(1)	39(1)	45(1)	13(1)	13(1)	6(1)
O(46)	31(1)	45(1)	26(1)	10(1)	6(1)	0(1)
O(56)	35(1)	49(2)	35(1)	14(1)	5(1)	-13(1)
N11	30(1)	60(2)	31(1)	5(1)	1(1)	-15(1)
C111	42(2)	66(3)	30(2)	11(2)	-5(1)	-23(2)
C121	67(3)	40(2)	33(2)	-1(1)	9(2)	-17(2)
C131	104(4)	48(2)	35(2)	4(2)	13(2)	-20(3)
C141	162(8)	76(4)	59(4)	-2(3)	37(4)	14(5)
C211	40(2)	62(2)	28(2)	3(2)	1(1)	-14(2)
C221	66(3)	59(3)	33(2)	7(2)	10(2)	-19(2)
C231	93(4)	65(3)	31(2)	-1(2)	18(2)	-14(3)
C241	156(7)	63(3)	68(4)	-4(3)	70(4)	-24(4)
C311	27(2)	72(3)	44(2)	16(2)	1(1)	-16(2)
C321	30(2)	79(3)	41(2)	11(2)	8(2)	-9(2)
C331	38(2)	83(3)	66(3)	19(3)	18(2)	-10(2)
C341	53(3)	90(4)	63(3)	31(3)	1(2)	-21(3)
C411	30(2)	64(2)	36(2)	-3(2)	6(1)	-14(2)
C421	35(2)	69(3)	52(2)	4(2)	14(2)	-7(2)
C431	48(2)	64(3)	44(2)	1(2)	20(2)	-10(2)
C441	87(4)	81(4)	85(4)	-14(3)	45(4)	-1(3)
N22	89(3)	69(3)	65(3)	22(2)	41(2)	48(2)
C112	82(4)	66(3)	65(3)	26(2)	37(3)	41(3)
C122	64(3)	53(2)	62(3)	20(2)	25(2)	24(2)
C132	58(3)	65(3)	62(3)	21(2)	22(2)	21(2)
C142	69(3)	61(3)	59(3)	13(2)	20(2)	17(2)
C212	76(3)	59(3)	64(3)	25(2)	40(3)	41(2)
C222	70(4)	83(4)	108(5)	40(4)	46(4)	36(3)
C232	72(4)	79(4)	98(5)	40(3)	46(3)	27(3)
C242	87(5)	91(5)	165(9)	49(6)	47(6)	10(4)
C312	143(6)	100(5)	75(4)	32(4)	63(4)	84(5)
C412	106(5)	71(4)	63(3)	2(3)	30(3)	37(3)
C422	140(8)	89(5)	116(7)	-16(5)	44(6)	37(5)

Table 5. Hydrogen coordinates (x 10^4) and isotropic displacement parameters ($Å^2$x 10^3) for km0801m.

	x	y	z	U(eq)
H(12A)	4528	5123	874	39
H(14A)	3939	7398	1385	54
H(15A)	3921	6858	2352	58
H(16A)	4217	5469	2596	54
H(22A)	3321	7503	321	56
H(24A)	5132	5967	247	44
H(25A)	5031	6557	-743	49
H(26A)	4075	7586	-1158	56
H11A1	7295	230	6752	60
H11B1	7573	1163	6900	60
H12A1	5999	592	6867	59
H12B1	6358	1491	7089	59
H13A1	6949	-34	7744	78
H13B1	7475	788	7922	78
H14A1	6785	562	8624	148
H14B1	5939	570	8062	148
H14C1	6467	1393	8242	148
H21A1	5743	1633	6033	55
H21B1	5931	1815	5396	55
H22A1	6941	2497	6571	65
H22B1	6922	2781	5885	65
H23A1	5635	3056	6402	76
H23B1	5552	3279	5690	76
H24A1	5887	4488	6321	131
H24B1	6616	4276	6060	131
H24C1	6692	4056	6771	131
H31A1	7876	705	5889	61
H31B1	7805	1663	6022	61
H32A1	6856	1771	4933	61
H32B1	7132	858	4824	61

H33A1	8550	1401	5153	75
H33B1	7980	1684	4470	75
H34A1	8696	2850	5034	109
H34B1	8316	2694	5583	109
H34C1	7745	2977	4901	109
H41A1	5835	144	5808	53
H41B1	5979	457	5181	53
H42A1	7013	-726	6021	62
H42B1	7123	-429	5373	62
H43A1	5715	-1310	5456	61
H43B1	5784	-978	4806	61
H44A1	6093	-2403	4910	120
H44B1	6812	-2235	5554	120
H44C1	6880	-1903	4903	120
H11A2	8712	10257	2459	81
H11B2	8189	9444	2227	81
H12A2	7783	10742	2944	70
H12B2	7181	9990	2660	70
H13A2	8776	9806	3559	73
H13B2	8186	9051	3270	73
H14A2	8153	9364	4296	94
H14B2	7273	9509	3793	94
H14C2	7850	10277	4074	94
H21A2	7425	11643	1327	75
H21B2	7483	11551	2046	75
H22A2	8887	11646	1649	100
H22B2	8911	11628	2368	100
H23A2	8135	12938	1511	95
H23B2	8242	12928	2244	95
H24A2	9202	13836	2050	169
H24B2	9570	13095	1761	169
H24C2	9669	13100	2494	169
H31A2	8746	10288	1390	119
H31B2	8108	9556	1155	119
H32A2	8027	11135	564	139
H32B2	7248	10548	385	139

H33A2	7856	10242	-392	100
H33B2	8158	9486	97	100
H34A2	9364	10247	-6	149
H34B2	9358	10287	704	149
H34C2	9050	11058	246	149
H32C2	7730	11145	570	139
H32D2	7343	10278	279	139
H33C2	9077	10648	500	100
H33D2	8627	9850	141	100
H34D2	8956	10890	-492	149
H34E2	8228	11416	-398	149
H34F2	8048	10545	-747	149
H41A2	6565	10496	1009	95
H41B2	6554	10426	1714	95
H42A2	6920	8987	1709	137
H42B2	6819	9081	978	137
H43A2	5498	9372	1472	182
H43B2	5407	9406	740	182
H44A2	4911	8173	1012	209
H44B2	5801	7961	1474	209
H44C2	5631	8012	731	209
H43C2	5488	9460	1429	182
H43D2	5614	8542	1227	182
H44D2	4612	9089	353	209
H44E2	5409	9096	148	209
H44F2	5105	9927	381	209

Table 6. Torsion angles [°] for km0801m.

Mo(1)-N(11)-C(11)-C(16)	-8.0(13)
Mo(1)-N(11)-C(11)-C(12)	172.5(9)
N(11)-C(11)-C(12)-C(13)	-179.9(3)
C(16)-C(11)-C(12)-C(13)	0.6(5)
C(11)-C(12)-C(13)-C(14)	-0.6(5)
C(11)-C(12)-C(13)-C(23)	-178.9(3)
C(12)-C(13)-C(14)-C(15)	0.1(6)
C(23)-C(13)-C(14)-C(15)	178.4(4)
C(13)-C(14)-C(15)-C(16)	0.4(7)
C(14)-C(15)-C(16)-C(11)	-0.4(7)
N(11)-C(11)-C(16)-C(15)	-179.7(4)
C(12)-C(11)-C(16)-C(15)	-0.1(6)
C(26)-N(21)-C(22)-C(23)	-0.7(8)
N(21)-C(22)-C(23)-C(24)	0.8(7)
N(21)-C(22)-C(23)-C(13)	-178.7(4)
C(12)-C(13)-C(23)-C(24)	-34.1(5)
C(14)-C(13)-C(23)-C(24)	147.5(4)
C(12)-C(13)-C(23)-C(22)	145.4(4)
C(14)-C(13)-C(23)-C(22)	-32.9(6)
C(22)-C(23)-C(24)-C(25)	-0.4(6)
C(13)-C(23)-C(24)-C(25)	179.1(4)
C(23)-C(24)-C(25)-C(26)	0.0(6)
C(22)-N(21)-C(26)-C(25)	0.1(7)
C(24)-C(25)-C(26)-N(21)	0.2(7)
C(11)-N(11)-Mo(1)-O(12)	167.9(11)
C(11)-N(11)-Mo(1)-O(15)	74.7(11)
C(11)-N(11)-Mo(1)-O(13)	-100.2(11)
C(11)-N(11)-Mo(1)-O(14)	-13.3(11)
C(11)-N(11)-Mo(1)-O(1)	-12(2)
N(11)-Mo(1)-O(1)-Mo(3)	-92.7(16)
O(12)-Mo(1)-O(1)-Mo(3)	87.26(11)
O(15)-Mo(1)-O(1)-Mo(3)	179.53(12)
O(13)-Mo(1)-O(1)-Mo(3)	-3.72(9)
O(14)-Mo(1)-O(1)-Mo(3)	-91.57(10)

N(11)-Mo(1)-O(1)-Mo(4)	-2.5(16)
O(12)-Mo(1)-O(1)-Mo(4)	177.44(11)
O(15)-Mo(1)-O(1)-Mo(4)	-90.29(11)
O(13)-Mo(1)-O(1)-Mo(4)	86.45(10)
O(14)-Mo(1)-O(1)-Mo(4)	-1.40(9)
N(11)-Mo(1)-O(1)-Mo(5)	87.2(16)
O(12)-Mo(1)-O(1)-Mo(5)	-92.89(11)
O(15)-Mo(1)-O(1)-Mo(5)	-0.62(11)
O(13)-Mo(1)-O(1)-Mo(5)	176.13(11)
O(14)-Mo(1)-O(1)-Mo(5)	88.28(10)
N(11)-Mo(1)-O(1)-Mo(2)	176.8(15)
O(12)-Mo(1)-O(1)-Mo(2)	-3.24(10)
O(15)-Mo(1)-O(1)-Mo(2)	89.04(11)
O(13)-Mo(1)-O(1)-Mo(2)	-94.22(10)
O(14)-Mo(1)-O(1)-Mo(2)	177.93(10)
N(11)-Mo(1)-O(1)-Mo(6)	-172(4)
O(12)-Mo(1)-O(1)-Mo(6)	8(5)
O(15)-Mo(1)-O(1)-Mo(6)	100(5)
O(13)-Mo(1)-O(1)-Mo(6)	-83(5)
O(14)-Mo(1)-O(1)-Mo(6)	-171(100)
O(3)-Mo(3)-O(1)-Mo(1)	109(5)
O(23)-Mo(3)-O(1)-Mo(1)	-89.30(10)
O(13)-Mo(3)-O(1)-Mo(1)	3.90(10)
O(36)-Mo(3)-O(1)-Mo(1)	-179.67(12)
O(34)-Mo(3)-O(1)-Mo(1)	93.29(10)
O(3)-Mo(3)-O(1)-Mo(4)	18(5)
O(23)-Mo(3)-O(1)-Mo(4)	179.01(11)
O(13)-Mo(3)-O(1)-Mo(4)	-87.79(10)
O(36)-Mo(3)-O(1)-Mo(4)	88.64(10)
O(34)-Mo(3)-O(1)-Mo(4)	1.60(9)
O(3)-Mo(3)-O(1)-Mo(5)	-67(6)
O(23)-Mo(3)-O(1)-Mo(5)	94(3)
O(13)-Mo(3)-O(1)-Mo(5)	-172(3)
O(36)-Mo(3)-O(1)-Mo(5)	4(3)
O(34)-Mo(3)-O(1)-Mo(5)	-83(3)
O(3)-Mo(3)-O(1)-Mo(2)	-160(5)

O(23)-Mo(3)-O(1)-Mo(2)	0.82(9)
O(13)-Mo(3)-O(1)-Mo(2)	94.02(10)
O(36)-Mo(3)-O(1)-Mo(2)	-89.54(10)
O(34)-Mo(3)-O(1)-Mo(2)	-176.58(10)
O(3)-Mo(3)-O(1)-Mo(6)	-72(5)
O(23)-Mo(3)-O(1)-Mo(6)	89.42(10)
O(13)-Mo(3)-O(1)-Mo(6)	-177.38(11)
O(36)-Mo(3)-O(1)-Mo(6)	-0.95(10)
O(34)-Mo(3)-O(1)-Mo(6)	-87.99(9)
O(4)-Mo(4)-O(1)-Mo(1)	156(3)
O(14)-Mo(4)-O(1)-Mo(1)	1.51(10)
O(34)-Mo(4)-O(1)-Mo(1)	-92.59(10)
O(46)-Mo(4)-O(1)-Mo(1)	177.57(10)
O(45)-Mo(4)-O(1)-Mo(1)	91.60(10)
O(4)-Mo(4)-O(1)-Mo(3)	-113(3)
O(14)-Mo(4)-O(1)-Mo(3)	92.43(10)
O(34)-Mo(4)-O(1)-Mo(3)	-1.67(9)
O(46)-Mo(4)-O(1)-Mo(3)	-91.51(9)
O(45)-Mo(4)-O(1)-Mo(3)	-177.48(10)
O(4)-Mo(4)-O(1)-Mo(5)	65(3)
O(14)-Mo(4)-O(1)-Mo(5)	-89.87(10)
O(34)-Mo(4)-O(1)-Mo(5)	176.03(10)
O(46)-Mo(4)-O(1)-Mo(5)	86.19(9)
O(45)-Mo(4)-O(1)-Mo(5)	0.23(9)
O(4)-Mo(4)-O(1)-Mo(2)	-3(5)
O(14)-Mo(4)-O(1)-Mo(2)	-158(3)
O(34)-Mo(4)-O(1)-Mo(2)	108(3)
O(46)-Mo(4)-O(1)-Mo(2)	18(3)
O(45)-Mo(4)-O(1)-Mo(2)	-68(3)
O(4)-Mo(4)-O(1)-Mo(6)	-24(3)
O(14)-Mo(4)-O(1)-Mo(6)	-178.73(11)
O(34)-Mo(4)-O(1)-Mo(6)	87.17(9)
O(46)-Mo(4)-O(1)-Mo(6)	-2.67(8)
O(45)-Mo(4)-O(1)-Mo(6)	-88.64(10)
O(5)-Mo(5)-O(1)-Mo(1)	61(4)
O(45)-Mo(5)-O(1)-Mo(1)	-91.92(11)

O(56)-Mo(5)-O(1)-Mo(1)	175.40(12)
O(15)-Mo(5)-O(1)-Mo(1)	0.62(11)
O(52)-Mo(5)-O(1)-Mo(1)	87.63(10)
O(5)-Mo(5)-O(1)-Mo(3)	-122(4)
O(45)-Mo(5)-O(1)-Mo(3)	84(3)
O(56)-Mo(5)-O(1)-Mo(3)	-8(3)
O(15)-Mo(5)-O(1)-Mo(3)	177(100)
O(52)-Mo(5)-O(1)-Mo(3)	-96(3)
O(5)-Mo(5)-O(1)-Mo(4)	153(4)
O(45)-Mo(5)-O(1)-Mo(4)	-0.24(9)
O(56)-Mo(5)-O(1)-Mo(4)	-92.92(11)
O(15)-Mo(5)-O(1)-Mo(4)	92.30(11)
O(52)-Mo(5)-O(1)-Mo(4)	179.30(11)
O(5)-Mo(5)-O(1)-Mo(2)	-29(4)
O(45)-Mo(5)-O(1)-Mo(2)	177.98(11)
O(56)-Mo(5)-O(1)-Mo(2)	85.29(11)
O(15)-Mo(5)-O(1)-Mo(2)	-89.49(11)
O(52)-Mo(5)-O(1)-Mo(2)	-2.48(9)
O(5)-Mo(5)-O(1)-Mo(6)	-117(4)
O(45)-Mo(5)-O(1)-Mo(6)	89.36(10)
O(56)-Mo(5)-O(1)-Mo(6)	-3.32(10)
O(15)-Mo(5)-O(1)-Mo(6)	-178.10(12)
O(52)-Mo(5)-O(1)-Mo(6)	-91.10(10)
O(2)-Mo(2)-O(1)-Mo(1)	55(3)
O(52)-Mo(2)-O(1)-Mo(1)	-88.74(11)
O(26)-Mo(2)-O(1)-Mo(1)	177.81(12)
O(12)-Mo(2)-O(1)-Mo(1)	3.19(10)
O(23)-Mo(2)-O(1)-Mo(1)	90.14(10)
O(2)-Mo(2)-O(1)-Mo(3)	-36(3)
O(52)-Mo(2)-O(1)-Mo(3)	-179.65(11)
O(26)-Mo(2)-O(1)-Mo(3)	86.89(11)
O(12)-Mo(2)-O(1)-Mo(3)	-87.73(10)
O(23)-Mo(2)-O(1)-Mo(3)	-0.78(9)
O(2)-Mo(2)-O(1)-Mo(4)	-146(4)
O(52)-Mo(2)-O(1)-Mo(4)	71(3)
O(26)-Mo(2)-O(1)-Mo(4)	-23(3)

O(12)-Mo(2)-O(1)-Mo(4)	163(3)
O(23)-Mo(2)-O(1)-Mo(4)	-110(3)
O(2)-Mo(2)-O(1)-Mo(5)	146(3)
O(52)-Mo(2)-O(1)-Mo(5)	2.65(10)
O(26)-Mo(2)-O(1)-Mo(5)	-90.81(11)
O(12)-Mo(2)-O(1)-Mo(5)	94.57(11)
O(23)-Mo(2)-O(1)-Mo(5)	-178.48(10)
O(2)-Mo(2)-O(1)-Mo(6)	-125(3)
O(52)-Mo(2)-O(1)-Mo(6)	91.52(10)
O(26)-Mo(2)-O(1)-Mo(6)	-1.94(11)
O(12)-Mo(2)-O(1)-Mo(6)	-176.56(11)
O(23)-Mo(2)-O(1)-Mo(6)	-89.60(10)
O(6)-Mo(6)-O(1)-Mo(1)	-76(7)
O(46)-Mo(6)-O(1)-Mo(1)	172(100)
O(36)-Mo(6)-O(1)-Mo(1)	80(5)
O(56)-Mo(6)-O(1)-Mo(1)	-98(5)
O(26)-Mo(6)-O(1)-Mo(1)	-9(5)
O(6)-Mo(6)-O(1)-Mo(3)	-155(4)
O(46)-Mo(6)-O(1)-Mo(3)	92.94(9)
O(36)-Mo(6)-O(1)-Mo(3)	0.97(10)
O(56)-Mo(6)-O(1)-Mo(3)	-176.93(11)
O(26)-Mo(6)-O(1)-Mo(3)	-88.62(11)
O(6)-Mo(6)-O(1)-Mo(4)	114(4)
O(46)-Mo(6)-O(1)-Mo(4)	2.78(9)
O(36)-Mo(6)-O(1)-Mo(4)	-89.19(11)
O(56)-Mo(6)-O(1)-Mo(4)	92.92(11)
O(26)-Mo(6)-O(1)-Mo(4)	-178.78(12)
O(6)-Mo(6)-O(1)-Mo(5)	25(4)
O(46)-Mo(6)-O(1)-Mo(5)	-86.86(9)
O(36)-Mo(6)-O(1)-Mo(5)	-178.83(11)
O(56)-Mo(6)-O(1)-Mo(5)	3.27(10)
O(26)-Mo(6)-O(1)-Mo(5)	91.58(11)
O(6)-Mo(6)-O(1)-Mo(2)	-65(4)
O(46)-Mo(6)-O(1)-Mo(2)	-176.54(10)
O(36)-Mo(6)-O(1)-Mo(2)	91.49(11)
O(56)-Mo(6)-O(1)-Mo(2)	-86.40(10)

O(26)-Mo(6)-O(1)-Mo(2)	1.90(11)
N(11)-Mo(1)-O(12)-Mo(2)	-175.75(16)
O(15)-Mo(1)-O(12)-Mo(2)	-74.10(15)
O(13)-Mo(1)-O(12)-Mo(2)	82.43(15)
O(14)-Mo(1)-O(12)-Mo(2)	7.2(4)
O(1)-Mo(1)-O(12)-Mo(2)	4.25(13)
O(2)-Mo(2)-O(12)-Mo(1)	178.7(2)
O(52)-Mo(2)-O(12)-Mo(1)	73.55(16)
O(26)-Mo(2)-O(12)-Mo(1)	-15.3(4)
O(23)-Mo(2)-O(12)-Mo(1)	-80.10(16)
O(1)-Mo(2)-O(12)-Mo(1)	-4.06(13)
O(3)-Mo(3)-O(13)-Mo(1)	176.74(17)
O(23)-Mo(3)-O(13)-Mo(1)	72.51(16)
O(36)-Mo(3)-O(13)-Mo(1)	-12.4(4)
O(34)-Mo(3)-O(13)-Mo(1)	-81.04(14)
O(1)-Mo(3)-O(13)-Mo(1)	-4.80(12)
N(11)-Mo(1)-O(13)-Mo(3)	-179.74(17)
O(12)-Mo(1)-O(13)-Mo(3)	-75.38(15)
O(15)-Mo(1)-O(13)-Mo(3)	13.1(4)
O(14)-Mo(1)-O(13)-Mo(3)	82.92(15)
O(1)-Mo(1)-O(13)-Mo(3)	5.04(13)
O(4)-Mo(4)-O(14)-Mo(1)	179.36(16)
O(34)-Mo(4)-O(14)-Mo(1)	75.00(15)
O(46)-Mo(4)-O(14)-Mo(1)	-10.0(3)
O(45)-Mo(4)-O(14)-Mo(1)	-77.86(15)
O(1)-Mo(4)-O(14)-Mo(1)	-1.82(12)
N(11)-Mo(1)-O(14)-Mo(4)	-178.17(16)
O(12)-Mo(1)-O(14)-Mo(4)	-1.1(4)
O(15)-Mo(1)-O(14)-Mo(4)	81.00(15)
O(13)-Mo(1)-O(14)-Mo(4)	-76.99(14)
O(1)-Mo(1)-O(14)-Mo(4)	1.92(12)
N(11)-Mo(1)-O(15)-Mo(5)	-174.41(18)
O(12)-Mo(1)-O(15)-Mo(5)	80.98(16)
O(13)-Mo(1)-O(15)-Mo(5)	-7.2(4)
O(14)-Mo(1)-O(15)-Mo(5)	-76.83(16)
O(1)-Mo(1)-O(15)-Mo(5)	0.82(14)

O(5)-Mo(5)-O(15)-Mo(1)	-178.6(2)
O(45)-Mo(5)-O(15)-Mo(1)	76.65(17)
O(56)-Mo(5)-O(15)-Mo(1)	-11.7(4)
O(52)-Mo(5)-O(15)-Mo(1)	-77.39(17)
O(1)-Mo(5)-O(15)-Mo(1)	-0.79(13)
O(3)-Mo(3)-O(23)-Mo(2)	178.42(16)
O(13)-Mo(3)-O(23)-Mo(2)	-77.09(15)
O(36)-Mo(3)-O(23)-Mo(2)	75.90(15)
O(34)-Mo(3)-O(23)-Mo(2)	4.5(3)
O(1)-Mo(3)-O(23)-Mo(2)	-1.07(12)
O(2)-Mo(2)-O(23)-Mo(3)	179.08(17)
O(52)-Mo(2)-O(23)-Mo(3)	3.5(3)
O(26)-Mo(2)-O(23)-Mo(3)	-77.16(16)
O(12)-Mo(2)-O(23)-Mo(3)	77.70(15)
O(1)-Mo(2)-O(23)-Mo(3)	1.08(12)
O(4)-Mo(4)-O(34)-Mo(3)	179.64(15)
O(14)-Mo(4)-O(34)-Mo(3)	-73.94(15)
O(46)-Mo(4)-O(34)-Mo(3)	78.23(14)
O(45)-Mo(4)-O(34)-Mo(3)	11.1(3)
O(1)-Mo(4)-O(34)-Mo(3)	2.20(12)
O(3)-Mo(3)-O(34)-Mo(4)	178.23(15)
O(23)-Mo(3)-O(34)-Mo(4)	-7.9(3)
O(13)-Mo(3)-O(34)-Mo(4)	74.71(14)
O(36)-Mo(3)-O(34)-Mo(4)	-80.04(14)
O(1)-Mo(3)-O(34)-Mo(4)	-2.21(12)
O(5)-Mo(5)-O(45)-Mo(4)	-178.56(17)
O(56)-Mo(5)-O(45)-Mo(4)	77.28(15)
O(15)-Mo(5)-O(45)-Mo(4)	-74.66(15)
O(52)-Mo(5)-O(45)-Mo(4)	-0.7(3)
O(1)-Mo(5)-O(45)-Mo(4)	0.31(12)
O(4)-Mo(4)-O(45)-Mo(5)	-177.84(16)
O(14)-Mo(4)-O(45)-Mo(5)	76.77(16)
O(34)-Mo(4)-O(45)-Mo(5)	-9.3(3)
O(46)-Mo(4)-O(45)-Mo(5)	-77.33(15)
O(1)-Mo(4)-O(45)-Mo(5)	-0.32(13)
O(2)-Mo(2)-O(52)-Mo(5)	178.61(17)

O(26)-Mo(2)-O(52)-Mo(5)	73.33(16)
O(12)-Mo(2)-O(52)-Mo(5)	-78.80(15)
O(23)-Mo(2)-O(52)-Mo(5)	-5.8(3)
O(1)-Mo(2)-O(52)-Mo(5)	-3.46(13)
O(5)-Mo(5)-O(52)-Mo(2)	-177.58(18)
O(45)-Mo(5)-O(52)-Mo(2)	4.5(4)
O(56)-Mo(5)-O(52)-Mo(2)	-74.65(16)
O(15)-Mo(5)-O(52)-Mo(2)	79.83(16)
O(1)-Mo(5)-O(52)-Mo(2)	3.52(13)
O(2)-Mo(2)-O(26)-Mo(6)	179.7(2)
O(52)-Mo(2)-O(26)-Mo(6)	-74.58(18)
O(12)-Mo(2)-O(26)-Mo(6)	13.8(4)
O(23)-Mo(2)-O(26)-Mo(6)	78.36(18)
O(1)-Mo(2)-O(26)-Mo(6)	2.66(15)
O(6)-Mo(6)-O(26)-Mo(2)	175.75(17)
O(46)-Mo(6)-O(26)-Mo(2)	0.7(4)
O(36)-Mo(6)-O(26)-Mo(2)	-79.99(18)
O(56)-Mo(6)-O(26)-Mo(2)	74.29(18)
O(1)-Mo(6)-O(26)-Mo(2)	-2.66(15)
O(6)-Mo(6)-O(36)-Mo(3)	177.99(17)
O(46)-Mo(6)-O(36)-Mo(3)	-77.92(16)
O(56)-Mo(6)-O(36)-Mo(3)	3.2(4)
O(26)-Mo(6)-O(36)-Mo(3)	75.41(17)
O(1)-Mo(6)-O(36)-Mo(3)	-1.31(14)
O(3)-Mo(3)-O(36)-Mo(6)	179.83(18)
O(23)-Mo(3)-O(36)-Mo(6)	-76.62(17)
O(13)-Mo(3)-O(36)-Mo(6)	9.0(4)
O(34)-Mo(3)-O(36)-Mo(6)	78.05(16)
O(1)-Mo(3)-O(36)-Mo(6)	1.33(14)
O(6)-Mo(6)-O(46)-Mo(4)	177.89(15)
O(36)-Mo(6)-O(46)-Mo(4)	73.06(14)
O(56)-Mo(6)-O(46)-Mo(4)	-80.25(14)
O(26)-Mo(6)-O(46)-Mo(4)	-7.1(3)
O(1)-Mo(6)-O(46)-Mo(4)	-3.73(11)
O(4)-Mo(4)-O(46)-Mo(6)	-177.20(16)
O(14)-Mo(4)-O(46)-Mo(6)	12.0(3)

O(34)-Mo(4)-O(46)-Mo(6)	-74.06(14)
O(45)-Mo(4)-O(46)-Mo(6)	80.82(14)
O(1)-Mo(4)-O(46)-Mo(6)	3.78(12)
O(5)-Mo(5)-O(56)-Mo(6)	-177.73(19)
O(45)-Mo(5)-O(56)-Mo(6)	-72.84(17)
O(15)-Mo(5)-O(56)-Mo(6)	15.3(4)
O(52)-Mo(5)-O(56)-Mo(6)	80.77(16)
O(1)-Mo(5)-O(56)-Mo(6)	4.54(14)
O(6)-Mo(6)-O(56)-Mo(5)	176.10(17)
O(46)-Mo(6)-O(56)-Mo(5)	72.51(16)
O(36)-Mo(6)-O(56)-Mo(5)	-9.0(4)
O(26)-Mo(6)-O(56)-Mo(5)	-81.58(17)
O(1)-Mo(6)-O(56)-Mo(5)	-4.53(14)
C211-N11-C111-C121	37.9(5)
C311-N11-C111-C121	159.1(4)
C411-N11-C111-C121	-80.0(5)
N11-C111-C121-C131	173.3(4)
C111-C121-C131-C141	167.1(5)
C311-N11-C211-C221	-52.7(4)
C411-N11-C211-C221	-174.7(3)
C111-N11-C211-C221	65.4(4)
N11-C211-C221-C231	-166.4(3)
C211-C221-C231-C241	-174.7(4)
C211-N11-C311-C321	-61.2(5)
C411-N11-C311-C321	57.8(5)
C111-N11-C311-C321	177.6(4)
N11-C311-C321-C331	167.5(4)
C311-C321-C331-C341	-75.9(6)
C211-N11-C411-C421	172.0(3)
C311-N11-C411-C421	50.2(5)
C111-N11-C411-C421	-67.3(5)
N11-C411-C421-C431	177.6(3)
C411-C421-C431-C441	176.8(4)
C412-N22-C112-C122	-52.4(7)
C212-N22-C112-C122	66.2(7)
C312-N22-C112-C122	-173.2(6)

N22-C112-C122-C132	173.5(5)
C112-C122-C132-C142	-179.0(5)
C412-N22-C212-C222	-176.2(5)
C112-N22-C212-C222	62.6(6)
C312-N22-C212-C222	-55.2(7)
N22-C212-C222-C232	175.2(5)
C212-C222-C232-C242	-175.0(6)
C412-N22-C312-C32A2	62.5(9)
C112-N22-C312-C32A2	-176.2(7)
C212-N22-C312-C32A2	-56.2(9)
N22-C312-C32A2-C33A2	-166.1(8)
C312-C32A2-C33A2-C34A2	-77.3(10)
C112-N22-C412-C422	-58.4(7)
C212-N22-C412-C422	-178.8(6)
C312-N22-C412-C422	60.0(7)
N22-C412-C422-C43A2	173.2(7)
C412-C422-C43A2-C44A2	-176.4(13)

Symmetry transformations used to generate equivalent atoms: